Investigation of the molecular mechanisms underlying the invasive phenotype in a panel of lung cancer cell lines

Mohan Kumar Muniyappa

Ph.D. Thesis 2009

Dedicated to my beloved

Parents, Family and Friends

A thesis submitted for the degree of Ph.D.

By

Mohan Kumar Muniyappa M.Sc.

The experimental work described in this thesis was carried out under the supervision of

Dr. Niall Barron Ph.D.

And

Prof. Martin Clynes Ph.D.

National Institute for Cellular Biotechnology

School of Biotechnology,

Dublin City University, Glasnevin, Dublin 9,

Ireland.

2009

I hereby certify that this material, which I now submit for assessment on the programme of study leading to the award of Ph.D. is entirely my own work and has not been taken from the work of others save and to the extent that such work has been cited and acknowledged within the text of my work.

Signed: Mohan Kumar Muniyappa *(Candidate) ID No.:* ***54162564***

Date: 28/08/2009

Aknowledgement

It has been quite an adventurous and memorable journey for me since 25th October 2004. Every single day past four years has been interesting, innovative, surprising sometimes even disastrous but I enjoyed every moment of it. And which made it possible for me to complete this PhD research thesis. Of course this would not have been possible if I hadn't had the guidance and help directly or indirectly from people with whom I have worked along with.

I would like to acknowledge and take this opportunity with great pleasure and heartfelt gratitude to thank Director of NICB and co-supervisor Prof. Martin Clynes, one of the most important personalities in my life, without whom I would only, dreamt of pursuing. The first stepping stone laid by him for my PhD dreams. His scientific knowledge combined with help and guidance during the course of my project was memorable one, especially the suggestion for carrying out microRNAs and the proteomic analysis work.

I would like to extend heartfelt gratitude to the second important and amazing personality my supervisor Dr. Niall Barron. A down to earth person, trouble shooter and working under his supervision led to inculcate independent thoughts. His supervision gave me lot of courage and enthusiasm, learnt new techniques and professionalized with some of the cutting edge technology in the molecular cancer research field and also helped me to improve my hidden leadership and management skills.

I would like to thank Dr. Paul Dowling for his enormous effort and help for the proteomics experiments. His professional way of working especially who has lot of patience and dedication for the work, something that I tried to imbibe from him.

I would also like to convey my gratitude to Mr. Michael Henry for his timely help in finshing proteomics experiments. Not only a dedicated prteomics personnel but also makes sure he is always in the news in NICB, cheers Mick.

I would like to convey special thanks to my examiners Prof.John Masters and Dr. Paula Meleady whos valuable comments and suggestion carved this Ph.D thesis to a much higher level than what it was. My sincere gratitude to Dr.Pula Meleady for the timely help and suggestion during proteimics experiments.

I would like to thank Dr. Finbarr O' Sullivan for timely help with confocal microscope work and also with FACS sorting experiments.

I would like thank to Dr. Norma O' Donovan who helped me at various stages during my project. I would also like to convey my gratitude to former senior scientist in NICB
Dr. Lorraine O'Driscoll for support and help during this project and also to former Manager of NICB Dr. Donnach O'Driscoll for the help and support.

I would like to thank former postdoctorate Dr. Patrick Gammell for his efforts and help during the start of microRNAs project. I would also like to thank Dr. Padraig Doolan for his timely advice and help.

I would like to thank Dr. Robert O'Connor and Mr. Julian McGovern for their help, advice and support with the computers whenever we had a breakdown in our lab.

I would like to convey my humble gratitude to all my friends here in Ireland and overseas, who always kept me going with their regular cultural activities, get together for an evening tea occasionally with a 'bajji' (Indian snack). Special mention to Ram, Jai, Sweta, Ramesh, Lisa, Alex, Dermot, Aoife, Noel, John, Paul, Kishore, Amitabh, James and Magali who made my stay in Dublin a memorable one.

I would like to convey my sincere and heartfelt gratitude to very special people in NICB, thanks Ms. Carol McNamara, Ms.Yvonne O' Reilly and Ms.Mairead Callan in the office for their nonstop support and help with finance and administrative section through out my stay in NICB. Heartiest thanks to Mr. Joseph Carey, Mr. Ultan and Mr.Shane in the prep room and

delivery section for their day to day help and making my cell culture and other related work to the project to carry on smoothly.

I would like to extend my special thanks to Dr. Olga Piskareva and previous lab members Dr.Aisling Pierce and Dr.Isabella Bray with their help i was able to master over some very important assays relevant to cancer research and who made my research work enjoyable during their presence. And finally I would like to say thanks from bottom of my heart to each and every single person in NICB who helped me and supported me during my project.

Abstract

The research described in this thesis aimed to increase our knowledge of the molecular mechanisms by which lung cancer cells acquire the capacity to invade. The research can be divided into two main sections a) Development of genetic tools for stable, targetable transgene overexpression, b) Investigation of the role of differential expression of a group of genes, including microRNAs, in cancer invasion. DLKP mildly invasive cell line derived from a non-small cell lung carcinoma and its Adriamycin resistant variant DLKPA highly invasive were used in this study to evaluate the roles of differentially expressed mRNAs and microRNAs.

We developed two targetable DLKP cell lines based on Cre-LoxP technology. These were generated by random and homologous recombination (site specific) targeting. These cell lines were developed to overcome challenges one faces with non-targetable systems including large discrepancies in target gene expression, genomic instability, and unpredictable phenotypes. A panel of thirty one DLKP single cell clones were assessed for stable and transgene overexpression, over four and a half months with regular passages and freeze thaw cycles. Many clones were found to display unstable transgene expression over time but several were identified with stable expression and at different levels. Two clones were selected based on stable expression level and on invasive phenotype, i) high expressing non invasive clone DLKP 17 and ii) low expressing invasive clone DLKP 11.

Microarray profiling studies done in this lab on a panel of lung cancer cell lines with various invasive phenotypes identified a list of differentially expressed genes. GLP1R, KCNJ8 and TFPI2 genes were stably overexpressed and all induced invasion in non-invasive DLKP 17. Furthermore GLP1-R induced invasion could be reversed through siRNA induced silencing of the transgene. GLP1-R overexpression in non-invasive MCF-7 also induced cellular invasion. These findings are the first time that GLP1-R has been linked to this phenotype.

MiRNA expression profiling was performed comparing low invasive DLKP (parent) and invasive DLKPA (Adriamycin selected) cell lines. Three differentially regulated miRNAs were selected for functional validation. Mir-21 and mir-27a were pro-invasive and mir-29a anti-invasive in DLKP and DLKPA cell lines. We later confirmed the impact on invasion and proliferation through stable overexpression studies with mir-29a. Pre-mir-29a overexpression in the invasive PANC-1 (pancreatic cancer line) resulted in reduced invasion suggesting that the effect of mir-29a was not cell line specific.

2D-DIGE proteomic profiling of cells transfected with mir-29a generated a list of differentially regulated protein spots, some of which were identified by MALDI-TOF and LC-MS analysis. Bioinformatic analysis revealed that the majority of these proteins were involved in cellular processes like apoptosis, proliferation, motility and differentiation. We chose GRB2, RAN, MIF and ANXA2 gene targets which were differentially downregulated due to mir-29a overexpression and performed siRNA induced knockdown in DLKPA cell line. Results revealed RAN to be anti-invasive and anti-proliferative in our cell line model. Knockdown of the other three targets did not affect the invasive or proliferative phenotype of DLKPA. GFP-RAN 3'-UTR reporter assay indicated a small (5-6%) but statistically significant reduction in GFP RAN-UTR expressing cell population when transfected with mir-29a. In conclusion we provide evidence that mir-29a may be an anti-invasive microRNA and that this effect is mediated via modulation of the expression of RAN and several other cellular proteins.

Table of Contents

Section 1.0 Introduction

Section 2.0 Materials and Methods

Results

Section A: 3.0

Section B:

Section C:

Section D:

Section E:

Discussion 4.0

Section IV:

Section V:

Section 5.0 Conclusions and Future work

ABBREVIATIONS

%	-	Percent
2D-DIGE	-	Two Dimensional- Differential in gel electrophoresis
3'UTR	-	3' Untranslated region
Ab	-	Antibody
AM	-	Anti-miRNA
AMP	-	Ampicillin
ANOVA	-	Analysis of variance
ANX2	-	Annexin 2
ATCC	-	American Tissue Culture Collection
ATP	-	Adenosine Triphosphate
BSA	-	Bovine Serum Albumin
BVA	-	Biological Variation Analysis
cAMP	-	Cyclic Adenosine Monophosphate
cDNA	-	Complementary DNA
CDR	-	Chemotherapeutic Drug Resistance
CHAPS	-	3-[(3-Cholamidopropyl) dimethylammonio]-1-propanesulfonate
CRE	-	Cre recombinase
DEPC	-	Diethyl Pyrocarbonate
DMEM	-	Dublecco's Minimum Essential Medium
DMSO	-	Dimethyl Sulfoxide
DNA	-	Deoxyribonucleic Acid
dNTP	-	Deoxynucleotide Triphosphate (N = A, C, T, G)
DTT	-	Dithiothreitol
ECM	-	Extracellular matrix
EDTA	-	Ethylene Diamine Tetraacetic Acid
EGF	-	Epidermal Growth Factor
EGFR	-	Epidermal Growth Factor Receptor
eIF	-	Eukaryotic Translation Initiation Factor
EMMPRIN	-	Extracellular matrix metalloproteinase inducer
EST	-	Express sequence tags
FBS	-	Foetal Bovine Serum

FSC	-	Forward Scatter
GAPDH	-	Glyceraldehyde-6-Phosphate Dehydrogenase
GF(s)	-	Growth Factor (s)
GFP	-	Green Fluorescent Protein
GLP1-R	-	Glucagon Like Peptide 1 Receptor
GRB2	-	Growth factor receptor bining protein 2
HEPES	-	N-[2-Hydroxyethyl] piperazine-N'-[2-ethanesulphonic acid]
HJ	-	Holiday Juntion
HR	-	Homologous Recombination
IC50	-	Inhibitory Concentration 50%
IEF	-	Isoelectric focussing
IMS	-	Industrial Methylated Spirits
IPG	-	immobilized pH gradient strips
LacZ	-	Lactose Z (β-galactosidase)
LB	-	Luria-Bertani
LC-MS	-	Liquid chromatography-mass spectrometry
LoxP	-	LoxP sequence
LINE-1	-	Long Interspersed Nuclear Element-1
KCNJ8	-	Inwardly rectifying potassium channel J8
KDa	-	Kilo Daltons
MALDI-TOF	-	Matrix-assisted laser desorption/ionization -Time of Flight
MAPK	-	Mitogen Activated Protein Kinase
MDR	-	Multiple Drug Resistance
MIF	-	Macrophage Migration Inhibitory Factor
Min	-	Minutes
mM	-	Milli Molar
μM	-	Micro Molar
miRNA	-	microRNA
MMLV-RT	-	Moloney Murine Leukaemia Virus- Reverse Transcriptase
MMPs	-	Matrix Metalloproteases
mRNA	-	Messenger RNA
nM	-	Nano Molar
NSCLC	-	Non-Small Cell Lung Cancer

ORF	-	Opening reading frame
PBS	-	Phosphate Buffered Saline
PCR	-	Polymerase Chain Reaction
PKA	-	Protein Kinase A
PM	-	Pre-miRNA
QC	-	Quality Control
qRT-PCR	-	Quantitative real time PCR
rAAV	-	Recombinant adeno viral vector
RAN	-	RAS related nuclear protein
RE	-	Restriction Enzyme
RISC	-	RNA-Induced Silencing Complex
RNA	-	Ribonucleic Acid
RNase	-	Ribonuclease
RNasin	-	Ribonuclease Inhibitor
RQ	-	Relative Quantity
RT-PCR	-	Reverse Transcriptase PCR
S100A13	-	S100 calcium binding protein A13
SCLC	-	Small Cell Lung Carcinoma
Scrm siRNA	-	Scrambled siRNA
SD	-	Standard Deviation
SDS	-	Sodium Doedecyl Sulphate
SE	-	Standard Error
SFM	-	Serum-Free Medium
shRNA	-	short hairpin RNA
siRNA	-	Small interfering RNA
TAE	-	Tris-acetic acid-EDTA buffer
TE	-	Tris-EDTA
TEMED	-	N, N, N', N'-Tetramethyl-Ethylenediamine
TF	-	Transcription factor
TFPI2	-	Tissue factor pathway inhibitor 2
TGFβ1	-	Transforming Growth Factor β1
TNFAIP8	-	Tumour necrosis Factor, Alpha-Induced Protein 8
Tris	-	Tris (hydroxymethyl) Aminomethane

TXT	-	Taxotere
TV	-	0.25% Trypsin/ 0.01% EDTA Solution in PBS
UHP	-	Ultra High Pure Water
uPA	-	Urokinase type plasminogen activator
uPAR	-	Urokinase type plasminogen activator receptor
UTR	-	Untranslated Region
UV	-	Ultraviolet
VCR	-	Vincristine
VEGF	-	Vascular Endothelial Growth Factor
VEGFR	-	Vascular Endothelial Growth Factor Receptor
v/v	-	Volume/Volume
w/v	-	Weight per Volume
X-Gal	-	5-Bromo-4-Chloro-3-indolyl-β-D-galactopyranoside

1.0 Introduction

1.1 Lung cancer

According to the Irish Cancer Society Lung cancer is one of the most prevalent in Ireland, with over 1,500 new cases each year. Currently lung cancer tops the list of most common cancers worldwide, not only in men but in women as well. The 5 year survival rate for lung cancer is < 15% from the time of diagnosis. This is largely due to the late stage of diagnosis and the lack of effective treatments, reflecting the need for a better understanding of the mechanisms that underlie lung carcinogenesis. Ultimately, this could improve the diagnosis, prognosis, and clinical management of patients with lung cancer. Other causes of lung cancer include exposure to chemicals such as asbestos, as well as the naturally occurring radioactive gas, ***radon*** (a colourless, odourless, tasteless, naturally occurring radioactive gas produced from the decay of the element radium, which occurs naturally in rocks and soil worldwide). Passive inhalation of environmental tobacco smoke (ETS) has also been linked with the development of lung cancer in non-smokers. Cells defective in the regulatory circuits that control proliferation and homeostasis pose a threat to become cancerous (Hanahan and Weinberg, 2000). Cancer is a multistep process and a distinguishing feature of malignant cells is their ability to invade surrounding normal tissue, metastasize through the blood and lymphatic systems, and re-establish at distant secondary locations. The choice of treatment for patients with lung cancer depends strongly on the clinical stage. Other details taken into account include pulmonary function and cell type. Surgery is the major therapeutic option for lung cancer patients, however approximately 75% of lung cancers are inoperable at time of diagnosis therefore surgery is only curative in patients with early stage lung cancer. Radiation therapy can also be curative for a small percentage of patients. To date, chemotherapy can offer improvement in short-term survival, but overall survival from lung cancer is poor. Unlike the study of a single gene, protein, or pathway, genomic and proteomic technologies enable a systematic overview that provides the potential to improve our understanding of this disease.

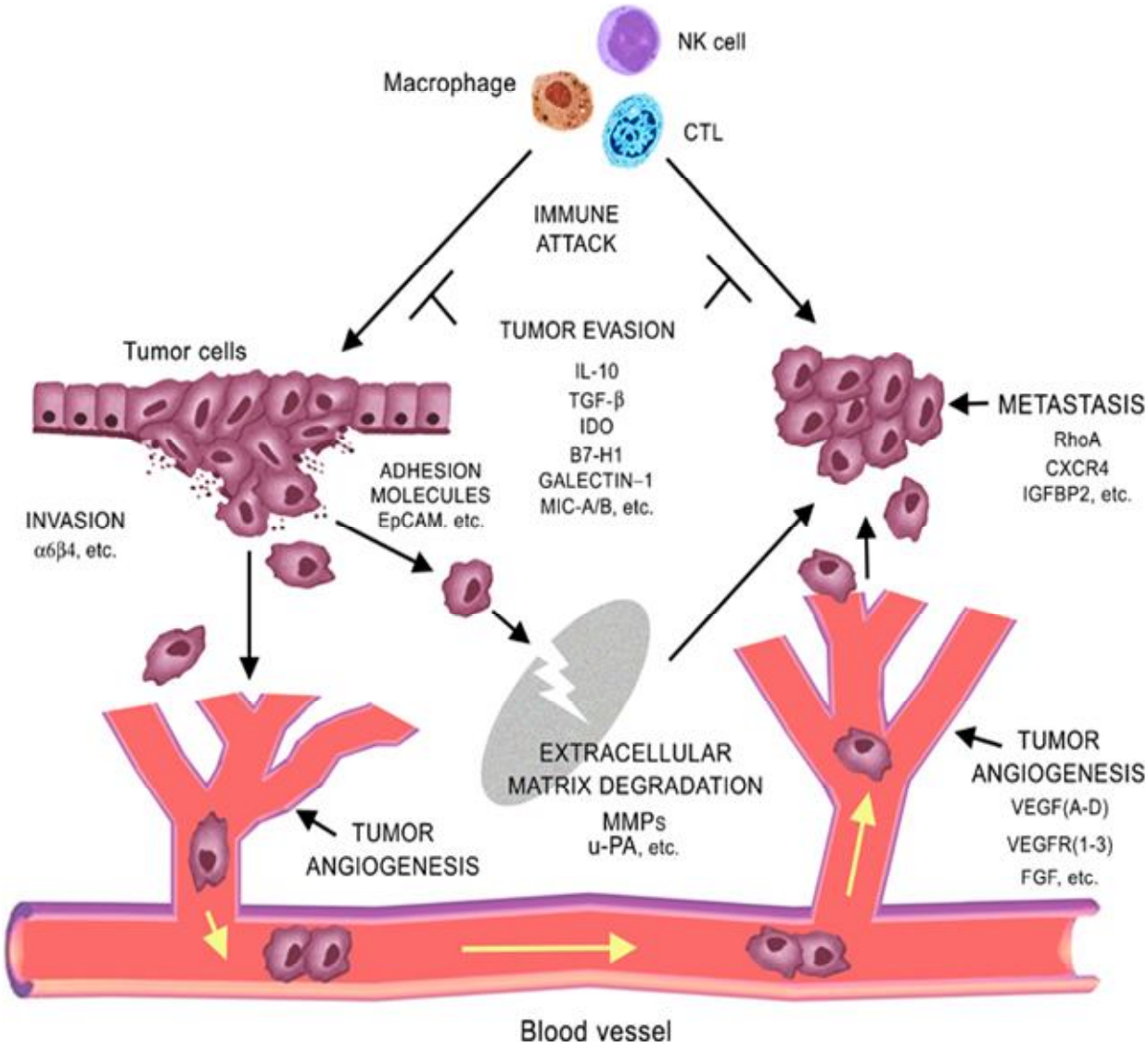

www.nature.com/.../v13/n6/fig_tab/3302694f2.html

Figure 1.0 Schematic diagram to illustrate gene targets important for tumor-host interaction. Gene targeting technology can be used to target molecules that are important for tumor angiogenesis, invasion, metastasis and immune evasion.

Symptoms associated with lung cancer are cough, dyspnoea, haemoptysis and post obstructive pneumonia, (Hoffman *et al,* 2000), although lung cancer can present with no initial symptoms. Diagnosis is achieved by invasive and non-invasive methods. Non-invasive methods for diagnosing lung cancer include sputum cytology and chest

radiography. After this point, invasive techniques such as bronchoscopy and lung biopsy are performed. While the location and size of the lung tumour can be estimated from a chest x-ray or CT scan, accurate diagnosis and staging requires a biopsy to histologically type the cells and determine if local nodes are involved. Staging of lung cancer is very important, since it will determine the type of treatment received. The international staging system classifies the cancer based on the Tumour, Node, and Metastasis (TNM) designation. The designation T1-4 refers to the size and location of the primary tumour. N0-N3 describes the extent of lymph node involvement. In cases where distant metastases are present (M1), the tumour is diagnosed as stage IV lung cancer. Early stage lung cancers are the most treatable, with later stage cancers such as stage IIIB and IV being virtually untreatable.

Lung cancer is divided into 2 main groups, small cell lung cancer (SCLC) and non-small cell lung cancer (NSCLC). The World Health Organisation (WHO) compiled this histologic classification. SCLC and the subtypes of NSCLC – adenocarcinoma, squamous cell carcinoma and large cell carcinoma, account for 95% of lung cancers. SCLC presents less frequently than NSCLC and generally originates from a central location in the lung. These tumours are very aggressive, have a rapid growth rate and generally present with distant metastases at diagnosis. These tumours have the poorest prognosis of all lung cancer subtypes. NSCLC is divided into three categories, squamous cell carcinoma (30% of all lung cancers), adenocarcinoma (40%) and large cell carcinoma (10%). Squamous cell carcinoma develops from within a central bronchus in the lung and frequently displays central cavitation from necrosis. They are characterised by keratin formation. Squamous cell carcinomas have slow growth rates and develop metastases at a late stage. Adenocarcinomas generally develop centrally from surface epithelial cells in larger bronchi. They are characterised by gland formation and mucus production. These tumours tend to metastasise early and have a rapid growth rate. Large cell carcinoma is characterised by large cells with large nuclei and prominent nucleoli. These tumours are usually poorly differentiated and tend towards large peripheral masses.

Lung cancer, particularly SCLC, is characterised by rapid growth and metastatic spread (Yano et al, 2005). By the time of diagnosis clinically undetectable micro metastasis may already have developed within the lung. Yano *et al,* (2005) injected immunodeficient mice with SCLC cell lines, SBC-3 and SBC-5 resulting in metastasis formation in liver,

bone and kidney. Lung cancer itself often arises as a metastasis from another site, for example, cancer of the breast (Horak and Steeg, 2005).

1.2 Invasion

Invasion is the active translocation of neoplastic cells across tissue boundaries and through host cellular and extracellular matrix barriers. Invasion is not only due to growth pressure but is attributed to additional genetic deregulation over and above those molecular events that cause uncontrolled proliferation. At the biochemical level, the mechanism of invasion used by tumour cells may be similar to that used by non-malignant cells which traverse tissue boundaries under normal physiological conditions. Mechanisms of invasion are known to involve a complex array of genetic and epigenetic changes many of which are specific for different types of tumours and different sites of metastasis. The roles of adhesion molecules such as integrins and cadherins in invasion have undergone a major transition over the past decade. It is now apparent that these molecules have a critical role in signalling from the outside to inside a cell thus controlling how a cell can interact with and sense its local environment. It has also become clear that proteolytic enzymes and their inhibitors not only degrade the ECM, but are involved in the release of factors that can positively or negatively affect the growth of tumour cells. In more recent years, the importance of the post-extravasional stages of invasion was highlighted, where adhesion and proteolysis are now known to play a role along with other processes including apoptosis, dormancy, growth factor-receptor interactions and signal transduction. It has also been found that it is not only the immediate cellular microenvironment, but also the extended cellular microenvironment that can modify cellular gene expression and enhance metastasis. Our improved understanding of the expanded roles of the individual molecules involved has resulted in a mechanistic blurring of the previously described discrete stages of the metastatic process (Cairns et al, 2003). In contrast to malignant invasion, physiological invasion is tightly regulated and ceases when the stimulus is removed. Invading tumour cells appear to have lost the control mechanism which prevents normal cells from invading neighbouring tissue at inappropriate times and places. Thus, the fundamental difference between normal and malignant cells is regulation. The difference must lie in the proteins that start, stop or maintain the invasion programme at times and places that are

inappropriate for non-malignant cells. A major goal is to understand what signals and signal transduction pathways are perpetually activated or deregulated in malignant invasion (Kohn et al, 1997).

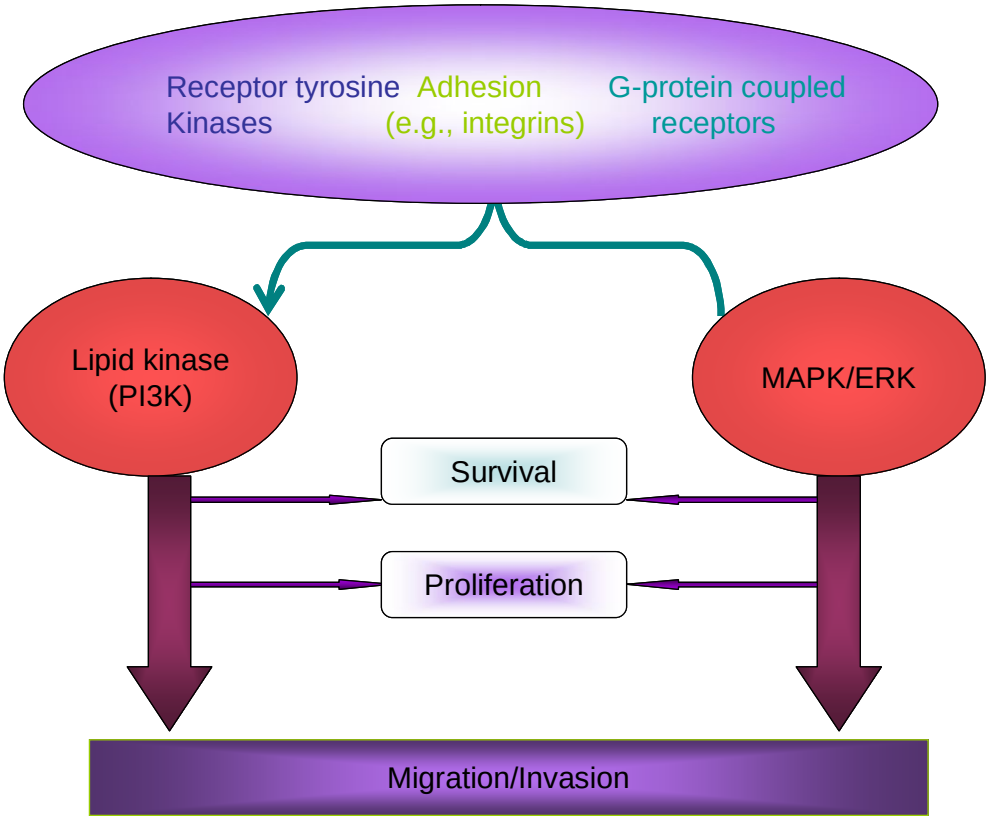

(Adopted from Physiology **20: 194-200, 2005)**

FIGURE 1.1 Schematic of molecular machinery involved during tumour cell transformation into a migratory cell, which involves signals for cellular processes like proliferation and survival responses.

Liotta et al, (1977) proposed a three step simplified theory of invasion: (1) Tumour cell attachment *via* cell surface receptors which specifically bind to the components of the extracellular matrix (ECM); (2) the anchored tumour cell secretes
hydrolytic enzymes, such as matrix metalloproteinases, to degrade the extracellular matrix; (3) tumour cell locomotion into the region of the matrix modified by the

proteolysis. Thus, regulation of the molecular events necessary for invasion requires spatial and temporal coordination at an individual cell level.

For cells migrating within a three dimensional extracellular matrix, such as penetrating a basement membrane, protrusion of a cylindrical pseudopod occurs prior to translocation of the whole cell body (Condeelis, 1993). A number of observations support the central role of the cytoskeleton-driven pseudopodia as organs of motility and invasion. Pseudopodia aggregate or concentrate cell surface degradative enzymes and adhesion receptors (Guirguis et al, 1987). A balance must switch from proteolysis to adhesion in order for the advancing pseudopod to grip the matrix and pull the cell forward. General unregulated proteolysis alone cannot be responsible for the entire invasion cascade. When the cell moves into the zone of lysis, adhesion is required and proteolysis must be shut down. At the rear of the cell, dissociation from adjacent cells, and detachment from previous attachment sites are necessary to release the cell. This type of motility is described as mesenchymal motility (Sahi et al, 2006).

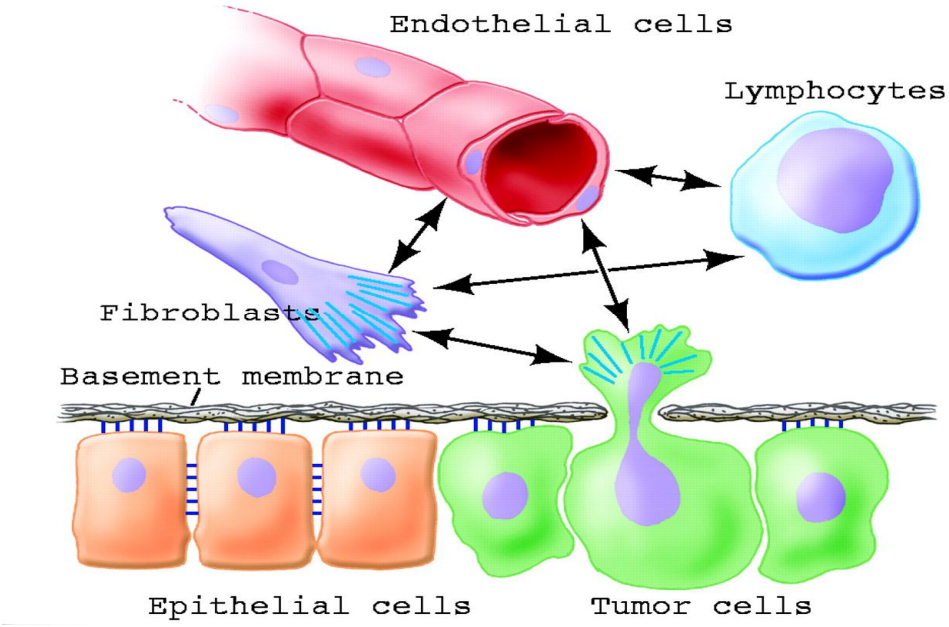

(Adopted from***Physiology* 20: 194-200, 2005)**

FIGURE 1.2A Schematic of active contribution of Stromal cells and ECM components to metastatic process. Through cell-cell contacts, cell-matrix contacts, and soluble mediators, complex communications initiate and sustain the invasion and migration of tumor cells.

The basement membrane and interstitial stroma also have important regulatory roles in invasion. They serve as a storage depot for latent proteinases, cytokines and growth factors, which can be activated or released by the invading cells. The critical pathological turning point is in the initiation of local invasion leading to the dissemination of tumour cells. Tumour-induced neovascularisation occurs in parallel with invasion and provides vascular entry necessary for dissemination. The molecular characterisation of invasion has led to the identification of two categories of checkpoints that constitute possible intervention targets. The first category includes cell surface and secreted proteins e.g. adhesion receptors, degradative enzymes and their inhibitors and motility stimulating cytokines. The second checkpoint category includes regulatory proteins and pathways such as calcium-mediated signalling, G-protein activation and tyrosine phosphorylation events. It is the molecular examination of these checkpoint molecules that may provide the basis for the development of therapeutics that can potentially block tumour invasion or growth (Kohn et al, 1997).

1.2.1 Survival during invasion

None of the functions of metastasizing cells are unique to cancer cells. An example of physiological invasion is smooth muscle cell migration from the tunica media (which contains smooth muscle fibres, elastic and collagenous tissue) to the intima (endothelial cell layer) of blood vessels. Angiogenesis, nerve growth cone extension and homing, embryogenesis and trophoblast implantation are also examples. During embryonic development, motile cells are tightly regulated in order to ensure proper homing and reversion to a non-motile phenotype after migration into a destined location (Hay, 1995). In contrast, cancer cells have lost the ability to recognise specific targets. Their inappropriate growth signals are accompanied by mechanisms to avoid apoptosis and the potential to elicit angiogenesis for independent nutrient supply.

Hood and Cheresh, (2002) and other studies suggest that invasion is not simply due to growth pressure but involves additional genetic deregulation over and above those molecular events that cause uncontrolled proliferation. The difference between the normal process and the pathogenic nature of cancer invasion is therefore one of regulation. Invading cells must be able to activate survival mechanisms and escape apoptosis. Indeed,

integrin-binding to ECM ligands initiates pro-survival mechanisms. Many anti-apoptotic pathways are the same as those that are involved in regulating migration. Many targets of FAK signalling such as RAS, RAC, PI3K and ERK have also been implicated in cell survival.

1.3 Metastasis

Cancer metastasis has been described as a complex series of sequential processes that involve: (1) the initial transforming event; (2) proliferation of transformed cells; (3) the ability of cancer cells to avoid destruction by immune mechanisms; (4) nutritional supply to the tumour mass requiring the release of tumour angiogenesis factors; (5) local invasion and destruction of extracellular matrix components and parenchymal cells; (6) migration of tumour cells away from the primary tumour mass; (7) penetration of cancer cells through the blood vessel wall; (8) embolisation of cancer cells in "clumps" to distant organs; (9) arrest of cancer cells in the lumen of small blood vessels or lymphatics; (10) reverse penetration of blood vessels; (11) repetition of the process beginning at step 2, resulting in the formation of a secondary tumour (metastases) (Fidler, 2002a). In many patients, metastases develop some years after the resection of the primary neoplasm

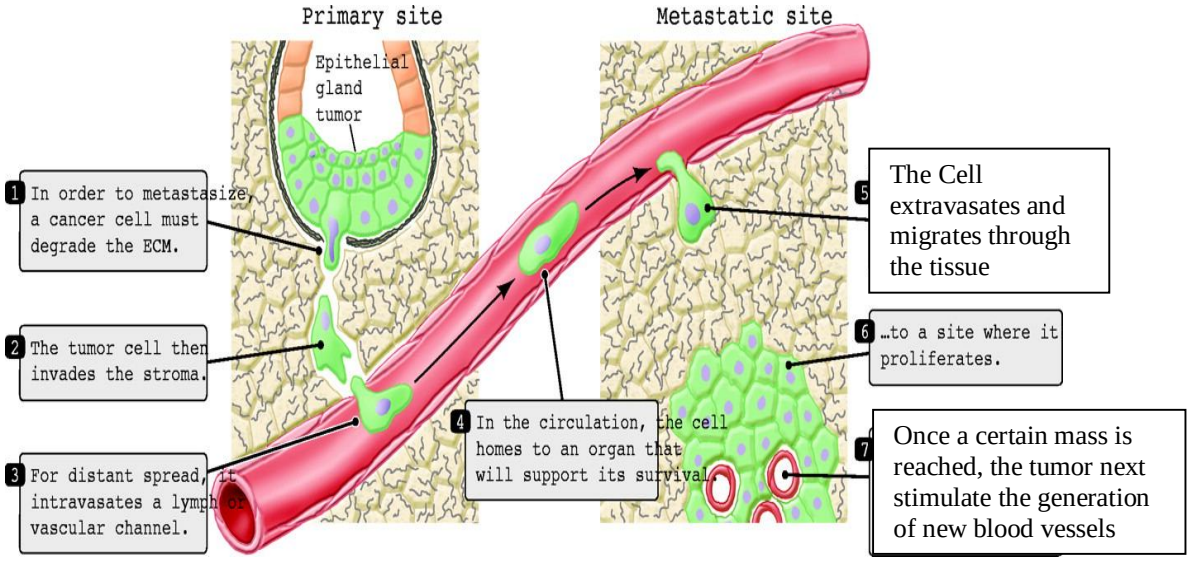

Physiology 20: 194-200, 2005

Figure 1.3A Schematic of a Metastatic sequence

By the time of diagnosis, a high proportion of patients have clinically detectable metastasis. It is assumed that dissemination is impossible until invasion has occurred. For breast cancer, the period of transition from hyper proliferative but non-invasive disease to invasive cancer is estimated to average 6 years (Sprat *et al*, 1986). The time period after the invasive carcinoma grows to reach the minimum threshold size of detection (0.25cm in diameter), to establishment of the first metastasis, can be less than one year (Sprat *et al*, 1986).

Thus transition of preinvasive carcinoma to invasion provides a much larger window for intervention compared to the conventional goal, which focuses on established invasive carcinoma. Most deaths from cancer are due to metastasis that are resistant to conventional therapies. Current therapies fail to eradicate metastasis for three major reasons. Firstly, when initially diagnosed, most tumours are well advanced and metastasis has already occurred. Secondly, specific organ environment can modify the response of a metastatic tumour cell to systemic therapy and alter the efficiency of anticancer agents. The third reason and the greatest obstacle to the success of therapy, is the heterogeneous composition of tumours, where highly metastatic cells can escape from the effect of therapeutic agents. Metastasis is considered to be an inefficient process, as a result large numbers of cells can be shed into the circulation from a primary tumour but only a small fraction of the cells will succeed in forming metastases. Results from a series of experiments using intravital video microscopy (IVVM), a technique which permits direct observation of the microcirculation *in vivo*, suggest that early steps in metastasis, including destruction of cells in circulation and extravasion, contribute less to metastatic inefficiency than previously assumed. Rather, regulation of growth of individual extravasated cells in target tissue appears to be the rate-limiting step (Chambers et al, 1995). Some metastases will arise on the basis of circulatory anatomy. The lungs are a common site of metastasis. The formation of metastases required the interaction of the right cells with the compatible organ environment.

Metastasis favours the survival and growth of a few subpopulations of cells that pre-exist within the parent neoplasm (Fidler and Kripke, 1977). Thus, metastases can have a clonal origin, and different metastases can originate from the proliferation of different single cells (Talmadge and Fidler, 1982). In the past inability to accurately diagnose patients at high risk for the development of metastasis has precluded the possibility of tailored

treatment, increased monitoring, or preventive action. However, advances in gene expression profiling have allowed many researchers including Euer, N. et al, (2002) to distinguish metastatic primary tumours from non-metastatic primary tumours. These results have led to much debate as to the mechanisms of metastatic development.

The ability to identify metastatic tumours using transcriptional signatures from bulk tumour tissues suggests that primary oncogenic mutations determine the metastatic potential of a tumour. This idea may be viewed as incompatible with the conventional theory of tumour progression which predicts that only a small number of cells from the primary tumour achieve metastatic potential. Both seemingly contradictory models have a variety of supporting data suggesting that both are correct to some extent (Hunter, 2006).

Organ microenvironment can influence the biology of cancer growth and metastasis in several different ways. During the interaction of metastatic cells with host tissues, signals from autocrine, paracrine or endocrine pathway can influence tumour cell growth and proliferation, due to the different concentrations of hormones in particular organs, local factors that are differentially expressed or paracrine growth factors concentrated in different tissues. In this way metastatic tumour cells can respond to physiological signals produced when homeostasis is disturbed. Tumour cells can also originate from or have an affinity for growth in a particular organ by responding to these physiological signals (Fidler, 2002b). For example, human colon carcinoma (HCC) cells implanted subcutaneously (ectopic site) into nude mice produce low levels of secreted type IV collagenase, whereas the same cells growing in the wall of the colon (orthotopic site) produce high levels of type IV collagenase (Nakajima et al, 1990). In another study by Fidler et al,. (2002) involving highly metastatic clones of human prostate cancer were implanted into the prostate (orthotopic site) and subcutis (ectopic site). Tumours growing in the prostate exhibited higher levels of epidermal growth factor receptor (EGF-R), basic fibroblast growth factor (bFGF), interleukin 8 (IL-8), type IV collagenase and the multidrug resistance (mdr-1) gene than those growing in the subcutis. This data indicates that the expression level of metastasis-regulating genes by metastatic cells can be induced by factors in the organ microenvironment Metastasis is the final stage in tumour progression from a normal cell to a fully malignant cell in some cases. The best-developed example is the characterisation of the molecular progression in colon cancer, in which specific changes (e.g. loss of tumour-suppressor genes and mutation of oncogenes)

are preferentially associated with specific changes of progression (Fearon and Vogelstein, 1990); (Kinzler and Vogelstein, 1996). However, the final stage in tumour progression to a metastatic phenotype remains to be elucidated at a molecular genetic level in colon and other cancers. Transfection with a variety of oncogenes (e.g. ras and src) has been shown to produce metastatic cells (Chambers and Tuck, 1993). For example, metastatic H-ras transfected NIH-3T3 cells had increased levels of a variety of gene products including proteinase and adhesive proteins (Tuck et al, 1991). Loss of tumour-suppressor gene function has also been implicated in the conversion to metastatic ability in specific tumour types, e.g. nm23 (Chambers et al, 1995), KAI1 (Dong et al, 1995), KiSS-1 (Lee et al, 1996), although none is likely to be universally implicated in all tumour types. It appears more likely that regulation of expression of genes that contribute functionally to metastasis can occur in a tissue-specific manner. The development of gene expression profiling may help to elucidate the genes that contribute to metastatic development in many cancer types.

1.3.1 The extracellular matrix and basement membrane

The extracellular matrix is a complex structure of carbohydrate- and protein-containing components that comprise the basement membrane underlying epithelial tissues and that surround structural tissues such as bone and muscle (Yurchenko et al, 2002). Almost all multicellular organisms have basement membranes. They are the first extracellular matrices that are produced during embryogenesis. Epithelial, endothelial and many mesenchymal cells are supported by this thin sheet-like ECM structure. The membrane acts as a solid regulator of cell attachment, differentiation and growth, as well as a passive barrier that segregates tissue compartments. Metastatic cancer cells have to penetrate the tumours own basement membrane, that of the vasculature and target tissue in order to establish secondary disease sites (Hood and Cheresh, 2002).

The basement membrane has a complex molecular architecture that consists of laminins, type IV collagen, entactin and heparan sulphate proteoglycans. Laminins are flexible four-armed, 850kDa glycoproteins. Laminin monomers polymerise into 3D structures in a time- and concentration- dependent manner. As an initial step in metastasis, many

epithelial tumours exhibit altered localisation or expression of laminin-binding integrins (e.g. $\alpha 6\beta 4$). This promotes invasion through the basement membrane and increases motility in the stroma, where tumour cells can remodel the matrix by depositing laminin (Hood and Cheresh, 2002). The most prevalent protein in the basement membrane is type IV collagen. Type IV collagen is a thread-like flexible molecule that can itself form a heterotrimer involving hydrophobic and disulphide bonds. The covalent binding of collagen provides mechanical stability to the basement membrane. Proteins such as entactin, which forms connections between networks of collagen and laminin, further stabilise the membrane. Many of the proteases with increased expression in metastatic tumours exhibit high enzymatic activity against type IV collagen. The basement membrane also contains heparan sulphate proteoglycans – a class of molecules that contain a protein core covalently linked to heparan sulphate chains. These molecules are linked to the membrane through interactions with laminin and may influence tumour biology by acting as a repository for growth factors including fibroblast growth factor.

1.4 Proteins involved in Invasion/Metastasis

1.4.1 Matrix Metalloproteinase (MMPs)

MMPs are synthesised and secreted in inactive zymogen form and depends on the presence of zinc and calcium ions. The production of active enzymes requires the proteolytic removal of the pro-domain. Over twenty MMP family members are known to exist (Polette et al, 2004). Most MMPs can cleave at least one component of the ECM. MMPs can also regulate cell growth, either directly through the release of growth factors or indirectly by changes in cell adhesion as described above. MMPs can degrade insulin-like growth factor (IGF) binding protein 3, which regulates the bioavailability and activity of IFG-II (Fowlkes et al, 1995). Powell et al, (1999) demonstrated that MMP-7 proteolytically generates active soluble Fas ligand and potentiates epithelial cell apoptosis. These different effects of MMPs and their inhibitors depend on the balance between them in the local microenvironment. MMPs are subdivided into collagenases, stromelysins, gelatinases and MT-MMPs based on their substrate preference. MMPs are physiologically expressed during various stages of development in processes requiring

cell migration, tissue remodelling, and wound healing, placentation or tumour progression. Many external stimuli can induce the expression of many MMPs.

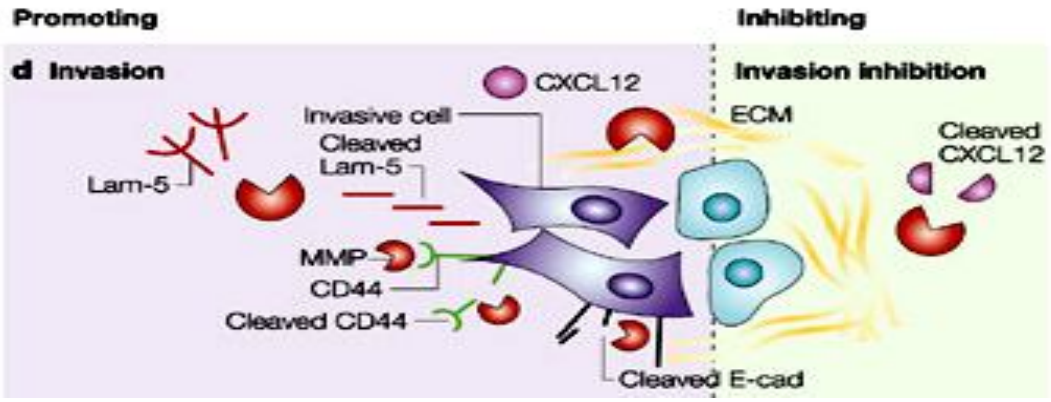

(Adopted from Nature Reviews Cancer 2, 161-174 (March 2002)

Figure 1.4.1A MMPs regulate invasion by degrading structural ECM components. Specifically, the MMPs promote invasion and migration by cleaving laminin 5 (Lam-5). MMPs also promote invasion by cleavage of the adhesion molecules CD44 and E-cadherin (E-cad). The released part of E-cad might then bind and inhibit the function of other uncleaved E-cad molecules. In addition, docking of MMP-9 to CD44 is required for cancer-cell invasion. MMPs might inhibit metastasis by cleavage of CXCL12, a chemokine of the CXC family that promotes breast cancer metastasis.

Plasmin has been described to proteolytically activate some latent MMPs (Mignatti and Rifkin, 1996) and the cooperation between MMPs and the plasminogen activator/ plasmin cascade have an important role in the regulation of tumour invasion *in vivo*. MMPs can auto activate in some cases and can also effect mutual activation. For example, MMP1 can activate latent MMP2 (Nagase et al, 1996). The proteolytic activity of MMPS is controlled by tissue inhibitors of MMPs (TIMPs), which specifically block activity of active MMPs by binding to the conserved zinc-binding site (Polette et al, 2004). Four TIMPs are currently known. According to Knauper et al, (1996) and Wang et al, (1997) studies it is revealed that TIMP-1 and –2 inhibit most MMP activity, while TIMP-2 and –3 inhibit MT1-MMP. TIMP-3 inhibits MMP-1, -2, -3, -7, -9 and –13. TIMP-4 inhibits MMP-2 and-7 It was originally thought that tumour cells were involved in the invasion process via secreted proteolytic enzymes. However, *in vivo* in situ hybridisation studies demonstrated that stromal cells were the source of MMPs. In 1990, Basset *et al*,

demonstrated that MMP11 was expressed specifically by fibroblasts in breast carcinomas and not by their benign counterparts. Thus, host cells have an important role in the production of MMPs and tumour invasion due to the cooperation of stromal and tumour cells. Extracellular matrix metalloproteinase inducer (EMMPRIN) is produced by tumour cells and can stimulate MMP-1 –2 and –3 by fibroblasts (Biswas et al, 1995). EMMPRIN mRNA is overexpressed in many carcinomas compared to benign and normal tissues, which suggests a role in invasion (Polette et al, 2004).

A complex interplay exists between cell adhesion molecule organisation and MMP expression that can also be involved in the development of an invasive phenotype by tumour cells. β-catenin is an intracellular attachment protein that can attach cytoplasmic actin bundles to cadherin transmembrane adhesion molecules at the site of cell-cell junctions. Since tumour cells detach from neighbouring cells in invasion abnormalities in the β-catenin/E- cadherin complex are likely to be involved (Curran and Murray, 2000). β-catenin and the DNA binding protein T Cell Factor 4/Transcription factor 4 (TCF4) also acts a transcriptional regulator of specific genes. Normally, the protein product of tumour suppressor gene adenomatous polyposis coli (APC) binds to cytoplasmic β-catenin and causes its degradation. In most colorectal cancers APC is mutated, so β-catenin accumulates and complexes with TCF which activates the transcription of target genes including cyclin D1 and c-myc. (Curran and Murray, 2000). Brabletz et al, (1999) report that MMP-7 is also a target of β-catenin/ TCF. Brooks et al, (1996) demonstrated that melanoma cells expressing integrin αvβ3 had the ability to bind active MMP-2 facilitating collagen degradation. Thus, a cell surface receptor known to be involved in directed cellular motility can also bind an enzyme that can degrade a major component of the basement membrane. Furthermore, the cell surface receptor determinant CD44 which is known to promote growth and metastasis of tumour cells, has been shown to associate with active MMP-9 at the cell surface of human melanoma cells (Yu and Stamenkovic, 2000). Disruption of MMP-9/CD44 aggregates decreases the invasiveness of tumour cells *in vivo*.

1.4.2 Cytokines

Cytokines also been shown to regulate MMPs. For example, interleukin –1 (IL-1) induces the transcription of MMP-1 and –3 (Borghaei et al, 1998). In a study by Bar-Eli, (1999) transfection of human melanoma cells with IL-8 increased the activity of MMP-2 and the invasiveness of the cells.

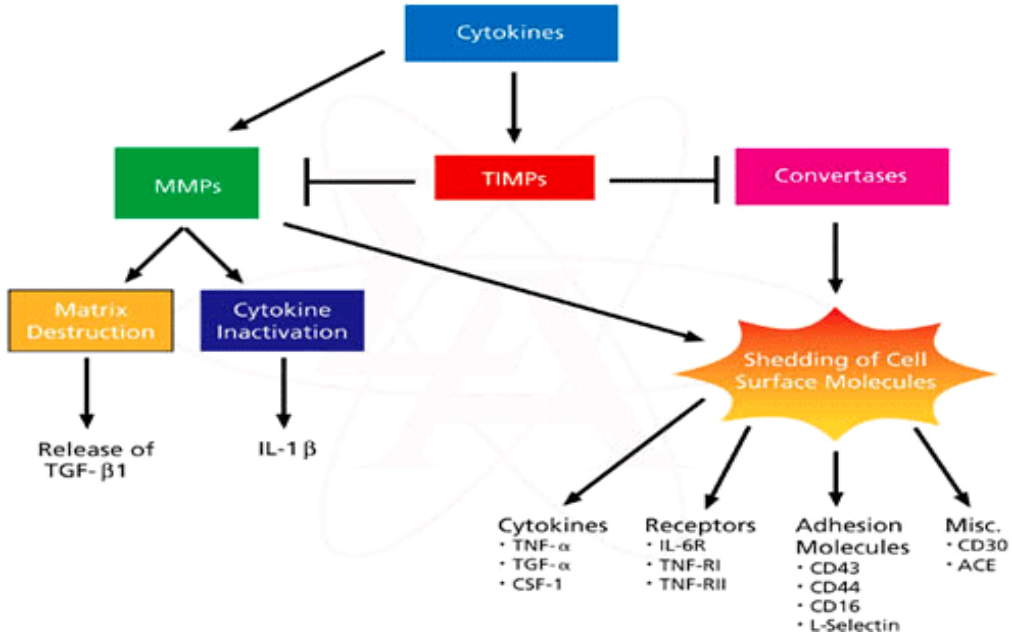

Figure1.4.2B Schematics Cytokines/MMPs connection (adoptedwww.sigmaaldrich.com)

MMPs can also regulate cell growth, either directly through the release of growth factors or indirectly by changes in cell adhesion as described above. MMPs can degrade insulin-like growth factor (IGF) binding protein 3, which regulates the bioavailability and activity of IFG-II (Fowlkes, 1994). Powell et al, (1999b) demonstrated that MMP-7 proteolytically generates active soluble Fas ligand and potentiates epithelial cell apoptosis. These different effects of MMPs and their inhibitors depend on the balance between them in the local microenvironment.

1.4.3 Cathepsin B

Increased cathepsin B expression, activity and changes in localisation have been observed in many different tumours including breast (Poole et al, 1978), colorectal (Campo et al, 1994) and lung (Sukoh et al, 1994). Koblinski et al, (2000) studies demonstrates that the increased expression of cathepsin B at the mRNA level is associated with gene amplification, increased transcription, the possible use of multiple promoters and alternatively spliced transcripts. Changes in the localisation of cathepsin B seem to precede the increase in protein levels, which suggests that alterations in trafficking of cathepsin B are independent of increased expression.

Proteases can interact leading to the activation of proteolytic cascades that can degrade ECM components. For example, Procathepsin B can be activated by cathepsin D, tPA, uPA, cathepsin G and elastases. Active cathepsin B in turn activates pro-uPA, which converts plasminogen to plasmin, which can degrade several ECM components and activate MMP-1, -3, -9, -12 and –13. The MMPs can then degrade other ECM components e.g. collagen -I and -IV, gelatins and activate further MMPs (Koblinski *et al*, 2000). Cathepsin B can activate MMPs indirectly via the plasminogen activator cascade and directly activate MMP-1 and –3. Thus, cathepsin B may be an important regulator of the activation of pro-uPA/ plasminogen and pro-MMPs.

Both direct and indirect interactions between tumour and stromal cells can increase the expression of proteases. For example the expression of gelatinases A and B are increased in fibroblasts upon contact with tumour cells. These fibroblasts then partake in further degradation of the ECM. Expression of cathepsin B and D can also be regulated by diffusible factors such as basic fibroblast growth factor (bFGF), insulin growth factor-1 (IGF-1) and epidermal growth factor (EGF). Paracrine factors secreted from tumour and stromal cells can thus regulate the expression of proteases (Koblinski *et al*, 2000).

1.4.4 Urokinase-type plasminogen activator

Urokinase-type plasminogen activator (uPA) is a serine protease that is involved in the progression of cancer particularly in invasion and metastasis. Many studies of breast cancer patients whose primary cancers have high uPA levels have significantly poorer outcome than those with low uPA levels. Paradoxically, high levels of plasminogen activator inhibitor-1 (PAI-1) a uPA inhibitor, is also predictive of poorer patient outcome (Duffy, 2002). The human uPA gene encodes a 53kDa protein that is initially synthesised as a catalytically inactive single chain peptide. Conversion to active form is brought about by a number of proteases including plasmin, cathepsin-B and –L. uPA is a multifunctional protein involved in both proteolysis and signal transduction. As a protease uPA catalyses the conversion of plasminogen to active plasmin. Plasmin can then promote the degradation of ECM substrates that include fibrin, fibronectin and laminin. It can also activate MMPs and activate or release specific growth factors such as FGF-2 and TGF-β. uPA-catalysed proteolysis occurs in vivo while the protease is attached to a membrane anchored protein receptor, uPAR (Andreasen et al, 1997).

Binding of uPA to its receptor enhances proteolysis and also results in signal transduction, including activation of mitogen-activated protein kinase (MAPK), extracellular signal-regulated kinases 1 and 2 and other signalling pathways that activate Fos and Jun (Ossowski and Aguirre-Ghiso, 2000). uPA activity can be neutralised *in vivo* by two inhibitors called as plasminogen activator inhibitors 1 and 2 (PAI-1 and PAI-2), which belong to the serpin family of protease inhibitors and inhibit apoptosis. PAI-1 can also modulate adhesion and migration independently of its role as a protease inhibitor (Duffy, 2002).

Andreasen *et al*, (1997) studies demonstrates a positive correlation between uPA levels and metastasis which have been found in both cell lines and animal tumours. Transfecting cell lines with uPA cDNA enhance the metastasis of the transfected cells. Inhibition of uPA activity or expression reduced metastasis in model systems. Blocking uPA:uPAR binding also decreases metastasis in systems studied. Tumours in uPA null mice exhibit less progression than those in mice expressing uPA. Since metastasis is the main cause of

death in cancer patients, and since uPA is an important mediator of this process, uPA is an ideal candidate for use as a marker to predict the likely formation of metastasis. Indeed, as a predictor of outcome for breast cancer patients, uPA acts as a potent biological marker. High levels of uPA are also correlated with poorer patient outcome in patients with stomach, colorectal, bladder, ovary, endometrium and brain cancers (Duffy, 2002b) (Wohn, 1997).

High levels of PAI-1 are also associated with aggressive disease and poorer patient outcome. Although the reason for this is not clear, there are many possible explanations. For example, a critical PAI-1 concentration may be needed to prevent excessive ECM degradation by uPA during cancer invasion, where excessive ECM degradation could leave insufficient substrate on which cancer cells could migrate. PAI-1 is also needed for angiogenesis to occur and can modulate both cell adhesion and migration and thus metastasis and can inhibit apoptosis; hence increased PAI-1 expression is a poor prognostic factor (Duffy, 2002; Duffy, 2002b). Both uPA and PAI-1 are possible targets for cancer therapeutics, specifically with applications in the prevention of metastases.

1.4.5 Integrins and cancer

Invasive cells undergo changes in integrin expression levels and integrin affinity for ECM substrates. Many studies have reported significant differences in the surface expression and distribution of integrins in malignant tumours when compared with pre-neoplastic tumours of the same type. For example, $\alpha 5\beta 3$ integrin is strongly expressed at the invasive front of melanoma cells and angiogenic blood vessels, but weakly expressed on pre-neoplastic melanomas and blood vessels (Brooks *et al*, 1994). While the expression of some integrins is increased during tumuorigenesis, the expression of others decreases. Cells can also assume a more migratory and invasive phenotype by altering their adhesive and signalling profile by increasing the affinity of integrins for their ligand (Hood and Cheresh, 2002).

The integrins, composed of α and β chain heterocomplexes, act as integral cell membrane receptors that form focal adhesion contacts with ECM ligands e.g. fibronectin, laminin, entactin, intercellular adhesion molecule (ICAM) and the collagens to name but a few.

Integrins also interact with cytoplasmic cytoskeletal filament-associated proteins e.g. actin, paxillin and talin. The family can form at least 25 distinct pairings of its 18 α and 8 β subunits, with each integrin consisting of a noncovalently linked α- and β-subunit. Each subunit has a large extracellular domain, a single membrane-spanning domain and a short, non-catalytic cytoplasmic tail (Mizejewski, 1999). In addition to regulating cell adhesion to the ECM, integrins relay molecular cues regarding the cellular environment that influence cell shape, proliferation, survival, migration and gene transcription.

Derangement of integrin expression may be responsible for many aberrant cellular activities during tumour onset, progression and metastasis. As integrins form connections with the extracellular environment, they provide structural support. They also mediate intracellular signalling through the activation of focal adhesion kinase (Guo and Giancotti, 2004). It is not surprising that the native ECM of a normal cell is a requisite for survival. Indeed, removal of a cell from its supportive matrix can cause that cell to die, also called "anoikis" (Frisch and Ruoslahti, 1997) Recent work has demonstrated that expression of TrkB protein, a neurotrophic receptor, enables a cell to survive, avoiding anoikis, when it has been removed from its native matrix (Douma et al, 2004). This protein enables the tumor cell to retool its signaling machinery, stimulating the phosphatidylionolistol-3-OH and AKT/PKB kinases, leading to inhibition of caspases, key mediators of anoikis.

In highly motile cells, initiation of migration is characterised by the reorganisation of actin to the cell edge, the protrusion of a leading lamellipodium and membrane ruffling at the advancing front of the lamellipodium. The RHO family of small GTPases can regulate these changes. Family members include RHO, CDC42 and RAC. RHO activation is dependent on integrins; syndecan-6 and other cell surface receptors, whereas RAC and CDC42 are activated by ligation of integrins (Ren et al, 1999). Activation of RHO leads to the formation of actin stress fibres and the assembly of focal adhesions. Activation of CDC42 is involved in the formation of filopodia and activation of RAC leads to membrane ruffling and cell migration (Hood and Cheresh, 2002). The expression of active RAC and CDC42 can depolarise differentiated mammary epithelial cells and induce integrin-mediated invasion through a 3D collagen matrix (Cotter et al, 1997).

During cell migration, the formation of new integrin contacts provides the cell with molecular signals that activate ERK signalling. Integrins regulate ERK activity through several FAK-dependent and independent pathways and also by modulating growth factor-stimulated ERK activity. ERK activation influences gene transcription cell survival and cell motility (Hood and Cheresh, 2002). During cell migration, the ERK signal decreases integrin-mediated adhesion and phosphorylates myosin-light-chain kinase (MLCK), which regulates the contractile force within the cell. Klemke et al, (1997) studies show that MLCK phosphorylates and activates myosin II, an ATPase found in leading lamellae and posterior regions of motile cells that generate force by promoting translational movement along actin cables. Activated myosin then generates contractile forces that pull the cell forward towards the new integrin contacts and breaks the contacts at the trailing edge of the cell. Phosphatidylinositol 3-kinase (PI3K) regulates integrin dependent cell movement by modulating integrin responses in normal and neoplastic tissue. PI3K activity is needed for CDC42 and RAC-induced cell motility and invasiveness in mammary epithelial cells (Cotter et al, 1997).

The Protein Kinase C (PKC) family of serine/threonine kinases are important in regulating integrin function and signalling. For instance, ligation of fibronectin by integrins and syndecan-4 recruits PKC to membrane adhesions where it is required for focal adhesion formation, phosphorylation of FAK, cell spreading, migration and SHC-dependent ERK activation (Hood and Cheresh, 2002).

1.5 Proteins with relevance to in vitro cancer cell invasion

Previously in the lab to study the molecular nature of invasion, the gene-expression profiles of five lung cancer cell lines (DLKP) with differing levels of invasiveness (as determined by an *in vitro* invasion assay) were analysed using expression microarray methodology. A panel of lung cancer cell lines with various levels of invasiveness, two invasive, non-drug exposed, variants of the DLKP cell line were used in the study along with a non-invasive Vincristine-selected (VCR) cell line, an invasive Taxotere (TXT) resistant variant and a non-invasive TXT- selected cell line that had lost its resistance to TXT. Differential regulated gene lists were generated from the array data containing genes that may potentially serve as transcriptional signatures for invasiveness and/or drug resistance in these cell lines. These were IGF-1R, KCNJ8, S100A13, SFN, TFPI2 and

GLP1R. Among them we selected four gene targets which were differentially upregulated across drug variant invasive cell lines.

1.5.1 Glucagon like Peptide 1 Receptor (GLP1R)

The glucagon-like peptide 1 receptor **(GLP1R)** is found on chromosome 6 (Thorens, 1992) (Dillon et al, 1993). The protein encoded by this gene is a member of the glucagon receptor family of G protein-coupled receptors (Brubaker and Drucker, 2002). GLP1R binds specifically the glucagon-like peptide-1 (GLP1) and has much lower affinity for related peptides such as the gastric inhibitory polypeptide and glucagon (Fehmann et al, 1994). GLP1R is known to be expressed in pancreatic beta cells. Activated GLP1R stimulates the adenylyl cyclase pathway which results in increased insulin synthesis and release of insulin (Drucker et al, 1987), Consequently GLP1R has been suggested as a potential target for the treatment of diabetes (Newcomb et al, 2004). GLP1R is also expressed in the brain where it is involved in the control of appetite (Kinzig et al, 2002). Studies suggest that mice which over express GLP1R display improved memory and learning (During et al, 2003).

1.5.2 Inwardly rectifying potassium channel J8 (KCNJ8)

(Inagaki et al, 1995) identified a K_{ATP} channel, uK_{ATP}-1 (KCNJ8/Kir6.1), which represented a new subfamily of the inwardly rectifying K^+ channel family. KCNJ8 is of particular interest as its role in cancer and invasion has not been previously reported in the literature. K^+ channels are a diverse class of ion channels in the cytoplasmic membrane. Ion channels are pores in the cell membrane that allow the passage of specific ions. They are opened and closed by changes in membrane potential, ligand binding, intracellular calcium concentration and membrane tension (Laniado et al, 2001). There is accumulating evidence that various K^+ channels in tumour cells play important roles in regulating tumour cell proliferation and apoptosis. There is also increasing interest in the potential implications of K^+ channels as pharmacological targets for cancer therapy and for use as biomarkers to aid diagnosis (Wang, 2004). The potassium channels termed “inward rectifiers” of which KCNJ8 is included pass currents over a hyperpolarized voltage range. They have an important role in the maintenance of resting membrane

potential in many cell types. The gating of some inward rectifiers (including KCNJ8) is tightly regulated by intracellular ATP levels, thereby providing a link between cellular metabolism and membrane potential.

1.5.3 Tissue Factor Pathway Inhibitor 2 (TFPI2)

Human TFPI2 is a 32kDa serine protease inhibitor that is associated with the ECM. It has high homology to TFPI1, a regulator of the extrinsic blood coagulation pathway (Miyagi et al, 1994). TFPI2 inhibits the tissue factor VIIa complex and many serine proteases including trypsin and plasmin. However, it does not inhibit uPA and tPA (Petersen et al, 1996). Many studies have demonstrated the down regulation of TFPI2 in the development of an invasive phenotype in cancer. For example, (Wojtukiewicz et al, 2003) used immunohistochemical procedures to examine TFPI2 expression in neoplastic cells of laryngeal, breast, gastric, colon, pancreatic, renal, endometrial cancer and in glial neoplasms. A higher staining intensity was observed in more differentiated tumours. This group also observed that TFPI2 expression decreased with increased malignancy. In a gene expression profile study of invasive cervical carcinomas versus normal cervical keratinocytes, TFPI2 expression was lower in the invasive carcinomas (Santin et al, 2005)

1.5.4 S100 calcium binding protein A13 (S100A13)

S100 proteins are small EF hand Ca^{2+} binding proteins of variable length and sequence. There are a number of functions associated with S100 proteins, many associated with tumour development. Wicki et al, (1996) identified a new S100 member termed S100A13 by screening expresses sequence tags (EST) databases. The C-terminus of S100A13 protein ends with the motif RKK, which is also seen in the metastasis-associated protein S100A4 and S100A10 (Kim and Helfman, 2003). The results described in Section 3.6 describe a novel function for S100A13 in the modulation of an invasive phenotype. S100A13 has been demonstrated to be overexpressed in brain tumours in concert with FGF-1 (Landriscina et al, 2001) and has been proven to be essential in the regulation and release of pro-angiogenic molecules FGF-1 and IL-1α in a copper dependent manner (Mandinova et al, 2003). Smirnov et al, (2005) identified S100A13 as a novel predictor of metastasis following its detection in circulating tumour cells in blood.

1.6 DNA Recombination

Recombination is an important phenomenon in genetic exchange. In living systems, recombination also plays an important role in the repair of mutations. Crossing over allows for a greater number of gene combinations than independent assortment. Gene conversion as a result of mismatch repair and recombination further increases the amount of change possible in the genome.

1.6.1 Homologous recombination

Homologous recombination is the exchange (“crossing over”) or replacement (“gene conversion”) of a DNA region by its homologous DNA sequence from the homologous chromosome or the sister chromatid (Fig. 1.12). Homologous recombination also occasionally occurs between similar DNA sequences on nonhomologous chromosomes or within a chromosome. A single gene conversion event changes one of the pair of homologous sequences without changing any other parts of the genome.

1.6.2 How it works

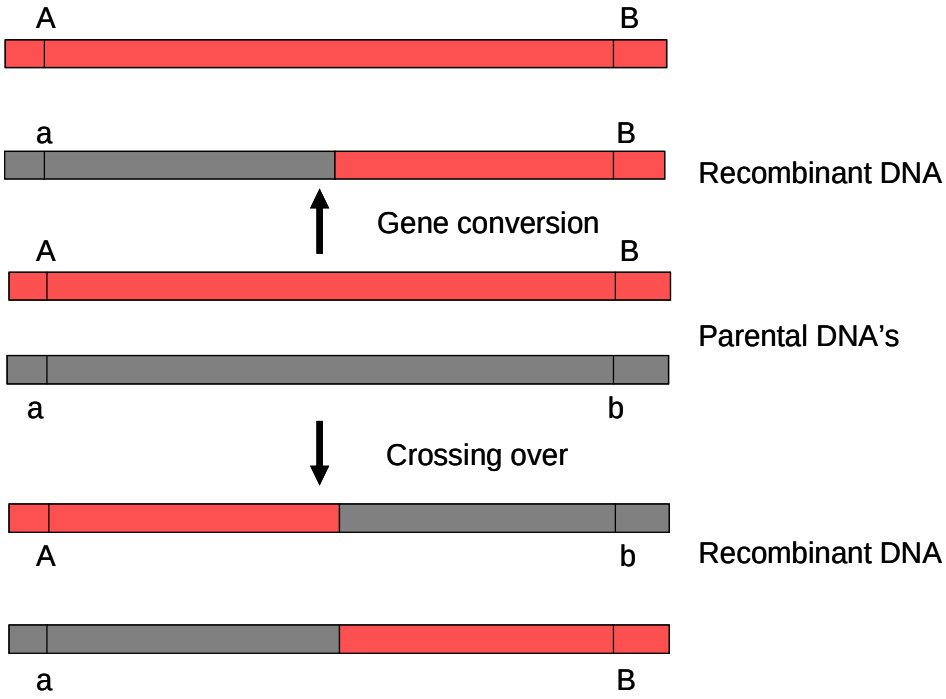

Figure 1.6.2A Schematics representing homologous recombination, involving gene conversion and/or crossover.

1.6.3 Holiday Model

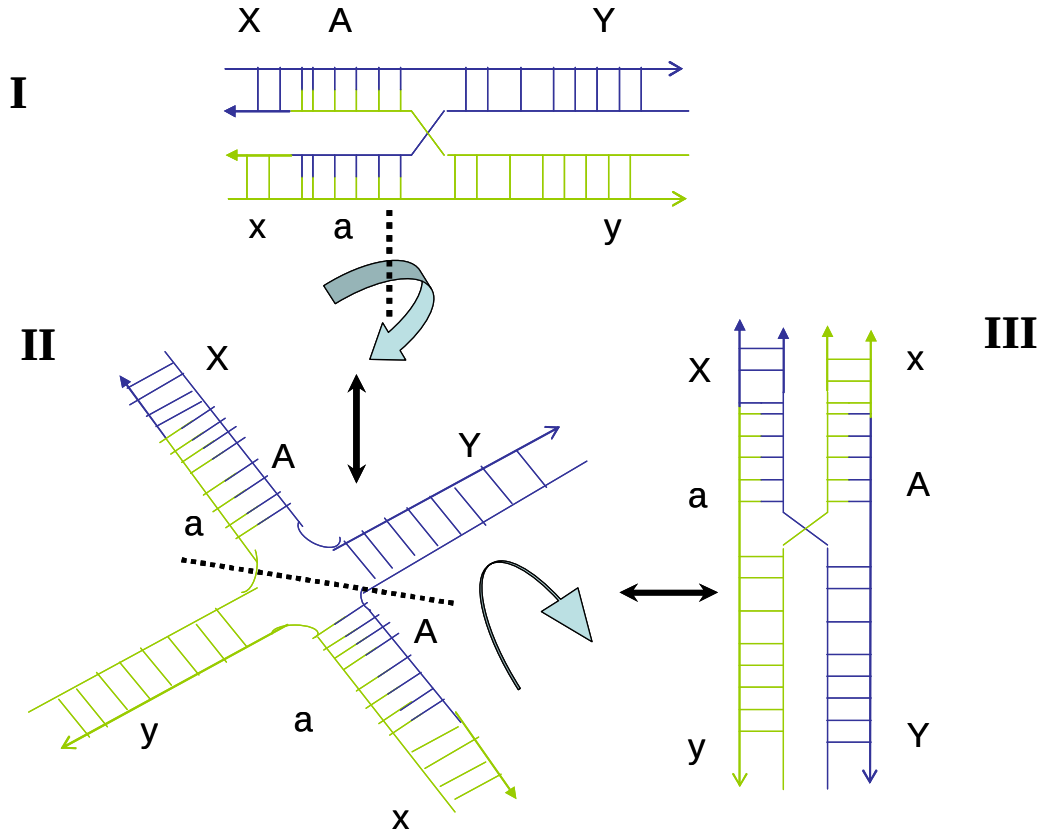

Figure 1.6.3A The Holliday model of DNA crossover. I) Two homologous DNA molecules line up (e.g., two nonsister chromatids line up during meiosis). Cuts in one strand of both DNAs. The cut strands cross and join homologous strands, forming the *Holliday structure* (or *Holliday junction*). II) Heteroduplex region is formed by *branch migration*, Resolution of the Holliday structure. The vertical cut will result in crossover between f-f' and F-F' regions. The Heteroduplex region will eventually be corrected by mismatch repair. III) A different view of the Holliday junction, DNA strands may be cut along either the vertical line or horizontal line.

Heteroduplex formation by the RecA/Rad51 family proteins involves homologous pairing and strand exchange. Homologous pairing is the formation of core heteroduplex joints by searching for homology between double-stranded DNA and single-stranded DNA, and strand exchange is the extension of the region of the heteroduplex. Although the ATP-binding motifs of proteins of this family are conserved, some human Rad51 paralogues have been shown to promote *in vitro* homologous pairing in an ATP-independent manner (Kurumizaka et al, 2001). Furthermore the human Rad52 protein which has no homology to Rad51 and is required for various homologous recombinations, promotes an ATP-independent homologous pairing (Kagawa et al, 2001).

In bacteria, the ATP-independent homologous pairing proteins were identified as RecT (Noirot and Kolodner, 1998) and RecO (Luisi-DeLuca, 1995) and it was shown that the RecT-dependent homologous recombination of plasmid DNA in bacteria does not require RecA. *E. coli* phage lambda also has its own recombination machinery that functions independently of the RecA/Rad51 family proteins. Thus it can be postulated that homologous recombination in small genomes does not require ATP-dependent homologous pairing proteins such as RecA. Although the ATP-hydrolysis-dependent reaction of RecA stabilizes heteroduplexes through strand exchange when the homologous region is sufficiently large, the same reaction results in the dissociation of previously formed heteroduplexes if the homologous region is small (Shibata et al, 1982). This suggests that the ATP-dependent reaction prevents heteroduplex formation between nonallelic sequences. This corrective system may not be required for the recombination of small genomes such as those of viruses and plasmids, or may be harmful to such recombination that uses a small homologous region in eukaryotes. This knowledge about the natural processes by which genetic information evolves will enable us to develop new technology for breeding useful agricultural or industrial organisms and gene therapy.

1.6.4 Homologous Recombination as a Genetic Tool

Homologous recombination is a reciprocal exchange of DNA sequences, as in between two chromosomes that carry the same genetic loci (Lewin et al, 2004). This process is conserved throughout evolution and was demonstrated in bacteria more than 50 years ago by the 1958 Nobel Laureate **Joshua Lederberg**. The modification of an endogenous gene into a designed sequence by homologous recombination, termed gene targeting, has broad implications for basic and applied research (Terada et al, 2007). **Mario R. Capecchi** (Capecchi, 1989) **Sir Martin J. Evans** (Evans et al, 1997) and **Oliver Smithies** (Smithies et al, 1984) had the vision that homologous recombination could be used to specifically modify genes in mammalian cells and they worked consistently towards this goal. In 2007 they were awarded the prestigious Nobel Prize for their contribution in field of Medicine in particular **"for their discoveries of principles for introducing specific gene modifications in mice by the use of embryonic stem cells".** Homologous recombination has significantly contributed to genome engineering, because it is the basis of homologous gene targeting. For example, a deficient gene can be replaced with a functional copy in situ, without any modification elsewhere in the genome.

1.7 Gene Targeting

Many genes that participate in interesting canonical pathways are essential for key cellular phenotypes. Because gene targeting can be controlled both spatially and temporally, the function of a given gene can be studied in the desired cell types and at a specific time point. Non targeted random insertion of foreign gene into the genome invariably leads to large discrepancies in target expression, genomic instability, unpredictable phenotypes, which in turn complicates and prolongs the screening process for sub clones suitable for experimentation. Conditional gene modification using **Cre-lox and Flp-Frt** technology allows the gene of interest to be knocked-out in only a subset of tissues or only at a particular time circumventing lethality. These genetic dissections facilitate researchers to evaluate gene function in development, physiology or behaviour.

1.7.1 FLP-FRT recombinase system

The FLP-FRT recombinase system of yeast can be used to mobilize FRT-flanked donor DNA and generate re-integration at a different chromosomal location (Golic et al, 1997). The donor DNA is introduced into the recipient chromosome flanked by repeats of the FRT recombinase recognition site. The FLP recombinase is introduced under control of a promoter, the action of FLP recombinase results in excision of the donor DNA followed by a second round of recombination at a target site where another FRT site is present. The phenomenon can be observed by having the target FRT site at the locus of a known gene where an altered phenotype is detectable. This method is limited by the requirement of a target FRT site near a known gene.

1.7.2 Cre-LoxP technology

Cre-Lox recombination is a special type of site-specific recombination which was patented in the 1980s by DuPont. Although Prof. Brian Sauer is credited with the discovery of this system, many workers from diverse fields have found useful applications of this recombination system including gene knockout technology and the development of Bacteriophage P1 based vectors - PACs (P1 derived Artificial Chromosomes). Cre-LoxP recombination involves the targeting of a specific sequence of DNA and splicing it with the help of an enzyme called Cre recombinase. Using this technology, specific tissue types or cells of organisms can be genetically modified; whilst other tissue remains unchanged. The Cre gene encodes a site specific DNA recombinase which can recombine DNA when it locates specific sites in the DNA sequence. These sites are known as LoxP (locus of X-over P1) sequences, which are 34 base pairs long, exists an asymmetric 8 bp sequence in between with two sets of palindromic, 13 bp sequences flanking it.

.

13bp **8bp** **13bp**

ATAACTTCGTATA - GCATACAT –TATACGAAGTTAT **LoxP sequence**

Direct Repeats
(Gene deletion)

Inverted Repeats
(Gene inversion)

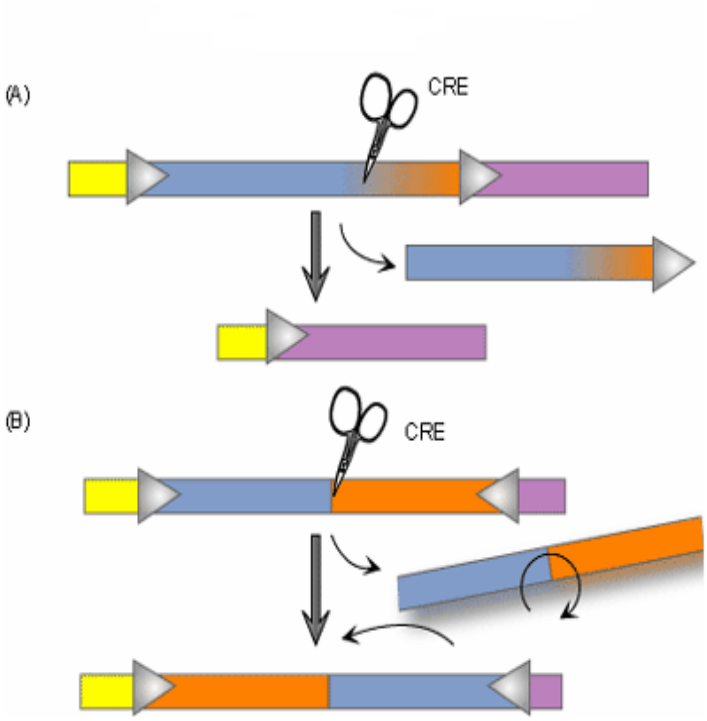

www.scq.ubc.ca/wp-content/creLoxP.gif

Figure 1.7.2A Cre-LoxP systems. The loxP site can be inserted on either side of a piece of DNA. If Cre recombinase is then expressed in the cell containing the LoxP sites insertion in the genome A) the loxP sites will be cut and joined together, removing the piece of DNA between the two sites if they are direct repeats. (B) Two loxP sites which are inserted on either side of a piece of DNA in opposite directions are cut and the piece of DNA inverted and reattached.

1.7.3 Vectors

In molecular biology, a **vector** is any vehicle used to transfer foreign genetic material into another cell. The vector itself is generally a DNA sequence that consists of an insert (transgene) and a larger sequence that serves of the "backbone" of the vector. Expression vectors specifically are for the expression of the transgene in the target cell, and generally have a promoter sequence that drives expression of the transgene. Replication vectors can be replicated in a target cell but not expressed, unlike expression vectors. Transcription vectors are used to amplify their insert. Insertion of a vector into the target cell is generally called transfection, although insertion of a viral vector is often called transduction. Two common vectors are plasmids and viral vectors.

The term *plasmid* was first introduced by the American molecular biologist Lederberg, (1998). A **plasmid** is an extra chromosomal DNA molecule separate from the chromosomal DNA and capable of sexual replication. In many cases, it is typically circular and double-stranded. It usually occurs naturally in bacteria, and is sometimes found in eukaryotic organisms (e.g., the *2-micrometre-ring* in *Saccharomyces cerevisiae*). Plasmid size varies from 1 to over 200 kilo base pairs (Russell and Klaenhammer, 2001). The number of identical plasmids within a single cell can be zero, one, or even thousands under some circumstances. Plasmids can be considered to be part of the mobilome, since they are often associated with conjugation, a mechanism of horizontal gene transfer.

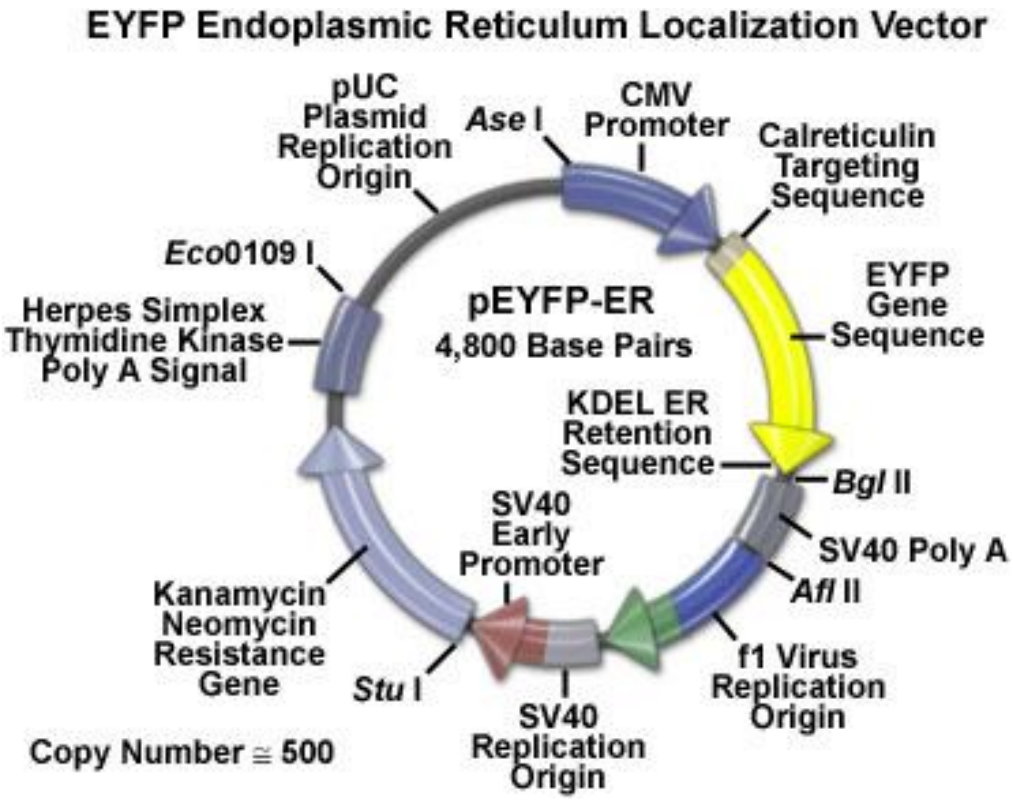

Figure 1.7.3A Plasmid vector (www.microscopyu.com)

Plasmids can be considered to be independent life-forms similar to viruses, since both are capable of autonomous replication in suitable (host) environments. However the plasmid-host relationship tends to be more symbiotic than parasitic (although this can also occur for viruses, for example with Endoviruses), since plasmids can endow their hosts with useful packages of DNA to assist mutual survival in times of severe stress. For example, plasmids can convey antibiotic resistance to host bacteria, who may then survive along with their life-saving guests who are carried along into future host generations.

Plasmid vectors minimalistically consist of an origin of replication that allows for semi-independent replication of the plasmid in the host and also the transgene insert. Modern plasmids generally have many more features, notably including a "multiple cloning site" which includes nucleotide overhangs for insertion of an insert, and multiple restriction enzyme consensus sites to either side of the insert. In the case of plasmids utilized as transcription vectors, incubating bacteria with plasmids generates hundreds or thousands of copies of the vector within the bacteria in hours, and the vectors can be extracted from the bacteria, and the multiple cloning site can be restricted by restriction enzymes to excise the hundredfold or thousand fold amplified insert. These plasmid transcription vectors characteristically lack crucial sequences that code for polyadenylation sequences

and translation termination sequences in translated mRNAs, making expression of transcription vectors impossible.

1.7.4 Insulators

In recent years the concept of domain boundaries or insulator elements has developed, based on the genetic properties of several eukaryotic genes. These elements serve to isolate chromosomal regions, confining regulatory effects of enhancers to the genes they are meant to serve. The need for them arises where two adjacent genes on a chromosome have very different transcription patterns, and it is critical that the inducing or repressing mechanisms of one do not interfere with the neighbouring gene (Burgess-Beusse et al, 2002). The chicken ß-globin insulator can inhibit activation of the gamma-globin gene promoter by the ß-globin locus control region. The Drosophila gypsy insulator functions similarly, conferring position-independent transcription to genes and preventing activation of promoters by enhancers separated from proximal promoters by insulator elements (Gdula et al, 1996).

1.7.4.1 Transcriptional regulator model

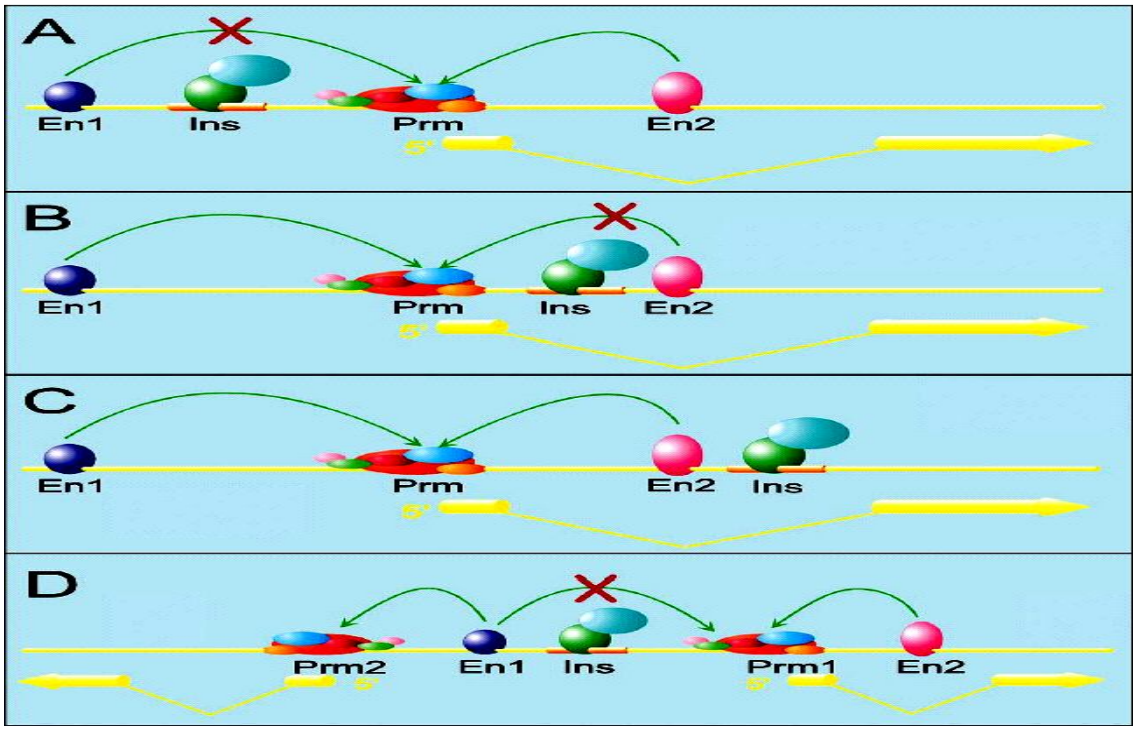

Annu. Rev. Genet. 2001.35:193-208.

Figure 1.7.4.1A Polar effect of an insulator on enhancer-promoter interactions.
The DNA and a hypothetical gene with two exons and one intron are shown in *yellow.* En1 and En2 represent two different enhancers and their associated transcription factors bound to nucleosomal DNA. Prm is the promoter of the gene where the different components of the transcription complex are present. Ins is an insulator element with its associated proteins. Solid arrows indicate a positive activation of transcription by the enhancer element; an X on the arrows indicates the inability of the enhancer to activate transcription. (*A*) An insulator (Ins), with two associated proteins, located in the 50 regions of the gene inhibits its transcriptional activation by an upstream enhancer (En1) without affecting the function of a second enhancer (En2) located in the intron of the gene. (*B*) When the insulator is located in the intron, expression from the downstream enhancer (En2) is blocked, whereas the upstream enhancer (En1) is active. (*C*) When the insulator is located in the intron but distal to the En2 enhancer, both enhancers are active and transcription of the gene is normal. This property distinguishes an insulator from a typical silencer. (*D*) If a second gene is located upstream of the En1 enhancer, although

this enhancer cannot act on the Prm1 promoter, it is still functional and able to activate transcription from the upstream Prm2 promoter.

1.7.4.2 Insulators as buffering agent during repressive action from neighbouring gene

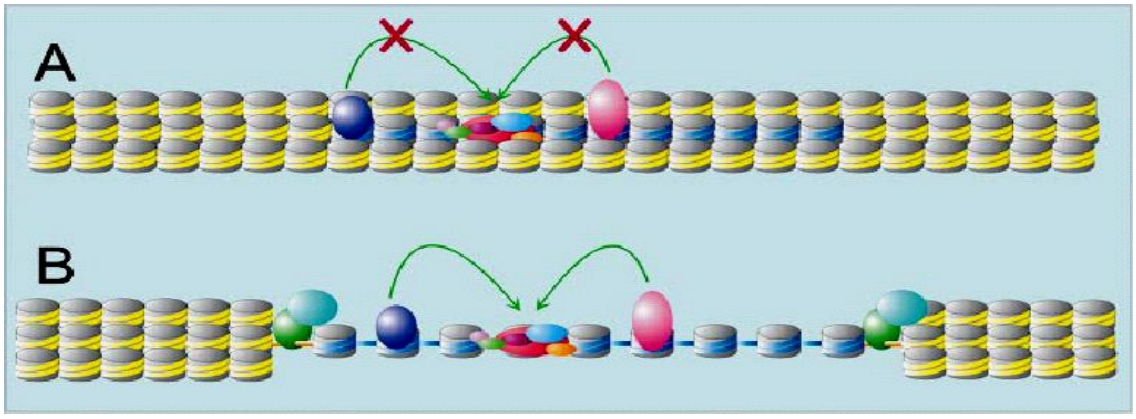

Annu. Rev. Genet. 2001.35:193-208.

Figure 1.7.4.2A Insulator elements buffer gene expression from repressive effects of adjacent chromatin. Symbols are as in Figure 1. (*A*) A transgene (represented by the *blue* DNA) integrated in the chromosome in a region of condensed chromatin is not properly expressed; the repressive chromatin structure of the surrounding region presumably spreads into transgene sequences, inhibiting enhancer-promoter interactions. (*B*) If the transgene is flanked by insulator elements (in *brown*), these sequences inhibit the spreading of the repressive chromatin, allowing an open chromatin conformation and normal transcription of the gene.

A study devised by Cai and Shen (2001) reveals a specialized chromatin structures (scs and scs') outside the coding sequence of the Drosophila *hsp70* gene. These sequences are associated with chromatin structures and serve as boundaries that can prevent activation by enhancer elements. Insulators or chromatin boundaries are frequently found in multiple copies, flanking enhancers or the genetic locus they regulate, such as the scs and scs' elements, the Mcp-1 and Fab boundaries, and the chicken ß-globin 5' and 3' boundaries. Selective interactions between neighbouring insulators may regulate the access of tissue-specific enhancers to target promoters by forming alternative chromatin loop domains. It is conceivable that these domains not only block inappropriate enhancers

but also facilitate interaction between distant enhancers and the target promoter. The best characterised system is the gypsy chromatin insulator of Drosophila. Gypsy is an infectious retrovirus consisting of two long terminal repeat regions that function in viral replication and integration and three retroviral genes: *gag*, *pol* and *env*, coding for nucleocapsid, reverse transcriptase and envelope proteins respectively (Song et al, 1994). The gypsy insulator is located in the 5' transcribed untranslated region of the gypsy element. The unlinked gene, *suppressor of Hairy-wing* plays an essential role in functioning of the gypsy insulator. SU (HW) binds to the insulator element, interacting directly with an octamer motif present in the gypsy insulator. SU (HW) binds to approximately 200 other sites on Drosophila polytene chromosomes, possibly corresponding to endogenous insulators that play a role in the organization of the genome into higher order chromatin domains that allow for the normal regulation of gene expression.

1.8 Micro RNA's

MicroRNAs (miRNAs) are small, non coding RNA molecules encoded in the eukaryotic genome which regulate gene expression at the translational level. They were first described in 1993 by Lee and colleagues in the Victor Ambros lab, yet the term *microRNA* was only introduced in 2001 in a set of three articles in Science (Ruvkun, 2001). These highly conserved, ~21-mer RNAs regulate the expression of genes by binding to the 3'-untranslated regions (3'-UTR) of specific mRNAs. MiRNAs are encoded by genes that are transcribed from DNA but not translated into protein (non-coding RNA); instead they are processed from primary transcripts known as *pri-miRNA* to short stem-loop structures called *pre-miRNA* and finally to functional miRNA. Mature miRNA molecules are partially complementary to one or more messenger RNA (mRNA) molecules, and their main function is to down regulate gene expression. This effect was first described for the worm *C. elegans* in 1993 by Victor Ambros and co-workers (Lee et al, 1993). MiRNAs have been confirmed in various plants and animals, including *C. elegans*, human and the plant *Arabidopsis thaliana*. Genes have been found in bacteria that are similar in the sense that they control mRNA abundance or translation by binding an mRNA by base pairing, however they are not generally considered to be miRNAs

because the Dicer enzyme is not involved. In plants, similar RNA species termed short-interfering RNAs *siRNAs* are used to prevent the transcription of viral RNA. While this siRNA is double-stranded, the mechanism seems to be closely related to that of miRNA, especially taking the hairpin structures into account. The siRNAs are also used to regulate cellular genes, as miRNAs do.

Approximately 3% of genome encodes for miRNAs and roughly around 30% of human protein coding genes are regulated by miRNAs (Barbarotto et al, 2008). The miRNAs can have pleiotropic effects on cell proliferation, apoptosis, and cell differentiation. They are generally believed to act by binding to imperfectly complementary sequences in the 3' untranslated region of target genes, resulting in decreased translation or in the degradation of the target transcript in cells as a result leading to tumourous tissue formation, referred to as **Oncomir** (Bagga, 2005). Pairs of oncogenes and the corresponding miRNAs that attenuate their expression have been recently identified. These miRNAs, or **"anti-oncomirs,"** can act as natural inhibitors of oncogene function, indicating the possibility that they might be developed as novel therapeutics (Goga, 2007). Examples of oncogene–anti-oncomir pairs include: *RAS*–let-7a; Regulation of *RAS* expression by let-7a is noteworthy because this oncogene–miRNA pairing has been conserved from *C. elegans* to humans, implying that oncogene–anti-oncomir pairs have co-evolved to regulate developmental programs (Johnson, 2005). *BCL2*–mir-15 and *BCL2*–mir-16 (Cimmino, 2005). *ERBB2*/*ERBB3*–mir-125a/b; mir-125a and mir-125b can co-ordinately regulate *ERBB2* and *ERBB3*, representing the first example of a single miRNA targeting two molecules in the same signalling cascade (Scott, 2007).

The mir-17-92b cluster functions as both an oncomir and anti-oncomir. In addition to its ability to cooperate with *MYC*, mir-17-92b can negatively regulate the expression of E2F, a transcription factor required for cell-cycle progression (O'Donnell, 2005). Finally, although no specific miRNA has yet been identified that directly targets *MYC* oncogene expression, *MYC* is likely a target of regulation by anti-oncomirs because loss of Dicer enzyme results in increased *MYC* expression (Kumar, 2007). Recent studies showed that the levels of the mir 17-92 cluster increased in lymphoma samples (He et al, 2005b). Also, the acceleration of tumor development was found to be increased in mice when c-Myc expression was acting simultaneously with mir-17-92 cluster expression.

1.8.1 MicroRNAs processing and gene regulation

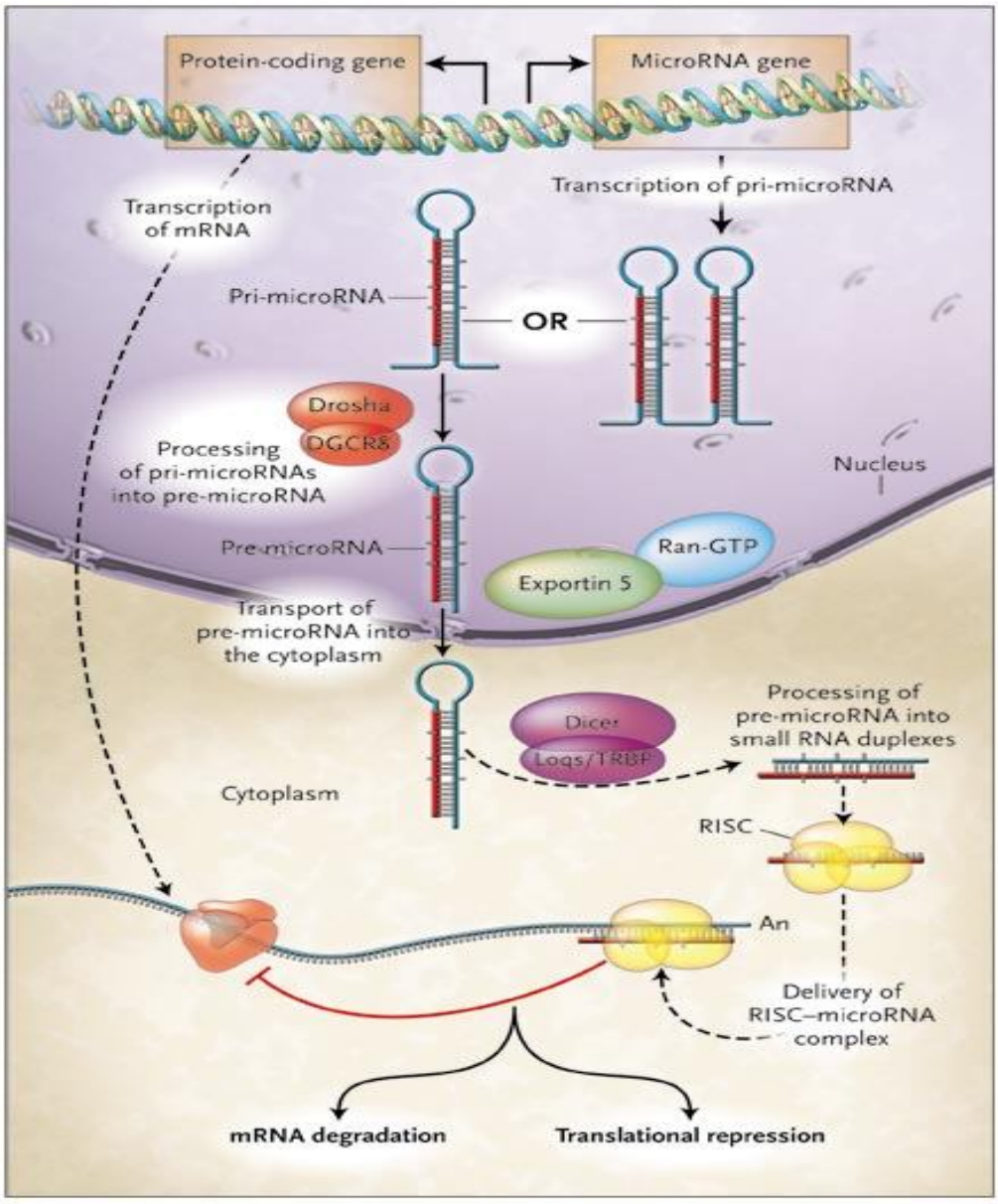

Figure 1.8.1A Represents miRNA processing and gene regulation in animals (Slack et.al. 2006)

---

1. **Transcription**

MicroRNAs are initially expressed as part of transcripts termed primary miRNAs (pri-miRNAs) (Lee et al, 2002). They are apparently transcribed by RNA Polymerase II, and include 5' caps and 3' poly (A) tails (Smalheiser, 2003); Cai et al, 2004). The miRNA

portion of the pri-miRNA transcript likely forms a hairpin with signals for dsRNA-specific nuclease cleavage.

2. Hairpin release in the nucleus

The dsRNA-specific ribonuclease Drosha digests the pri-miRNA in the nucleus to release hairpin, precursor miRNA (pre-miRNA) (Lee et al, 2003). Pre-miRNAs appear to be approximately 70 nt RNAs with 1–4 nt 3' overhangs, 25–30 bp stems, and relatively small loops. Drosha also generates either the 5' or 3' end of the mature miRNA, depending on which strand of the pre-miRNA is selected by RISC (Lee et al, 2003; Yi et al, 2003).

3. Export to the cytoplasm

Exportin-5 (Exp5) seems to be responsible for export of pre-miRNAs from the nucleus to the cytoplasm. Exp5 has been shown to bind directly and specifically to correctly processed pre-miRNAs. It is required for miRNA biogenesis, with a probable role in coordination of nuclear and cytoplasmic processing steps. (Lund et al, 2004; Yi et al, 2003).

4. Dicer processing

Dicer is a member of the RNase III superfamily of bidentate nucleases that has been implicated in RNA interference in nematodes, insect, and plants. Once in the cytoplasm, Dicer cleaves the pre-miRNA approximately 19 bp from the Drosha cut site (Lee 2003, Yi 2003). The resulting double-stranded RNA has 1–4 nt 3' overhangs at either end (Lund 2003). Only one of the two strands is the mature miRNA; some mature miRNAs derive from the leading strand of the pri-miRNA transcript, and with other miRNAs the lagging strand is the mature miRNA.

5. Strand selection by RISC

To control the translation of target mRNAs, the double-stranded RNA produced by Dicer must strand separate, and the single-stranded mature miRNA must associate with the RISC (Hutvagner and Zamore, 2002). Selection of the active strand from the dsRNA appears to be based primarily on the stability of the termini of the two ends of the dsRNA

(Schwarz et al, 2003), (Khvorova et al, 2003). The strand with lower stability base pairing of the 2–4 nt at the 5' end of the duplex preferentially associates with RISC and thus becomes the active miRNA (Schwarz et al, 2003).

In plants, gene regulation/silencing occurs via the RNA-mediated interference (RNAi) pathway, in which miRNAs bind with perfect complementarity to protein coding mRNA sequences. mRNA transcripts are then cleaved by ribonucleases in the miRNA-associated, multiprotein RNA-induced-silencing complex (miRISC), which results in the degradation of target mRNAs (Chan and Slack, 2006). In animals, miRNAs exert their regulatory/silencing effects by binding to imperfect complementary sites within the 3' untranslated regions (UTRs) of their mRNA targets. Here, they repress target-gene expression post-transcriptionally as well as degrading mRNA via RNA-induced silencing complex (RISC) (Esquela-Kerscher and Slack, 2006).

1.8.2 MicroRNA Bio-Arrays

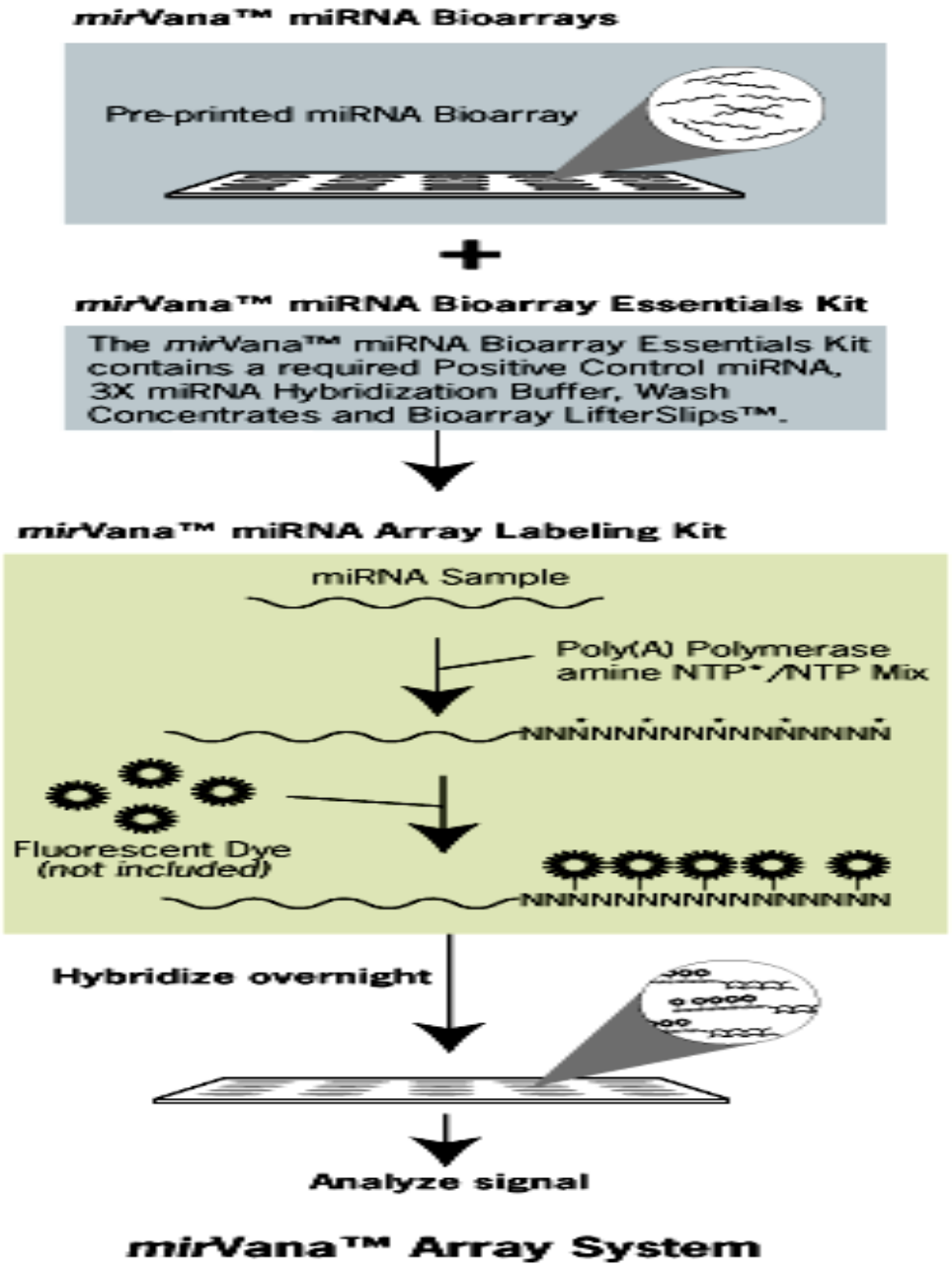

Figure 1.8.2A Overview of the *mir*Vana™ miRNA Array System (source www.ambion.com)

Ambion® *mir*Vana™ miRNA Bioarrays Version 9.2 are high-quality microarrays with probes representing a comprehensive panel of human, mouse, and rat microRNAs. Version 9.2 of *mir*Vana miRNA Bioarrays coincides with Version 9.2 of miRBase Sequence Database, which is curated by the Sanger Institute

(microrna.sanger.ac.uk/sequences). Version 9.2 also features probes to detect an exclusive set of 153 human miRNAs. Called Ambi-miRs, these novel miRNAs have been identified through a combination of bioinformatics prediction, cloning, and detection in human total RNA samples.

Table 1.1 Version 9.2 Content for Ambion® *mir*Vana™ miRNA Bioarrays

Probe Sets	**Number**
Human	471
Mouse*	380(221)
Rat**	238(41)
Ambi-miRs™	153
Controls***	22
Total	908

(Source www.ambion.com)

---

* Unique probes those are not human.

** Unique probes that are not human or mouse.

*** The positive control provided with the Ambion® *mir*Vana™ miRNA Labelling Kit is complementary to multiple control probe spots on the Ambion *mir*Vana miRNA Bioarray, which allow for alignment of the array for scanning.

1.8.3 MiRNA detection

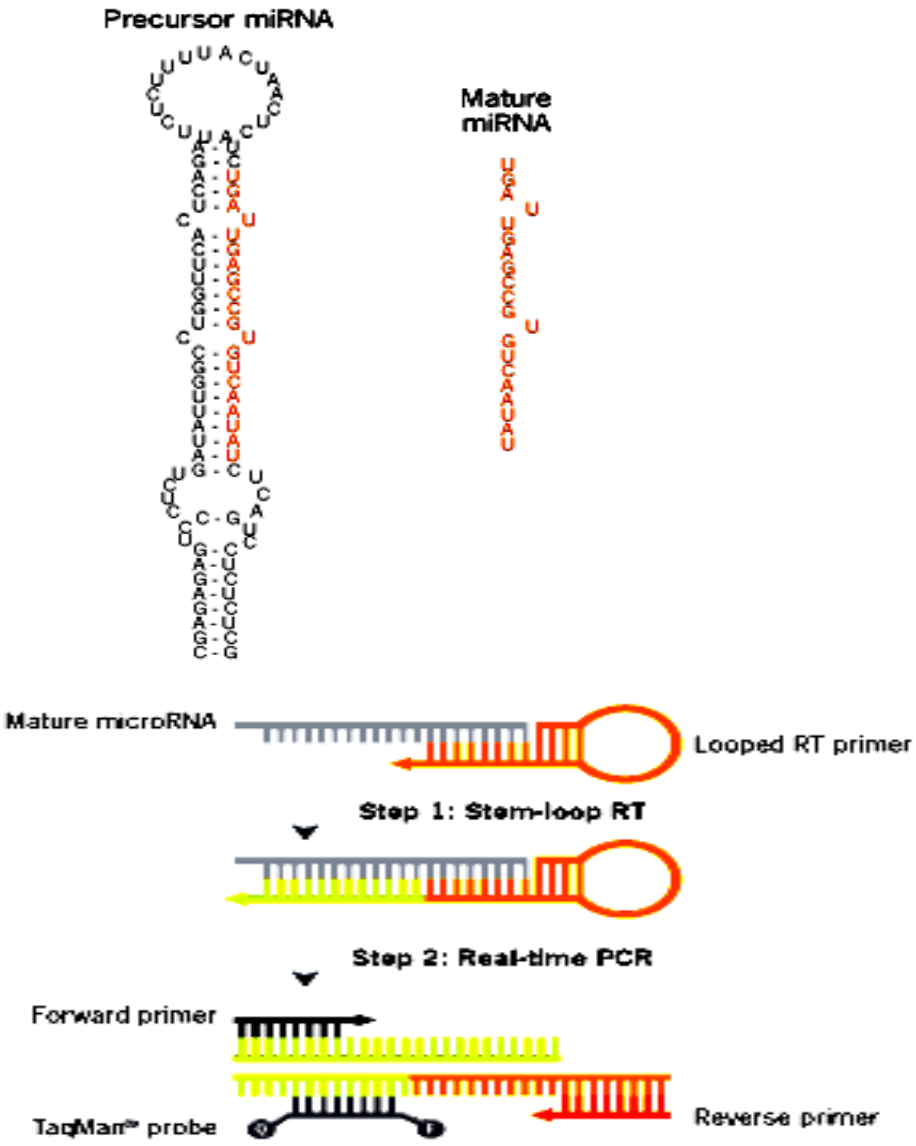

(Source www.ambion.com)

Figure 1.8.3A A represents pre-miRNA and matured miRNA after Dicer processing. Figure B shows schematics of TaqMan based MicroRNA assays, the advantages of stem-loop primer: (I) specificity for only mature miRNA target, and (II) formation of a RT primer/mature miRNA–chimera, extending the 5' end of the miRNA. The resulting longer RT amplicon presents a template amenable to standard real-time PCR, using TaqMan assays.

.

1.8.4 MicroRNAs as tumour suppressors and Oncomir

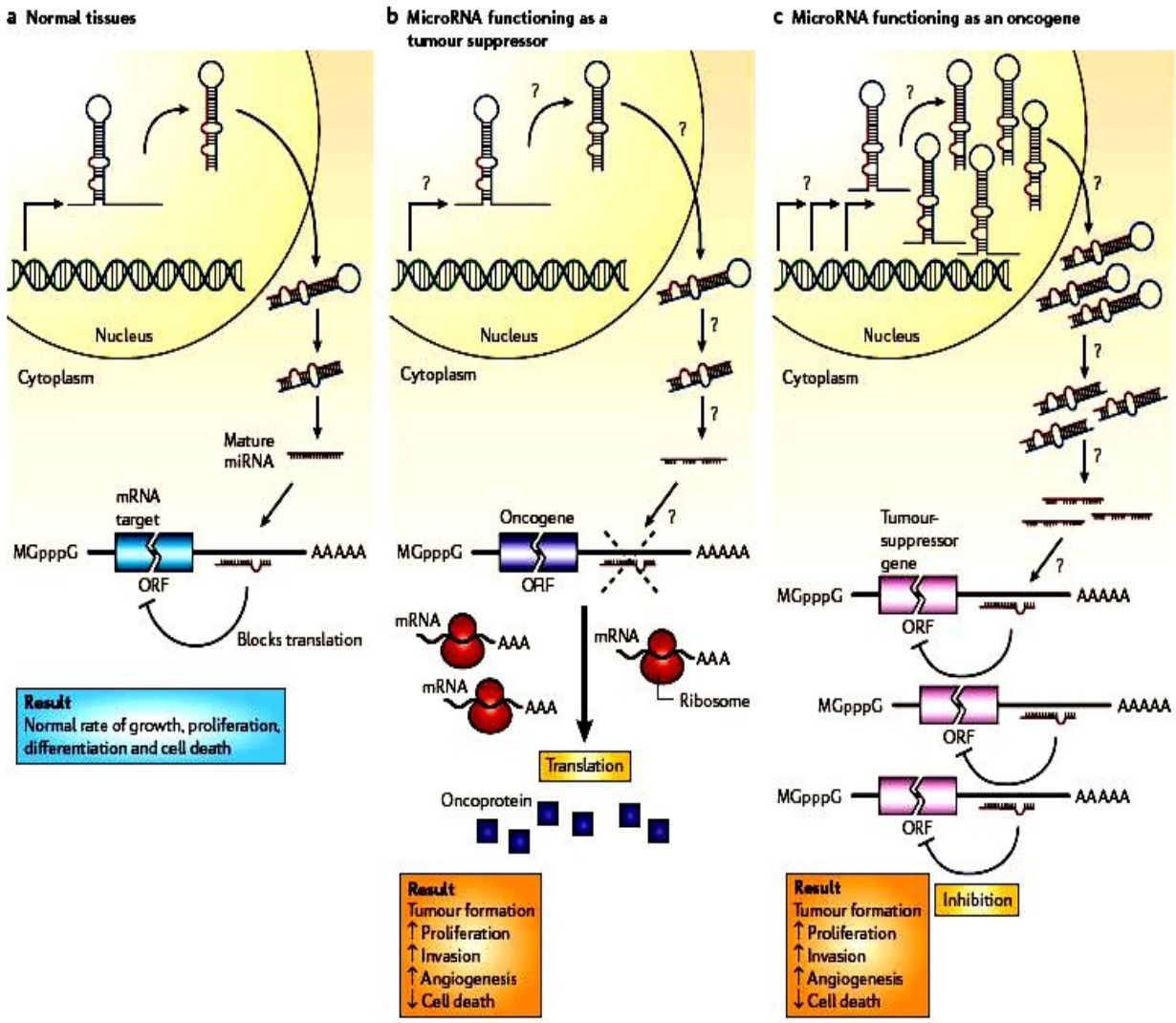

Figure 1.8.4A Schematic of roles of miRNA (http://rogermallak.tripod.com).

a) MiRNA biogenesis in normal tissues, as a result of normal rates of cellular growth, proliferation, differentiation and cell death, b) microRNAs as tumor suppressors, a defect in miRNA biogenesis represented in fig b as (?) at different levels, as a result inappropriate expression of miRNA target- oncoproteins, c) As oncogene, increased amounts of a miRNA, which might be produced at inappropriate times or in the wrong tissues, would eliminate the expression of a miRNA-target tumor-suppressor gene and lead to cancer progression (Slack et.al. 2006).

Studies reveal possible links between miRNAs and viral disease, neurodevelopment, and cancer. MiRNA expression in brain development (Krichevsky et al, 2003), chronic lymphocytic leukemia (Calin et al, 2004a), colonic adenocarcinoma (Michael et al, 2003), Burkitt's lymphoma (Metzler et al, 2004), and viral infection (Pfeffer et al, 2004). Lately miRNAs had been shown to act as both tumour suppressors and oncogenes. More than 50% of miRNA genes have been found localised in cancer-associated genomic regions or in fragile sites (Calin et al, 2004b). Expression profiling methods were developed to analyse 217 mammalian miRNAs from a panel of 200 human cancers. Results showed an overall reduction in expression of miRNAs in cancer compared to normal samples. This indicates that miRNAs act predominately as tumour suppressors (Yang et al, 2005). However, a cluster of miRNAs, miR-17 ~ 92, is overexpressed is some lymphoma and solid tumours. Ectopic expression of these miRNAs in a mouse model of Burkitt's lymphoma led to accelerated and disseminated disease (He et al, 2005a)

A study was carried out in 2004 in which Chronic Lymphocytic Leukemia (CCL) samples were analysed to investigate the involvement of miRNA in cancer. They obtained 41 tissue samples from CLL patients. The results they found suggested that miRNA played important roles in the pathogenesis of human CLL (Calin et al, 2004b). They observed that when both pre-miRNA and mature miRNA were dysregulated (such as miR-123, miR-132, or miR-136), the same type of variation in CLL samples were observed in normal samples. They found that upon deletion of the 13q14 chromosome, miRNAs (miR-24-2, miR-195, miR-203, miR-220, and miR-221) are reduced as well as other miRNAs (miR-7-1, miR-19a, miR-136, miR-154, miR-217, precursor miR-218-2) which were significantly increased (Calin et al, 2004b). This indicates that deletion or down-regulation of miRNAs is associated with human tumours. They also reinforced that a large portion of miRNAs are encoded at fragile sites, suggesting that miRNA had an important role in the pathogenesis of human cancer (Calin et al, 2004b).

In 2005, the affect of c-Myc on the regulation of miRNA expression was studied by (Mendell, 2005). The c-Myc is a helix-loop-helix leucine zipper transcription factor which regulates cell proliferation, growth and apoptosis. They found with Chromatin

immunoprecipitation experiments that c-Myc activates expression of six miRNAs grouped together on human chromosome 13. Mendell et al, (2005) also discovered that the transcription factor E2F1 is down-regulated by two miRNAs (miR-17-5p and miR20a) located in the activated group of miRNAs. E2F1 promotes cell cycle progression and is also targeted by c-Myc. Therefore, c-Myc simultaneously
Up-regulates and down-regulates E2F1 translation causing a proliferation signal
(Mendell et al, 2005).

The emergence of miRNAs as potential cancer interventions is likely to have a large effect on gene therapies that are designed to block tumor progression. Large-scale expression screens, to compare miRNA levels in tumors versus normal tissues, will be useful in identifying novel miRNAs that are involved in cancer. Also, functional screens that are designed to select miRNA genes that specifically control cancer-related processes, such as cell proliferation and apoptosis, will also help in this search.

1.9 MicroRNAs and Proteomics

1.9.1 Proteomics Background

Proteomics includes not only the identification of proteins but also the determination of their locations, modifications, interactions, activities and ultimately their functions. Proteomics is regarded as the sister technology to genomics (Scott et al, 2000) complementing the knowledge derived from genomic analysis. The ultimate goals of proteomics go beyond a catalogue of proteins expressed by healthy and diseased cells. The eventual objective is to elucidate the organisation and dynamics of the metabolic, signalling and regulatory networks through which the life of the cell is transacted. Cancer proteomics seeks to understand how networks become dysfunctional, predict how their function can be manipulated through interventions by drugs or genetic manipulations (Anderson et al, 2001) and enables the identification of disease-specific proteins, drug targets and markers of drug efficacy and toxicity. Furthermore, cancer proteomics seeks to identify markers to improve diagnosis, classification of tumours and also to define

targets for more effective therapeutic measures (Simpson and Dorow, 2001). Given the late stage at which cancers often present, the identification of early detection biomarkers by proteomic analysis will offer better prognosis and aid in individualizing treatments for certain cancers.

The first proteomic study of lung cancer was published in 2002 and in contrast, several dozen microarray studies of lung cancer have been published since 1999. Proteomics analysis attempts to identify the protein complement expressed by the genome (Pedersen et al, 2003) and is the systematic separation, identification and characterisation of proteins present in a biological sample (Scott et al, 2000). Validation of changes in gene expression at the protein level would improve many of these studies, because changes in protein expression provide a more functional readout. Although evaluating protein expression may not be necessary to develop fingerprints for diagnostic use, it is necessary if markers that are identified by this method are to be used in their own right as diagnostic markers or as targets for therapy. Thus, despite the fact that many genes were identified as potential biomarkers, all of them require further validation. Even though proteomics provides a more functional approach than genomics, proteomics alone might provide an insufficient readout because post-translational modifications such as phosphorylation control the stability and function of many proteins. The development of sophisticated proteomic techniques such as phospho-proteomics will add another level of complexity to these systematic analyses (Blagoev and Pandey, 2001).

1.9.2 Impact of Advanced Proteomics on MiRomics

Analysis of the proteome has added layers of complexity compared to the genome. A simple gene can encode multiple different proteins by alternative splicing of the mRNA transcript, by varying translation start or stop sites, by frameshifting during which a different set of triplet codons in the mRNA is translated or by posttranslational modifications (Anderson and Seilhamer, 1997). A single protein may be multifunctional and conversely similar functions may be performed by different proteins (Fields, 2001). The result is a proteome estimated to be an order of magnitude more complex than the genome. The fact that miRNAs can cause degradation of their targets has been widely

exploited to identify such targets through microarray analysis. However, targets that are not susceptible to degradation would be missed. Vinther et al, (2006) showed with a method known as SILAC (stable-isotope labeling by amino acids in cultured cells), it is possible to label proteins during translation through incorporation of “heavy” amino acids. Proteomes from cells grown in the presence of different labels, exposed to different experimental manipulations, can be compared side by side with the analyzed peptides showing up as distinct peaks in the mass spectrometer. A new approach by Selbach et al, (2008) and co-workers used a particular implementation of SILAC termed pulsed SILAC (pSILAC). In this approach, labeling is restricted to newly synthesized proteins, permitting the determination of protein synthesis rates and providing high sensitivity. In contrast, conventional SILAC quantifies changes in protein concentrations, which respond to additional factors including intrinsic protein half-lives and regulated turnover. However, assuming that the total concentration of a protein rather than its current rate of synthesis determines biological outcomes, changes identified by SILAC might be equally relevant, such that SILAC and pSILAC should be viewed as complementary approaches (Großhans H. 2008).

A recent study by Iliopoulos D. et al, (2008) involving microRNA profiling of patient-derived osteoarthritic cartilage in comparison to normal cartilage, revealed a 16 microRNA osteoarthritis gene signature. Using reverse-phase protein arrays in the same tissues they were able to detected 76 differentially expressed proteins between osteoarthritic and normal chondrocytes. Reverse phase protein microarray technology offer a new opportunity to measure and profile signaling pathways, providing data on post-translational phosphorylation events not obtainable by gene microarray analysis. Proteins such as SOX11, FGF23, KLF6, WWOX and GDF15 not implicated previously in the genesis of osteoarthritis were identified. Iliopoulos D group were able to identify potential "interactome" network consisting of 11 microRNAs and 58 proteins linked by 414 potential functional associations by integrating microRNAs and proteomic data with microRNAs gene-target prediction algorithms. Such comparison of the molecular and clinical data, revealed specific microRNAs (miR-22, miR-103) and proteins (PPARA, BMP7, IL1B) to be highly correlated with Body Mass Index (BMI). Further experimental validation revealed that miR-22 regulated PPARA and BMP7 expression and its inhibition blocked inflammatory and catabolic changes in osteoarthritic chondrocytes (Iliopoulos D. et al, 2008).

As alternatives to SILAC there exists iTRAQ (isobaric tag for relative and absolute quantitation) is a non-gel based technique used to identify and quantify proteins from different sources in one single experiment. It uses isotope coded covalent tags. iTRAQ is used in proteomics to study quantitative changes in the proteome (Aggarwal K et al, 2006). Shadforth IP et al, (2005) evaluated the advantage of iTRAQ over SILAC and metabolic labelling which is more robust and high throughput which can analyse four samples simultaneously, thereby reducing the amount of mass spectrometry time needed for analysis. In addition, the b- and y- ions derived from peptides labelled with the four iTRAQ tags are indistinguishable, resulting in higher MSMS intensity and therefore more confident peptide identifications in comparison to SILAC and metabolic labelling, in which the MSMS spectra for the differentially labelled peptides are acquired independently. The marriage of miRomics and proteomics might help delineating the spectrum of targets that are regulated by miRNAs. New knowledge about the functional roles of oncomiRs is revolutionizing cancer biology and will open up new opportunities in biomedical research (William CS Cho, 2007).

1.15 Aims of Thesis

The research work carried out in this thesis can be divided into two main sections,

a) **Development of genetic tools for stable, targetable transgene overexpression**

Major complicating factors with in vitro transgene integration and exogenous gene expression in mammalian cells include instability and inconsistency due to chromosomal position effects and/ or copy number variation between different clones. To address this variation we set out to design and construct two different Cre-LoxP based mammalian expression plasmid vectors to generate targetable cell lines. We planned to modify these for random insertion of LoxP sites and LINE-1 site-specific insertion of LoxP sites in a model lung cancer cell line (DLKP) using the following strategies:

- Random insertion of a targeting site with a plasmid vector carrying a reporter fusion gene Geo (GFP+Neo) flanked by LoxP sites, followed by selection of stable GFP positive and neomycin resistant DLKP clones.

- Use of LINE-1 elements as targeting arms for homologous recombination. The rationale behind using LINE-1 elements was a) they constitute 17-20% of the genome which should make them easily available targets and b) using human L1 element as target would help avoid targeting and disrupting endogenous functional genes.

- To address stability issues with transgene overexpressing cell lines, we planned to subject the GFP positive DLKP clones to selection and multiple passaging with freeze thaw cycles while monitoring GFP expression, in order to identify stable clones.

b) Investigation of the role of differential expression of a group of genes including microRNAs, in cancer invasion.

- Based on existing microarray data from our laboratory and qRT-PCR analysis to stably overexpress four genes (invasion related) KCNJ8, TFPI2, S100A13 and GLP1R in the targetable DLKP cell lines as a proof-of-concept of their utility.

- To investigate roles of miRNAs in cancer invasion in DLKP Vs DLKPA cell lines, as well as to identify possible invasion and proliferation related targets through comprehensive proteomic profiling studies and to investigate further roles of these proteins using siRNA knockdown.

2.0 Materials and Methods

2.1. Water

Ultra pure water was used in the preparation of all media and solutions. This water was purified by a reverse osmosis system (Millipore Milli-RO 10 Plus, Elgastat UHP) to a standard of 12-18MΩ/cm resistance.

2.2. Glassware

Solutions pertaining to all cell culture and maintenance were prepared ad stored in sterile glass bottles. Bottles and lids and all other glassware used for any cell related work were prepared as follows: - all glassware lids were soaked in a 2% (v/v) solution of RBS-25 (AGB Scientific) for at least 1 hour. Following scrubbing and several rinses in tap water, the bottles were then washed by machine using Neodisher detergent, an organic, phosphate-based acid detergent. The bottles were then washed with distilled water, followed by a rinse with ultrapure water and were sterilised by autoclaving.

2.3. Sterilisation

Water, glassware and all thermostable solutions were sterilised by autoclaving at 121^{o}C for 20 minutes (min) under a pressure of 1bar. Thermolabile solutions were filtered through a 0.22μm sterile filter (Millipore, millex-gv, SLGV-025BS). Low protein-binding filters were used for all protein containing solutions.

2.4. Media Preparation

Medium was routinely prepared and sterility checked by Joe Carey (lab technician). The basal media used during routine cell culture were prepared according to formulations shown in Table 2.1 10x media were added to sterile ultrapure water, buffered with HEPES and $NaHCO_3$ and adjusted to a pH of 7.45-7.55 using sterile 1.5M NaOH and 1.5M HCl. The media were then filtered through sterile 0.22μm bell

filters (Gelman, 121-58) and stored in 500ml sterile bottles at 4°C. Sterility checks were carried out on each 500ml bottle of medium as described in section 2.6.4 The basal media were stored at 4°C up to their expiry dates as specified on each individual 10x medium container. Prior to use, 100ml aliquots were supplemented with 5% foetal calf serum (BATCH #) and this was used as routine culture medium. This was stored for up to 2 weeks at 4°C, after which time, fresh culture media was prepared. For all DLKP cell lines ATCC (Hams F12/DMEM (1:1) supplemented with 5% FCS was routinely used. For the RPMI cell lines, Minimum Essential Medium (MEM) supplemented with 5% FCS, 1% Sodium pyruvate, 1% Non essential amino acids (NEAA) and 1% L-glutamine was used.

Table 2.1 Preparation of basal media

	DMEM (Dulbecco's Modified Eagle Medium) (mls) (Sigma, D-5648)	**Hams F12 (mls) (Sigma, N-6760)**
10X Medium	500	Powder
Ultrapure H_2O (UHP)	4300	4700
1M HEPES[1]	100	100
7.5% $NaHCO_3$	45	45

[1] The weight equivalent of 1M N- (2-Hydroxyethyl) piperazine-N'- (2-ethanesulfonic acid) (HEPES) was dissolved in an 80% volume of ultra-pure water and autoclaved. The pH was adjusted to 7.5 with 5M NaOH.

2.5 Cell Culture

All cell work was carried out in a class II down-flow re-circulating laminar flow cabinet (Nuaire Biological Cabinet) and any work that involved toxic compounds was carried out in a cytoguard (Gelman). Strict aseptic technique was adhered to at all

times. The laminar flow cabinet was swabbed with 70% industrial methylated spirits (IMS) before and after use, as were all items used in the cabinet. Each cell line was assigned specific media and waste bottles. Only one cell line was worked with at a time in the cabinet, which was allowed to clear for 15min between different cell lines. The cabinet itself was cleaned each week with industrial detergents (Virkon, Antec International; TEGO, TH. Goldschmidt Ltd.), as were the incubators. The cell lines used during the course of this study, their sources and their basal media requirements are listed in Table 2.2 Lines were maintained in 25cm^2 flasks (Costar; 3050), 75cm^2 (Costar; 3075) or 175cm^2 flasks (Corning, 431079) at 37^{o}C and fed every two to three days.

Table 2.2 Cell lines used in this study

Cell Line	Cell type	Basal Media	Source	FCS (%)
DLKP	Poorly differentiated squamous cell lung carcinoma	ATCC**	NICB*	5
DLKPA	Adriamycin resistant variant of DLKP	ATCC**	NICB*	5
DLKP-17	Targetable Clonal subpopulation of DLKP with LoxP site	ATCC**	NICB*	5
DLKP-11	Targetable Clonal subpopulation of DLKP with LoxP site	ATCC**	NICB*	5
DLKP-17-GLP1R	GLP1R transfected DLKP 17 clone	ATCC**	NICB*	5
DLKP-17-KCNJ8	KCNJ8 transfected DLKP 17 clone	ATCC**	NICB*	5
DLKP-17-TFPI2	TFPI2 transfected DLKP 17 clone	ATCC**	NICB*	5
DLKP-17-S100A13	S100A13 transfected DLKP 17 clone	ATCC**	NICB*	5
DLKP-11-GLP1R	GLP1R transfected DLKP 11 clone	ATCC**	NICB*	5
DLKP-11-KCNJ8	KCNJ8 transfected DLKP 11 clone	ATCC**	NICB*	5
DLKP-11-TFPI2	TFPI2 transfected DLKP 11 clone	ATCC**	NICB*	5
DLKP-11-S100A13	S100A13 transfected DLKP 11 clone	ATCC**	NICB*	5
DLKPA-mir29a-1	hsa-mir-29a transfected DLKP A clone 1	ATCC**	NICB*	5
DLKPA-mir29a-3	hsa-mir-29a transfected DLKP A clone 3	ATCC**	NICB*	5
DLKPA-mir29a-4	hsa-mir-29a transfected DLKP A clone 4	ATCC**	NICB*	5
DLKPA-mir29a-11	hsa-mir-29a transfected DLKP A clone 11	ATCC**	NICB*	5
DLKPA-mir-negative control	Mir-negative control transfected DLKP A	ATCC**	NICB*	5
MCF-7	Human Breast adenocarcinoma	DMEM****	ATCC***	10
PANC-1	Pancreatic Ductal carcinoma	DMEM****	ATCC***	5

---

* NICB, National Institute for Cellular Biotechnology, Dublin, Ireland
** ATCC Basal media consists of a 1:1 mixture of DMEM and Hams F12.
*** ATCC, American Type Culture Collection, Rockville, MD, USA
**** DMEM, Dulbecco's Modified Eagles Medium

2.6 Subculture of Adherent Lines

During routine sub culturing or harvesting of adherent lines, cells were removed from their flasks by enzymatic detachment. Waste medium was removed from the flasks and the cells were rinsed with a pre-warmed (to 37^{o}C) trypsin/EDTA (TV) solution (0.25% trypsin (Gibco, 5090-028), 0.01% EDTA (Sigma, EDS) solution in PBS A (Oxoid BR14a)). The purpose of this was to remove any naturally occurring trypsin inhibitor that could be present in the residual serum. Fresh TV was then placed on the cells (2ml/25cm^2 flask, 4ml/75cm^2 flask) and the flask incubated at 37^{o}C until the cells were seen to have detached (5-10min). The trypsin was then deactivated by addition of an equal volume of complete (*i.e.* containing 5% FCS) growth medium. The entire solution was transferred to a 30ml sterile universal tube (Sterilin; 128a) and centrifuged at 1,000rpm for 5 min. The resulting cell pellet was resuspended in pre-warmed fresh complete growth medium, counted (Section 2.6.1) and used to re-seed a flask at the required cell density or to set up an assay.

2.6.1 Cell Counting

Cell counting and viability determinations were carried out using a trypan blue (Gibco, 15250-012) dye exclusion technique. An aliquot of trypan blue was added to a sample from a single cell suspension in a ratio of 1:5. After 3 min incubation at room temperature, a sample of this mixture was applied to the chamber of a haemocytometer over which a glass coverslip had been placed. Cells in the 16 squares of the four outer corner grids of the chamber were counted microscopically; an average per corner grid was calculated with the dilution factor being taken into account, and final cell numbers were multiplied by 10^4 to determine the number of cells per ml. The volume occupied by the chamber is 0.1cm x 0.1cm x 0.1cm *i.e.* 0.0001cm^3. Therefore cell number x 10^4 is equivalent to cells per ml. Non-viable cells were those that stained blue while viable cells excluded the trypan blue dye and remained unstained.

2.6.2 Cell Freezing

To allow long-term storage of cell stocks, cells were frozen and cryo-preserved in liquid nitrogen at temperatures below –180^{o}C. Once frozen properly, such stocks should survive indefinitely. Cells to be frozen were harvested in the log phase of growth (*i.e.* actively growing and approximately 60-70% confluent) and counted as described in Section 2.6.1. Pelleted cells were resuspended in serum. An equal volume of a DMSO/serum (1:9, v/v) was slowly added drop wise to the cell suspension to give a final concentration of at least 5x10^{6} cells/ml. This step was very important, as DMSO is toxic to cells. When added slowly the cells had a period of time to adapt to the presence of the DMSO, otherwise cell lysis can occur. The suspension was then aliquoted in cryovials (Greiner, 122278), which were then quickly placed in the vapour phase of liquid nitrogen containers (approximately –80^{o}C). After 2.5 to 3.5 hours, the cryovials were lowered down into the liquid nitrogen where they were stored until required.

2.6.3 Cell Thawing

Immediately prior to the removal of a cryovial from the liquid nitrogen stores for thawing, a sterile universal tube containing pre-warmed complete growth medium was prepared for the rapid transfer and dilution of thawed cells to reduce their exposure time to DMSO freezing solution which is toxic at room temperature. The suspension was centrifuged at 1,000rpm for 5 min, the DMSO-containing supernatant removed and the pellet resuspended in fresh growth medium. Cell count was carried out (Section 2.6.1) to determine the efficiency of the freezing/thawing procedures. Thawed cells were placed into tissue culture flasks with an appropriate volume of medium (5ml/25cm^{2} flask and 10ml/75cm^{2} flask) and allowed to attach overnight. After 24 hours, the cells were re-fed with fresh medium to remove any residual traces of DMSO.

2.6.4 Sterility Checks

Sterility checks were routinely carried out on all media, supplements and trypsin used for cell culture. Samples of basal media were inoculated into Columbia (Oxoid, CM331) blood agar plates, Sabauraud (Oxoid, CM217) dextrose and Thioglcollate (Oxoid, CM173) broths, which detect most contaminants including bacteria, fungus and yeast. Complete growth media were sterility checked at least two days prior to use by incubating samples at 37^{o}C, which were subsequently examined for turbidity and other indications of contamination.

2.7 Specialised Techniques in Cell Culture

2.7.1 Isolation of sub-population of cell lines by limited dilution single cell cloning

To obtain single cell clones the cell lines were plated in 96 well plates, the plate was divided into two sections of 6 columns each so that two sets of cloning can be done in a single plate

a) The initial concentration of 1000 cells per ml was obtained as described in (section 2.6.1)
b) Wells in first columns of two sets in 96 well plates were seeded with 125µl of media with cells (125 cells per well).
c) The adjacent wells were pipetted with 100µl normal media without cells
d) With a multichannel pipette 25µl of cell suspension from the first column was pipetted out and seeded into adjacent wells in the second column, and from second column to the third, and so on in a serial manner.
e) This technique resulted in one cell per well, with a minimum of 12-15 single cells per plate.

2.7.2 X-Gal staining of DLKP cells grown in monolayer

This method is used for the detection of β-galactosidase on formalin-fixed, monolayer cells, for cells in 6 well plates:

a) Cells washed twice with 3ml cold 1X PBS and aspirated

b) 5ml ice cold 0.5% glutaraldehyde (made in 1X PBS) was added on to cells

c) Incubated 5 minutes at room temperature and then aspirated

d) washed twice with cold 1X PBS and aspirated

e) X-gal staining solution (table 2.3) added (approx. 1.5ml) and incubated at 37^0C

f) the staining evaluated after 24 hrs.

Tabe 2.3 X-gal staining solution preparation for 30ml

Components	Requirements
1M $MgCl_2$	**39µl**
5M NaCl	**90µl**
0.5M HEPES, pH 7.3	**2.64ml**
30mM potassium ferricyanide	**3ml**
30mM potassium ferrocyanide	**3ml**
2% X-gal(dissolved in DMSO)	**750µl**
Distilled water	**To 30ml**

2.7.3 Assessing GFP stable overexpresssion using Guava EasyCyte flowcytometer

Guava EasyCyte system was used for cell cycle monitoring as well for GFP stable overexpression screening. Stable GFP overexpressing cell lines were trypsinised from 24 well plates and resuspended by diluting 1:6 (50µl cell suspension, 300µl final volume). Initial system check was performed with manufacturer provided control to avoid any flaw in the flow. So according to manufacturer recommendations $1/20^{th}$ dilution of control beads was prepared and monitored for bead flow, and ensured that there is no block in the system. The samples in 96 well U-bottom plates were placed in the plate holder, the cell flow was adjusted for ~ 200cells/µl. Forward scatter gating as well as % fluorescence (log) gating were fixed at 600volts . The data acquired was based on these settings and always maintained for the entire experiments.

2.7.4 Cell Cycle analysis using Guava EasyCyte flowcytometer

The Guava® Cell Cycle Assay was used for measuring G0/G1, S, and G2/M phase distributions. Whole-cell staining was prepared with propidium iodide (PI). The guava cell cycle software was set for assessment of G0/G1, S, and G2/M phase cell cycle percentages. The cells were seeded in multiple wells for time point based data acquisition. The cells were serum starved 24 hrs before the experiment to synchronize the majority of cells at a similar cell cycle stage. After 24 hrs cells were fed media with serum and samples collected at time points 0, 2, 4, 8, 12, 16, 24, 32 hrs. The cells were processed with cell cycle assay kit (Catalogue No. 4500-0220, 100 tests) and data acquired on a Guava EasyCyte flow-cytometer.

Culturing and harvesting adherent cells in 24-well tissue culture plates

1. Cell concentration seeded at $2x10^3$ cells in 2 mL of medium to each well of a 24-well cell culture plate.
2. Incubated the cells at 37°C to allow the cells to attach to the plate and to grow to 60-80% confluency before proceeding.

• Cells were first synchronized in G0 by culturing cells for 24hrs in basal medium without serum.

3. 24 hrs later cells were supplemented with serum media and from then every 0, 2, 4, 8, 12,16,24,32 hrs cells were harvested

4. Harvest the cells from the 24-well plates (Section 2.6)

Cell Fixation

A. Cell fixation in a 96-well plate

1. Cell samples were transferred from the 24-well plate to a 96-well round bottom plate if the cells are not already in a round bottom plate.

2. Centrifuged cells at 450 x g for 5 minutes with the brake on low and at room temperature.

3. Discarded the supernatant and care taken not to touch the pellet.

4. 200 µL of 1X PBS added to each well using a multi-channel pipettor.

5. Cells in the well mixed by pipetting up-and-down several times.

6. Centrifuged the cells in the round bottom plate at 450 x g for 5 minutes with the brake on low and at room temperature.

7. Discarded the supernatant.

8. Using a multi-channel pipettor, thoroughly resuspended the cells by repeat pipetting in the residual PBS, pipetting up and down several times.

9. Placed the round bottom plate containing the resuspended cells on a lab shaker.

10. 200 µL of ice-cold 70% ethanol added dropwise into the wells while shaking at low speed (speed 3).

11. Sealed the plate with a microplate sealer and refrigerate cells for at least one and up to 12 hours prior to staining. Fixed cells are stable for several weeks at 4°C and for two to three months at –20°C.

12. Proceeded to Cell Staining Protocol in 96-well format.

NOTE: It is important to have a single cell suspension prior to fixation. Otherwise the fixation process will result in a high percentage of doublet cells that will decrease the accuracy of the results.

Cell Staining Protocol

A. Cell staining in 96-well format

1. Warm Guava Cell Cycle Reagent to room temperature; shield from excessive light exposure. Warm 1X PBS to room temperature.

2. 200 µL of the samples transferred into the wells of a 96-well round bottom plate if the samples have not yet been transferred.

3. Centrifuged the 96-well round bottom plate containing the samples at 450 x g for 5 minutes with the brake on low and at room temperature.

4. Removed and discard the supernatant being careful not to touch the pellet. (After centrifugation, the well should contain a visible pellet or a white film on the bottom of the plate.)

5. Using a multi-channel pipettor 200 µL of 1X PBS was added to each well. Cells were mixed in the wells by pipetting up and down several times. The plate was allowed to stand at room temperature for one minute.

6. Centrifuged the 96-well round bottom plate at 450 x g for 5 minutes with the brake on low and at room temperature.

7. Remove and discard the supernatant being careful not to touch the pellet.

NOTE: The PBS washing step (steps 5 to 7) can be omitted if the user has first shown that this wash step is not necessary to minimize the %CV of the G0/G1 peak. However, the cells should still be centrifuged once to remove the ethanol. The Guava Cell Cycle Reagent should not be added to cells still in ethanol.

8. 200 µL of Guava Cell Cycle Reagent was added to each well.

9. Mixed by pipetting up and down several times.

10. Incubated the 96-well round bottom plate at room temperature shielding away from light for 30 minutes.

11. Acquire the samples on the Guava PCA-96 system.

EXPECTED RESULTS

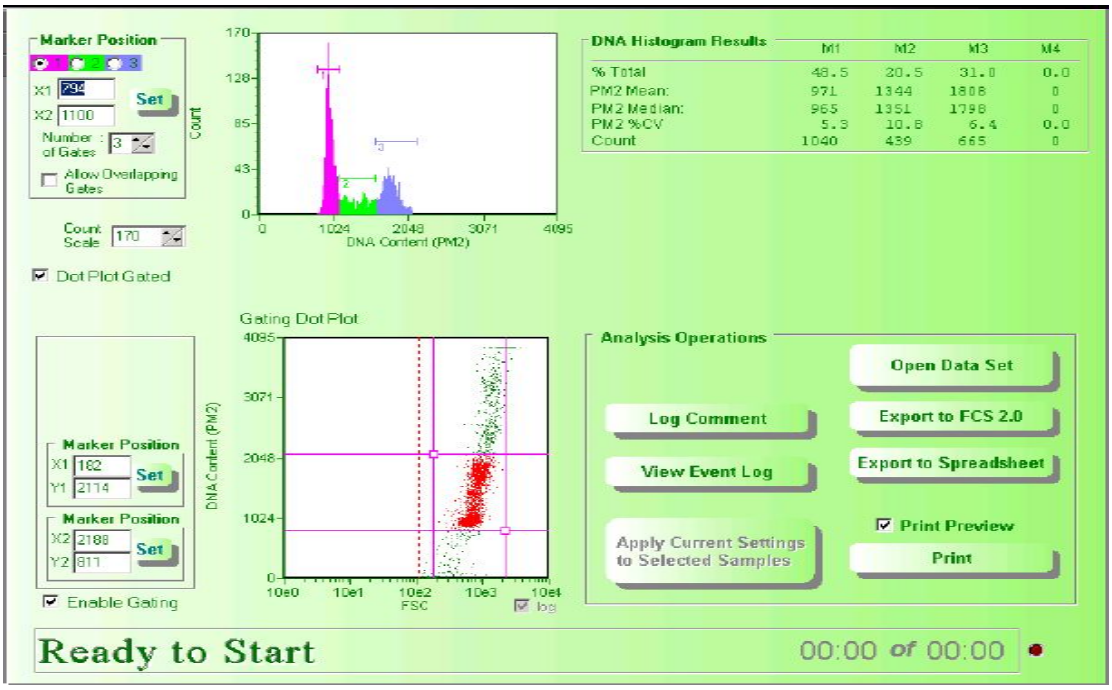

Figure represents Cell cycle phases (http://guavatechnologies.com)

Figure show typical results obtained with the Guava Cell Cycle Reagent. Log-phase cells were serum starved for 24 hours and treated with media containing serum. Ethanol fixed overnight and stained in 96-well plates according to the protocol described above. The upper plot shows the distribution of the cell cycle phases (G0/G1, S and G2/ M) in histogram format. The DNA Histogram Results show the result for the percentage of cells in G0/G1 (M1), S (M2) and G2/M (M3) under % Total. The bottom plot shows the Forward Scatter (FSC) versus DNA content of the cell sample.

2.8 Transfection

2.8.1 Optimisation of Transfection of cDNA's

Lipofectamine 2000 (Invitrogen, 11668019) and Green Fluorescent Protein (GFP) plasmid DNA was prepared with the volumes of Lipofectamine 2000 and cDNA being varied. The conditions investigated to ascertain the most efficient transfection conditions were as follows, briefly, the Lipofectamine 2000 and optiMEM (serum free media) were incubated at room temperature for 5min. During this time the plasmid and optiMEM were also incubating at room temperature. Both incubations were combined, mixed gently and formed complexes over 20min at room temperature. 1ml of this complex (DNA:Lipofectamine 2000) was added on top of adherent cells per well. The cells were viewed using a fluorescent microscope after 24-48hrs and the optimum transfection efficiency determined for each cell line by comparing the number of cells that fluoresced green with the number of cells in a particular field (Section 3.5.1). The Lipofectamine 2000 had a toxic effect on the cells, thus the lowest volume of transfection reagent was used while maintaining high transfection efficiencies. 5µl Lipofectamine 2000 was used to transfect 2µg plasmid cDNA in all transient cDNA transfections in this study.

2.8.2 Transfection of miRNAs and siRNAs

The siPORT NeoFX (Ambion) transfection agent volume was optimised for the cell lines i.e., 0.15µl for 96 well cell culture plate to transfect 50nM or 100nM of miRNAs and 50nM or 100nM of siRNA. Cell concentrations of $4x10^4$ cells per ml (100µl/each well) in 96 well cell culture plates for proliferation assay was used. In 24 well cell

culture plates, 2µl of NeoFX to transfect 50nM or 100nM of miRNAs and 50nM or 100nM of siRNA was used. Cell concentration of $3x10^5$ per ml for 24 well cell culture plates was used for the invitro invasion assay. Scrambled siRNA and/or negative miRNA controls were also used in our studies (Table 2.4 and 2.5). Kinesin specific siRNA was used as positive control (Ambion Inc., 16704).

	96 well plate/well	24 well plate/well
siPORT NeoFX	0.15µl	2µl
siRNAs	50 – 100nM	50-100nM
miRNAs	50 – 100nM	50-100nM
Opti-MEM	Made up to 10µl	Made up to 100µl
Cell seeding density	$4X10^3$ cells/well	$3X10^5$ cells/well

The miRNAs with 50nM and/or 100nM concentration was prepared in optiMEM (Gibco^{TM}, 31985) media. Similarly siRNAs with 50nM and/or 100nM concentration was prepared in optiMEM (Gibco^{TM}, 31985) media. The siPORT NeoFX and optiMEM mix was also prepared simultaneously. These mixtures were incubated at room temperature for 10min. After incubation NeoFX: optiMEM solution was added to each tube containing target miRNAs, negative miRNA controls as well as kinesin siRNA. For siRNA experiments similar method was followed with scrambled siRNA as controls along with kinesin as positive control. These solutions were mixed well and incubated for a further 10 minutes at room temperature. 10µl/well of 96 well cell culture plates and 100µl/well for 24 wells cell culture plates of siRNA and/or miRNA/NeoFX solutions were added. 100µl cell suspension for each well in 96 well cell culture plate or 1ml of cell suspension in each well of 24 well cell culture plate were added on top of miRNA: NeoFX or siRNA: NeoFX complex. The plates were mixed gently and incubated at 37°C for 24 hours. After 24hr, the transfection mixture was removed from the cells and the plates were fed with fresh medium. The plates were assayed for changes in proliferation at 72hr using the acid phosphatase assay (Section 2.7.8) or in vitro invasion assay (section 2.7.9).

Table 2.4 Synthetic miRNA Oligo nucleotides

MiRNA	Catalogue No.	Product ID
Pre-hsa-mir-21	AM17100	PM10206
Anti-hsa-mir-21	AM1700	AM10206
Pre-hsa-mir27a	AM17100	PM10939
Ani-hsa-mir27a	AM1700	AM10939
Pre-hsa-mir29a	AM17100	PM10932
Anti-hsa-mir-29a	AM1700	AM10932
Pre-mir-control	AM17110	----
Anti-mir-control	AM17010	----

Table 2.5 Synthetic siRNA Oligo nucleotides

siRNA	Ambion ID
Scrambled	4390843
Kinesin	4392420
GLP1R	s194615(1) s5826(2)
RAN	s11768(1) s11767(2)
MIF	s194615(1) s194614(2)
ANX2	s1384(1) s1385(2)
GRB2	s6119(1) s6120(2)

2.8.3 Selection of transgenic clones

5-6 hrs post transfection with cDNA (section 2.8), fresh media was added. 48hrs post transfection the cells were fed with media containing (400µg, 600µg or 800µg/ml G418 disulphate salt (Sigma A1720; cell culture tested). Every second day the cells were fed with fresh selection media, and observed until the non transfected cells were all killed due to selection pressure. The minimum concentration at which cells were killed and the time required to achieve this was found to be 800µg/ml for 5-6 days. The surviving cells were expanded and used for single cell cloning as mentioned (2.7.1).

2.9 Assessment of cell number –Acid Phosphatase Assay

1. Following the incubation period of either cDNA transfection or siRNA/miRNA treatments (48-72hrs) in cells, media was removed from the 96 well cell culture plates.
2. Each well on the plate was washed with 100 µls PBS. This was removed and 100 µls of freshly prepared phosphatase substrate (10mM *p*-nitrophenol phosphate (Sigma 104-0) in 0.1M sodium acetate (Sigma, S8625), 0.1% triton X-100 (BDH, 30632), pH 5.5) was added to each well. The plates were wrapped in tinfoil and incubated in the dark at 37°C for 2 hours.
3. The enzymatic reaction was stopped by the addition of 50 µls of 1M NaOH to each well.

   The plate was read in a dual beam plate reader at 405 nm with a reference wavelength of 620 nm.

2.10 *In vitro* invasion assay – experimental procedure

Invasion assays were performed using the method of Albini (1998) using commercial invasion assay kits (Beckton Dickinson, CAT # 354480). The invasion assay kits were allowed to come to room temperature before use, were rehydrated on the top and bottom of the insert with 0.5ml pre-warmed serum-free media for 2 hours at 37^{o}C.

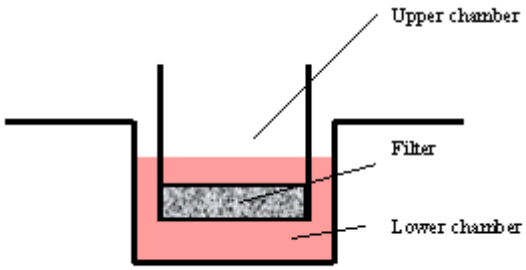

Following this incubation, the media underneath the insert was replaced with pre-warmed media containing 5% FCS. The cells were trypsinised, counted and resuspended in pre-warmed media containing 5% FCS at a density of 1x10^{6} cells/ml. 100µl of the cell suspension was added to each insert. The cells were incubated at 37^{o}C for 24 hours. After this time, the inside of the insert was wiped with a wet cotton

swab and the underside of the insert stained with 0.25% crystal violet for 10 minutes, followed by washing with UHP and allowed to air dry. The inserts were then viewed under the microscope and photographed. The number of invasive cells was determined by microscopically counting 10 representative fields at 20X.

2.11 Molecular Biology Techniques

2.11.1 Genomic DNA extraction from 96 well plate cultures

This simple method, based on a protocol described by Miller et al.(1998), involves precipitation of genomic DNA out with a saturated NaCl solution.

Reagents required : Lysis buffer (10mM Tris[pH 7.7],10mM EDTA, 10mM NaCl, 05%[w/v] sarcosyl), adding 1mg/ml proteinase K just before use , 5M NaCl and absolute ethanol mixture (150µl of 5M NaCl to 10ml of cold absolute ethanol), multichannel pipettor , paper towels, 70% ethanol.

Procedure:

a) Cells were cultured in 96 well plates until 80-90 % confluency, media removed and washed twice with 1X PBS.

b) 50µl lysis buffer was added in each well, incubated the plate in humid atmosphere at 60^0C overnight (by placing plates into closed plastic Tupperware-type container with wet paper towels in a conventional oven.)

c) Next day 100µl of ethanol/NaCl added into each well using multichannel pipettor.

d) 96 well plate allowed to stand at room temperature on the bench for 30 minutes without mixing. (The nucleic acid precipitates as a filamentous network).

e) The 96 well plate carefully was inverted onto paper towel to discard NaCl/ethanol solution,

f) The bound nucleic acid in the wells was washed three times by dripping 150µl of 70% ethanol per well and discarded by inverting after each wash.

g) After the final 70% ethanol rinse, 96 well plates were inverted to dry on the bench, and the DNA resuspended in TE buffer.

2.11.2 Preparation of total RNA from cells using Rneasy Mini Prep Kit® (QIAGEN, 74104)

RNA extraction was achieved using the Qiagen RNeasy mini kit (Qiagen, 74104). This extraction is based on the guanidine thiocyanate method of extraction and yields high quality RNA. The procedure was performed as follows:

1. To harvest RNA, culture media was removed from cells in culture and the cells were washed with PBS.
2. Cells were then lysed directly in the culture dish by the addition an appropriate volume of buffer RLT containing 10µl β-mercaptoethanol per ml of buffer RLT. 350µl RLT was used to lyse less than 5 x 10^6 cells, while 600µl RLT was used to lyse between 5 x 10^6 and 1 x 10^7 cells.
3. This suspension was then homogenised by passing it through a 20-guage needle fitted to an RNAse free syringe at least five times.
4. One volume of 70% ethanol was then added to the homogenised sample and mixed well by pipetting. This sample was then applied to an Rneasy mini column placed in a 2ml collection tube and centrifuged for 15s at 10,000rpm. The flow through was discarded.
5. 700µl of buffer RW1 was applied to the Rneasy column. The tube was closed and centrifuged for 15s at 10,000rpm to wash the column. The flow through and the collection tube were discarded at this point and the Rneasy column transferred to a new collection tube.
6. 500µl of buffer RPE was applied to the column, the lid closed and the tube centrifuged for 15s at 10,000 rpm to wash the column. The flow through was discarded and a further 500µl of buffer RPE applied to the Rneasy column. The tube was then closed and spun for 2 min at 10,000rpm to dry the silica-gel membrane.
7. The RNA was then eluted in a new 1.5ml collection tube using 20µl Rnase-free water. The tube was closed and allowed to stand for 1min and then spun for 1 min at 10,000rpm.
8. The RNA was then quantified and diluted as appropriate.

RNA concentrations were calculated by measuring OD at 260nm and 280nm and using the following formula:

$$OD_{260nm} \text{ x Dilution Factor x } 40 = \mu g/\mu l \text{ RNA}$$

The purity of the RNA extraction was determined by calculating the A_{260}:A_{280} ratio. An A_{260}:A_{280} ratio of 2 in indicative of pure RNA. Only those samples with ratios between 1.7 and 2.1 were used in this study.

2.11.3 Using the Nanodrop to measure nucleic acids

The NanoDrop is a cuvette free spectrophotometer. It uses just 1µl to measure from 5 ng/µl to 3000 ng/µl of nucleic acids in solution. Before applying the RNA sample the pedestal was wiped down using a lint-free tissue dampened with UHP. 1µl of UHP was then loaded onto the lower measurement pedestal. The upper sample arm was then brought down so as to be in contact with the solution. "Nucleic acid" was selected on the Nanodrop software to read the samples. After the equipment was initialised the "blank" option was chosen, and after a straight line appeared on the screen the "measure" option was selected. All sample readings were automatically saved as text files which could be viewed using Microsoft excel. The upper and lower pedestals were cleaned with a clean dry wipe between samples. When finished, the pedestal was cleaned with a wipe dampened with UHP followed by drying with a dry wipe. The purity of the RNA extraction was determined by calculating the A_{260}:A_{280} ratio. An A_{260}:A_{280} ratio of 2 is indicative of pure RNA. Only those samples with ratios between 1.7 and 2.1 were used in this study.

2.11.4 Relative qRT-PCR

The number of copies of an mRNA transcript of a gene in a cell or tissue is determined by the rates of its expression and degradation. The **real-time PCR** system is based on the detection and quantitation of a fluorescent reporter (Lee, 1993; Livak, 1995). There are two conventional real time PCR methods SYBR® Green and TaqMan probe based. The former was the first to be used in real-time PCR. It is a fluorescent dye that binds to double-stranded DNA and emits light when excited. Unfortunately, it binds to any double-stranded DNA which could result in a non-

specific signal, especially compared with the specificity found with TaqMan probe based method. This uses a fluorogenic probe which is a single stranded oligonucleotide of 20-26 nucleotides and is designed to bind only the DNA sequence between the two PCR primers. So total RNA was extracted (Section 2.8.2 or 2.8.3) and cDNA synthesised as per Section 2.8.5 and experiments were performed in triplicate, according to the manufacturer's instructions. Reverse transcriptase (RT) reactions were performed using micropipettes which were specifically allocated to this work. To form cDNA, high-capacity cDNA reverse transcription kit (Applied Biosystems) was used the following reagents were thawed and mixed on ice (Table 2.6) in a 0.5ml eppendorf (Eppendorf, 0030 121.023)

Table 2.6 to prepare 2X RT Master mix (per 20 µl reaction)

Components	In 20 µl reaction
10X RT buffer	**2.0**
25X dNTP mix(100mM)	**0.8**
10X RT Random Primers	**2.0**
MultiScribe™ reverse transcriptase	**1.0**
RNase inhibitor	**1.0**
Nuclease free H_2O	**3.2**
Total per reaction	**10.0**

The master mix was placed on ice and mixed gently, cDNA reverse transcription reaction was prepared by adding 10 µl 2X RT master mix into an individual tube, 10 µl of RNA sample (200-500ng final concentration recommended) was pipetted into master mix containing tubes, sealed briefly, centrifuged and loaded onto thermal cycles(Hybaid)

Thermal cycles

Temperature Hold	Time duration in min.
25^0C	10
37^0C	120
85^0C	5
4^0C	∞

After completion of the reaction cDNA was ready for quantitative PCR.

Component	Per Reaction
2x Sybergreen master mix	12.5
Forward & Reverse primer (10µM)	1µl each
UHP	8.5µl
cDNA	2.0µl
Total	25µl

Thermal cycles

Step	Temperature Hold	Time	Cycle
Denature	95^0C	10 minutes	1
Denature	95^0C	15 seconds	
Annealing & Extend	60^0C	30 seconds	40

2.11.5 Non-Quantitative Polymerase chain reaction

A standardised polymerase chain reaction (PCR) procedure was used in this study. The reactions were carried out in 0.5ml safe-lock eppendorf tubes (Eppendorf, 0030 121.023). All reagents had been aliquoted and stored at –20^{o}C and all reactions were

carried out in a laminar flow cabinet. Primers and annealing temperatures are detailed in the Table 2.9. A typical PCR tube contained the following:

Component	Per Reaction
25mM $MgCl_2$	1.5µl
10x PCR Buffer	2.5µl
Forward & Reverse primer (10µM)	1µl each
UHP	6.5µl
DNA	2.5µl
Taq/dNTP mixture*	10µl
Total	25µl

*= 0.5µl 10mM dNTP's (10mM of each dNTP; Sigma, D 5038)

0.25µl of 5U/µl *Taq* DNA polymerase enzyme (Sigma, D-4545), 9.25µl of UHP

Platinum Supermix based PCR reaction

Component	Per Reaction
DNA	2.5µl
Forward primer(10µM)	1µl
Reverse primer (10µM)	1µl
Platinum Supermix	21.5µl
Total	25 µl

DNA was amplified by PCR as follows:

Step	Temperature Hold	Time	Cycle
Denature	95^0C	5 minutes	1
Denature	95^0C	30 seconds	*35
Anneal	X^0C	30 seconds	
Extend	72^0C	30 seconds	
Final Extension	72^0C	10minutes	1
Hold	4^0C	∞	

*The cycle number varied with primers used but was generally 35 cycles.

X = the annealing temperature varied with primer set used (see over)

The reaction tubes were then stored at 4^oC for analysis by gel electrophoresis.

Table 2.9 PCR primers used for developing targetable plasmid vector

Primer Name	**Sequence => 5'->3' Direction**	**Tm.*(^{0}C)**
pEGFP-C1-2864.s	GTG CTC GAC GTT GTC ACT GAA	59.8
pEGFP-C1-3012.as	GCC GGA TCA AGC GTA TGC	58.2
gfp1079F	ACA AGC AGA AGA ACG GCA TCA	57.9
gfp1231R	CGG ACT GGG TGC TCA GGT A	61.0
CMV(FseI).s	AAA CGT GGC CGG CCT AGT TAC TTA AT	63.2
CMV(SpeI).as	AAC TGA CTA GTG GAT CTG ACG GT	60.6
Cla_loxp_Avr.s	ATC GAT ATA ACT TCG TAT AAT GTA TGC TAT ACG AAG TTA TC	65.4
Cla_loxp_Avr.as	CCT AGG ATA ACT TCG TAT AGC ATA CAT TAT ACG AAG TTA TAT	66.5
Mlu_Ase_linker.s	ACG CGT GGT CAG CAT AGT TAA GTA T	61.3
Mlu_Ase_linker.as	TAA TAC TTA ACT ATG CTG ACC A	52.8

pEGFP-C1-810F	CTA CGG CGT GCA GTG CTT C	61.0
pEGFP-C1-1309R	CGA GAG TGA TCC CGG CG	60.0
cmv-C1-532F	TAG GCG TGT ACG GTG GGA G	61.0

*** Anneal Temperature typically =Tm-5^{0}C**

Table 2.10 PCR primers used for screening LINE-1 specific homologous recombination

Primer Name	Sequence => 5'->3' direction	Tm.*(^{0}C)
L15'arm(FseI).as	ACA TTT GGC CGG CCT CGG TTTGC	66.0
L15'orf2_3360.s	CCA GAT TCA TAA AGC AAG TCC TCA	59.3
L1Cmv_5351.as	TTA TAT AGA CCT CCC ACC GTA CAC G	63.0
5'L1orf2_3358.s	ACC CAG ATT CAT AAA GCA AGT CCT C	61.3
5'L1orf2_4532.as	TGG CCT CAT AAA ATG AGT TAG GG	58.9
L1(1)-2611.s	GAG AGA AAG GTC GGG TTA CCC TCAA	64.6
L1(1)-5895.as	TCA GGA TGA TCT GGA CGA AGA GCA T	63.0
L1(2)-2615.s	GAA AGG TCG GGT TAC CCT CAA A	60.3
L1(2)5898.as	CGA TCA GGA TGA TCT GGA CGA A	60.3
L1(3)-2612.s	AGA GAA AGG TCG GGT TAC CCT CAA	62.7
L1(3)-3439.as	AGG ATG ATC TGG ACG AAG AGC AT	60.6
L1(4)-2632.s	TCA AAG GAA AGC CCA TCA GAC TAAC	61.3
L1(4)-3444.as	CGA TCA GGA TGA TCT GGA CGA AGA	62.7
PL1-7.s	TAC GTC TGA TTG GTG TAC CTG AAA GTG ATG T	65.5
PL1-7.as	CTA ATG ACC CCG TAA TTG ATT ACT ATT AAT AAC GG	64.8
PL1-8.s	TCC TGA AGG AAG CGC TAA ACA TGG AAA GG	66.7
PL1-8.as	CAT TTA CCG TAA GTT ATG TAA CGC GGA ACT CCA T	67.1
PL1-9.s	TCA TGC CAA AAT GTA AAG ACC ATC GAG ACT AG	65.6
PL1-9.as	CAG TTT ACC GTA AAT ACT CCA CCC	68.3

	ATT GAC GTC AAT	
PL1-10.s	AGA AAC TGC ATC AAC TAA TGA GCA AAA TCA CC	64.4
PL1-10.as	ATT CTA GTT GTG GTT TGT CCA AAC TCA TCA ATG T	64.7

*** Anneal Temperature typically =Tm-5^{0}C**

Table 2.11 PCR primers used for Transgene overexpression studies

Primer Name	Sequence => 5'->3'Direction	Tm.*(^{0}C)
glp1r.s_rea	CTC CTT CCA GGG GCT GAT GGT G	65.8
glp1r.as_rea	CTG GTG GGA CAC TTG AGG GGC T	65.8
kcj8.s_rea	GTG GAA TGG AGA AAA GTG GTT TG	58.9
kcj8.as_rea	TGA TCA AAC CCA CAA TAT TCT GG	57.1
tfpi2.s_rea	AGC TAC TTG TAT GGG CTT CTG C	60.3
tfpi2.as_rea	TTT GCA ATC CTC CCT GCT AAC AA	58.9
s100a13.s_rea	ACC TCT TCA GGA AAG CCA TCT GA	60.6
s100a13.as_rea	TTC CGG CCC TCC TGC CTT GCA AA	66.0
actinB.s	TGG ACA TCC GCA AAG ACC TGT AC	62.4
actinB.as	TCA GGA GGA GCA ATG ATC TTG A	58.4

*** Anneal Temperature typically =Tm-5^{0}C**

Table 2.12 PCR primers used for mir-29a cloning

Primer Name	Sequence=> 5'->3' direction	Tm.*(^{0}C)
mk29a.s	AAA CCG GAT CCG AGC CCA ATG TAT GCT GGA TTT AG	70

mk29a.as	CCC AAC TCG AGT TAA GCT TTG TTT TCT TAG TTC TTG TCC ATG G	69

*** Anneal Temperature typically =Tm-5^{0}C**

Table 2.13 PCR primer used for siRNA knockdown studies

Primer Name	Sequence=> 5'->3' direction	Tm.*(^{0}C)
ran_mk-160F ran_mk-285R	GTT GGT GAT GGT GGT ACT GGA A TCC TCT GTT GGT GTG GAA CAC T	60.3 60.3
mif_mk-216F mif_mk-317R	GAA CCG CTC CTA CAG CAA GCT TTG GCC GCG TTC ATG TC	61.8 55.2
anxa2_mk-136F anxa2_mk-286R	TGT TCA CGA AAT CCT GTG CAA CTC ATC CAC ACC TTT GGT CTT G	55.9 60.3
grb_mk-464F grb_mk-964R	TGG TAC AAG GCA GAG CTT AAT GG AGG CAG CTT GTG GGT TTA ATT C	60.6 58.4
myc-MK-1312F myc-MK-1457R	CCA GCA GCG ACT CTG AGG A GAC CAG TGG GCT GTG AGG AG	61.0 63.5

*** Anneal Temperature typically =Tm-5^{0}C**

Table 2.14 PCR primers used for 3'RAN UTR cloning

Primer Name	Sequence => 5'->3' direction	Tm.*(^{0}C)
ran_3'utr-753F	AAA AAG CTT TGA GAA TGA AGC TGG AGC CCA G	66.8
ran_3'utr-1656R	CCC GGA TCC CGG CTT GCG TAT CAA CTT CAC A	72.1

*** Anneal Temperature typically =Tm-5^{0}C**

2.12 MicroRNAs

2.12.1 Organic RNA extraction using MirVana miRNA isolation Kit

The mirVana^{TM} miRNA isolation kit (catalogue # 1560, 1561) designed for purification of RNA suitable for studies of both siRNA and miRNA. The kit employs organic extraction followed by immobilization of RNA on glass-fibre filters to purify either total RNA, or RNA enriched for small species, from cells or tissue samples. The total RNA from cell samples was isolated as per the manufactures protocol a recommended 10^2-10^7 cells were used for RNA extraction.

I Cell lysis

a) Trypsinised cells (section 2.6) were washed cells by gently re-suspending in 1ml of 1XPBS and pelleted at low speed.

b) PBS removed and cells resuspended in 300-600µl lysis/binding solution.

c) Samples vortexed vigorously to ensure complete lysis of the cells and to obtain a homogenous lysate.

II Organic Extraction

a) MiRNA homogenate was added, 1/10th volume of cell lysate and vortexed and left on ice for 10 minutes.

b) Equal volume of Acid-phenol: Chloroform added to lysed homogenate samples and vortexed for 30-60s.

c) Centrifuged samples for 5 min at maximum speed (10,000xg) at room temperature to separate the aqueous and organic phases

d) The upper aqueous phase was pipetted out into fresh tube without disturbing the lower phase and volume removed was noted

III Final RNA isolation

a) 1.25 volumes of room temperature 100% ethanol was added to aqueous

phase.

b) Pipetted lysate/ethanol mixture onto filter cartridge placed in collection tube, and centrifuged for ~15 sec to pass the mixture through the filter at 10,000xg.

c) Flow through was discarded , and to the filter cartridge 700µl of miRNA wash solution 1 was added and centrifuged for ~ 5-10 sec.

d) Flow through discarded and to the filter cartridge 500µl wash solution 2/3 was added and centrifuged, these steps repeated and flow through discarded.

e) The filter cartridge was transferred to a new collection tube , 100µl of pre-heated (95^0C) nuclease free water added to the center of the filter, and the cap closed. Centrifuged for ~20-30 sec at maximum speed to recover the RNA. The collected eluate was quantified as mentioned Section 2.11.3 and stored at -80^0C until further use.

2.12.2 Relative quantity of mirs by qRT-PCR

Reagent preparation

Dilution of *mir* Vana RT primer to 1X concentration

mirVana gene-specific RT Primers are supplied as 10X stock solutions. These were diluted to 1 X concentration with nuclease-free water to make a working stock. They were mixed thoroughly by vortexing and briefly centrifuged.

Volume and amount

RNA concentration was adjusted with nuclease-free water so that 1 µL of RNA solution was used per reaction (25ng/µl).

Preparation for reverse transcription (RT) Master Mix

a) Vortex all the RT reagents, except the Array Script™ Enzyme which is mixed just before use. RT reagents were kept on ice.

b) A RT Master Mix was prepared with the reagents that were shared across most of samples using Table 2.7

Table 2.7 Final composition of the RT reaction

Per Reaction	Component
to 10µl	Nuclease free water
2µl	mirVana 5X RT buffer
1µl	1X mirVana RT primer*
1µl	25ng/µl RNA
0.4 µl	ArrayScript Enzyme mix
10µl	Final volume

Diluted from the 10X stock supplied

a) 9µl of RT master mix was aliquoted into individual wells of a 96 well PCR plate

b) 1µl RNA samples were added to each aliquot of RT master mix aliquoted wells,

c) For the no-template control reactions, nuclease-free water was added. For the primer control, nuclease free water was substituted instead of primers

d) The RT reaction was performed by incubating for 30 min at 37°C, then for 10 min at 95°C in thermal cycler (Applied Biosystems 7500) After completion of reaction sample plate was placed on ice and PCR was performed immediately.

For real-time PCR, add SYBR Green I to the *mir* Vana 5X PCR Buffer

To prepare the PCR master mix the components shown in table (2.8) were assembled on ice. SYBR Green I (provided at 10,000 X concentration) was diluted, 1:7 (v/v) with dimethyl sulfoxide or nuclease-free water. Then 1.2 µL of the diluted dye was added to the *mir* Vana 5 X PCR Buffer supplied with the kit. Vortex to mix followed by a brief centrifuge.

Table 2.8 PCR Master Mix

Per Reaction	Component
5µl	mirVana5X PCR buffer
0.5µl	50X ROX
1U(0.2µl)	Thermostable DNA polymerase
0.5µl	mirVana PCR primers
to 15 µl	Nuclease free water

f) The PCR master mix was mixed gently and 15µl was added to each RT reaction

g) Thermal cycling was done as follows

Step	Temperature Hold	Time	Cycle
Denature	95^0C	3 minutes	1
Denature	95^0C	15 seconds	
Annealing & Extend	60^0C	30 seconds	40

2.13 Plasmid DNA isolation

E.coli cultures were streaked on LB agar (table surface was sterilised before use), containing appropriate selection antibiotic (Ampicillin or Chloramphenicol) and incubated at 37°C overnight. From these, a single colony was inoculated into 5ml LB broth (table 2.5, autoclaved before use) containing appropriate selection antibiotic and was grown for 8 hours with shaking at 37°C and was subject to a DNA mini preparation using the Qiagen Plasmid DNA Extraction Mini Kit (Qiagen, 12143) according to the manufacturer's instructions. The DNA concentration was determined by measuring the OD_{260nm}. Plasmid was stored at –20°C until required.

2.13.1 Restriction Enzyme Digestion

5 µls of each isolated plasmid sample was run out on a 1% agarose gel to check for degradation. Restriction digestion was then carried out to confirm orientation of the insert. All digestions were carried out using the recipe as outlined in Table 2.15

Table 2.15 Standard DNA digestion mix

Component	Volume (µls)
DNA sample (0.5-1µg)	2
undiluted enzyme (5units)	1
BSA (10mg/ml)	0.2
10X appropriate buffer	2
UHP	14.8

All 20 µls were run out on a 1% agarose gel together with 3 µls loading dye (Section 2.8.12). From this information, samples were selected for large-scale plasmid preparation.

2.13.2 Plasmid DNA Ligation or sub cloning

A known quantity (section 2.8.7) of each plasmid or PCR product was digested with the appropriate restriction endonuclease for 3hr at 37^{o}C to remove the sequence of interest for insertion into the target expression vector. These restriction digests were analysed by TAE low melt 1% gel electrophoresis and the relevant fragment size excised from the gel using a fresh clean blade for each excision. The DNA was purified from the gel by the addition of PB buffer (Qiagen Gel Purification Kit) to each gel slice; this was melted at 55^{o}C for 10min and applied under vacuum to a gel purification column. The DNA was column washed with 750µl of PE buffer under vacuum and centrifuged at 13,000rpm for 1min to dry. The pellet was re-dissolved in 15µl EB buffer and a portion of this run out on a 1% TAE agarose gel. This ensured that the cDNA fragment was not contaminated and thus suitable for ligation. Each insert was ligated with known plasmid vector backbone (digested with matching REs)

at 15°C overnight in a mastermix typically containing expression vector (100ng), target insert cDNA (300ng), water, 10X ligation buffer and T4 ligase (2.5U) in a total volume of 10µl.

2.13.3 Transformation procedure

A bacterial cell suspension (100µl) of competent JM109 (Promega, L2001) or XL Blue-1 (Stratagene, # 200130) was mixed with ligated DNA and placed on ice for 40min after which the mixture was heat-shocked at 42°C for 30 to 90s and then placed on ice for 3min. LB broth (1ml as mentioned in table 2.8 autoclaved before use) was added to the competent cell suspension and incubated at 37°C for 1hr. Different volumes of this suspension was spread on a selecting agar plates LB agar (table 2.16) containing appropriate antibiotic concentration of Ampicillin or chloramphenicol) and incubated overnight at 37°C. Single colonies that grew on these selecting plates were incubated into 5ml LB broth containing appropriate selection antibiotic. Single colonies inoculated into 5ml LB broth (table 2.16,autoclaved before use) containing appropriate selection antibiotic and were grown for 8hr with shaking at 37°C and were subject to a DNA mini preparation (Section 2.8.7) or Large Scale Preparation (Section 2.8.13). For a large scale DNA preparation this culture was then inoculated into 270ml LB broth containing 0.3ml Ampicillin (100mg/ml) in 1L baffled flask with shaking overnight at 37°C.

Table 2.16 LB Media preparation

Requried materials	LB broth	LB Agar
NaCl (Merk, K1880814)	10g	10g
Tryptone(Oxoid, L42)	10g	10g
Yeast extract(Oxoid, L21)	5g	5g
Bacto Agar	-	20g
Distilled water	1000ml	1000ml

2.13.4 Agarose Gel Electrophoresis of Plasmid DNA or PCR Products

A 1% agarose gel (Sigma, A-9539) was prepared in 1X TAE buffer (diluting 50X TAE buffer) (242g Tris base, 57.1ml Acetic acid, 100ml 0.5M EDTA, 996ml UHP) and melted in a microwave oven. After being allowed to cool down, 0.003% (v/v) of a 10mg/ml ethidium bromide solution was added to the gel which was then poured into an electrophoresis apparatus (BioRad). Combs were placed in the gel to form wells and the gel allowed to settle. 5µl of loading buffer (50% glycerol, 1mg/ml xylene cyanol, 1mg/ml bromophenol blue, 1mM EDTA) was added to 20µl plasmid restriction digestion reaction or 25µl PCR samples and 10µl was run on the gel at 80-90mV for approximately 2 hours. When the dye front was seen to have migrated the required distance, the gel was removed from the apparatus and examined on a UV-transluminator and photographed.

2.13.5 Plasmid DNA sequencing

In order to fully confirm the orientation and the origin of the inserted DNA in the plasmids, each plasmid was sent for sequencing (MWG DNA sequencing facility, Germany, typically plasmid sample with known primer sequence sent) and approximate 500-900bp sequence read out were received from each successful sequencing reaction. Once these parameters had been confirmed, transfection could be carried out.

2.13.6 Maxi preparation of Plasmid DNA

Plasmid DNA was purified using an endofree plasmid maxi kit (Qiagen, 12362). Following growth of plasmid culture in into 270ml LB (table 2.16) broth containing 0.3ml ampicillin (100mg/ml) in 1L baffled flask with shaking overnight at 37^{o}C, the culture was split into 2 x 250ml centrifuge bottles and spun at 3,500rpm for 15min at 4^{o}C. Pellets were weighed and either frozen at –80^{o}C until required or processed further. The bacterial pellet was resuspended in 10ml buffer P1. To this, 10 ml buffer P2 was added, mixed gently and incubated at room temperature for 5min. A volume

of 10ml chilled buffer P3 was added to the lysate and mixed immediately and gently. The lysate was poured into the barrel of the QIA-filter cartridge and incubated at room temperature for 10min. The cap from the QIA filter outlet nozzle was removed and the plunger was gently inserted in to the cartridge. The cell lysate was filtered into a 50ml tube. To the lysate, 2.5ml buffer ER was added and mixed by inverting repeatedly. This was incubated on ice for 30min. Quiagen-tip 500 was equilibrated by applying 10ml buffer QBT and the column was allowed to empty by gravity flow. The filtered lysate was then applied to the Quiagen-tip and allowed to enter the resin by gravity flow. The Quiagen-tip was washed twice with 30ml buffer QC. The DNA was eluted by addition of 15ml buffer QN and the eluate was collected in a 30ml tube. The DNA was precipitated by adding 10.5ml isopropanol to the eluted DNA. This was mixed and centrifuged at ~10,000rpm for 30min at 4^0C. The DNA pellet was washed with 5ml of 70% ethanol and this was centrifuged at ~10,000rpm for 10min. The pellet was air-dried and dissolved in 500µl buffer TE. The DNA concentration was determined by measuring the $OD_{260nm.}$

2.14 Western Blot analysis

Proteins for western blot analysis were separated by SDS-polyacrylamide gel electrophoresis (SDS-PAGE).

2.14.1 Sample preparation

Cells were scraped directly on culture dishes using lysis buffers: (8M urea (Sigma, U6504), 4 % (w/v) CHAPS (Sigma, C5070), 2M thiourea (Sigma 88810) 30mM, Tris Base (Sigma, T1378), pH to 8.5 with dilute HCl). Lysis was carried out over twenty min on ice and following vortexing, the lysate was spun at 4^oC for 15 min at maximum speed to remove any insoluble debris. The protein was quantified using the method of Bradford (Bio-Rad; 500-0006) and the protein samples were supplemented with 2X Lamelli sample buffer (contains loading dye, Sigma-Aldrich S 3401) and water to a final stock concentration of 2µg/µl. Sample and then boiled for 2 min and stored at -20^oC until required.

2.14.2 Quantification of protein

Protein levels were determined using the Bio-Rad protein assay kit (Bio-Rad; 500-0006) with a series of bovine serum albumin (BSA) (Sigma, A9543) solutions as standards. A stock solution of 2 mg/ml BSA(Bio-Rad) was used to make a standard curve. 10 µl samples were diluted into tubes in a stepwise fashion from 0 – 2 mg/ml BSA. The Biorad was first filtered through 3MM filter paper (Schleicher and Schuell, 311647) and then diluted 1/5 with UHP as it was supplied as a 5-fold concentrate. The diluted dye reagent (490 µls) was added to each standard and sample tube and the mixtures vortexed. The 500 µl samples were diluted out in 100 µl aliquots onto a 96-well plate (Costar, 3599). After a period of 5 min to 1h, the OD_{570} was measured, against a reagent blank. From the plot of the OD_{570} of BSA standards versus their concentrations, the concentration of protein in the test samples was determined. From this, a relative volume for each protein sample was determined for loading onto the gels. Usually 10-20 µg protein per lane was loaded.

2.14.3 SDS Acrylamide Gel electrophoresis

Resolving and stacking gels were prepared as outlined in (Table 2.17) and poured into clean 10cm x 8cm gel cassettes that consisted of 2 glass plates separated by a plastic spacer. The resolving gel was poured first and allowed to set. The stacking gel was then poured and a comb placed in the stacking gel in order to create wells for sample loading. Once set, the gels could be used immediately or wrapped in aluminium foil and stored at $4^{o}C$ for 24 hours.

Table 2.17 Preparation of electrophoresis gels

Components	Resolving gel (10%)	Resolving gel (12%)	Stacking gel
30% Acrylamide stock[*1]	2.38 mls	2.8 mls	330 µls
Ultrapure water	2.66 mls	2.24 mls	1.4 mls
1.5M-Tris/HCl, pH 8.8	1.82 mls	1.82 mls	-
0.5M-Tris/HCl, pH 6.8	-	-	250µls
10% SDS (Sigma, L-4509)	70 µls	70 µls	20 µls
10% Ammonium persulphate (Sigma, A-1433)	70 µls	70 µls	20 µls
TEMED (Sigma, T-8133)	2.8 µls	2.8 µls	2µls

[1] Acrylamide stock solution consists of 29.1g acrylamide (Sigma, A8887) and 0.9g NN'-methylene bis-acrylamide (Sigma, 7256) dissolved in 60ml UHP water and made up to 100ml final volume. The solution was stored in the dark at 4°C for up to 1 month. All components were purchased from Sigma, SDS (L-4509), NH_4-persulphate (A-1433) and TEMED, N,N,N,N'-tetramethylethylenediamine (T-8133).

2.14.4 Protein transfer and Western blotting

Following electrophoresis, the acrylamide gels were equilibrated in transfer buffer (25mM Tris, 192mM glycine (Sigma, G-7126) pH 8.3-8.5 without adjusting) for 20 min. Proteins in gels were transferred onto Hybond ECL nitrocellulose membrane (Amersham, RPN 2020D) using a semi-dry transfer cell (Biorad). Eight sheets of Whatman 3mm filter paper (Whatman, 1001824) were soaked in transfer buffer and placed on the cathode plate of a semi-dry transfer cell. Excess air was removed from between the filters by moving a glass pipette over the filter paper. Nitrocellulose membrane, cut to the same size of the gel, was soaked in transfer buffer and placed

over the filter paper, ensuring that there were no air bubbles. The acrylamide gel was placed over the nitrocellulose and four more sheets of pre-soaked filter paper were placed on top of the gel. Excess air was again removed by rolling the pipette over the filter paper. The proteins were transferred from the gel to the nitrocellulose membrane at 0.34 Amps (15 Volts) for 30 min.

From this point on, all further steps were carried out on a revolving apparatus to ensure even exposure of the membrane blot to all reagents. Following transfer, the membranes were blocked in fresh filtered 5% non-fat dried milk (Cadburys; Marvel skimmed milk) in PBS (20mM Tris, 0.15M NaCl)/0.1% Tween 20 (Sigma, P1379), pH 7.4 for 2 hours. After blocking, the membranes were rinsed with TBS/0.1% Tween and incubated with primary antibody overnight at 4^{o}C. Primary antibodies used are listed in Table 2.18. The following day the primary antibody was removed and the membranes rinsed three times with PBS/0.1% Tween. The membranes were then incubated in 1/1000 dilution of suitable HRP-labelled secondary antibody (Anti-Mouse (abcam); anti-Rabbit (abcam) or Goat;) in 1% marvel for 1 hour at room temperature (R.T.). The secondary antibody was then removed and blots were washed three times for 15 min in PBS/0.1% Tween. Bound antibody was detected using enhanced chemiluminescence (ECL) (Section 2.9.4).

All incubation steps from now on, including the blocking step, were carried out on a revolving apparatus (Stovall, Bellydancer) to ensure even exposure of the blot to all reagents. The Nitrocellulose membranes (Amersham,) were blocked for 2 hours at room temperature with fresh filtered 5% non-fat dried milk (Cadburys, Marvel skimmed milk) in Phosphate-buffered saline (PBS) with 0.5% Tween (Sigma, P-1379) pH 7.5. After blocking, the membranes were rinsed once in 1X PBS and incubated with 5 to 10 mls primary antibody. The specific conditions for each antibody are outlined in table 2.18 below. Bound antibody was detected using enhanced chemiluminescence (ECL).

Table 2.18 List of primary antibodies used for western blot analysis

Antibody	Dilution/ concentration	Supplier	Catalogue no.
GFP (R)[2]	1/500	Abcam	ab610270
GAPDH (M)[1]	1/5,000	Abcam	ab 9482
GLP1R(R)[2]	1/1000	Abcam	ab1583816
KCNJ8 (C)[3]	1/1000	Gift	---
TFPI2(M)[1]	1/200	Gift	----
RAN(R)[2]	1/1000	Abcam	ab4781

(M)[1] = Mouse anti-human IgG

(R)[2] = Rabbit anti-human IgG

(C)[3] = Chicken IgG

Table 2.19 List of secondary antibodies used for western blot analysis

Antibody	Dilution/ concentration	Supplier	Catalogue no.
Mouse	1/1000	Abcam	abP0260
Rabbit	1/1000	Abcam	abP0448
Goat	1/1000	Abcam	abE0466
Chicken	1/1000	Abcam	ab49710

2.14.5 Enhanced chemiluminescence detection

Protein bands were developed using the enhanced chemiluminescence kit (ECL) (Amersham, RPN2109) according to the manufacturer's instructions.

After blots were washed in PBS/0.1% Tween three times for 5 min, a sheet of parafilm was flattened over a smooth surface, *e.g.* a glass plate, ensuring all air bubbles were removed. 1.5ml of ECL detection reagent 1 and 1.5ml of reagent 2 were mixed and covered over the membrane. Charges on the parafilm ensured the fluid remained on the membrane. The reagent was removed after one min and the membrane wrapped in cling film. The membrane was exposed to autoradiographic film (Roche) in an autoradiographic cassette for various lengths of time, depending on the strength of signal obtained. The autoradiographic film was then developed for 5 min in developer (Kodak, LX24), diluted 1:6.5 in water. The film was briefly immersed in water and transferred to a Fixer solution (Kodak, FX-40) diluted 1:5 in water, for 5 min. The film was transferred to water for 5 min and then air-dried.

2.14.6 2-D Fluorescence Difference Gel Electrophoresis

The proteomics work mentioned in the thesis was carried with the help of Dr. Paul Dowly and Mr. Michael Henry, NICB). Cell samples were collected (section 2.7.7). The cell samples were lysed in 2D-DIGE lysis buffer ((8M urea (Sigma, U6504), 4 % (w/v) CHAPS (Sigma, C5070), 2M thiourea (Sigma 88810) 30mM, Tris Base (Sigma, T1378), pH to 8.5 with dilute HCl) and protein quantified (section 2.14.1 and 2.14.2). 3 biological replicates with 4 conditional transfection were used in the study. The protein samples were cleaned up using Ready Prep^{TM} 2D clean up kit (Bio-Rad, catalogue # 163-2130). DIGE analysis or for the identification of proteins of interest by mass spectrometry was used (see section 2.20)

2.14.7 Preparation of dye stock solution (1 nmol/µl)

The three CyDye DIGE Fluor Minimal dyes (Cy3, Cy5 and Cy2 (Amersham, 25-8010-65) were thawed from –20 ^{o}C to room temperature for 5 minutes. To each microfuge tube dimethylformamide (DMF) (Aldrich, 22,705-6) was added to a

concentration of 1 nmol/ µl. Each microfuge tube was vortexed vigorously for 30 seconds to dissolve the dye. The tubes were then centrifuged for 30 seconds at 14,000rpm in a microcentrifuge. The reconstituted dyes were stored at –20 ^{o}C for up to two months.

2.14.7.1 Preparation of 10 µl working dye solution (200 pmol/µl)

On thawing, the dye stock solutions were centrifuged in a micro centrifuge for 30 seconds. To make 10 µl of the three working dye solutions, 8 µl of DMF was added to three fresh eppendorf labelled Cy2, Cy3 and Cy5. A 0.2 nmol/µl volume of each of the reconstituted dye stock solutions was added to their respective tubes. The dyes were stored at -20 ^{o}C in tinfoil in the dark for 3 months.

2.14.7.2 Protein sample labelling

4 samples equivalent to 50 µg was placed into twelve eppendorf tubes in biological triplicates and were used for labelling. They are Anti microRNA inhibitor negative control , Anti hsa-mir-29a inhibitor(treated with each 1µl Cy3) and Pre microRNAs negative control, Pre hsa-mir-29a(treated with Cy5) 3 treated protein (6 for Cy3 and the other 6 for Cy5). Each tube was mixed by vortexing, centrifuged and then left on ice for 30 minutes in the dark. To stop the reaction, 1µl of 10 mM lysine was added; the tubes were vortexed, centrifuged briefly and left on ice for 10 minutes in the dark. The labelled samples were stored at –80 ^{o}C. The Cy2 pool for each gel (50 µg) to this tube 1µl of working dye solution was added.

2.14.7.3 Preparing the labelled samples for the first dimension

The protein samples labelled with Cy2 (pooled internal standard), Cy3 and Cy5 were thawed on ice (in the dark), combined by placing into a single eppendorf tube and mixed. An equal volume of 2X sample buffer (2.5 ml rehydration buffer stock solution (8M urea, 4 % CHAPS), pharmalyte broad range pH 3-11 (2%) (Amersham, 17-6000-86), DTT (2%) (Sigma, D9163) was added to the labelled protein samples. The mixture was left on ice for at least 10 minutes then applied to Immobiline DryStrips for isoelectric focussing.

2.14.7.4 Strip rehydration using Immobiline DryStrip reswelling tray

Isoelectric focussing of all samples was carried out using immobiline pH gradient (IPG) strips. The protective lid was removed from the Immobiline Dry Strip Reswelling tray. The tray was levelled using the spirit level. A 350µl volume of rehydration buffer solution (with 2 % pharmalyte broad range pH 3-11 and 2 % DTT) was slowly pipetted into the centre of each slot, all air bubbles generated were removed. The cover film from the IPG strip (pH range 3-11, Amersham, 17-1233-01) was removed and positioned with the gel side down and lowered. To ensure the entire strip was evenly coated the strip was gently lifted and lowered onto the entire surface of the solution avoiding trapping air bubbles. Each strip was overlaid with about 3 ml of IPG Cover Fluid (Amersham, 17-1335-01) starting on both ends of the strip, moving to the centre. The protective lid was then replaced and the strips were left at room temperature to rehydrate overnight (or at least 12 hours).

2.14.7.5 Isoelectric focussing using the IPGphor manifold

Following the rehydration procedure, the Manifold (Amersham) was placed onto the IPGphor unit by inserting the "T" shape into the hollow provided. A 9 ml volume of Cover Fluid was placed into each of the twelve lanes in the tray in order to cover the surface. Two wicks (Amersham, 80-6499-14) per strip were placed on tinfoil and 150 µl of UHP was pipetted onto each one to rehydrate them. The rehydrated strips were placed in the correct orientation (+ to anode) and aligned just below the indented mark, to allow for the wicks to overlap the strip. The rehydrated wicks were then placed over both the cathodic and anodic ends of all the strips. The wicks were checked to ensure they were positioned over the gel portion of the strip and avoiding the indent in the lane so as to guarantee a good contact with the electrodes. The sample cups (Amersham, 80-6498-95) were then positioned approximately 1 cm from the cathodic end of the strip and an insertion tool was used to securely "click" the cups into place. The electrodes were then fitted with their "Cams" open and in direct contact with the wicks.

The amount of protein loaded per strip was 75ug for screening, 150ug for DIGE or 300ug for spot picking. The protein samples were prepared by centrifuging to remove any insoluble material and the appropriate volume was loaded with a pipette tip placed just beneath the surface of the cover fluid. The cover of the IPGphor unit was closed and the desired programme selected. The temperature was set for 20^{o}C with 50μA/strip. The IEF parameters are as follows: step 1: 300 volts for 3 hours (step-and-hold), step 2: 600 volts for 3 hours (gradient), step 3 1000 volts for 3 hours (gradient), step 4: 8000 volts for 3 hours (gradient). The IEF was left at 8000 volts (step-and –hold) until ready for SDS-PAGE step. On completion of the IEF run, the strips were drained of the cover fluid and stored in glass tubes at –80^{o}C or used directly in the second dimension.

2.15 Second Dimension – SDS polyacrylamide gel electrophoresis

2.15.1 Casting gels in the ETTAN Dalt-12 gel caster

The 12.5 % acrylamide gel solution was prepared in a glass beaker (acrylamide/bis 40 %, 1.5 M Tris pH 8.8, 10 % SDS). Prior to pouring, 10 % ammonium persulfate and neat TEMED were added. Two types of plates were used, low fluorescent for DIGE experiments and hinged for preparative and screening silver stained gels. All plates (both normal hinged and low fluorescent) and casting equipment were inspected to ensure they were clean. The gel caster frame was placed on a level bench leaning on its “legs” so that the back of the caster was open and facing the operator. The plates were assembled so that the front and back plates were evenly aligned and all seals and hinges in place. A thin spacer was placed in the gel caster unit followed by an assembled plate followed by a thin spacer then another plate. The plates were positioned in the caster unit so that the lower, front plate was the furthest away from the operator and the spacers packed with their curved edges to the top. This layering was repeated until all 6 plates and spacers were in place. All plates and spacers were checked to ensure they were packed tightly together so as to minimise any gaps and air pockets. If all 6 gels were not required, up to 4 dummy plates could be substituted instead of the glass plates. When the desired amount of plates had been added, the thicker spacers were placed next to bring the level marginally over the edge of the back of the caster. The backing plate was then added to the caster frame and screwed

into place with the 6 screws provided. The silicone tubing was added to the outlet of the glass beaker and the glass tube was inserted to the other end of the silicone tubing. The glass tube was inserted into the inlet of the reservoir and the glass beaker containing the gel solution was then clamped to a retort stand. The gel solution was held in place using arterial clamps on the top tube and the tube running down from the reservoir to the caster chamber. The top tube was unclamped and the gel solution was allowed to fill the tubing and the reservoir drain. Air bubbles that had been generated were dislodged by flicking the tube. When all air bubbles had been removed the bottom clamp was released allowing the gel solution into the gel caster. When the gel solution reached the indicator line across the top of the caster, the bottom and top tubes were reclamped. The displacement solution (0.375M Tris-Cl 1.5M pH 8.8, 30% glycerol, UHP and bromophenol blue) was added to the reservoir and the glass tubing was slowly removed from the reservoir inlet. The clamp was removed from the bottom tube allowing the displacement solution into the tube and forcing the remaining gel solution into the gel caster. The gels were overlaid with 1 ml saturated butanol or sprayed with 0.1 % SDS solution. The gels were left to set for at least three hours at room temperature. Following this, the caster was gently unlocked and the gels removed and rinsed with distilled water. If the gels were not used immediately they were stored for up to four days in 1X running buffer at 4 ^{o}C. If gels were to be used for "spot picking" the plates were silanised to stick the acrylamide mixture to the plates. A volume of 2ml of (8ml ethanol, 200µl glacial acetic acid, 10µl bind-silane and 1.8ml UHP) was pipetted over the glass plate and wiped over with a lint free cloth. This was left to air dry for 15 minutes, after which 2ml ethanol and 2 ml UHP were each pipetted over the plate and wiped off respectively. The plate was left to air dry for approximately 1 hour 30 minutes.

2.15.2 Preparing the ETTAN DALT 12 electrophoresis unit

The electrophoresis chamber was prepared by adding 6.48 litres of UHP and 720 ml of 10X SDS running buffer. The pump was then turned on to cool the system to 10 ^{o}C.

2.15.3 Equilibration of focussed Immobiline DryStrips

The SDS equilibration buffer (30% glycerol, 6M urea, 50mM 1.5M Tris-Cl pH 8.8, 2% SDS, bromophenol blue and UHP) which had been prepared, aliquotted into 30 ml volumes and frozen at –20^{o}C was allowed to thaw to room temperature. Two SDS equilibration buffer solutions with DTT (65 mM) or iodoacetamide (240 mM) (Sigma, I1149) were then prepared. Using a forceps, the IPG strips* were removed from the IPGphor unit, the cover fluid was drained off by holding the strips at an angle and they were placed into individual glass tubes with the support film toward the wall. Equilibration buffer (10 mls containing DTT) was added to each tube and incubated for 15 minutes with gentle agitation using an orbital shaker. During this equilibration step, the gel cassettes were rinsed with UHP and then the tops rinsed with 1X running buffer. After the first equilibration, DTT containing equilibration solution was removed and 5 mls of the iodoacetamide containing equilibration buffer added. The strips were incubated for 10 minutes with gentle agitation. During this equilibration step, the agarose overlay solution (0.5% agarose in running buffer) was prepared and 50 ml of 1X running buffer was placed in a glass tube.

*If the strips had been frozen at this stage they were left at room temperature to thaw before the DTT-containing equilibration solution was added.

2.15.4 Loading the focussed Immobiline DryStrips

Using a forceps and holding the anode end, the IPG strips were rinsed in 1X SDS electrophoresis running buffer and placed between the two glass plates of the gel. The strip was pushed down gently using a thin plastic spacer until it came in contact with the surface of the gel. Any air bubbles trapped between the gel surface and the strip were gently removed. Approximately 1 ml of the 0.5 % agarose overlay solution was applied over the IPG strip to seal it in place.

2.15.5 Inserting the gels into the Ettan DALT 12 electrophoresis buffer tank

When the running buffer reached the desired temperature (10^{o}C) the loaded gel cassettes were wetted with UHP and inserted into the tank through the slots provided in the same orientation. When all 12 slots were filled, 2X running buffer was added to the upper chamber until the mark on the side of the chamber was reached. The cover of the unit was replaced and the required running conditions selected. The unit was run for 18–24 hours at 1.5 Watts per gel at 10°C or until the bromophenol blue dye front reached the bottom of the gel. When the run was completed, the gel cassettes were removed from the tank one at a time using the DALT cassette removal tool and rinsed with UHP to remove the running buffer.

2.16 Method for scanning DIGE labelled samples

The Typhoon Variable Mode Imager (GE Healthcare) was turned on and left to warm up for 30 minutes prior to scanning. The scanning control software was opened and the fluorescence mode was selected. The appropriate emission filters and lasers were then selected for the separate dyes (Cy2 520 BP40 Blue (488), Cy3 580 BP30 Green (532) and Cy5 670 BP 30 Red (633)). The first gel was placed in the scanner and pre-scanned at a 1000 pixel resolution in order to obtain the correct photo multiplier tube (PMT) value was always maintained between 60,000-80,000 for every scan event (to prevent saturation of the signal from high abundant spots). Once the correct PMT value was found, the gel was scanned at 100 pixel resolution, resulting in the generation of three images, one each for Cy2, Cy3 and Cy5. Once the scanning was completed, the gel images were imported into the ImageQuant software. All gels were cropped identically to facilitate spot matching in the Decyder 6.5 BVA module.

2.17 Analysis of gel images

2.17.1 Differential in-gel analysis (DIA)

The DIA module processes a triplet of images from a single gel. The internal standard is loaded as the primary image followed by the secondary and tertiary image, derived from, for example, a control and treated sample. Spot detection and calculation of spots properties were performed for each image from the same gel. The Batch process programme determined the margins of the spots, quantified the spot intensities and calculated the relative spot intensity as the ratio between the total intensity of the gel and the intensity of each individual spot. The protein spots were then normalised using the in-gel linked internal standard. The data from the first gel was XML formatted and exported into the Biological Variation Analysis (BVA) software for further analysis. This procedure was repeated for each gel in the experiment.

2.17.2 Biological variation analysis (BVA)

Once all gels from the experiment were loaded into the BVA module, the experiment design was set up and the images were assigned into three groups (standard, control and treated). The spots on the gels were then matched across all gels in the experiment. This module detects the consistency of the differences between samples across all the gels. The software standardises the relative spot intensity of the Cy5 image to that of the Cy3 image in the same gel. The standardised spot intensity was then averaged across the triplicate gels. The BVA module detected the consistency of the differences between samples across all the gels and applied statistics to associate a level of confidence for each of the differences. The protein spots with statistically significant protein expression changes were designated “proteins of interest” and placed in a pick list. Preparative gels for spot picking with 300 ug of protein/gel were focussed and run out on SDS-PAGE gels. The gels were then stained with colloidal coomassie (section 2.18). Spots that showed differential protein expression were picked with the ETTAN Spot Picker (section 2.19).

2.18 Brilliant blue G Colloidal coomassie staining of preparative gels for spot picking

After electrophoresis, the smaller lower plates with the gels attached were placed in the gel boxes containing fixing solution (7% glacial acetic acid in 40% (v/v) methanol (Aldrich, 200-659-6)) for at least one hour. During this step a 1X working solution of Brilliant Blue G colloidal coomassie (Sigma, B2025) was prepared by adding 800ml UHP to the stock bottle. When the fixing step had nearly elapsed a solution containing 4 parts of 1X working colloidal coomassie solution and 1 part methanol was made, mixed by vortexing for 30 seconds and then placed on top of the gels. The gels were left to stain for 2 hours. To destain, a solution containing 10% acetic acid in 25% methanol was poured over the shaking gels for 60 seconds. The gels were then rinsed with 25% methanol for 30 seconds and then destained with 25% methanol for 24 hours. The glass surface was dried and two reference markers (Amersham) attached to the underside of the glass plate before scanning. The resulting image was imported into the ImageMaster software (Amersham) and the spots were detected, normalised and the reference markers selected. While keeping the shift key depressed, all spots of interest were manually selected. The resulting image was saved and exported into the Ettan Spot Picker software.

2.18.1 Spot picking

The stained gel was placed in the tray of the Ettan Spot Picker (Amersham, 18-1145-28) with reference markers (Amersham, 18-1143-34) aligned appropriately and covered with UHP. The imported pick list was opened, the syringe primed and the system was set up for picking the spots from the pick list. The spots were robotically picked and placed in 96-well plates, which were stored at 4^{o}C until spot digestion.

2.19 Spot digestion and identification with MALDI-TOF

The 96-well plate was placed in the Ettan Digester (Amersham, 18-1142-68) to digest the protein as follows: Step 1 – the gel plugs were washed three times for 20 minutes each with 50µl 50mM ammonium bicarbonate (Sigma, A6141) in 50% methanol. Step 2 – the gel plugs were washed twice for 15 minutes with 50µl 70% acetonitrile

(Sigma, 34967). The gel plugs were left to dry for at least 60 minutes. After drying, the individual gel pieces were rehydrated in 10µl digestion buffer (12.5ng trypsin (Promega, V5111) per µl of 10% acetonitrile, 40mM ammonium bicarbonate). Exhaustive digestion was carried out overnight at 37^{o}C. After digestion, the samples were transferred as follows: Step 1 – A volume of 40µl of 0.1% trifluoroacetic acid (Sigma, 302031) in 50% acetonitrile was added to the wells, mixed and left for 20 minutes. A volume of 60µl of this solution was transferred to a fresh 96-well plate. Step 2 - A volume of 30µl of 0.1% trifluoroacetic acid in 50% acetonitrile was added to the wells, mixed and left for 20 minutes. A volume of 50µl of this solution was transferred to the fresh 96-well plate. The liquid in the plate was vacuum-dried in a maxi dry plus. After drying, the 96-well plate was placed in the Ettan Spotter (Amersham, 18-1142-67) for spotting onto the target plates. A volume of 3µl of 0.5% trifluoroacetic acid in 50% acetonitrile was added to the desiccated peptides and mixed 5 times. A volume of 0.3µl of this mixture was spotted onto the target plate after which a volume of 0.3µl matrix solution [7.5mg/ml a-cyano-4-hydroxycinnamic acid (LaserBio labs, 28166-41-8) in 0.1% trifluoroacetic acid in 50% acetonitrile].

Peptide-mass fingerprinting was performed using Ettan MALDI-ToF Pro. The instrument setting was reflector mode with 175 ns delay extraction time, 60-65% grid voltage and 20kV accelerating voltage. Laser shots at 250 per spectrum were used to acquire the spectra with mass range from 600-3000Da with 8-shot mode. A total of three spectra were generated for each sample analysed. MALDI-generated mass spectra were internally calibrated using trypsin peaks or commercially available peptide standards (Pep4 Laser BioLabs). The peptide masses were searched against the National Centre for Biotechnology Information (NCBI) Homo-sapien database using ProFound^{TM}. One missed cleavage per peptide was allowed and an initial mass tolerance of 100ppm was used in all searches. Fixed carbamidomethylation of cysteines and partial oxidation for methionine was assumed.

MALDI-time of flight (ToF) MS was carried out using Ettan pro MALDI-ToF Mass Spectrophotometer (GE Healthcare). Peak lists were generated and calibrated against internal trypsin autolysis peaks (m/z 842.501 and 2211.104) and or commercially available peptide standards (Pep 4 LaserBio Lab). PMF identifies a protein by measuring the molecular mass of all major trypsin products and matching these

molecular masses using the NCBI database with ProFound. Proteins were identified using ProFound with a mass tolerance of +/- 0.2 m/z, a maximum of 1 missed cleavage, fixed carbamidomethylation of cysteines and partial oxidation of methionines.

Mass spectra were recorded operating in the positive reflector mode at the following parameters: accelerating voltage 20 kV; and pulsed extraction: on (focus mass 2500). Internal and external calibration was performed using trypsin autolysis peaks at 842.509 m/z, 2211.104 m/z and PepMix 4 respectively. Calibration using Pep4 was performed as follows: Once two spectra were generated for the PepMix 4 mix (position 1 on the slide), the acquisition of spectra was stopped. The first spectrum of sample one was selected and the calibrant peaks readjusted for accuracy. The five individual peaks cover the 500-3500 Da mass range and include bradykinin fragment 1-5 (573.315), angiotensin II human (1046.5424), neurotensin (1672.9176) and insulin B chain oxidised (3494.6514). Once calibration was completed it was saved as the new "system calibration". The MALDI was then restarted. The mass spectra generated for each of the proteins were analyzed using MALDI evaluation software (Amersham Biosciences). Protein identification was achieved with the PMF Pro-Found search engine for peptide mass fingerprints with expectation value < 0.01 (this refers to the probability that the identification is 99% accurate).

2.20 Spot digestion and identification with nanoLC-MS/MS

Tryptically digested samples were resuspended in 20µL of a LC-MS grade water containing 0.1%TFA and analysed by one-dimensional LC-MS using the Ettan^{TM} MDLC system (GE Healthcare) in highthroughput configuration directly connected to a Finnigan^{TM} LTQ^{TM}(Thermo Electron). Samples were concentrated and desalted on RPC trap columns (Zorbax^{TM} 300SB C18, 0.3mm x 5mm, Agilent Technologies) and the peptides were separated on a nano-RPC column (Zorbax^{TM} 300SB C18, 0.075mm x 100mm, Agilent Technologies) using a linear acetonitrile gradient from 0-60% Acetonitrile (Riedel-de Haën LC-MS grade) over 60 minutes directly into the LTQ via a 10µm nanoESI emitter (Presearch FS360-20-10-CE-20). Thermo linear ion trap

mass spectrometer was used for MS/MS. A scan time of ~0.15 s (one microscans with a maximum ion injection time of 10ms) over an m/z range of 300-2000 was used followed by MS/MS analysis of the 3 most abundant peaks from each scan which were then excluded for the next 60 seconds followed by MS/MS of the next next three abundant peaks which in turn were excluded for 60 seconds and so on. A "collision energy" setting of 35% was applied for ion fragmentation and dynamic exclusion was used to discriminate against previously analysed ions (data dependent analysis).
All buffers used for nanoLC separations contained 0.1% Formic Acid (Fluka) as the ion pairing reagent. Full scan mass spectra were recorded in profile mode and tandem mass spectra in centroid mode. The peptides were identified using the information in the tandem mass spectra by searching against SWISS PROT database using SEQUEST^{TM} using an Xcorr value of 1.5 for singly charged peptides, 2.0 for doubly charged peptide and 2.5 for triply charged peptides.

2.20 Overview of Bioinformatic Analysis

2.20.1 Pathway Assist ®

Pathway Assist is a product aimed at the visualisation and analysis of biological pathways, gene regulation networks and protein interaction maps. It comes with a comprehensive database that gives a snapshot of all information available in PubMed, with the focus on pathways and cell signalling networks. This product was useful in assisting in the interpretation of proteomics results. It allowed visualisation of results in the context of pathways, gene regulation networks and protein interaction maps. This was done using curated and automatically created pathways. Graph drawing, layout optimisation, data filtering, pathway expansion and classification and prioritization of proteins were all possible. Pathway Assist worked by identifying relationships among genes, small molecules, cell objects and processes and built pathways based on these relationships.

2.20.2 Pubmatrix

Molecular experiments using multiplex strategies such as cDNA microarrays or proteomic approaches generate large datasets requiring biological interpretation. Text based data mining tools have recently been developed to query large biological

datasets of this type of data, (Kevin G Becker 2003). PubMatrix is a web-based tool that allows simple text based mining of the NCBI literature search service PubMed using any two lists of keywords terms, resulting in a frequency matrix of term co-occurrence. In this way, lists of terms, such as gene names, or functional assignments can be assigned, genetic, biological, or clinical relevance in a rapid flexible systematic fashion (http://pubmatrix.grc.nia.nih.gov/).

2.20.3 PANTHER (Protein Analysis Through Evolutionary Relationships)

The PANTHER classification system is a unique resource that classifies genes by their functions, using published scientific experimental evidence and evolutionary relationships to predict function even in the absence of direct experimental evidence. Proteins are classified by expert biologists into families and subfamilies of shared function, which are then categorized by molecular function and biological process ontology terms. For an increasing number of proteins, detailed biochemical interactions in canonical pathways are captured and can be viewed interactively (http://www.pantherdb.org/).

2.21 Statistical Methods

The Statistics applied to analyze the significance of our research findings were by unpaired t-Test for proliferation and invasion assay and 1 way ANOVA for proteomics. The unpaired *t* test compares the means of two groups, assuming that data are sampled from Gaussian populations. The **one-way analysis of variance** (abbreviated **one-way ANOVA**) is a technique used to compare means of two or more samples (using the F distribution). This technique can be used only for numerical data. The ANOVA tests the null hypothesis that samples in two or more groups are drawn from the same population. To do this, two estimates are made of the population variance. The error bar in the graphs represents standard deviation (SD) or standard error mean (SEM) as mentioned in the figure legends.

Results: 3.0 ; SECTION A

3.1 Design and Construction of targetable plasmid vectors for random integration

In order to evaluate the mode of action and function of a gene product it is often useful to alter the expression levels of individual genes. The challenges one faces during gene overexpression studies include genetic instability, loss of observed phenotype in real time, and as a result unreliable data may be observed. So the aim of this study was to develop genetically stable and transcriptionally active targetable cell lines. Refer to Figure 3.1.5 and 3.1.7 for an overview of the way the Cre-LoxP system works.

A random targeting plasmid was designed and constructed, then used for developing targetable stable cell lines. The random targeting plasmid vector was basically a modified pBluescript vector, which was cut with *NotI-KpnI* restriction enzyme (Section 2.13.1). A LoxP (target sequence of Cre recombinase) linker was designed and the sequence was synthesized by MWG Biotech, Germany. The LoxP linker sequence had the following restriction enzyme sites **5' *NotI, XhoI, FseI, SpeI,* LoxP, *AseI, MluI,* LoxP, *HindIII, Cla, KpnI* 3'**. The two LoxP sequences were designed in such a way that they were oriented in the same direction, to facilitate knock out of intervening sequence. The synthesized sense and antisense LoxP linker sequences were annealed, cut with *NotI-KpnI* restriction enzymes and ligated (section 2.13.1) into pBluescript with *NotI-KpnI* cut ends.

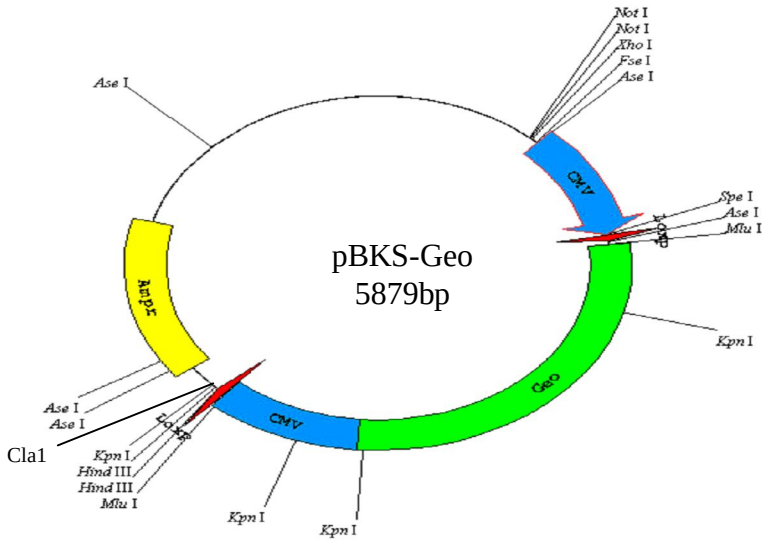

Figure 3.1.1a Schematic representation of plasmid used to generate targetable DLKP cell lines.

Primers were designed to PCR amplify the *Neo* gene. These primers also contained *BglII-HpaI* restriction enzyme sites (Fig. 3.1.2a), to facilitate insertion in frame with *GFP* gene from the pEGFP-C1 plasmid (Fig. 3.1.3). The entire fusion construct including promoter [CMV-Geo (GFP+Neo)] was cut out using *AseI* and *MluI* restriction and cloned into pBluescript vector with *AseI-MluI* cut ends, from now on called as pBKSgeo (Fig. 3.1.1a). Another CMV promoter was amplified using the pEGFP-C1 vector as a template and with *AseI* and *SpeI* sites in the primer sequences. The pBKSgeo plasmid and the amplified CMV promoter fragment were digested with *AseI-SpeI* and the CMV was ligated upstream of the Geo sequence and 5' LoxP construct.

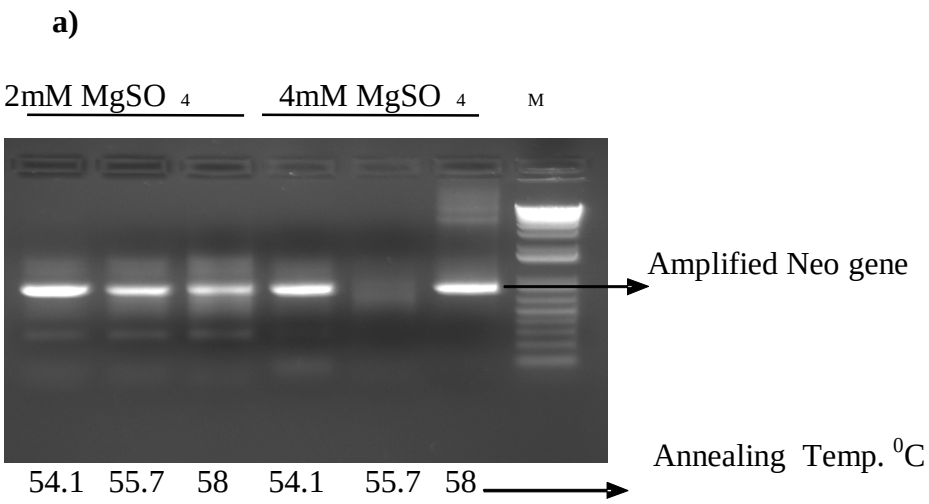

Figure 3.1.2 a) PCR conditions optimization for amplifying *Neo* gene from pEGFP-C1 plasmid with different temperature conditions and with different $MgSO_4$. b) Restriction enzyme digestion. M: DNA molecular weight marker, N: *Neo* PCR product cut with BglII and G: pEGFP-C1 cut with BglII and HpaI restriction enzyme.

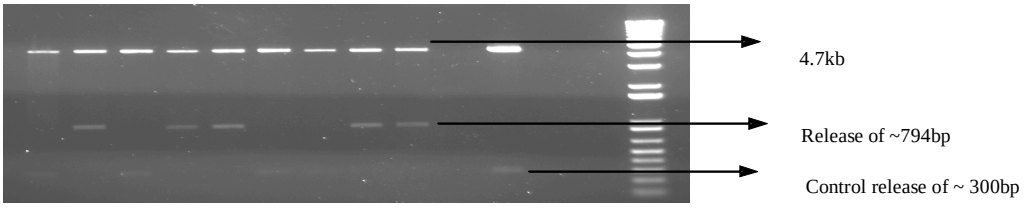

Figure 3.1.3 Neo fused with GFP in pEGFP-C1 confirmed through restriction digestion. The *neo* gene was released by BglII and HpaI digestion.

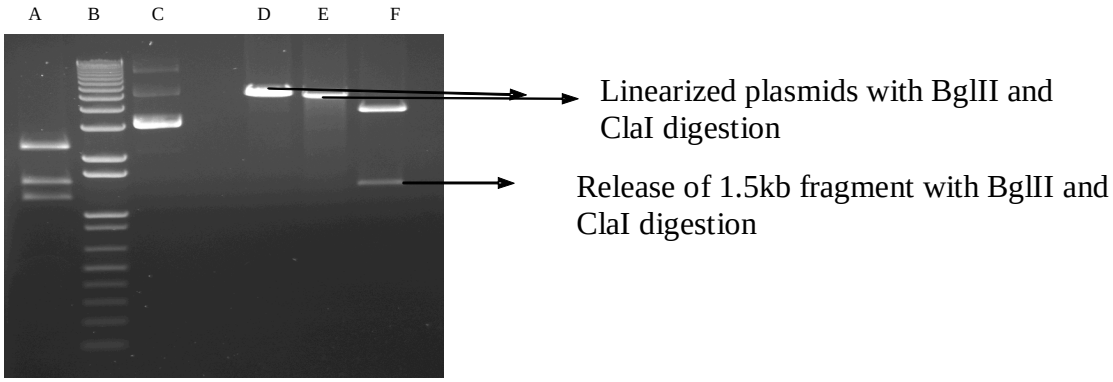

Figure 3.1.4 Restriction Enzyme digestion analysis of pBKS-geo clone. Lane A: MluI cut pBKSgeo construct, B: 1kb plus DNA ladder, C: uncut, pBKSgeo plasmid cut with BglII and ClaI in lane D, E, F. An expected release of 1.5kb fragment from clone in lane F .

To obtain stable single cell stable clones the plasmid was transfected into the DLKP cell line. A ratio of 1:3 of DNA to Lipofectamine 2000 was used for 6 well cell culture plates as it was observed to be minimally toxic with maximum transfection efficiencies.

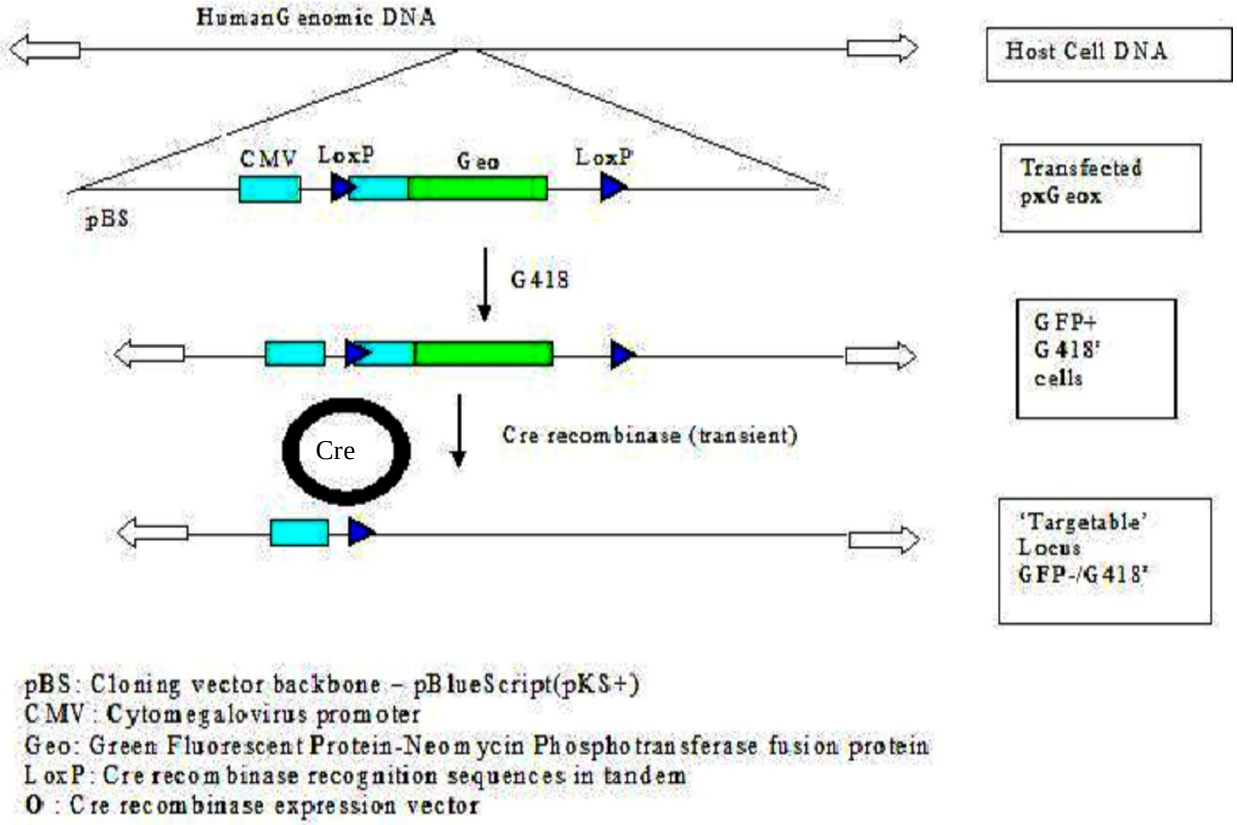

Figure 3.1.5 schematic representation of targetable cell line development.

In conclusion the fusion protein GFP+Neo is functional as evident from figure 3.1.6, although the GFP was less brighter compared to wild type plasmid and neomycin phosphotransferase was conferring resistance to G418 selection.

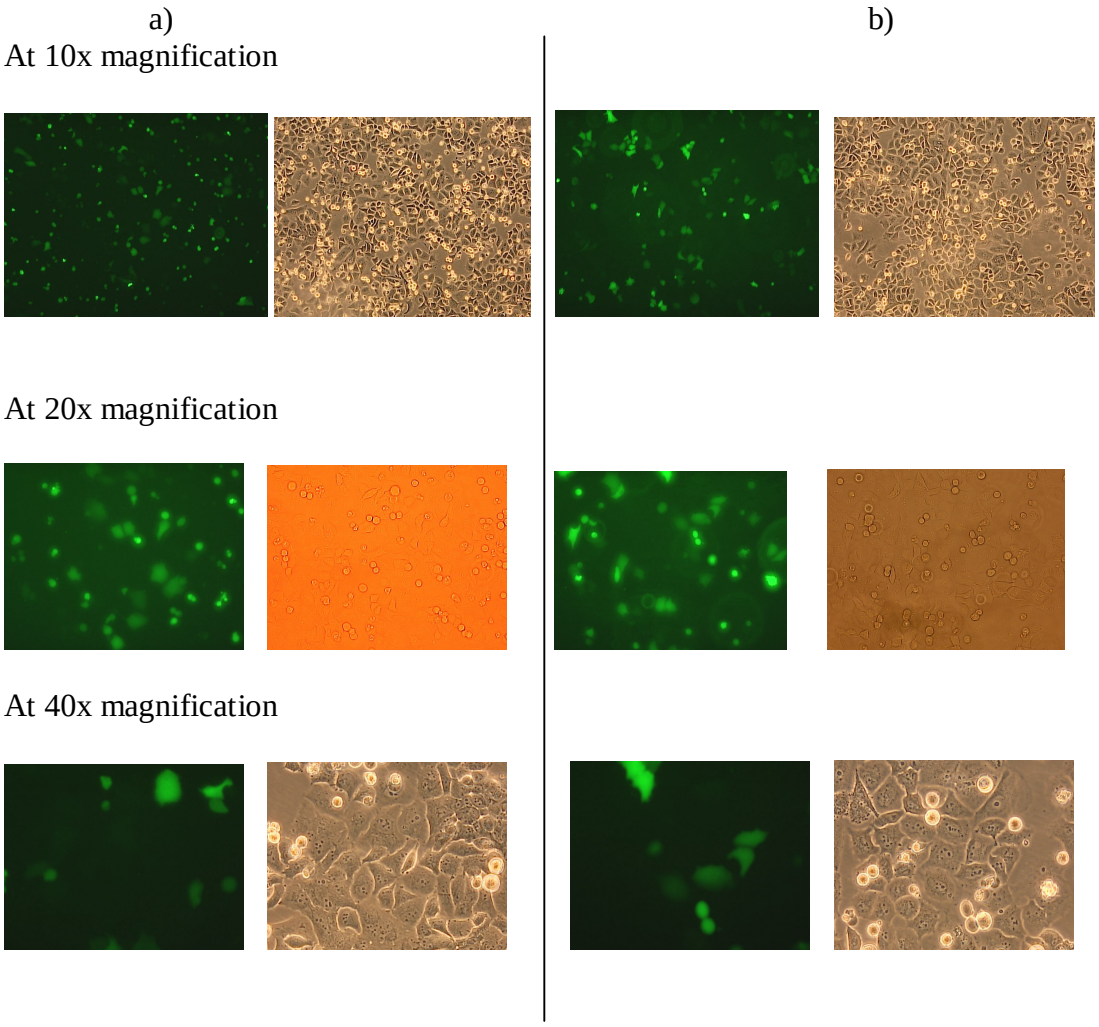

Figure 3.1.6 Photographic representation of the transfection optimization. a) Geo (GFP+Neo) in pEGFP vector (b) represents the wild type pEGFP-C1 vector transfected in DLKP cells using lipofectamine as transfection reagent, and observed through FITC and Normal light filter at different magnification.

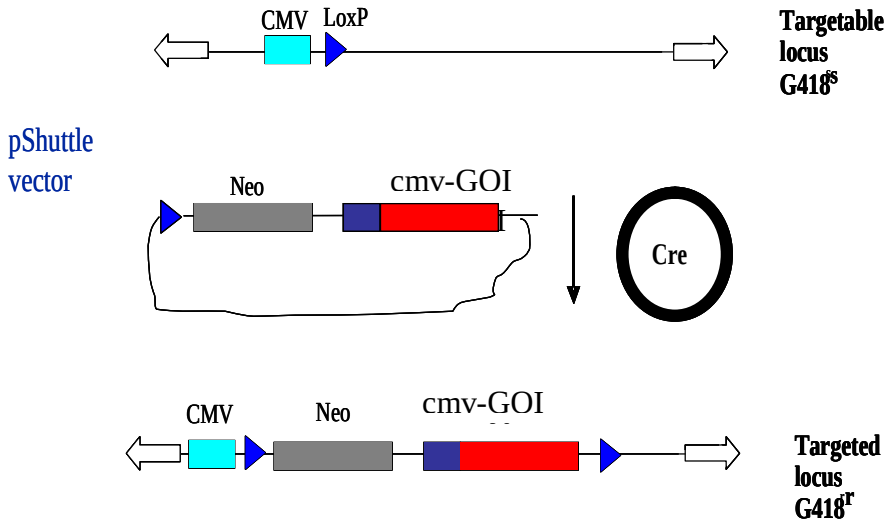

Figure 3.1.7 Schematic representation of retargeting the targetable locus with pShuttle plasmid.

GFP positive/ G418 resistant DLKP clones were transiently transfected with a *cre* recombinase expressing plasmid. Cells with LoxP sites in their genome express with Cre, the protein catalyzes a reciprocal recombination event between the LoxP sites. As a result, the DNA in between the *LoxP* sites is excised and subsequently degraded (refer fig. 3.1.7). In this case the *geo* fusion gene was excised (fig.3.4.3) resulting in a cell containing a randomly generated targetable locus with a CMV promoter upstream of LoxP sequence.

The developed targetable cell lines were GFP negative/G418 sensitive. These constituted our master targetable cell lines, and could now be re-targeted by using a shuttle plasmid. This consisted of a single LoxP site with a promoter less selection marker gene (Neo), and gene of interest for overexpression. This shuttle plasmid was co-transfected in GFP negative/G418 sensitive cell lines along with cre expressing plasmid. Once again due to Cre-LoxP targeting mechanism the cells incorporate the construct, in our case promoterless Neo and gene of interest (schematics represented in fig 3.1.7). The promoter at the targetable site facilitates transcription of the inserted Neo gene, resulting in G418 resistant cells. G418 selection pressure was applied to generate stable DLKP cell lines that overexpress the transgene of interest for use in subsequent gene-specific functional studies.

3.2 Stability and transgene expression level assessment of DLKP geo clones using flowcytometer analysis

Before removing the geo sequence by Cre expression to generate the 'master' targetable cell lines we wished to assess a panel of clones for stability of expression The reason for this was that potential problems that are often incurred during transgene overexpression include variability in gene expression levels and sudden loss in transgene expression and constitute a significant hurdle in gene functional studies. To investigate the stability of transgene overexpression we decided to perform a time course assessment by using thirty three "stable" DLKP clones expressing geo. These were generated as described in section 3.1. The clones were grown over a 20 week period with regular passaging and each was measured for GFP positivity at each passage. Two freeze thaw cycles were also included as this process is often a trigger for loss of transgene overexpression in unstable clones. At the outset the 33 clones had varying levels of GFP expression (figure 3.2.2, 3.2.3, 3.2.4, 3.2.5, 3.2.6). An example of the read-out by flow cytometry is shown in fig. 3.2.1. To gate the populations correctly GFP negative cells were analyzed first and the voltage of the PMT detector adjusted to place these cells below 15 on the green fluorescence scale. The population was also gated based on forward scatter to exclude small particles in the culture (fig. 3.2.1a). As a positive control, DLKP cells transfected with the vector pEGFP-C1 were analysed with the established gating and settings. These cells represented a stable mixed population with varying degrees of green fluorescence. This was reflected in the broad spread of fluorescence observed (fig.3.2.1b). In contrast, a clonal population of DLKP cells transfected with the Geo fusion construct displayed a much more uniform signal across the population. What is notable is the small percentage of GFP negative (green dots) cells in what would be expected to be a homogenous population (fig.3.2.1c). This flow cytometry analysis was applied to all clones which were cultured in presence of G418 selection pressure, using the same settings over several months to observe any variations in this expression pattern with time in culture.

DLKP

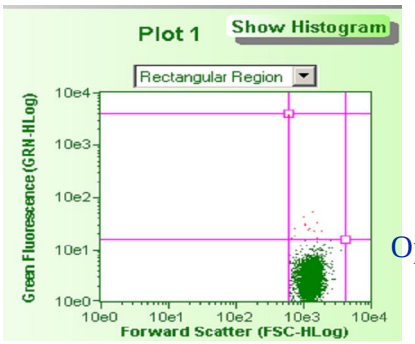

a

Optimising Gating

b

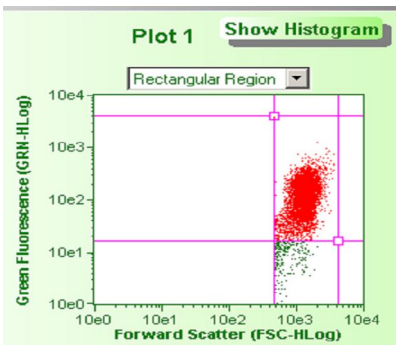

c

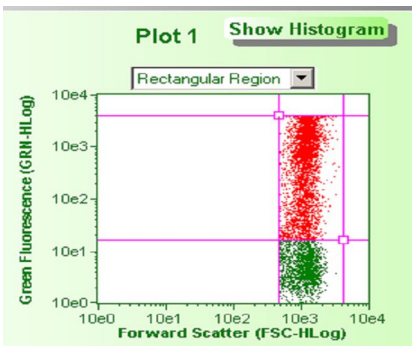

DLKP Geo clone

DLKP GFPC1 mixed population

Figure 3.2.1 Gating standardisation on flowcytometer. a) GFP negative cells (group of green cells) b) mixed population of GFP +ve cells (red cells) c) One of the stable DLKPgeo clones(group of red cells). Forward scatter optimised at (FSC-HLog 10e2.4) and Green fluorescence at (GRN-HLog 10e1.5)

To gate the populations correctly GFP negative cells were analyzed first and the voltage of the PMT detector adjusted to place these cells below 15 on the green fluorescence scale. The population was also gated based on forward scatter to exclude small particles in the culture (fig. 3.2.1a). As a positive control, DLKP cells transfected with the vector pEGFP-C1 were analysed with the established gating and settings. These cells represented a stable mixed population with varying degrees of green fluorescence. This was reflected in the broad spread of fluorescence observed (fig.3.2.1b). In contrast, a clonal population of DLKP cells transfected with the Geo fusion construct displayed a much more uniform signal across the population. What is notable is the small percentage of GFP negative (green dots) cells in what would be expected to be a homogeneous population (fig.3.2.1c). This flow cytometry analysis was applied to all clones which were cultured in presence of G418 selection pressure, using the same settings over several months to observe any variations in this expression pattern with time in culture.

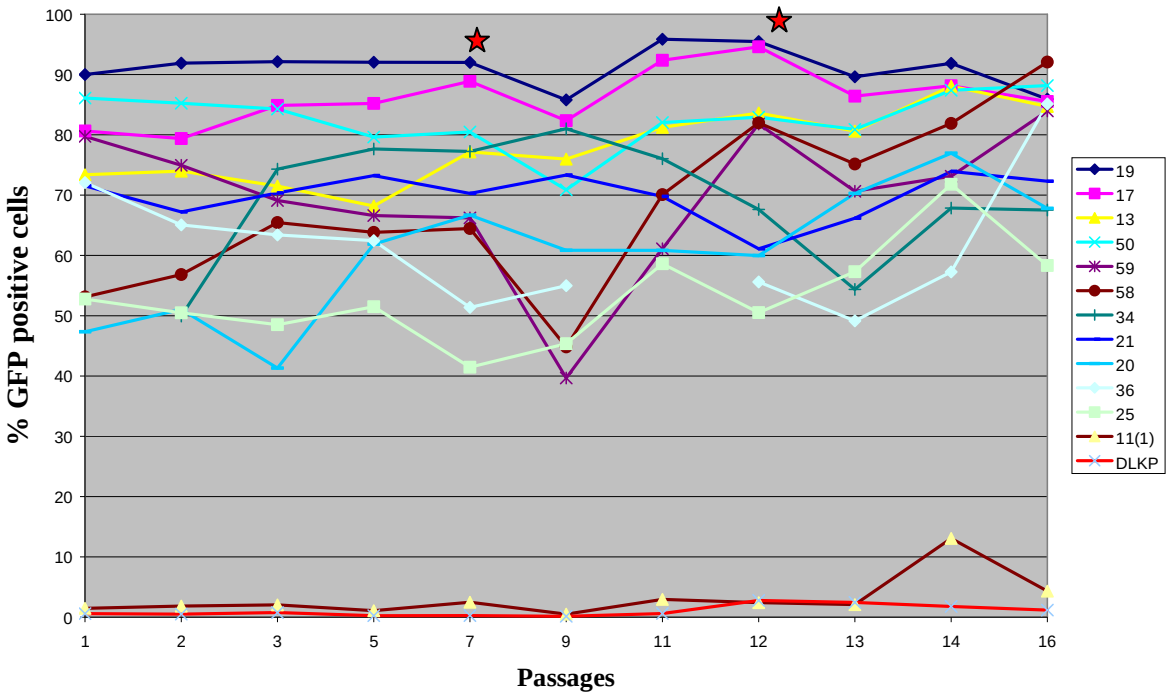

Figure 3.2.2 Percentage GFP fluorescence of DLKP Geo clones over 16 passages. DLKP parent and DLKPgeo negative cell line 11(1) used as negative controls. The eleven clones included here represent those with a high percentage of the population being GFP positive. The two stars represent freeze thaw cycles included during the experiment.

The above graph illustrates a subgroup of DLKP clones displaying consistent GFP expression levels over a period of four and half months. Within this subgroup there is a broad range in terms of percentage GFP positivity. The stars represent the time at which all clones were subjected to a freeze thaw cycle (24hrs at -80^{0}C). It is notable that clones 58 and 59 in particular had considerably reduced percentage of GFP positive cells subsequent to the first freeze thaw. Both clones appeared to have recovered within a couple of passages.

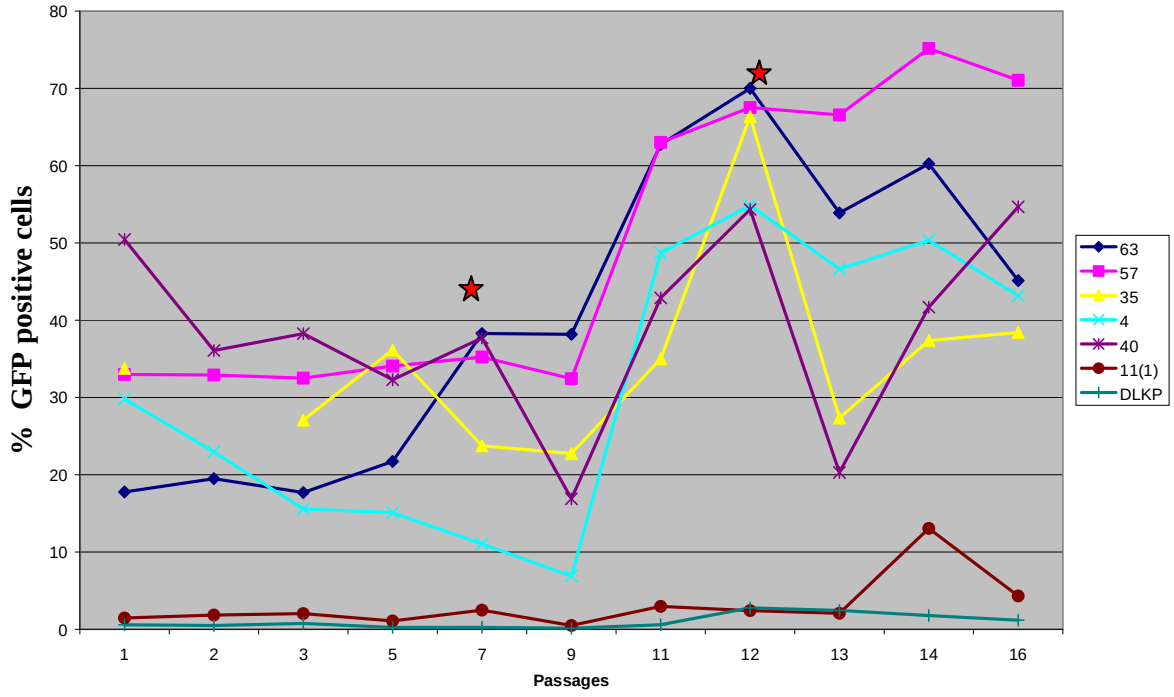

Figure 3.2.3 Percentage GFP fluorescence of a subset of DLKP Geo clones over 16 passages. DLKP parent and DLKPgeo negative cell line 11(1) used as negative controls. The five clones included here represent those with increased percentage GFP expressing population. The two stars represent freeze thaw cycles included during the experiment.

The above graph illustrates a subgroup of DLKP clones displaying increased GFP expression levels over a period of four and half months. The stars represent the time at which all clones were subjected to a freeze thaw cycle. It is notable that all clones have a considerably increased percentage of GFP positivity after the first freeze thaw, and after the second freeze thaw clone 57, in particular, had no reduction in GFP expressing population compared to the rest.

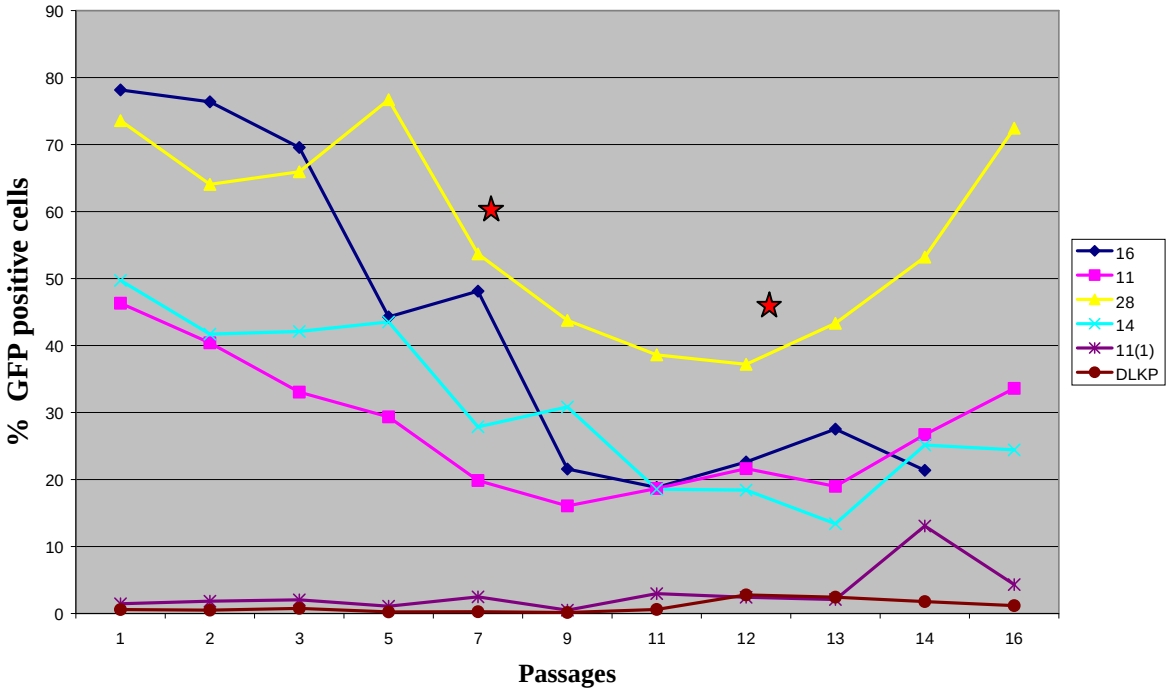

Figure 3.2.4 Percentage GFP fluorescence of DLKP Geo clones during 16 passages. DLKP parent and DLKPgeo negative cell line 11(1) were used as negative controls. The four clones included here represent those with decreased percentage GFP expressing population. The two stars represent freeze thaw cycles introduced during the experiment.

The above graph illustrates a subgroup of DLKP clones displaying decreased GFP expression levels over a period of four and half months. The four clones initially had very high GFP expressing populations, and as the passages continued this fell to as low as 20%. But one clone in particular (28) was interesting in that it was showing reduced GFP expression until just after the second freeze thaw when this trend was reversed to show an increased GFP expressing population. The stars represent the time at which all clones were subjected to a freeze thaw cycle (24hrs at -80^0C).

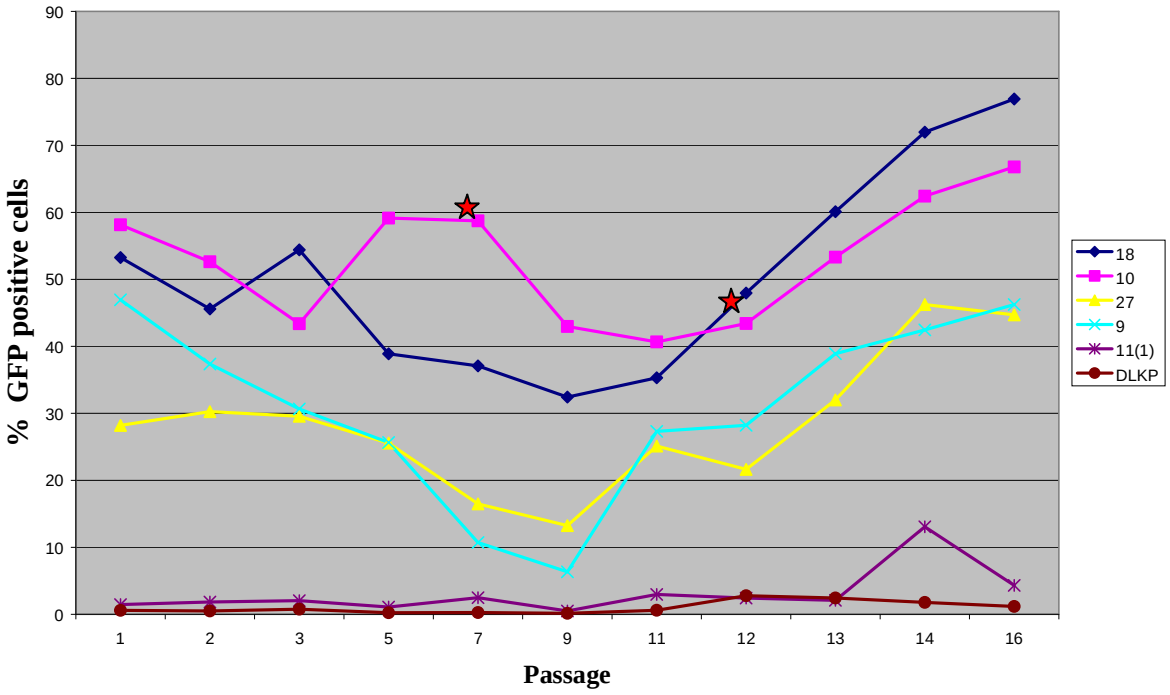

Figure 3.2.5 Percentage GFP fluorescence of DLKP Geo clones representing 16 passages. DLKP parent and DLKPgeo negative cell line 11(1) were used as negative controls. The four clones included here represent those with medium level of GFP expressing population. The two stars represent freeze thaw cycles included during the experiment.

The above graph illustrates a subgroup of DLKP clones displaying medium GFP expression levels over a period of four and half months. The four clones displayed a relatively broad GFP positivity (30-60%) and as the passages progressed the detection level was reduced as low as 10% (clone 9 and 27). The stars represent the time at which all clones were subjected to a freeze thaw cycle (24hrs at -80^0C). Subsequent to freeze thaw cycles it was observed that the clones regained the initial GFP positive levels.

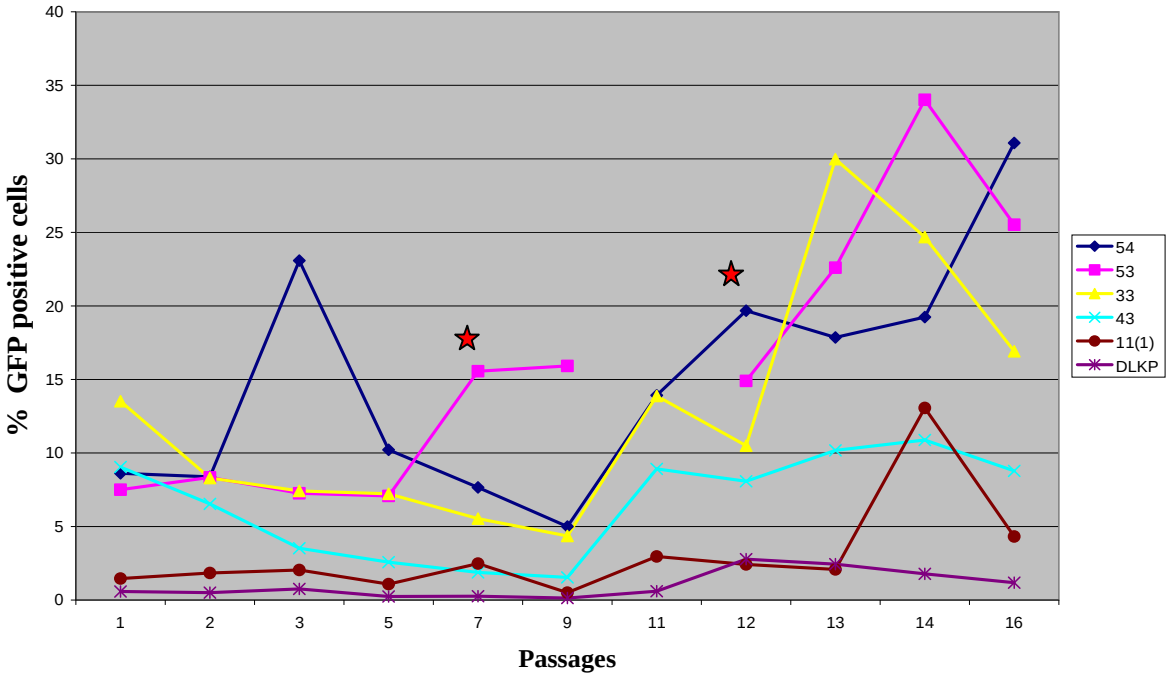

Figure 3.2.6 Percentage GFP fluorescence of DLKP Geo clones over 16 passages. DLKP parent and DLKPgeo negative cell line 11(1) were used as negative controls. The four clones included here represent those with low levels of GFP expressing cells. The two stars represent freeze thaw cycles included during the experiment.

The above graph illustrates a subgroup of DLKP clones displaying low and somewhat erratic GFP expression levels over the duration of the experiment. The four clones from the beginning were observed to have low GFP positivity and as the experiment continued the expression levels became inconsistent. The stars represent the time at which all clones were subjected to a freeze thaw cycle (24hrs at -80^0C). The break in the clone 53 line accounts for the fact that no data was acquired during that passage.

This study provided us with a substantial amount of information about the stability issues one has to face during gene overexpression studies. From the stability assessment of a panel of DLKP geo overexpressing clones we learned that, although the clones are from an isogenic population they had very different stability profiles. This may be due to genomic integration at different sites demonstrating clearly the problems with generating transgenic clones. Out of 33 clones only clones 19,17,13,21 and 50 were stable and all the remaining clones were observed to have stochastisity in their stability and expression levels.

3.3 Cell cycle assay for Stable GFP expressing DLKP cell lines

One of the most striking observations made during the stability assessment (section 3.2) of the DLKP geo clones was that cells derived from a single cell clone appeared to have both GFP positive and negative cells within the population. One would expect to see variations between clones but not within them. To further investigate this observed phenomenon an experiment was designed to measure variations in fluorescence which we thought was related to cell cycle (section 2.7.4).To address this a propidium iodide (DNA binding dye) based cell cycle assay was performed. The comparison between DLKP vs. DLKP geo clones over 32 hrs showed no dramatic difference either in GFP expressing population (fig. 3.3.1), monitored by flow cytometry although we observed variation in cell percentage at different cell cycle checkpoints (G0/G1, S and G2/M) (fig. 3.3.2).

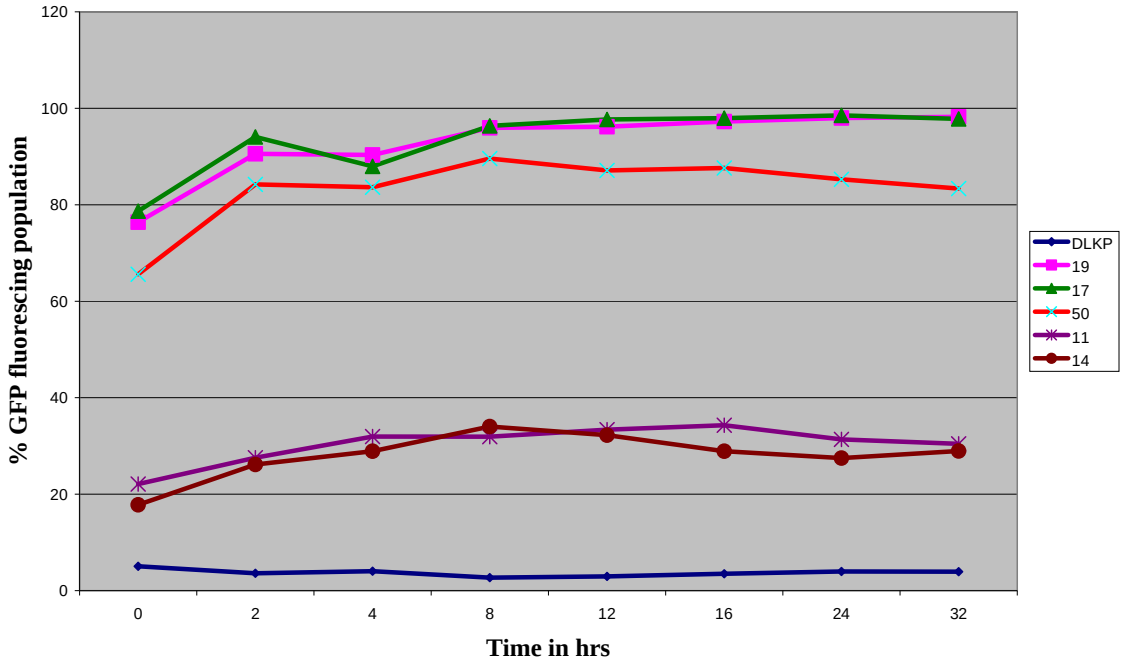

Figure 3.3.1 Percentage of GFP positive cells of DLKP Geo clones over time. DLKP parent was used as negative control. The five DLKP geo clones 19,17,59,11 and 14 included here were representative of a broad range of GFP expressing populations.

Figure 3.3.1 illustrates a subgroup of DLKP clones displaying broad range of GFP positivity. The rationale behind selecting such varied DLKP geo clones was to represent every kind of expression that we observed during our stability assessment. The GFP expression level of five clones was consistent across (2-32hrs) time, suggesting that there was no difference in GFP expression during cell division. The doubling time of DLKP is

approximately 22hrs (data not shown). Most notable was the sudden increase in GFP positivity observed 2hrs after addition of serum media. This was possible due to reduced translation under serum starved conditions used to synchronize the cultures followed by a burst of translation upon addition of serum.

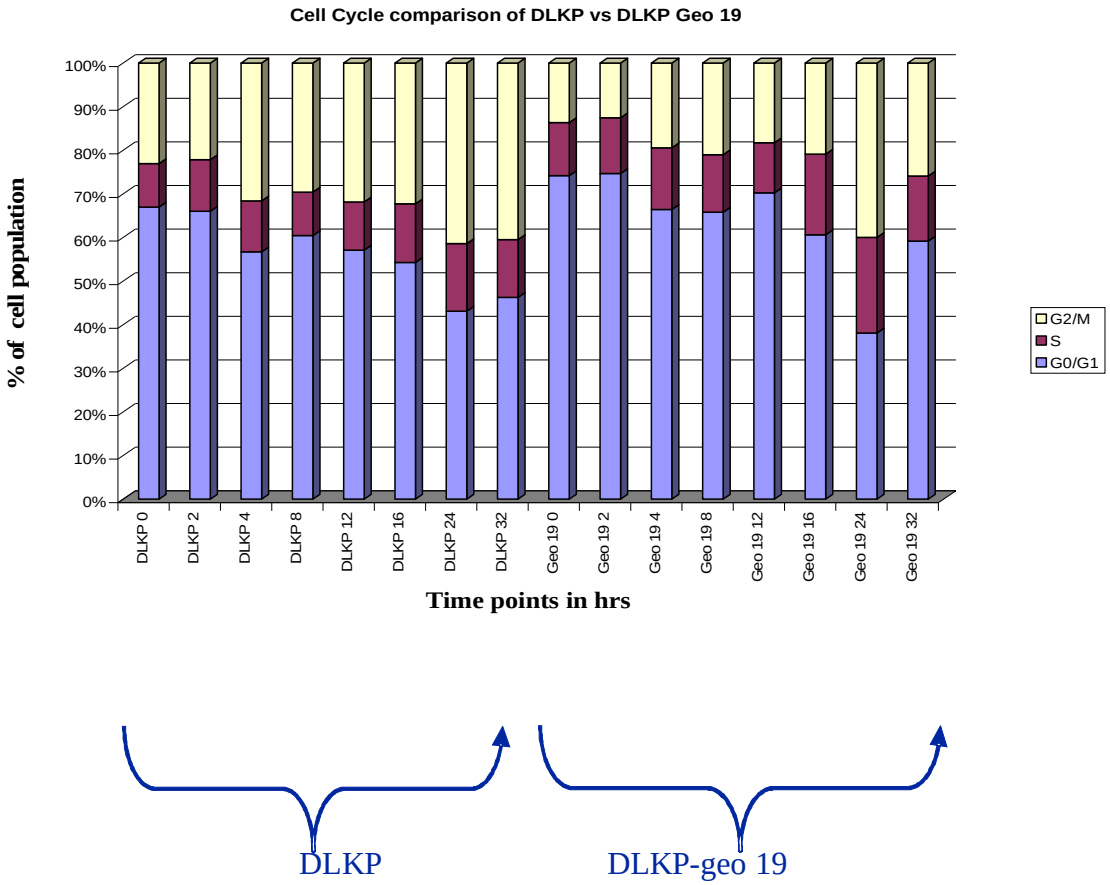

Figure 3.3.2 Cell cycle assay performed with DLKP and a stable DLKPgeo clone at 0, 2, 4, 8, 12, 16, 24, 32 hrs intervals. Y axis represents the percentage of cells at each phase of the cell cycle (G0/G1, S and G2/M) at each time point.

Figure 3.3.2 illustrates the comparison of parent DLKP with one of the GFP expressing DLKP clones (high expresser), the different shades of colour in each bar

Figure 3.3.2 represents cell population content captured at different cell cycle stages. The doubling time for DLKP is approximately 22hrs (data not shown). Cell cycle trend was observed, though there was no drastic change in cell number at different cell cycle stages.

So the stochastic GFP positivity observed was unlikely to be due to cell cycle dependent variation in expression. It would appear that the *geo* clone generally had a higher percentage of cells in the G0/G1 phase and less in the G2/M phase than the parental control. However, the pattern observed over time was similar for both cell lines and, more importantly, didn't correlate with any fluctuations in GFP positivity.

3.4 Generation of geo knockout cell lines.

The method chosen to develop targetable, master DLKP cell lines was based on the Cre-LoxP system. After the stability assessment (Section 3.2), we selected a range of DLKP geo clones with high to low expression levels. The clones chosen in this experiment were DLKP geo 17, 19 and 11. These cell lines were transiently transfected (section 2.8) with a Cre expressing plasmid vector. 48hrs after transient transfection the cells were trypsinised (section 2.6) and were single cell cloned in 96 well plates (section 2.7.1). Upon reaching confluency the cells were trypsinised and seeded in duplicate 96 well plates. One set of clones was incubated with G418 media selection (800μg/ml). The clones that lost the Geo gene were killed. These were the clones of interest to us (fig 3.4.1). These clones were GFP negative/G418 sensitive and constituted the master targetable DLKP clones.

To confirm that these clones were genuine "geo knock outs", we screened them both at the transcriptional and translational level. Western blot analysis (section 2.14) of the parent DLKP-geo clones and their geo knock out progeny was performed (refer fig. 3.4.2). An expected band of 55kDa (Geo) was observed in the DLKP-geo parents and no band in their knock out counterparts, confirming absence of expression. Similarly genomic DNA was isolated from DLKP-geo (section 2.11.1) and their geo knockout derivative cell lines and PCR was performed (section 2.11.5) to confirm removal from the genome (refer fig 3.4.3). The expected 600bp amplicon product was observed in DLKP geo clones but no product in the knock out clones. Two DLKP geo knockout master targetable clones were chosen for future functional studies. They were DLKP 17(high expresser) and DLKP 11 (low expresser).

Figure 3.4.1 illustrates the screening process to identify the knockout of geo gene from DLKP geo clones. The knockout was confirmed both by applying G418 selection and visualising through fluorescent microscope. From the figure it's evident that the clones which were sensitive to G418 selection are also GFP negative. Figure 3.4.2 confirms the functionality of the molecular tool that was explored based on the Cre-LoxP system. The three DLKP geo clones 17, 19 and 11 were subjected to transient Cre overexpression, resulting in Cre-LoxP mediated knockout of the Geo gene. In the western blot DLKP parent was used as a negative control. DLKP transfected with pEGFP-C1 was used as positive control. A 55kda band was detected in Geo expressing DLKP cell lines (GFP+Neo fusion product), and a 27 kDa (GFP) band in the wild type control was observed. Conversely no 55 kda band was observed in Cre treated DLKP geo clones, confirming the knockout.

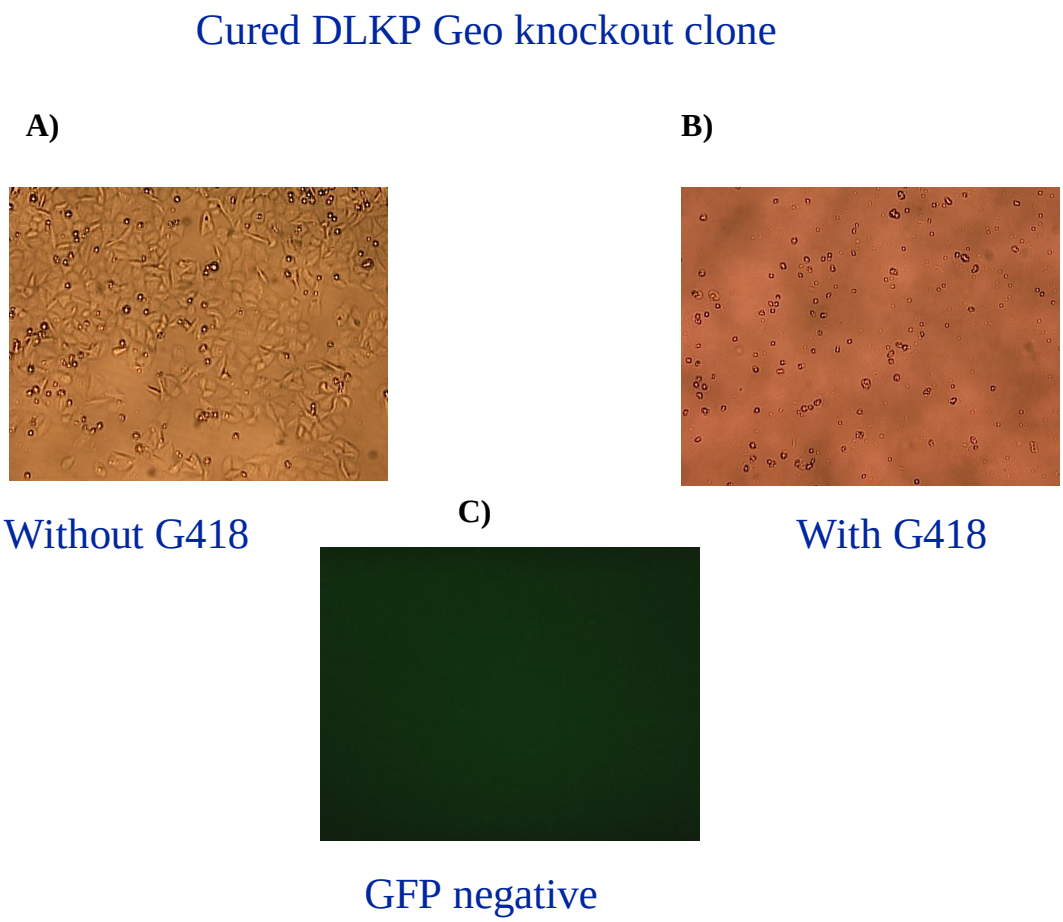

Figure 3.4.1 Cured clone (geo knockout), which is GFP negative and G418 sensitive. A+B; phase contrast, C; FITC filter, A+C; no G418 in media, B; with G418 in media.

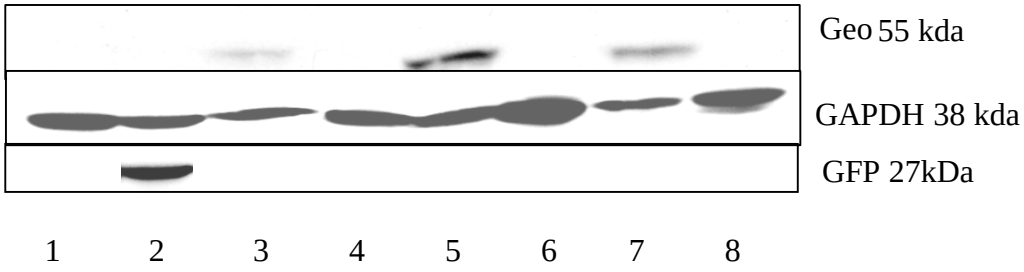

Figure 3.4.2 Western blot analysis of DLKP-geo clones and their knockout sub clones. Lane 1: DLKP parent negative control, lane 2: DLKP-GFP-C1 expressing cell line, 27 kDa GFP band detected, lane 3,5and7: DLKP-geo 11,17 and 19 expressing cell lines, 55 kDa band detected, lane 4,6and8: DLKP-geo 11,17 and19 'knockout' sub clones, no *geo* band detected. GAPDH loading control identified 38 kDa.

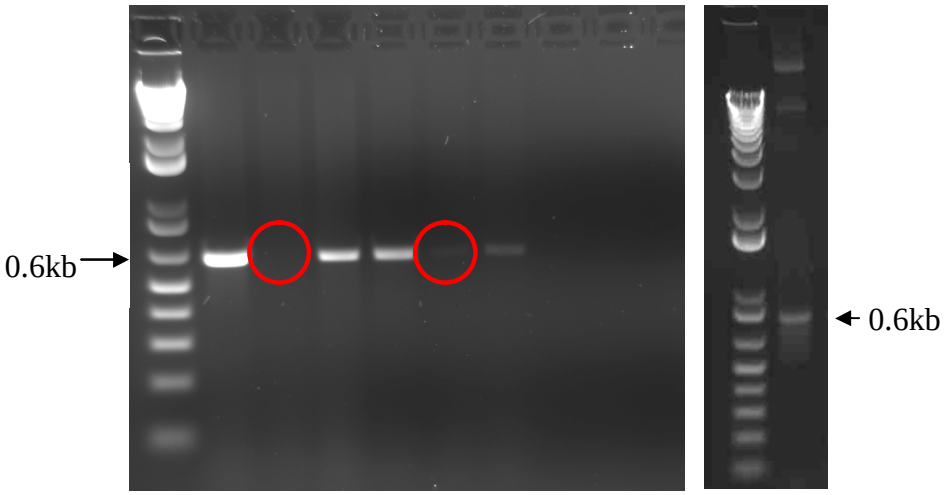

Figure 3.4.3 PCR analysis of genomic DNA from DLKP geo and their cre treated sub clones. Lane M : DNA Marker , 11 : DLKP 11geo clone, 11(1) : DLKP 11(1) cre treated, 11(2) : DLKP 11(2) cre treated, 14 : DLKP 14 geo clone, 14(1) : DLKP 14(1) cre treated, 14(2) : DLKP 14(2) cre treated, W: wild type DLKP, Es: mouse embryonic stem cell DNA, Ntc : no template.

Figure 3.4.3 illustrates Geo knockout in DLKP-geo cre treated genomic DNA samples. Genomic DNA was extracted from GFP negative and G418 sensitive clones along with their GFP positive and G418 resistant parental cell lines. GFP-specific primers were used in a PCR- based screen for geo knockout in DLKP geo clones, transiently transfected with Cre. Several different gDNA controls were used involving wild type DLKP, Mouse embryonic stem cells, GFP positive DLKP and no template control.

3.5 Design and construction of re-targeting vector, pTarshuttle

To develop targetable cell lines we utilized the Cre-LoxP based system, and accordingly the two LoxP sequence were oriented in the same direction. Subsequently geo knock out DLKP clones are left with a single LoxP sequence with a CMV promoter upstream of it in the genome. To make use of this targetable locus we designed and constructed a shuttle vector to be used for knock in of any gene of interest. This pShuttle was constructed in the Invitrogen pTarget vector background (mammalian expression vector). As the pTarget vector was a TA open ended cloning vector we used Klenow polymerase and ligase enzyme to re-circularise the vector. A screen of 14 plasmid extracted from XL-Blue 1 competent *E. coli* colonies (section 2.13) revealed that pTarget vector was successfully circularized (fig. 3.5.2). The pTarget vector was further modified by removing the CMV promoter region upstream of Neo and cloning in its place a LoxP sequence. The LoxP sequence was synthesized (MWG Biotech, Germany) with ***ClaI-AvrII*** restriction enzyme sites at the ends. The synthesized sense and antisense sequences were annealed and digested with ClaI-AvrII as was the pTarget vector. The double stranded LoxP sequence was ligated with the pTarget plasmid vector. Restriction enzyme screening of miniprep (refer section 2.13.1) of *E.coli* colonies confirmed six out of twelve plasmids contained the insert (fig 3.5.2)

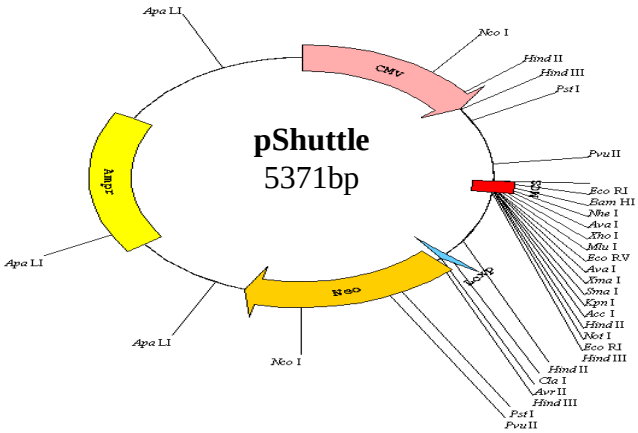

Figure 3.5.1 Schematic representation of pShuttle LoxP vector used for transgene targeting studies.

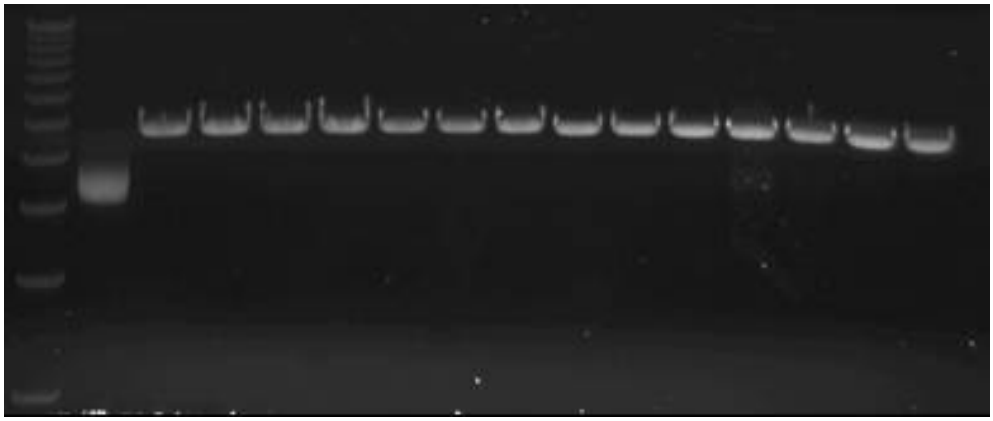

M uncut 1 2 3 4 5 6 7 8 9 10 11 12 13 14

Figure 3.5.2 pTarget vector, circularized by treatment with klenow polymerase followed by ligation. Lane M: 1kb plus DNA ladder, lane uncut: circularized plasmid, lane 1 to 14 linearized plasmid preps by digestion with *ClaI*.

3.6 Proof of concept of targeting tool with pShuttle *LacZ* in DLKP targetable cell line.

The final step in validating the use of the DLKP targetable cell lines as a research tool was to demonstrate that a transgene could be specifically introduced at the LoxP site in the cells. As proof of concept we cloned the LacZ gene into pShuttle vector (which has promoterless Neo and LoxP site). The pShuttle LacZ plasmid was co-transfected along with pCre into targetable DLKP clones. The pSVGal containing LacZ under control of SV40 promoter was included as a positive control. X-gal staining (section 2.7.2) was done with transiently transfected cells to estimate efficiency and ensure successful expression of the galactosidase enzyme from the pShuttle-LacZ. G418 selection was also applied to select for stable clones that had incorporated the plasmid.

Figure 3.6.1 illustrates the process that is undergone during re-targeting the LoxP site in targetable cell lines. The re-targeting vector has a single LoxP site, downstream of it a promoter-less Neo gene. Upstream of LoxP, we have cloned in LacZ reporter gene followed by its own CMV promoter. The re-targeting plasmid was co-transfected with pCre. LoxP reciprocal recombination is triggered which facilitates LacZ insertion

between the two regenerated LoxP sites along with the promoter less Neo upstream. The CMV promoter already present in the targetable locus facilitates Neo expression to confer resistance in cell lines for G418 stable selection. The stable cell lines are assayed for β-galactosidase activity to confirm LacZ translation. The cells with non-targeted, randomly integrated plasmid should be sensitive to G418 selection due to inactive Neo and hence killed.

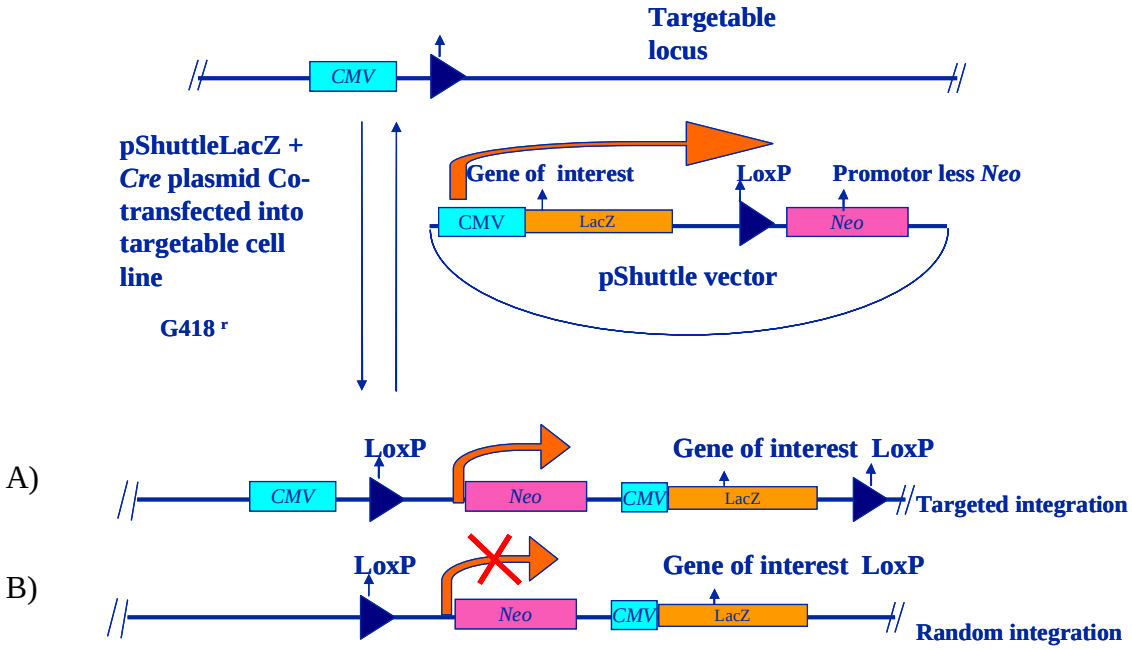

Figure 3.6.1 Schematic representation of re-targeting the loxP site in targetable cell lines. A) Targeted integration, promoterless neo being driven by CMV at integration site. B) Random integration, neo still being inactive due to random insertion and hence cells killed during selection.

3.7 Design and construction of targeting LacZ reporter plasmid vector

The LacZ gene was cut from pSVGal reporter plasmid vector with ***XhoI-KpnI***; similarly the pShuttle vector was digested with ***XhoI-KpnI.*** The LacZ gene was ligated with pShuttle and screening the mini-preped plasmid samples confirmed two out of three positives (fig 3.7.3). The pShuttle-LacZ targeting vector was transiently co-transfected with the Cre expressing plasmid in the targetable DLKP clones and the cells were stably selected for G418 resistance. The surviving cells were stained for β-gal activity (section 2.7.2). From the results it was confirmed that although the transfection worked not all cells which survived selection were X-gal positive (fig. 3.7.4).

This suggested that the pShuttle targeting vector may be leaky, i.e. LacZ negative /G418 resistant cells with or without Cre expression. This may be due to two possible reasons. Though Neo is promoterless in the pShuttle vector and should only become active upon Cre-mediated insertion at the genomic LoxP site, it may be that independent of Cre, the plasmid 1) randomly integrates in the genome near an endogenous promoter/enhancer element (As shown in fig 3.7.1) or 2) randomly integrates in the genome in an orientation that facilitates activation of transcription from the CMV on the plasmid. The most likely reason is (1) and the lack of X-gal staining is due to inactivation of the LacZ gene before or during insertion in the genome by endogenous exo & endonucleases.

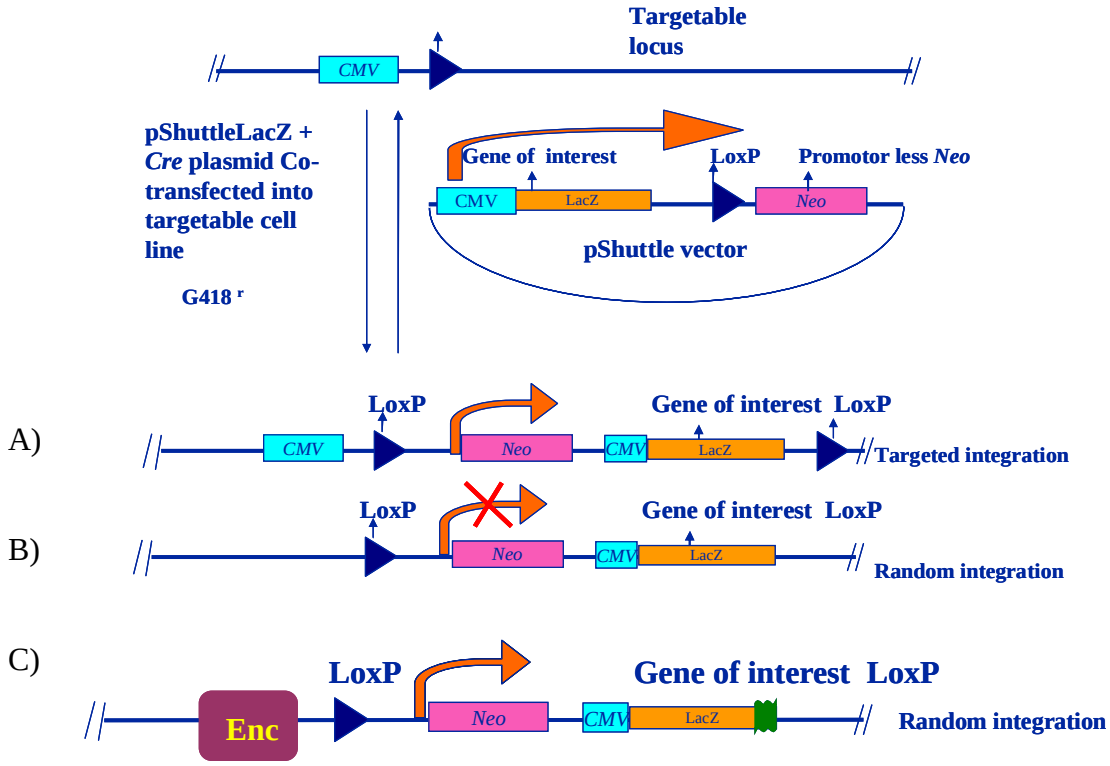

Figure 3.7.1 Schematic representation of possible random integration at Enhancer sites in the Genome. A) Targeted integration, promoterless neo being driven by CMV at the integration site. B) Random integration, neo still being inactive due to random insertion and hence cells killed during selection. C) Random integration in the vicinity of endogenous enhancer/promoter which drives neo and hence resistance to G418 selection. Nucelase activity may be responsible for inactivation of LacZ sequence prior to integration to give X-gal negative cells (green)**.**

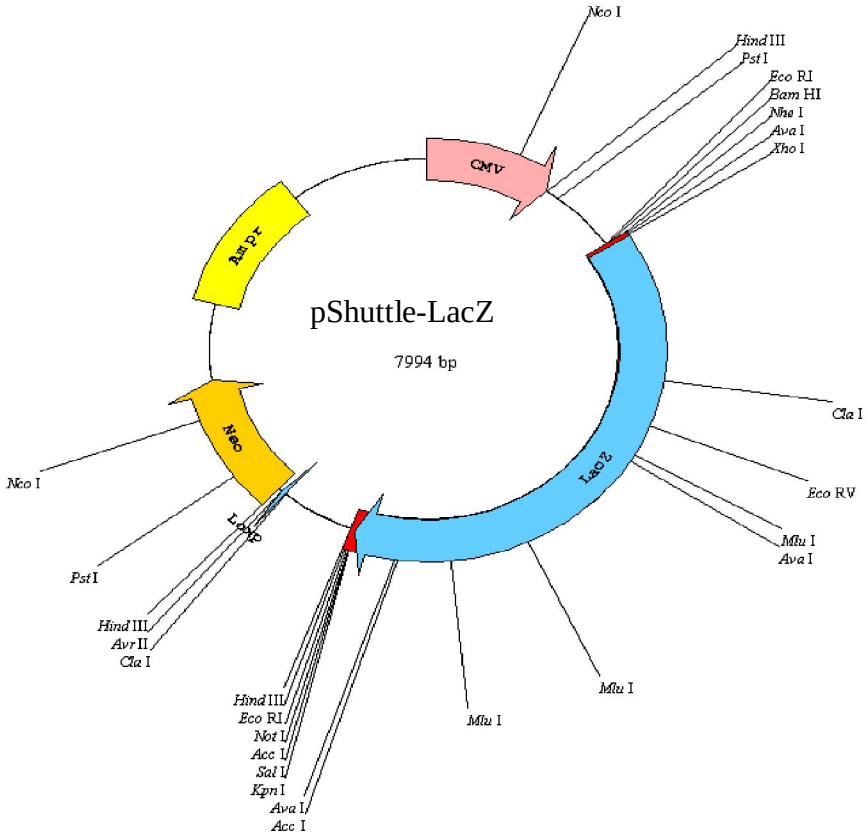

Figure 3.7.2 Schematic representation of shuttle vector carrying LacZ reporter gene which was used as proof of concept for our developed targetable system.

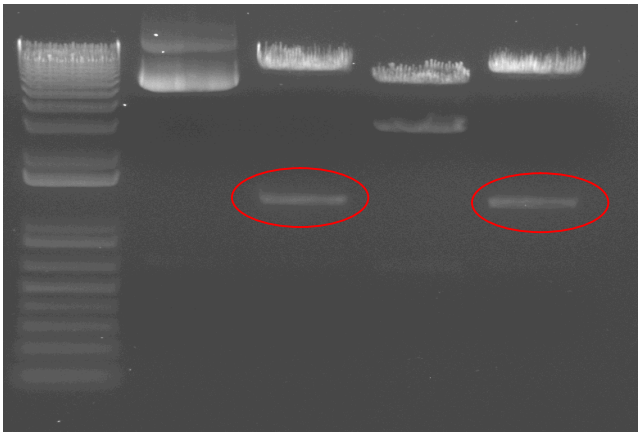

M uncut 6 14 16

Figure 3.7.3 LacZ gene cloning confirmation in pShuttle vector. *XhoI* and *EcoRV* enzymes were used to check for the desired fragment release, lane M: 1kb plus DNA ladder, uncut plasmid, 6 and 16 confirmed released of the desired fragment length and 14 was a negative clone.

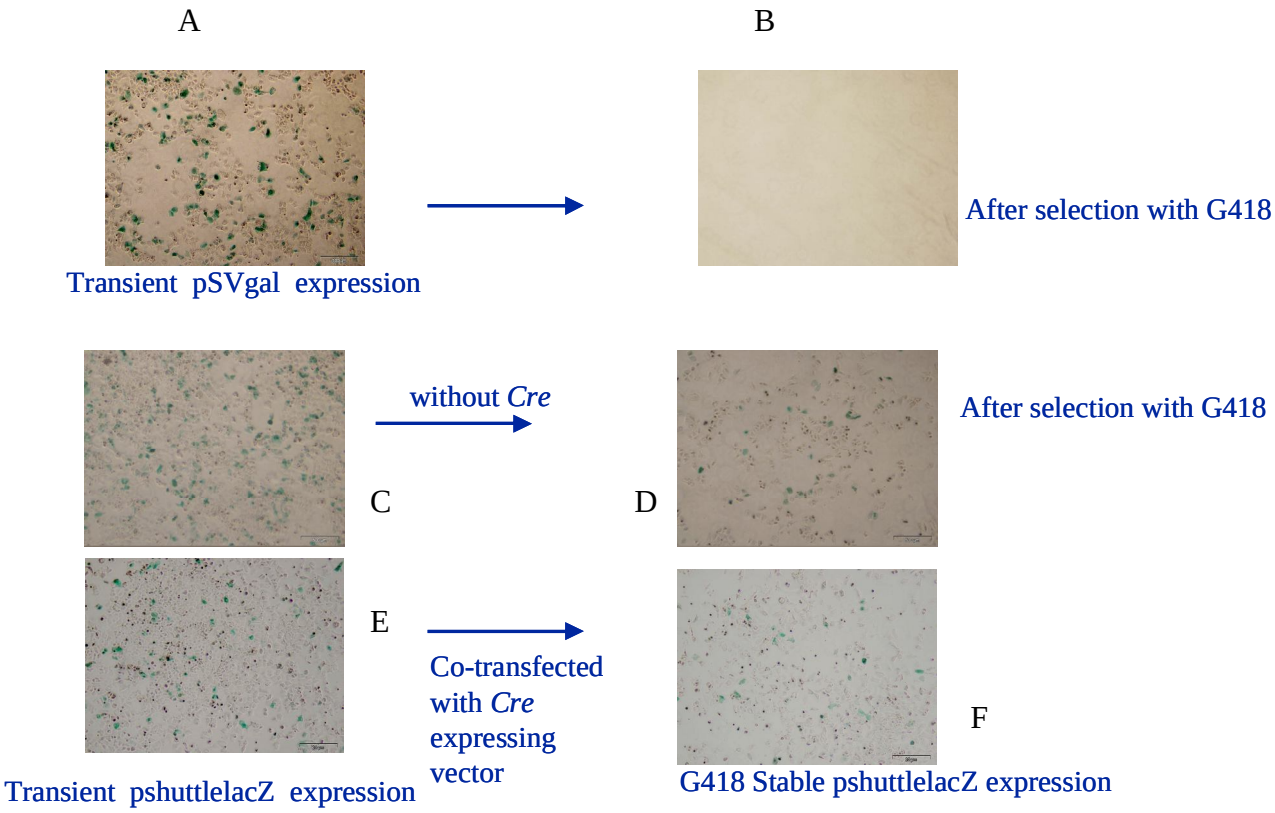

Figure 3.7.4 Transfection of targetable DLKP cell line with pSVGal & pShuttle-LacZ with pCre. Blue colour indicates positive cells. C&D cells transfected with pShuttle LacZ & without pCre. E&F cells transfected with pShuttle LacZ & pCre. A,C&E cells stained for gal activity before selection. B,D&F cells stained for gal activity after selection in G418 for 4-5 days.

3.8 β-Galctosidase staining with pShuttle LacZ & pShuttle-INS transfected DLKP targetable cell line

From this result it was clear that the genetic tool required improvement. We thought the phenomenon was most likely due to endogenous enhancer/promoters and not due to the CMV in the plasmid. So to avoid any positional effect we used an insulator sequence to counteract the effect of local promoters upon random insertion. Insulators possess two properties: an anti-enhancer activity that blocks enhancer-promoter communication, and an anti-silencer activity that prevents the spread of repressive chromatin (Emily J Kuhn et al 2003). Figure 3.8.2 provides proof of the insulator element being cloned in pShuttle-INS-LacZ plasmid. A restriction digestion enzyme confirmed (fig. 3.8.2) that six out of

twelve minipreped samples were positive for desirable fragment release when digested with ***HpaI-AvrII*** enzymes.

Figure 3.8.1 illustrates a schematic representation of the re-targeting vector similar to that mentioned in section 3.7.1, but with one modification, i.e., incorporation of an insulator element upstream of LoxP. The rationale was to try to prevent inappropriate transcription of the Neo gene, which was resulting in survival of cells with non-specific integration events. Accordingly re-targeting plasmid was co-transfected with Cre in the targetable cell lines. The Cre-LoxP reciprocal recombination should facilitate LacZ insertion in between LoxP sites along with the promoter-less Neo. The CMV promoter already present at the targetable locus should allow transcription of Neo to confer G418 resistance on cell lines correctly targeted. The stable cell lines were assayed for β-galactosidase activity to confirm LacZ expression.

Figure 3.8.3 demonstrates X-gal staining of cells transfected with pSVGal and pShuttle-LacZ–INS plasmid vector. From the observed results it is evident that there was a dramatic reduction in cell survival post selection (figure 3.8.3f (i)). These DLKP cells were co-transfected with pShuttle LacZ-Ins plasmid and pCre. This result suggested that the insulator worked, however a small population still remained negative for β-gal activity (figure 3.8.3f (ii)). However, the number of cells surviving selection was greatly reduced compared to previously, in the absence of an insulator sequence.

In conclusion though we were able to overcome the inappropriate transcription of the Neo gene, it was not 100% “clean”. There were always surviving cells which were β-gal negative/G418 resistant. This necessitated an extra step where transgene expression needed to be verified.

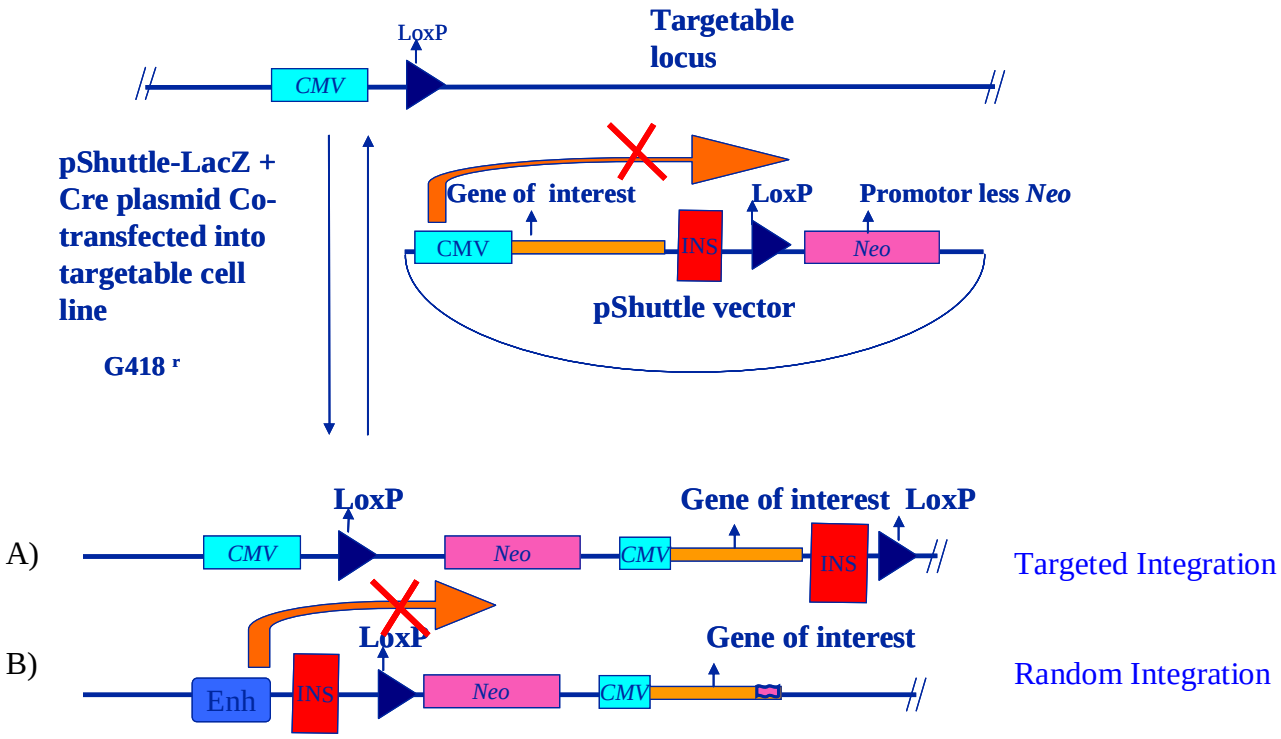

Figure 3.8.1 Schematic representation of re-targeting the loxP site in targetable cell lines with pShuttle containing an insulator. A) Targeted integration, promoterless neo being driven by CMV at integration site. B) Random integration, promoter/enhancer effect being blocked by insulator sequence

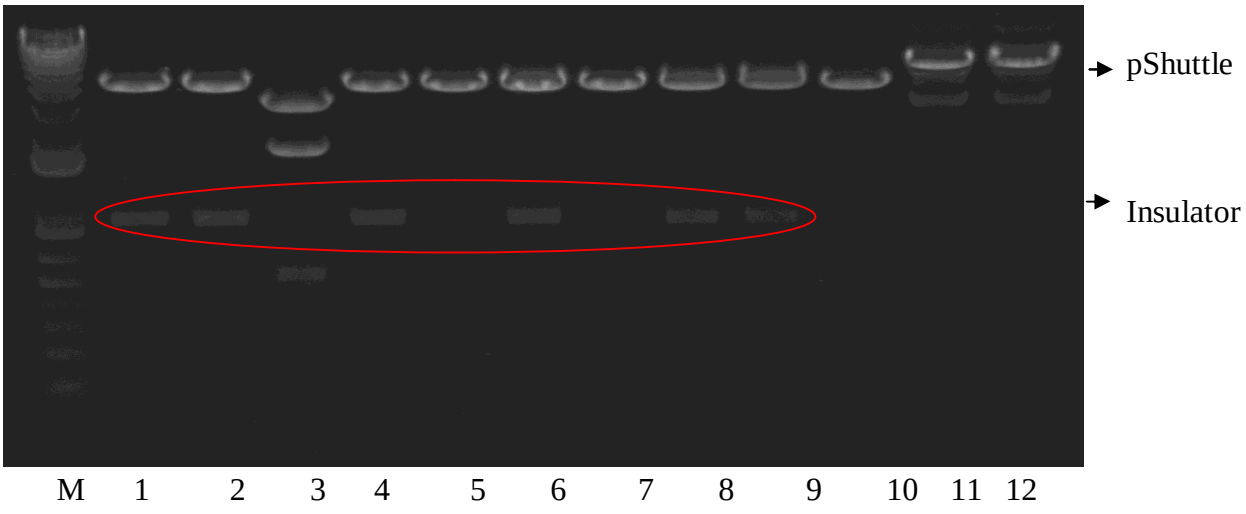

Figure 3.8.2 Restriction enzyme digestion analysis of plasmids to confirm insulator sequence cloning in pShuttle vector. Restriction enzyme digestion with HpaI and AvrII released desired fragment confirming successful cloning, lane M: 1kb plus DNA ladder, lane 1, 2,4,6,8 and 9 indication of desired fragment release.

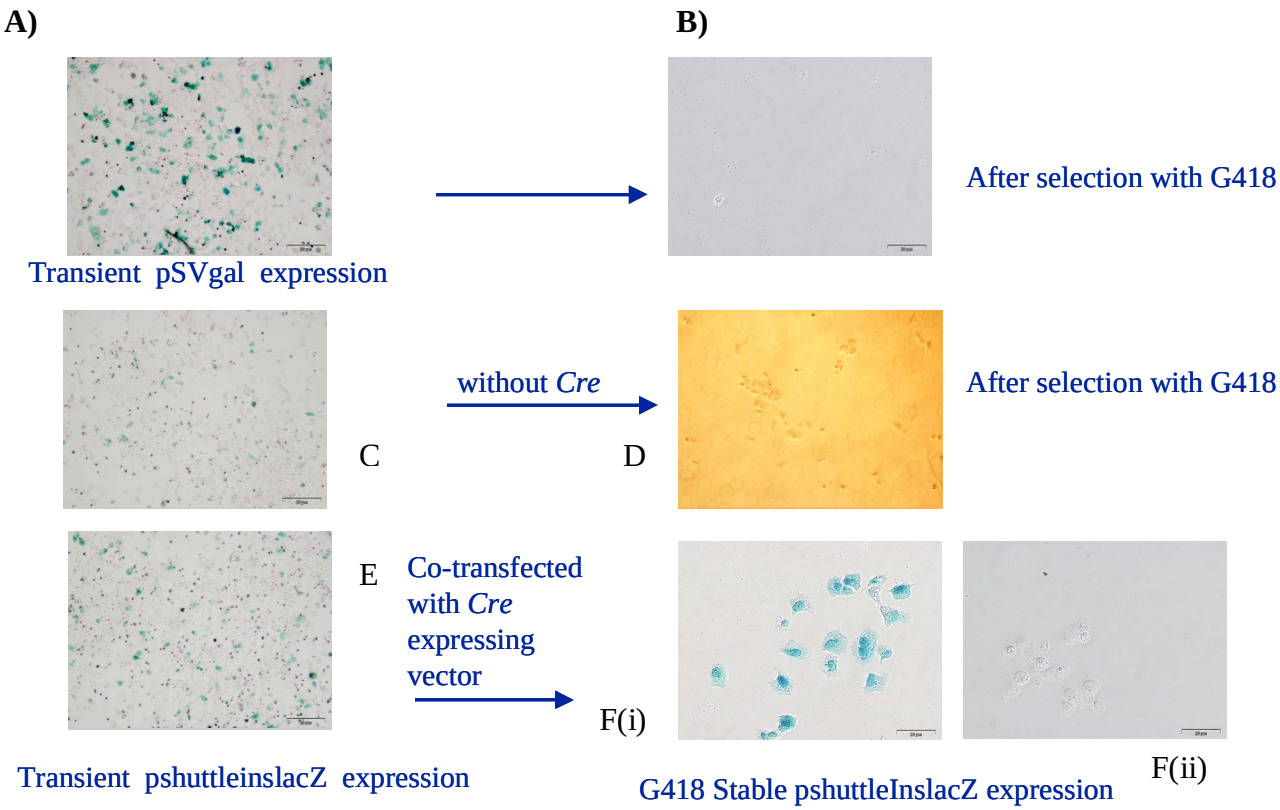

Figure 3.8.3 A& B transfection of DLKP targetable cell line with pSVGal & pCre. Blue colour indicates positive cells. C&D cells transfected with pShuttle LacZ & without pCre. E&F (i) cells transfected with pShuttle LacZ & pCre. A, C&E cells stained for gal activity before selection. B, D&F (i&ii) cells stained for gal activity after selection in G418 for 4-5 days. F (ii) illustrates an example of LacZ –ve colony of cells.

SECTION: B

3.9 Design and construction of LINE-1 sequence specific targeting plasmid vector

In the previous section, the first step in generating the master targetable cell lines involved insertion of the plasmid containing the LoxP flanked "Floxed" *geo* into the genome in a random manner. Clones were then screened for expression and other properties but the site of insertion was unknown.

In this next experiment we wished to avoid this random first step and attempt to insert the "floxed" *geo* into a chosen location or locations in the genome. We planned to use an approach relying on Homologous Recombination (HR) to achieve this. This method was developed in the late 1980's as a means of 'knocking out' genes in ES cells to study gene function in vivo. The technique relies on HR mechanism that occurs during meiosis where sister chromosomes swap alleles to introduce genetic diversity. By flanking a selection marker with sequence that matches a genomic locus, the marker is targeted to that locus, albeit at low efficiency. This phenomenon occurs at very low efficiency in somatic cells so in this case we chose target loci that occur at very high frequency in the genome- Long Interspersed Nuclear Element 1 (LINE1 or L1 elements).

There are approximately 80-100 transcriptionally active copies of this element in the human genome. The rationale behind using L1 elements was a) they constitute 17-20% of the genome which should make them abundantly available targets and b) using L1 element as target should help avoid targeting endogenous genes. This approach would hopefully overcome the problem of low frequencies of homologous recombination in somatic cells and a possible development of a gene targeting system. The plasmid that was designed contained the following elements: a reporter fusion gene [Geo (GFP+Neo)] with two LoxP sequences flanked by split 5' and 3' portions of the ORF-2 sequence of human L1 element. A thymidine kinase outside the 5' end arm of the L1 element was included for negative selection i.e. to reduce or eliminate non-targeted recombination.

The background vector used was a modified pBluescript (Fig 3.1.1). The 1.7kb 5' arm was PCR amplified from pSP52 plasmid vector with NotI-XhoI restriction enzyme sequence overhangs. Later the PCR amplicon and pBluescript were digested with NotI-XhoI, ligated to each other and restriction enzyme digestion analysis of the resulting plasmid (pBKS 5'L1) preps confirmed two positives out of six screened (fig 3.9.3).

Similarly a 2.4kb 3' arm of the L1 ORF2 was subcloned from pSP52 plasmid vector with HindIII-ClaI restriction enzymes and ligated with pBKS 5'L1 vector. Restriction digestion screening revealed one positive out of three (Fig. 3.9.3.1) and this plasmid was designated pBKS 5'-3'L1. Upstream of the 5'arm we cloned the Herpes Simplex Thymidine Kinase gene at the NotI site (fig. 3.9.3.2). The thymidine kinase produced by cells that have incorporated it phosphorylates ganciclovir making it toxic and killing incorrectly targeted cells. This L1 element-targeting vector containing reporter gene, was linearized with HindIII and transfected into DLKP cells. Conditions for maximum transfection efficiency were optimized (fig 3.9.4).

Figure 3.9.1 illustrates the procedure involved in generating LINE-1 specific stable targetable cells by homologous recombination. The targeting vector was comprised of a reporter/selection fusion gene Geo (GFP + Neo) as represented by the green bar in the diagram, flanked by LoxP stie on either side to facilitate Cre mediated removal. A CMV promoter upstream of LoxP was also included. The LoxP sites were flanked by ORF 2 segments of the LINE-1 element. Upstream of the 5' end a negative selection marker gene thymidine kinase was cloned. The DLKP cells transfected with this plasmid were grown in G418 and Ganciclovir containing media to select for homologous integration events. Upon identifying correctly targeted clones the geo sequence could be removed by transient Cre expression as described previously, leaving behind a single LoxP site and a CMV promoter within the ORF2 of an endogenous LINE-1 element.

From the transfection data it was confirmed that the plasmid was transcriptionally active. Figure 3.9.4 demonstrates the transfection optimization conditions for pBKS-L1 targeting plasmid in DLKP cells. Different DNA: Lipofectamine 2000 ratios were used to achieve maximum transfection with minimum damage to the cells. From the results it was evident that 2μg:5μl of DNA to Lipofectamine ratio was optimal (Fig 2b). Although figure 2c appears to have brighter cells, more cells were killed.

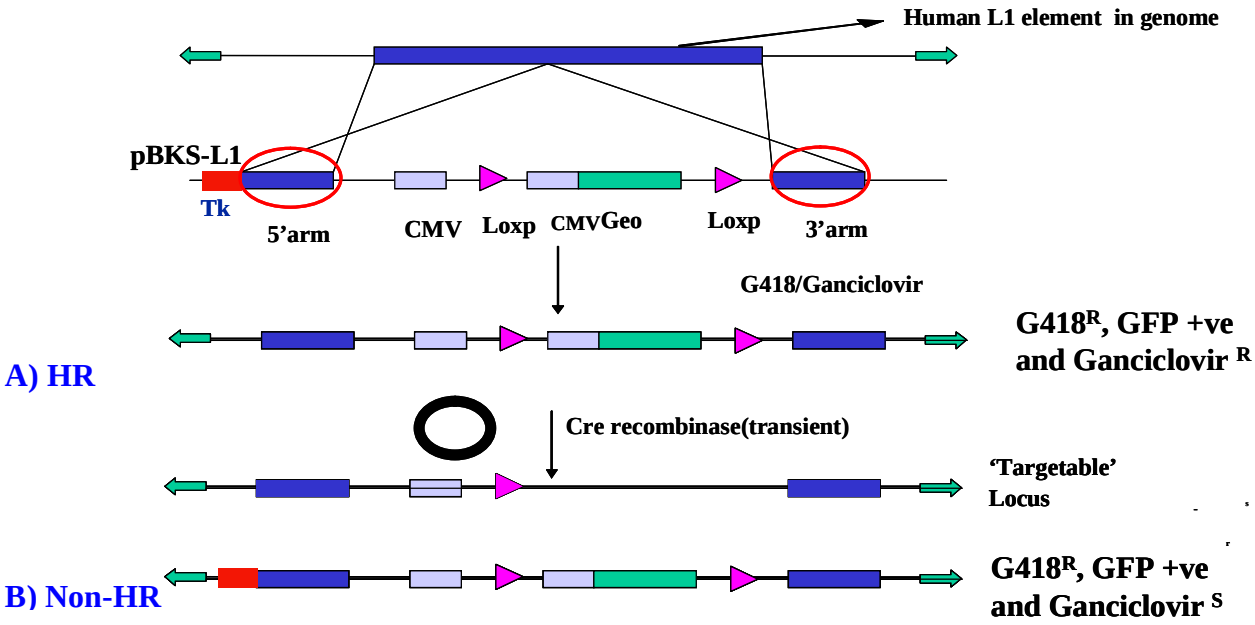

Figure 3.9.1 Schematic representation of L1 element specific targeting mechanism and subsequent knockout of geo to create a single re- targetable LoxP site. A) HR event: cells are G418 resistance, GFP positive and Ganciclovir resistance. B) Non-HR: cells G418 resistance, GFP positive but Ganciclovir sensitive.

The two blue boxes represent split ORF2 region of L1NE 1 element. The pink boxed arrows represent LoxP sites. The red box represent Thymidine kinase gene. The purplish box represents CMV promoter.

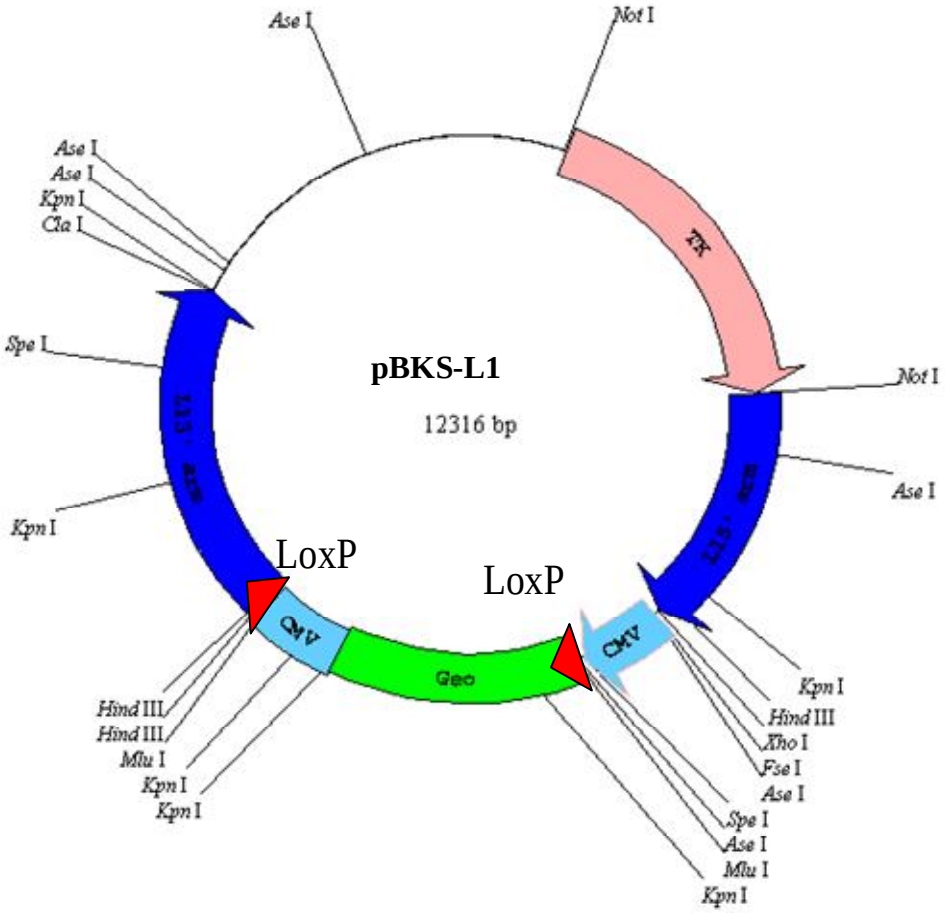

Figure 3.9.2 Schematic representation of pBKS-L1 targeting plasmid. LINE-1 element ORF2 region was split into two with 5' 1.7kb (NotI and XhoI) and 3' 2.4 kb (HindIII and ClaI) fragments cloned on either side of two LoxP sites. The geo selection/reporter cassette was inserted between the LoxP sites and a HSV-thymidine kinase expression cassette was placed upstream of the 5'arm.

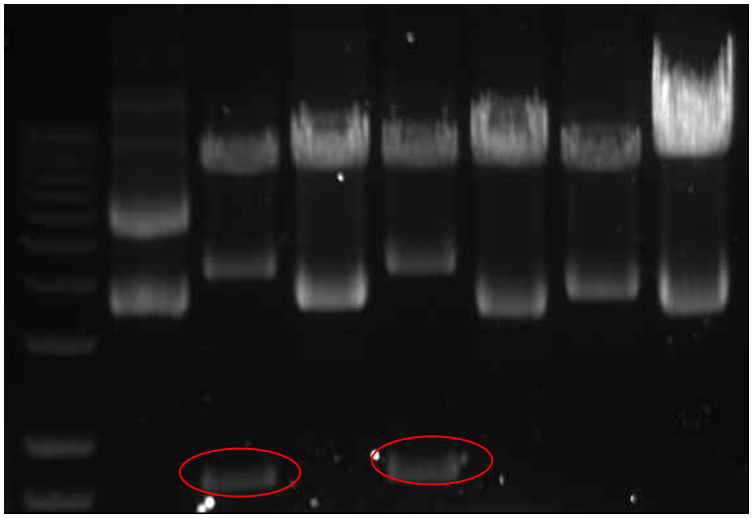

M 1 2 3 4 5 6 7

Figure 3.9.3 DNA agarose gel confirmation of 5'arm cloning. NotI and XhoI restriction enzyme digestion to check cloning of 5' arm of ORF2 of LINE-1 element in pBKSgeo vector, lane 2 & 4 release of expected size of ~1.7kb, lane 1: uncut plasmid, lane 3, 5, 6, 7: cut with NotI and XhoI

M 1 2 3 4

Figure 3.9.3.1 DNA agarose gel confirmation of LINE1 3'arm cloning. HindIII and ClaI restriction enzyme digestion to check cloning of 3' arm of ORF2 of LINE-1 element in pBKSgeo vector, lane 4: release of expected size of ~2.4kb, lane 1: uncut plasmid, lane 2, 3: cut with HindIII and ClaI

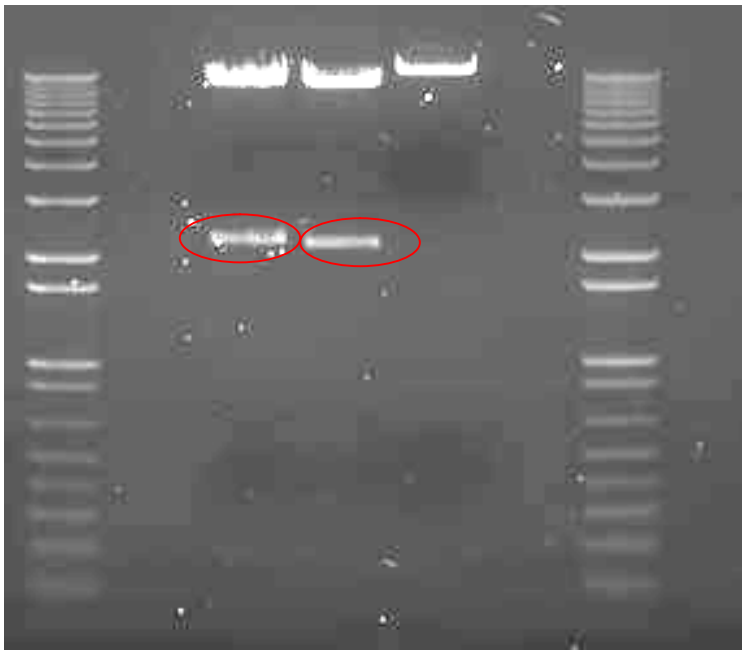

M 1 2 3 M

Figure 3.9.3.2 DNA agarose gel confirmation of Thymidine kinase (Tk) cloning. NotI and SacI restriction enzyme digestion to check cloned Tk gene in pBksgeoL1 plasmid lane 1: NotI cut, 2: SacI cut release of ~2.1kb fragment, M: DNA ladder, 3: Linearized plasmid cut with ClaI.

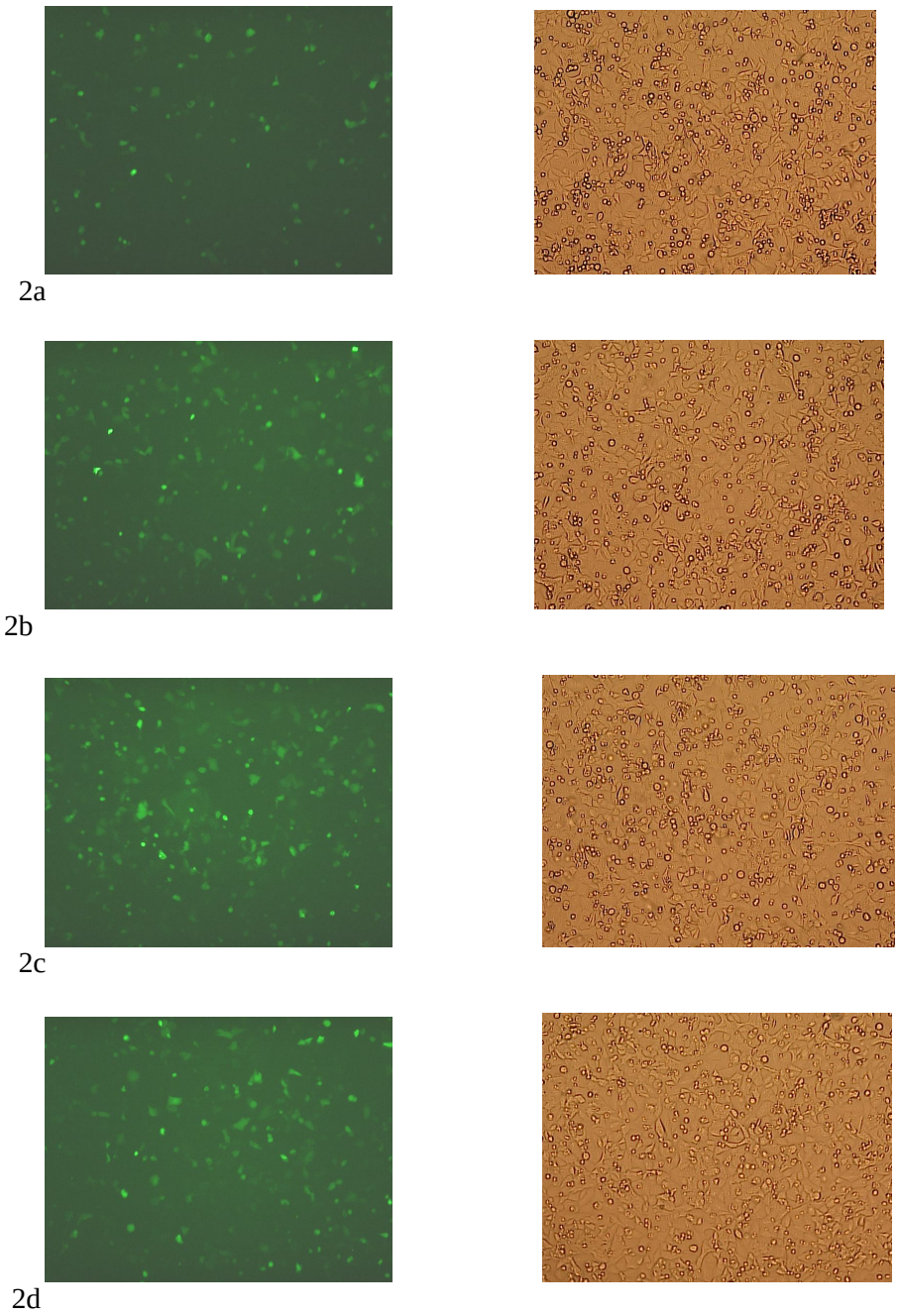

Figure 3.9.4 Transfection optimization with LINE-1 targeting plasmid. 2a, 2b, 2c, 2d represent the different DNA to Lipofectamine 2000 concentrations. While the DNA concentration was kept constant at 2µg the Lipofectamine 2000 concentration was varied from 2, 5, 7 and 10 µl. The cell concentration was kept constant at $3x10^5$ cells/ml and picture view is at 10X optical magnification.

3.10 Transfection of DLKP with LINE-1 specific targeting plasmid and isolation of single cell clones

The transfected cells were stably selected with G418/Ganciclovir containing media and surviving cells were subjected to limiting dilution, single cell cloning in 96 well cell culture plates. We were able to isolate 600 single cell clones which were expanded for genomic DNA isolation (section 2.8.6). PCR screening was performed using primers which were validated with positive controls (fig 3.10.1). Several pairs of primers were designed and used in the screen. Sense primer designed outside the 5' arm but still in the L1 element (in-between ORF1 and ORF2) and an antisense primer in the *geo* region. If a HR event occurs, these would amplify ~2kb product (Fig. 3.10.2). Since we did not have a perfect positive control we used sP52 plasmid which has ORF1 and ORF2 regions of L1 element and pBKS 5'-3' L1 targeting plasmid as control to make sure the primers were binding properly with expected amplicon. Unfortunately despite screening 600 clones we were not able to find a single positive clone with a successful L1 homologous recombination event. This suggested that the homologous recombination frequency in these cells was at the minimum less than one in six hundred compared to random integration.

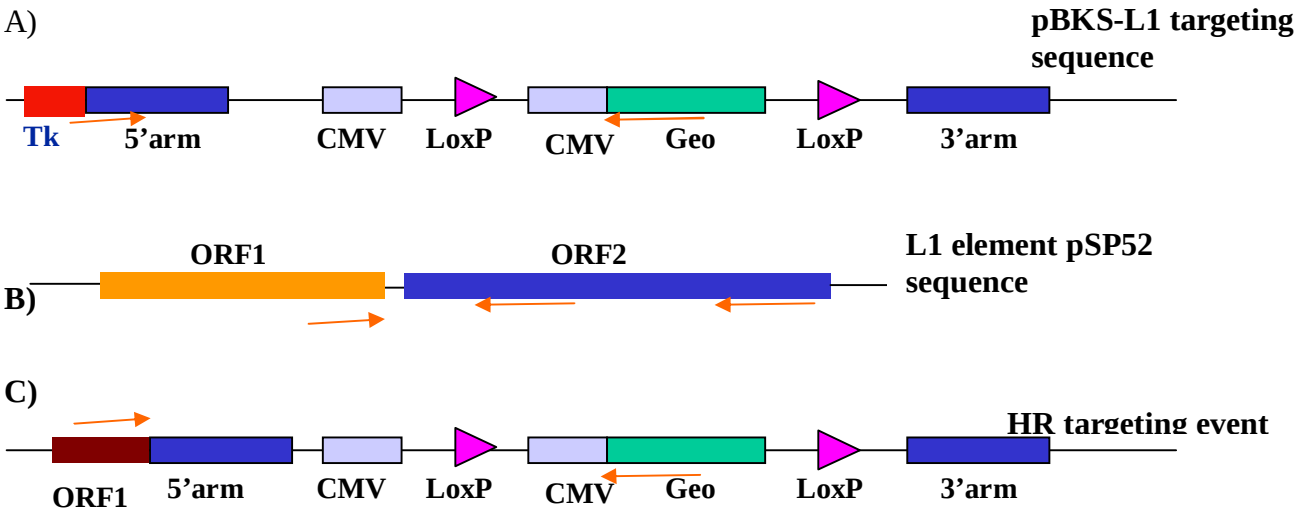

Figure 3.10.1 schematic representation of primer designed regions for HR Screening. A) Represents several sets of primers designed at 5'arm of ORF2 in L1 element as well as from the Geo sequence. B) Primers designed in pSP52 plasmid containing ORF1 and ORF2 full length L1 element. C) The primers designed amplify in the event of HR .

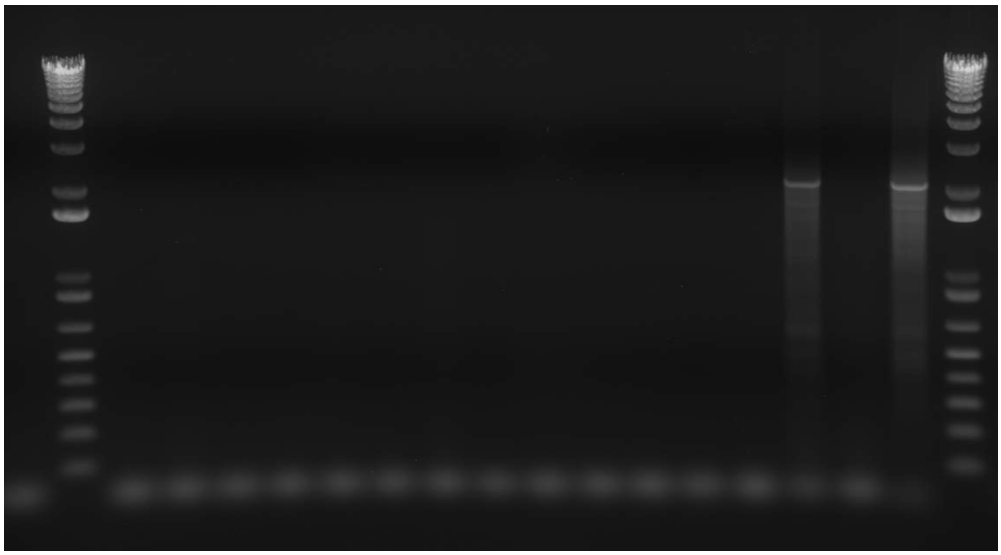

M clones 1 2 3 M

Figure 3.10.2 Represents large scale gDNA PCR screening for homologous recombination. Lane M: 1kb plus DNA ladder, Clones: screened, lane 1: sp52 plasmid control, 2: DLKP-genomic DNA, 3: pBKS-5'-3'L1 plasmid**.**

SECTION: C

3.11 Sub cloning of selected gene targets for stable overexpression studies.

In order to evaluate the mode of action and function of a gene product it is often useful to alter the expression of the gene. This is accomplished through powerful gene manipulation methods including overexpression or knockdown/knockout. Major obstacles with transgene integration and stable transgene expression in mammalian cells are instability either due to chromosomal position effects and/or copy number and variation in expression between different clones. Studies done by Fukushige and Sauer, (1992) addressed the problem of gene transfer into mammalian cells and site specific integration of transgenes at pre-selected sites in the genome with the *Cre-LoxP* based targeting system.

We also applied this system to overcome the above challenges in gene manipulation studies; we developed stable targetable DLKP clones. We checked the robustness of Cre-LoxP targeting by transfecting a pShuttle LacZ reporter vector (section 3.8). From the initial LacZ reporter based results, we realised the targetable system was not 100% efficient. We improved this efficiency to an acceptable level by including an insulator element.

The reason we put the effort into creating these targetable cell lines was to study gene function in a more predictable system. The genes that we were interested in investigating were identified in microarray studies in this lab [Pierce A. PhD thesis NICB, (2006)] comparing parent DLKP with drug resistant cell lines with variable invasive phenotypes. From this study, we selected 4 target genes whose differential expression was validated by qRT-PCR analysis. This validation confirmed that these 4 genes were differentially upregulated compared to mildly invasive parent DLKP cell line. These were GLP1-R, KCNJ8, TFPI2 and S100A13.

The cDNA coding for these targets were subcloned into pShuttle vector, for transfection in two targetable DLKP master cell lines: DLKP-17(high expresser) and DLKP-11(low

expresser). The rationale behind selecting these clones was to study the dosage effect of transgene overexpression. Investigation of these target genes at two different expression levels in the same cell line background was performed. Their functional impact on cellular invasion and proliferation was investigated.

3.11.1 Design and construction of GLP1-R gene in targeting plasmid vector

Glucagon like Peptide 1 Receptor (GLP1-R) cDNA was purchased from OpenBiosystems as a cloned sequence in pCR4-TOPO plasmid vector (cat. no. MHS4426-99238938). Both pCR4-TOPO and pShuttle-Ins vector were digested with ***EcoRI*** enzyme (section 2.13.1) and ligated with pShuttle-Ins plasmid (refer fig.3.11.1a and section 2.13.2), restriction digestion screening of mini-prepped (section 2.13) plasmid DNA confirmed two out of eighteen samples were positive (fig. 3.11.1b). One of the positive clones was selected and maxi preparation (section 2.13.6) of plasmid DNA was performed. The pShuttle-Ins-GLP1-R plasmid was co-transfected with pCre into DLKP-11 and 17 (section 2.8) and selected with G418. The cells surviving selection pressure were subjected to single cell cloning in 96 well plates (section 2.7.1).

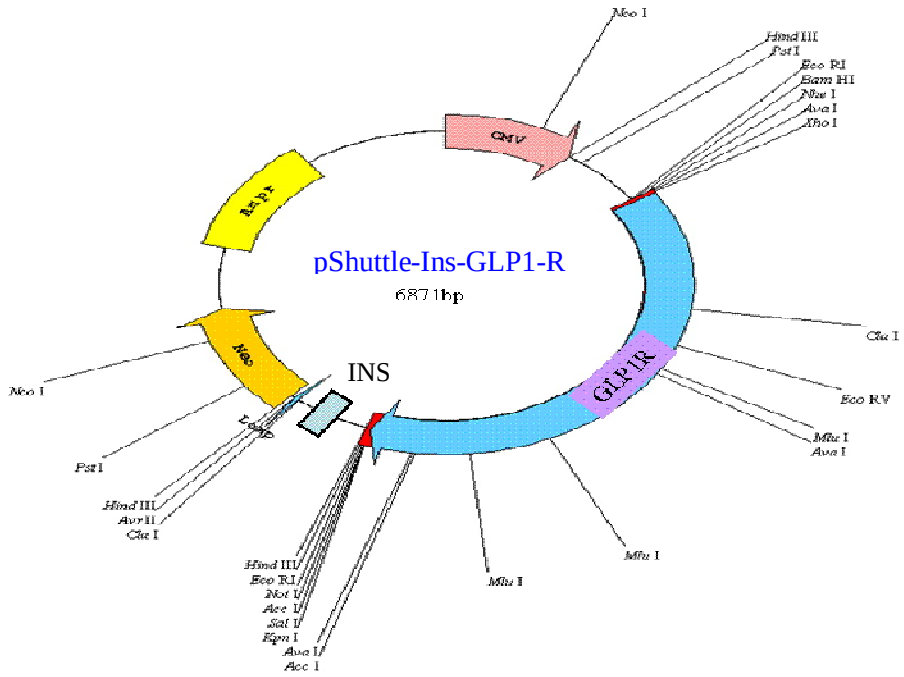

Figure 3.11.1a Schematic representation of pShuttle-Ins targeting vector carrying GLP1-R gene, EcoRI restriction enzyme was used to clone the cDNA construct.

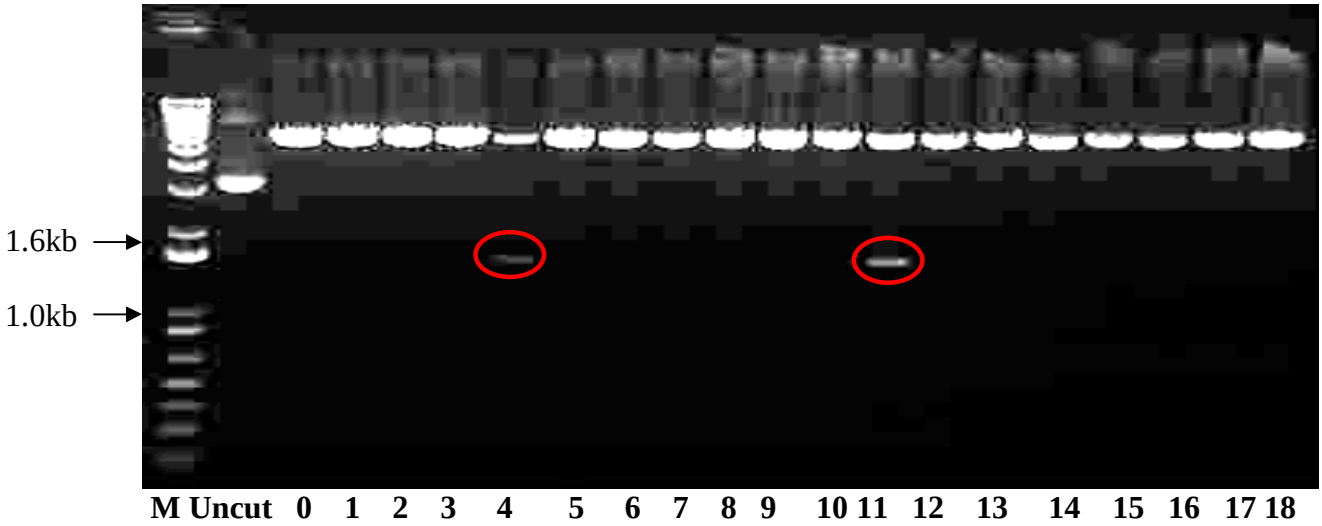

Figure 3.11.1b DNA agarose gel confirmation of GLP1-R cloning. Panel of clones (18) screened for insertion of GLP1-R gene in pShuttle vector. EcoR1 restriction enzyme digestion reveals two clones (4 and 11) had the expected fragment size (~ 1.5kb release), lane 4 and 11 represents GLP1-R clones with the desired release of fragment

3.12 Design and construction of KCNJ8 gene in targeting plasmid vector

KCNJ8 cDNA was purchased from OpenBiosystems as a cloned sequence in pCMV-Sport6 plasmid vector (cat. no. MMM1013-63162). Both pCMV-Sport6 and pShuttle-Ins vector were digested with ***BamHI-XhoI*** enzyme (section 2.13.1) and an insert from pSport ligated with pShuttle-Ins vector (refer fig.3.12.1 and section 2.13.2). Restriction digestion screening of mini-prepped (section 2.13) plasmid DNA confirmed that two out of four samples were positive (fig. 3.12.2). One of the positive clones was selected and maxi preparation (section 2.13.6) was performed. The pShuttle-Ins-KCNJ8 plasmid was co-transfected with pCre into DLKP-11 and 17 (section 2.8) and selected with G418. The cells surviving selection pressure were subjected to single cell cloning in 96 well plates (section 2.7.1).

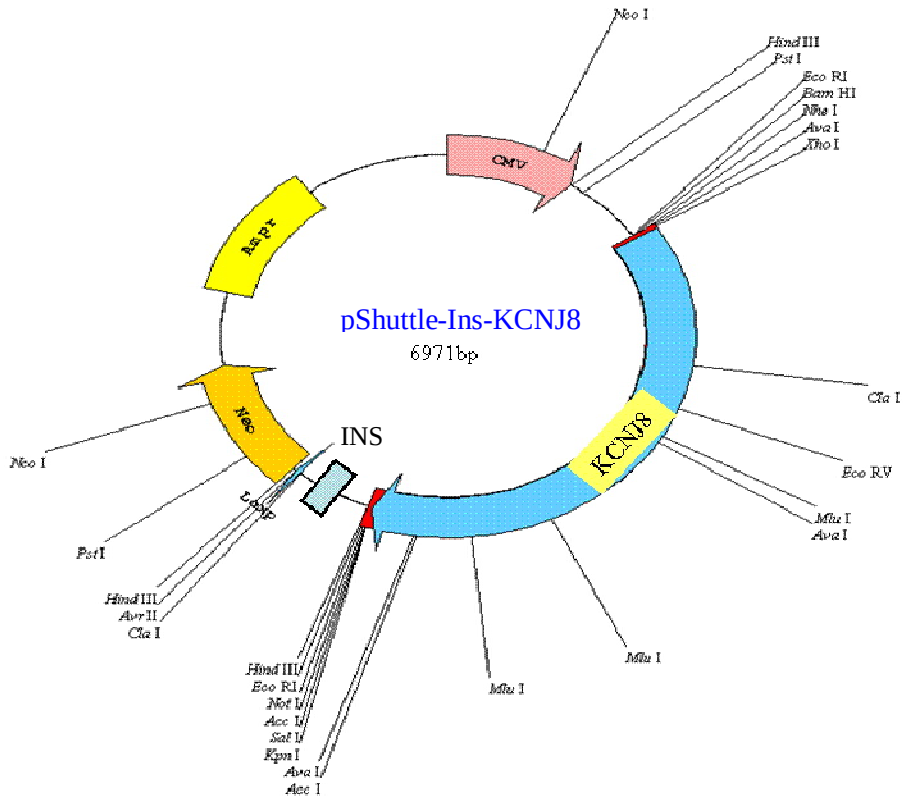

Figure 3.12.1 The pShuttle-Ins targeting vector containing KCNJ8 (Potassium ion channel) gene. *BamHI* and *XhoI* restriction enzymes were used to sub-clone the cDNA into the construct.

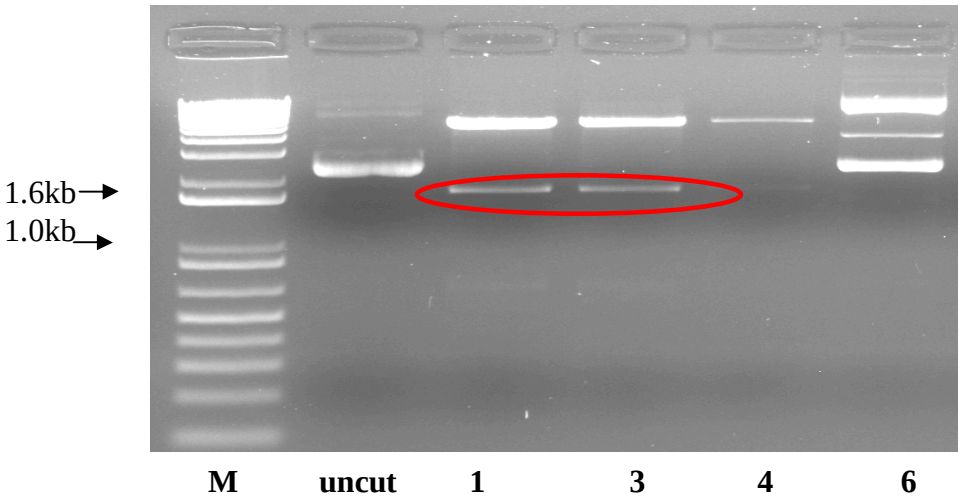

Figure 3.12.2 DNA agarose gel confirmation of KCNJ8 cloning in pShuttle-Ins vector. Restriction enzyme digestion BamH1:Xho1 released the expected ~1.6kb fragment from clones 1, 3 and 4 confirming KCNJ8 gene insertion.

3.13 Design and construction of TFPI2 gene in targeting plasmid vector

Tissue Factor Pathway Inhibitor 2 (TFPI2) cDNA was purchased from Openbiosystems as a cloned sequence in pCMV-Sport6 plasmid vector (cat. no. MMM1013-64874). Both pCMV-Sport6 and pShuttle-Ins vector were digested with ***BglII-XbaI*** enzyme (section 2.13.1) and ligated to in pShuttle-Ins vector (refer fig.3.13.1 and section 2.13.2). Restriction digestion screening of mini-prepped (section 2.13) plasmid DNA confirmed that six out of ten samples were positive (fig. 3.13.2). One of the positive clones was selected and maxi preparation (section 2.13.6) of plasmid DNA was performed. The pShuttle-Ins-TFPI2 plasmid was co-transfected with pCre into DLKP-11 and 17 (section 2.8) and selected with G418. The cells surviving selection pressure were subjected single cell cloning in 96 well plates (section 2.7.1).

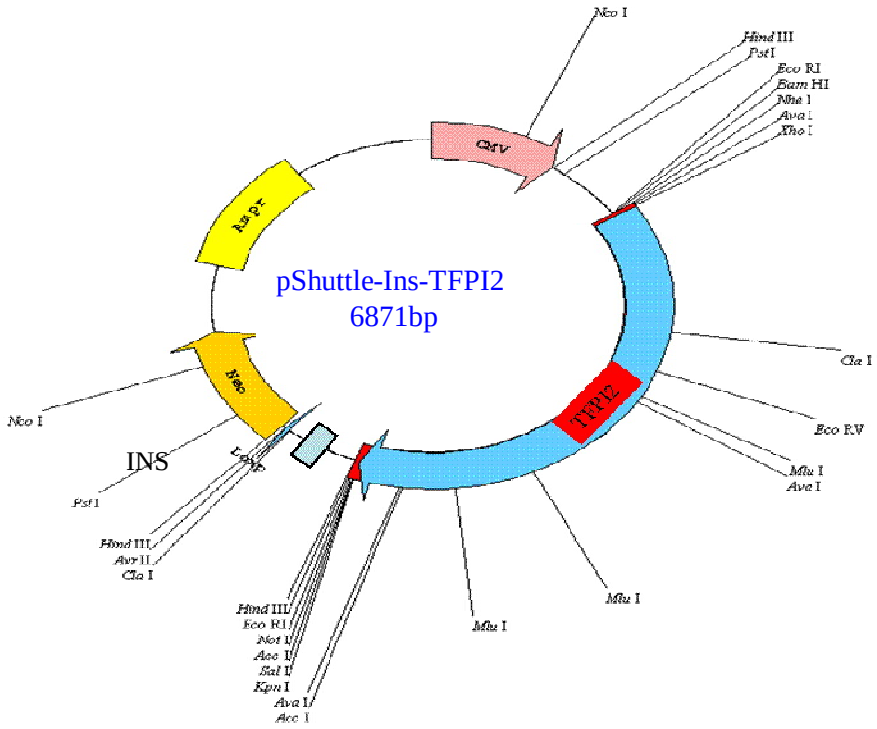

Figure 3.13.1 the pShuttle-Ins targeting vector carrying TFPI2 (Tissue factor pathway inhibitor 2) gene. *XbaI* and *BglII* restriction enzyme were used to sub-clone the cDNA construct.

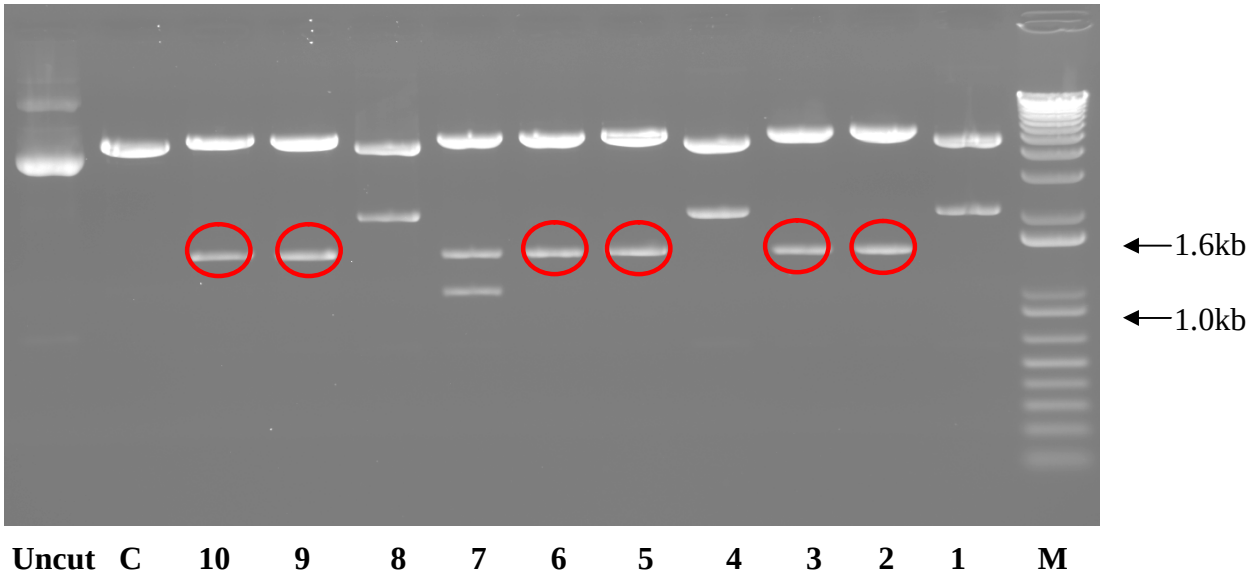

Figure 3.13.2 DNA agarose gel confirmation of TFPI2 gene cloning in pShuttle vector. BglII: XbaI restriction enzyme digestion released expected fragment of ~ 1.5kb from clones 2, 3,6,7,9 &1

3.14 Design and construction of S100A13 gene in targeting plasmid vector

S100 calcium binding protein A13 (S100A13) cDNA was purchased from Openbiosystems as cloned sequence in pOTB7 plasmid vector (cat. no. MHS1011-59294). Both pOTB7 and pShuttle-Ins vector were digested with ***BamHI-XhoI*** enzyme (section 2.13.1) and ligated in pShuttle-Ins plasmid vector (refer fig.3.14.1 and section 2.13.2). Restriction digestion screening of minipreped (section 2.13) plasmid DNA confirmed that one clone was positive (fig. 3.14.2). The positive clone was selected and maxi preparation (section 2.13.6) of plasmid DNA was performed. The pShuttle-Ins-S100A13 plasmid was co-transfected with pCre into DLKP-11 and 17 (section 2.8) and selected with G418. The cells surviving selection pressure were subjected to single cell cloning in 96 well plates (section 2.7.1).

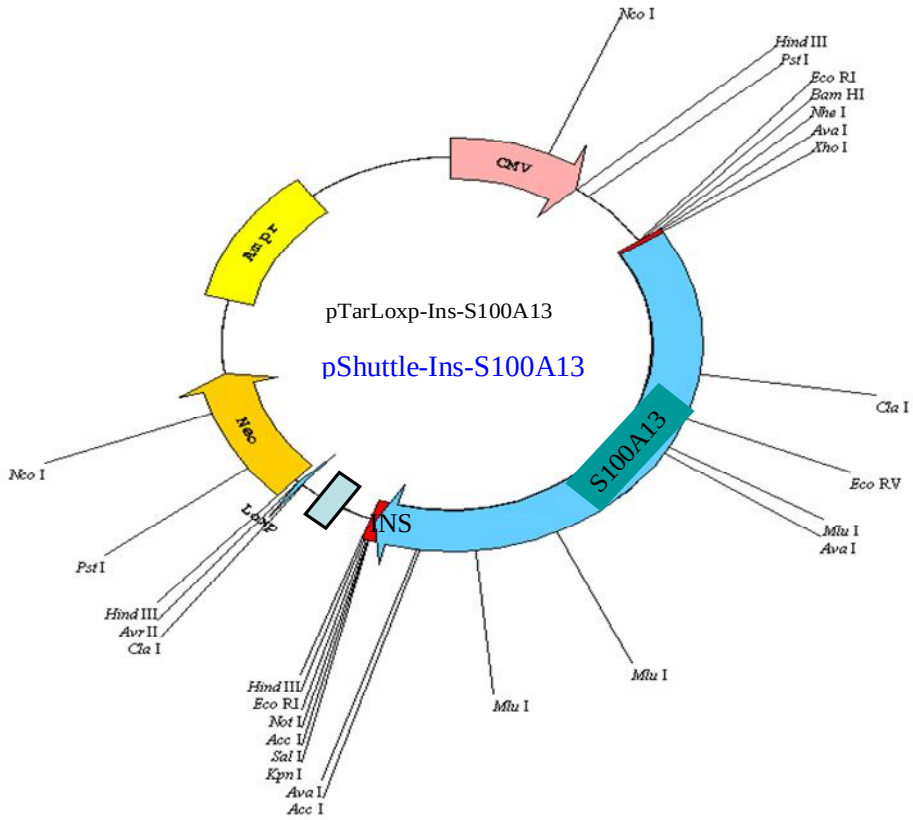

Figure 3.14.1 the pShuttle-Ins targeting vector carrying S100A13 (calcium ion binding protein) gene. *BamHI* and *XhoI* restriction enzyme were used to sub-clone the cDNA construct.

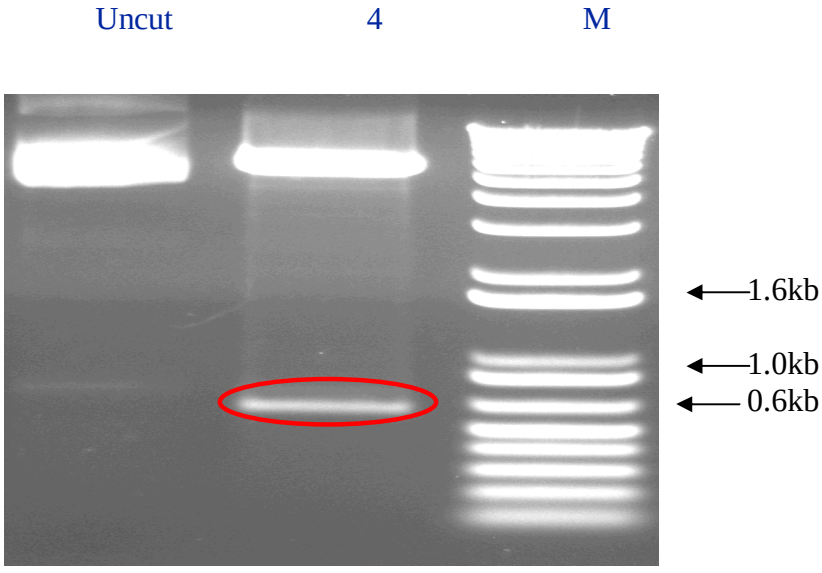

Figure 3.14.2 DNA agarose gel picture of S100A13 gene cloning in pShuttle vector. BamH1:Xho1 restriction digestion revealed that clone (4) contained the S100A13 insert with the expected ~ 0.6kb release.

3.15 Assessment of Invasion phenotype of DLKP 17 and 11 master targetable clones

To investigate the role of the chosen genes on invasion and proliferation we initially assessed the baseline invasive phenotype of the master targetable clones. Invasion assays were performed (section 2.7.1) on DLKP 17 (high expresser) and DLKP 11(low expresser). The experiment was performed in biological triplicates to ensure the consistency of the observation. DLKP 17 was found to be non invasive and DLKP 11 was highly invasive (fig. 3.15.1). Also we had demonstrated previously from the stability and expression level assessment (section 3.2) that DLKP-17 had a high level of transcription from its integration site and DLKP-11 was a low expressing clone.

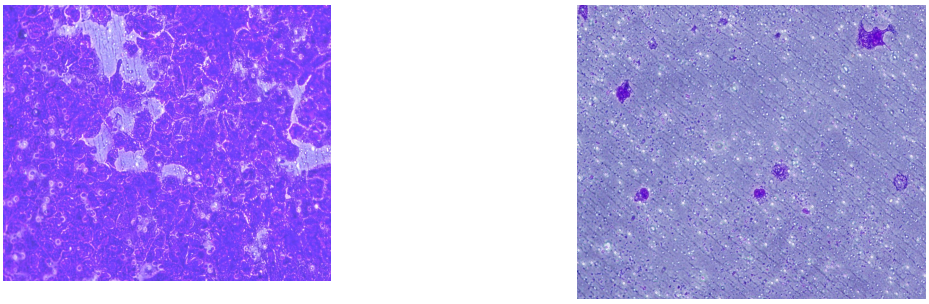

DLKP 11 **DLKP 17**

Figure 3.15.1 Invasive phenotype of targetable master clones DLKP 17 and DLKP 11.

3.16 To determine the targeting event through PCR screening

Two DLKP targetable clones 17 and 11 were selected from our stability studies (section 3.2), which were different in their transgene expression levels. They were *Cre* 'cured' to remove *geo* leaving a LoxP site as an endogenous, targetable locus. Stable co-transfections were carried out (section 2.8.1), with constructed transgene shuttle vectors. From stable clones genomic DNA was isolated (section 2.11.1) for PCR screening.

Figure 3.16.1A shows a schematic representation of primers designed to screen the re-targeted locus. The sense and antisense primers are represented as red arrows. These primers only result in an amplicon if re-targeting is successful. Figure 3.16.1B shows PCR screening of transgene re-targeting event. The agarose gel illustrates an example where re-targeting screen has been performed. A faint but expected band of ~170bp was observed in DLKP 17a clone. But we were not able to visualise in DLKP 11a could be due to much lower copy than DLKP 17a.

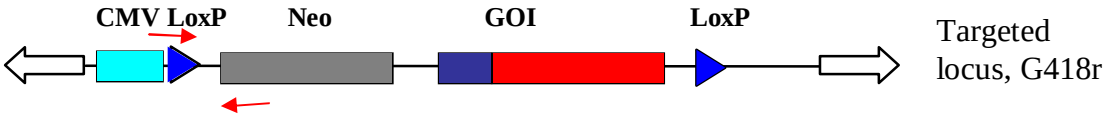

Figure 3.16.1A Schematic representation of targeted locus and primers location.

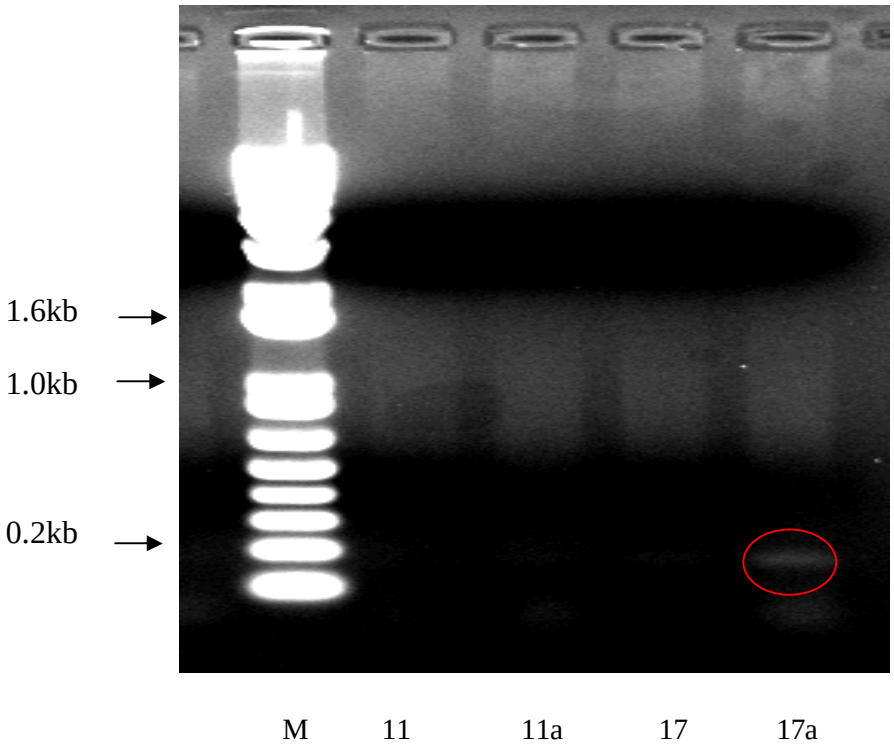

Figure 3.16.1B PCR analysis confirming GLP1-R targeting event in DLKP. Template used was DNA from DLKP 11 and 17 re-targeted cell lines and their targetable clones as controls. Lane M: 1kb plus DNA ladder, 11: DLKP 11, 11a: DLKP retargeted, 17: DLKP 17 and 17a: DLKP 17 retargeted. Amplicon had expected size of ~ 170bp amplified in DLKP 17a but not in parent cell line.

3.17 Investigation of the effect of stable GLP1-R overexpression in DLKP 17 and DLKP 11 cell lines

The protein encoded by this gene is a member of the glucagon receptor family of G protein-coupled receptors. GLP1-R cDNA was cloned into the pShuttle-Ins vector and co-transfected with pCre in DLKP 17 and DLKP 11 targetable cell lines. The transfected cells were selected for G418 resistance and limiting dilution, single cell cloning was performed.

The single cell clones were bulked up and RNA was extracted (section 2.11.2). Initial overexpression of GLP1-R at transcript level was monitored by qRT-PCR analysis (section 2.11.4). The qRT-PCR analysis revealed (fig. 3.17 A&B) that DLKP 17 and 11 clones had distinctively different GLP1-R expression as observed in the original stability screen. For all the qRT PCR studies b-actin was used as an endogenous control, which was used to normalize the expression levels across the samples. The protein lysates were also extracted from these cell lines and western blot analysis was performed (section 2.14) revealing that the two clones expressed GLP1-R (Fig. 3.17C). For all western blot analysis anti-GAPDH antibody as was used to ensure equal quantity of sample loading.

A) **DLKP-17-GLP1-R**

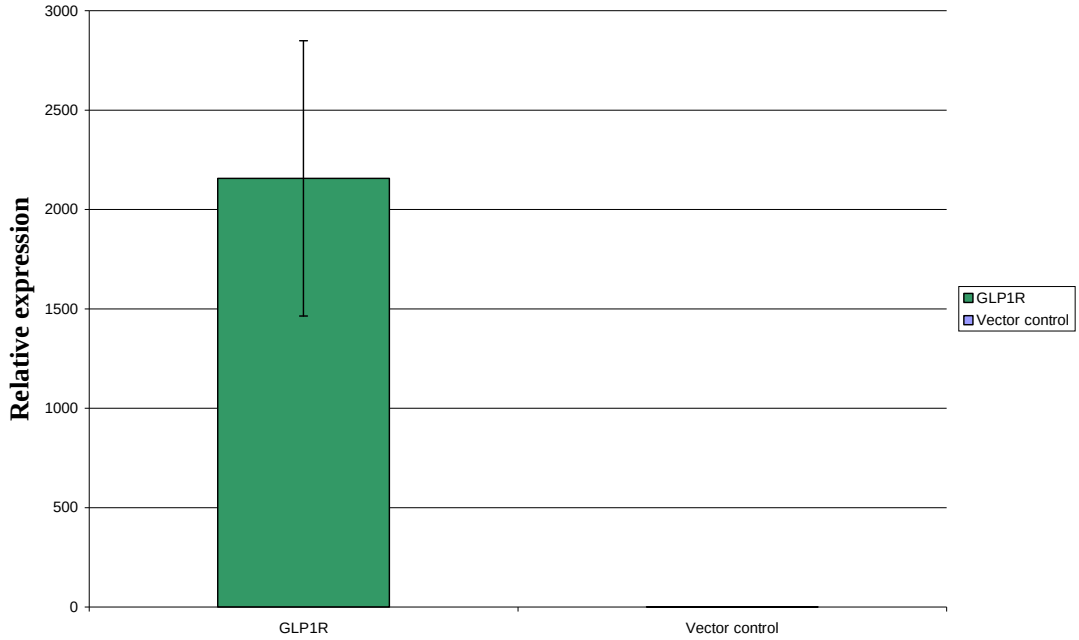

B)**DLKP-11-GLP1-R**

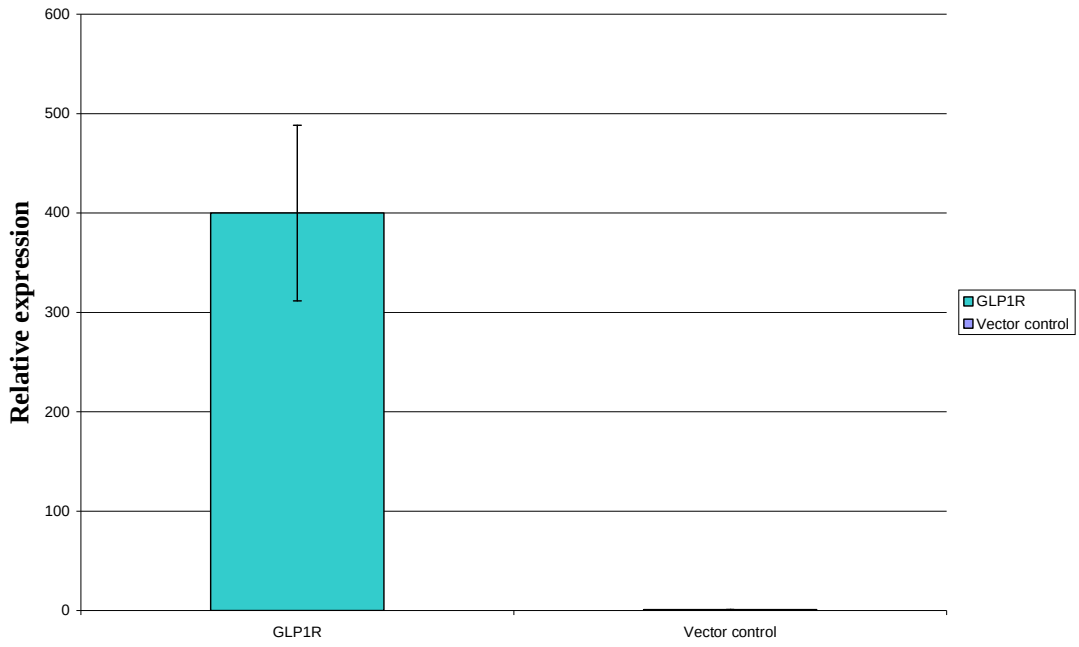

Figure 3.17A&B qRT-PCR confirmation of stable GLP1-R transgene overexpression in DLKP 17 and DLKP 11. (A) Illustrates relative qRT PCR analysis of stable GLP1-R overexpression in DLKP 17 clone compared to empty vector control. The values were normalised to endogenous β-actin levels. A relative fold difference of 2300 (SEM ± 692%) was observed. Similarly, figure (B) illustrates the stable GLP1-R overexpression in DLKP 11 cell line, with a relative fold difference of 400 (SEM ± 88.3%).

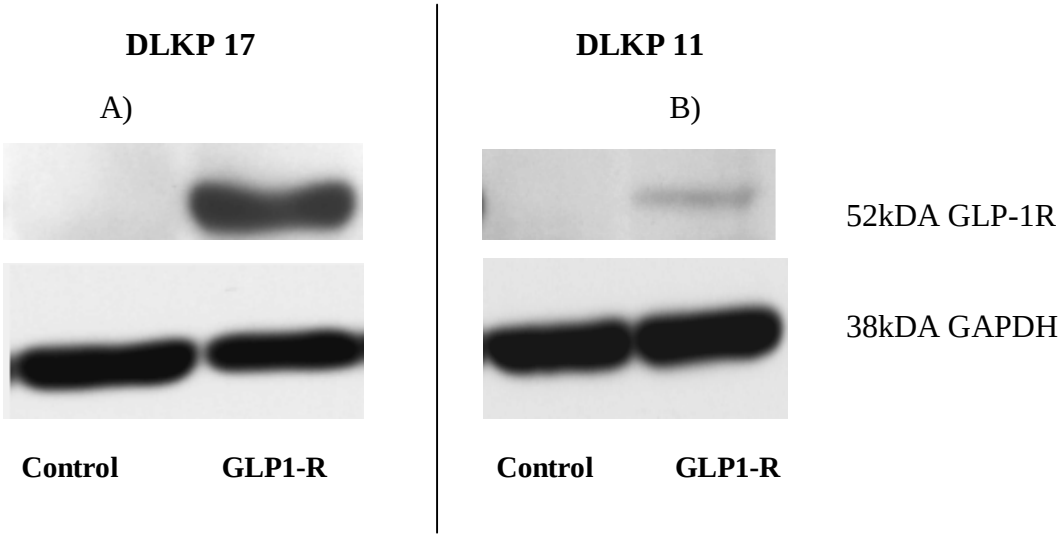

Figure 3.17C Western blot analysis of GLP1-R expression in DLKP 11 GLP1-R and DLKP 17-GLP1-R compared to control. A&B illustrates a 52kDa band specific to GLP1-R, both in DLKP 17 and DLKP 11 overexpressing cell lines. Conversely no band was detected in empty vector control transfected cells. Anti GAPDH antibody was used to ensure similar protein loading on the gel.

3.17.1 To evaluate the effect of stable GLP1-R overexpression on proliferation in DLKP 17 and 11 cell lines.

To determine if there was any impact on proliferation due to constitutive GLP1-R overexpression, we performed a proliferation assay (section 2.9). The effect on cell growth was investigated by seeding 100µl of $3x10^4$ cells per ml of GLP1-R overexpressing DLKP 17 and 11 cell lines and their empty vector controls for relative measurements. 48 hrs after seeding, growth in each well on the plate was measured using the acid phosphatase assay as described in Section 2.9

As can be seen in Fig. 3.17.1 A&B stable overexpression of GLP1-R in DLKP 17 and DLKP 11 decreased cell proliferation relatively. Significant decrease of around 40% in cell number was observed compared to control vector in DLKP 17 cells. Similarly relative to empty vector transfected DLKP 11, GLP1-R overexpressing DLKP 11 clones showed a significant 20% reduction in cell number.

A) DLKP-17

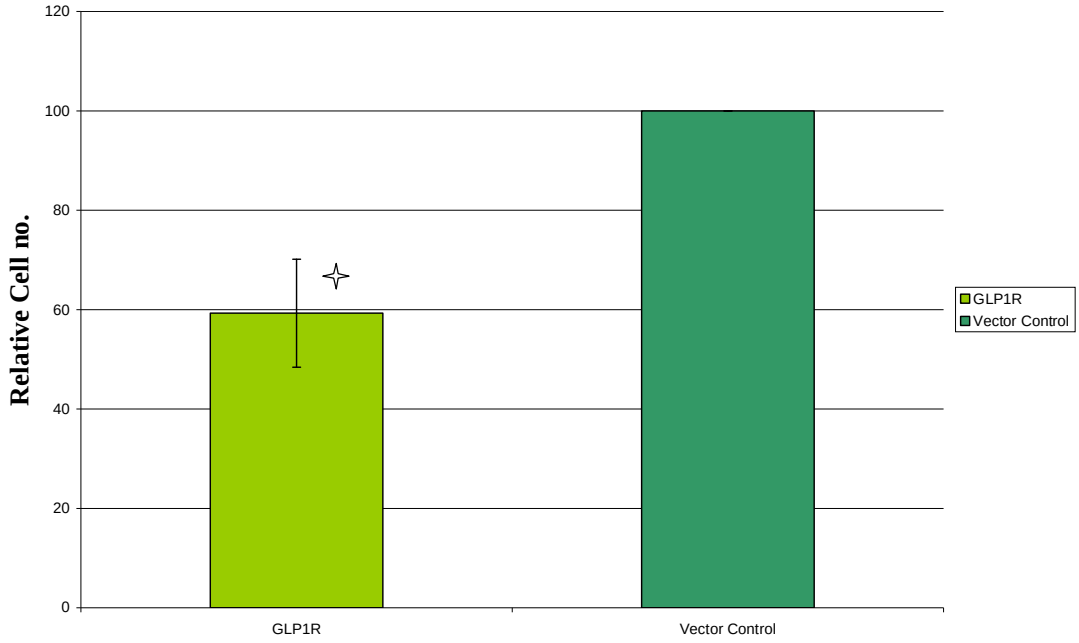

B) DLKP-11

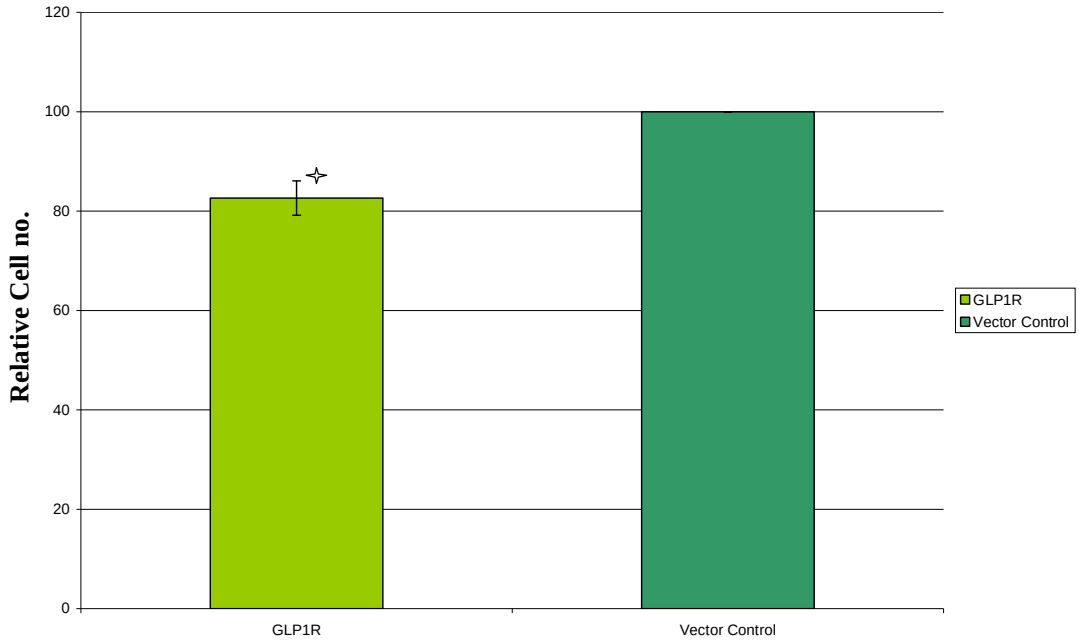

Figure 3.17.1 A & B Stable GLP1-R overexpression Proliferation assay relative to empty vector transfected cells in DLKP 17 and DLKP 11 cell lines. A) DLKP 17: a significant decrease in proliferation relative to control with [p-value (<0.05)]. B) DLKP 11: also significant decrease relatively with p-value (<0.05) and N=3.

3.17.2 To evaluate the effect of stable GLP1-R overexpression on the invasive phenotype of DLKP 17 and DLKP 11 cell lines.

From our previous experiment to establish the baseline invasive phenotype of DLKP 17 and DLKP 11 cell lines it was observed that DLKP 17 was non invasive and DLKP 11 was highly invasive. To evaluate the effect of GLP1-R overexpression on DLKP 17 and DLKP 11 invasion we performed an in vitro invasion assay. The invasion assays were performed over 48 hours using a commercial invasion assay kit containing inserts pre-coated with Matrigel (ECM) without a serum gradient. This was to avoid induced invasion due to extra serum levels in the media. The cells were seeded at 10^5 cells per insert. They were incubated at 37^{o}C for 48 hours after which the undersides of the inserts were stained; ten fields of view were counted per insert at 20X magnification and averaged. At least two inserts were used for the analysis of each condition.

The effect of GLP1-R stable overexpression on DLKP 17 was dramatic (~ 700%) i.e. a significant induction from non a invasive to an invasive phenotype was observed in DLKP17 GLP1-R overexpressing cells (Fig.3.17.2A). Conversely in DLKP 11 which was already invasive, there was no apparent impact on invasion visually but the cell counts suggested that there was a small but significant (20%) decrease in invasion compared to empty vector control.

A)

DLKP 17 Vector control DLKP 17 GLP1-R

Figure 3.17.2A Photographic representation of invasion assay in stable GLP1-R overexpressing DLKP 17 cell line. Invading cells stained purple.

B)

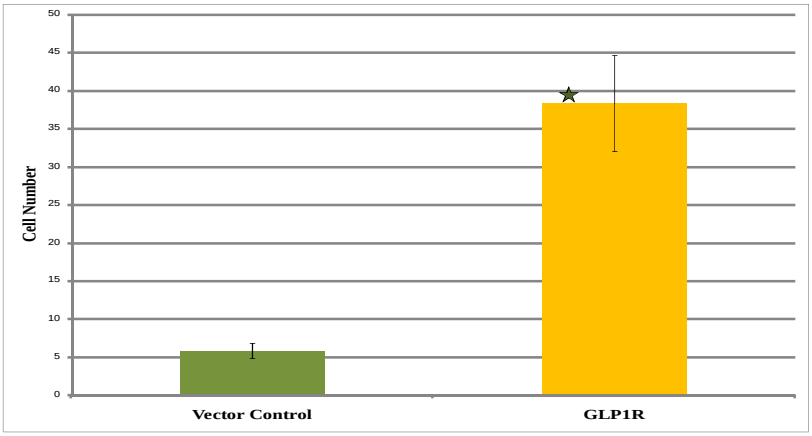

Figure 3.17.2B Invasion assay in stable GLP1-R overexpressing DLKP 17 cell line. Significant increase in invasion was observed relative to DLKP 17 vector control with * [p-value (<0.05)] and N=3.

C)

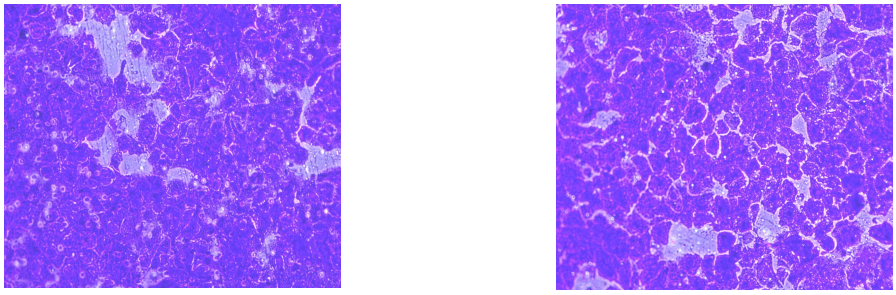

DLKP 11 Vector control DLKP 11 GLP1-R

Figure 3.17.2C Photographic representation of invasion assay results in stable GLP1-R overexpressing DLKP 11 cell line

D)

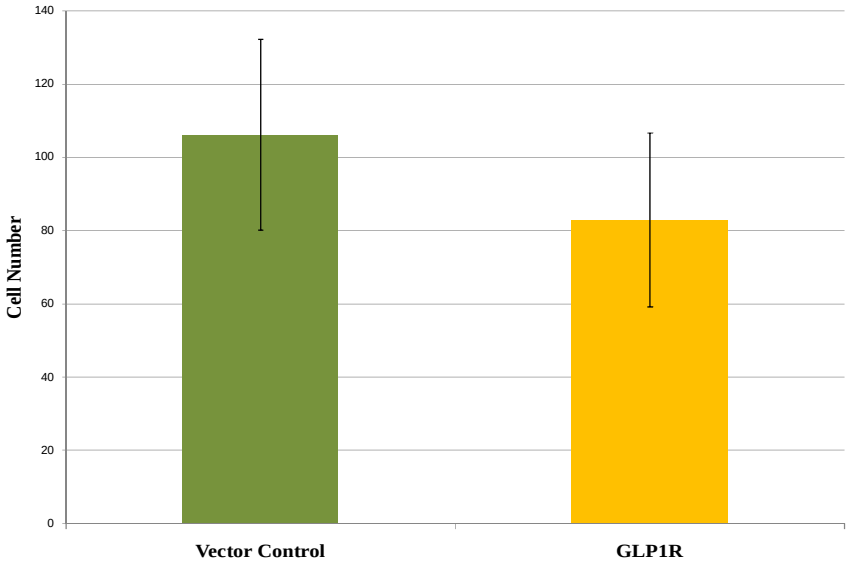

Figure 3.17.2D Invasion assay results in stable GLP1-R overexpressing DLKP 11 cell line. A decrease in invasion was observed relative to DLKP-11 vector control. However it was not significant. N=3.

3.18 Investigation of the role of GLP1-R overexpression in non-invasive MCF-7 cell line.

The pro invasive effect of GLP1-R overexpression in non invasive DLKP-17 was dramatic but, was it cell line specific? To address this we transiently overexpressed GLP1-R in MCF-7 (breast cancer cell line), which has been previously reported as a non invasive cell line. Overexpression was confirmed by western blot analysis.

3.18.1 Western blot analysis of GLP1-R transient overexpression in MCF-7 cell line.

Transient overexpression of GLP1-R in transfected MCF-7 cell line was evaluated at the protein level. Briefly the cells were transfected with pShuttle-Ins-GLP1-R plasmid and 48 hrs post transfection protein was extracted from cells and used for GLP1-R specific western blot analysis (section 2.14) using a GLP1-R specific antibody (table 2.10). Blots were incubated using a 1/1000 dilution of antibody which generates a 52kDa band specific to GLP1-R. Anti GAPDH antibody was used as loading control and generated a 38 kDa GAPDH specific band. Figure 3.18.1A illustrates immunoblot confirmation of transient GLP1-R overexpression in MCF-7 compared to empty vector control. The quantity of GLP1-R in the transfected MCF-7 cells was considerably higher considering the difference in endogenous loading control.

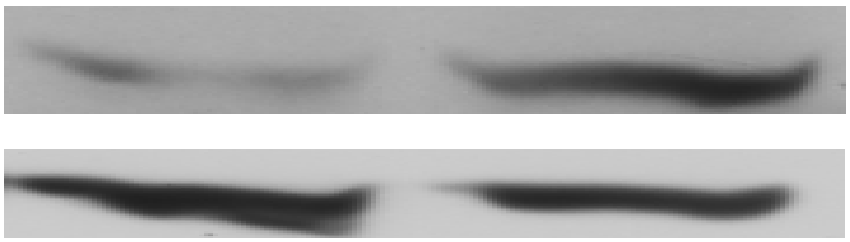

Figure 3.18.1A Western blot analysis of transient GLP1-R overexpression in MCF-7 cell line.

3.18.2 Investigate GLP1-R transient overexpression on invasion in non-invasive MCF-7 cell line

Stable GLP1-R overexpression in DLKP 17 (non invasive) targetable cell lines resulted in induction of the invasive phenotype. To evaluate the effect of GLP1-R as a modulator of cellular invasion we performed transient overexpression of GLP1-R in a known non invasive breast cancer cell line MCF-7. The pShuttleGLP1-R or empty pShuttle was transfected in MCF-7 cell lines and invasion assay analysis was performed 48hrs later.

The invasion assays were performed over 48hrs using commercial invasion assay kit containing inserts pre-coated with Matrigel (ECM) without a serum gradient. The effect of transient GLP1-R overexpression on MCF-7 was dramatic (7 fold induction) with a significant induction of a non invasive to an invasive phenotype. There were occasional invading cells in control inserts which facilitated the fold-change calculation (not seen in Fig. 3.18.2A1)

A)

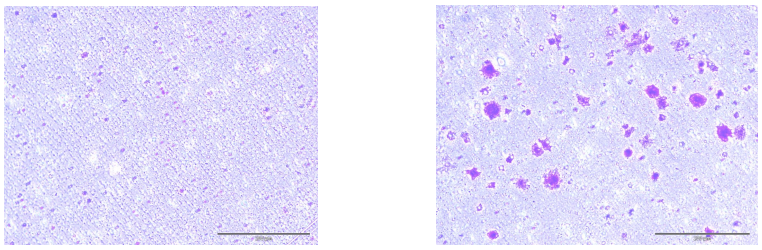

Control Vector GLP1-R overexpression

Figure 3.18.2A Invasion assay in MCF-7 cells due to transient GLP1-R expression. a1) Control vector transient overexpression, a2) GLP1-R transient overexpression.

B)

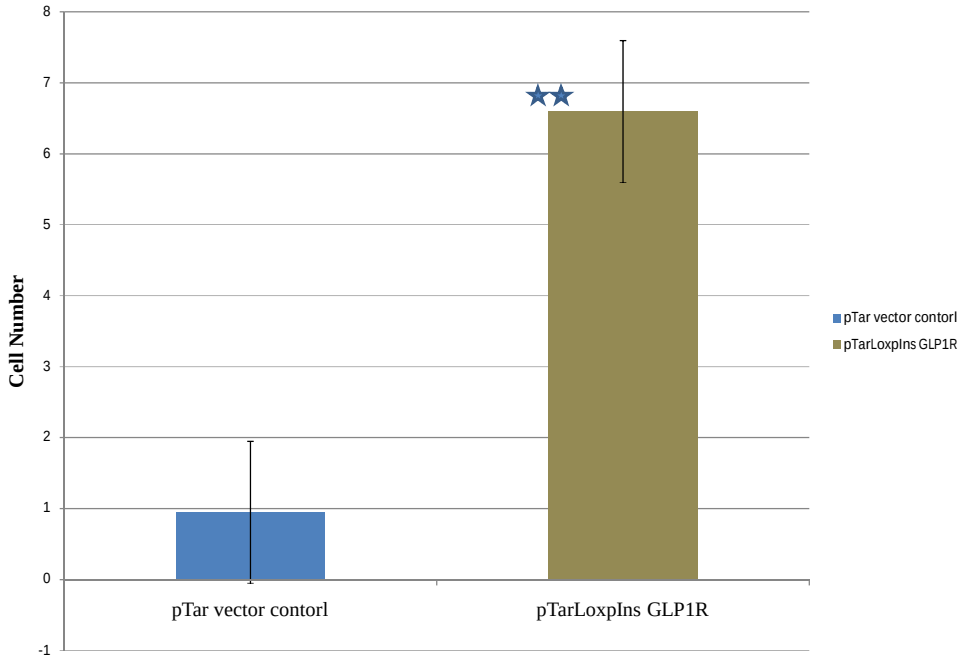

Figure 3.18.2B Transient GLP1-R overexpression invasion assay counts relative to empty vector transfected cells in MCF-7 cell line. Relative invasion assay counts comparing vector control transfected MCF-7 to MCF-7 GLP1-R transient overexpressing cell lines with** [p-value (≤0.01)] and N=3.

3.19 Investigation of the effect of GLP1-R siRNA knockdown in GLP1-R stable overexpressing cell lines.

Western blot analysis of DLKP 17 cells that were stably transfected with GLP1-R or the empty vector revealed that there was no detectable endogenous expression of this protein. Exogenous expression was strong. This pattern correlated with an observed induction of the invasive phenotype in the GLP1-R expressing cells (Fig.3.17.2B). This trend was reflected in MCF-7 cells also. To further establish the causal role of GLP1R in this induction of invasiveness we attempted to reverse the phenotype using RNAi. GLP1-R specific knockdown using siRNA was performed in DLKP 17 and 11 GLP1-R overexpressing clones (section 2.8.2) and cell proliferation and invasion was assayed as described previously. The knockdown of GLP1-R at the translational level was confirmed by western blot analysis.

3.19.1 Western blot confirmation of GLP1-R knockdown post siRNA treatment in DLKP GLP1-R overexpressing cell lines

Two independent siRNAs specific to GLP1-R were transfected into DLKP GLP1-R stable overexpressing cell lines and validated by western blot analysis (section 2.14). 2µl of NeoFX transfection reagent per well of a 24-well plate was used to transfect 100nM of target siRNA into the cells (section 2.8.2). 72hrs later the cells were trypsinised and protein was extracted.

To exclude non-specific effects on target protein expression we used scrambled siRNA sequence and NeoFX transfection agent as controls. To ensure transfection efficiency we used Kinesin-specific siRNA. Kinesin facilitates cellular mitosis, therefore silencing kinesin facilitates cell arrest. In the absence of kinesin dividing cells adopt a rounded morphology in advance of microtubule formation, and this is where the cells arrest. Hence the round morphology of cells transfected with kinesin siRNA. In proliferation assays, non-transfected control cells divide normally while the kinesin siRNA transfected cells do not. The difference in control cell number compared to kinesin siRNA-transfected cells is not a measure of transfection efficiency or related to any cell death. It is a measure of how many times the control cells divided beyond the stage at which Kinesin levels became limiting in the transfected cells and they stopped dividing. Figure

3.19.1A illustrates the effect of two siRNA sequences used for specific GLP1-R knockdown. It is evident from the blot that GLP1-R (2) siRNA has a greater impact on knockdown than GLP1-R (1) relative to scrambled siRNA (Scr) treatment.

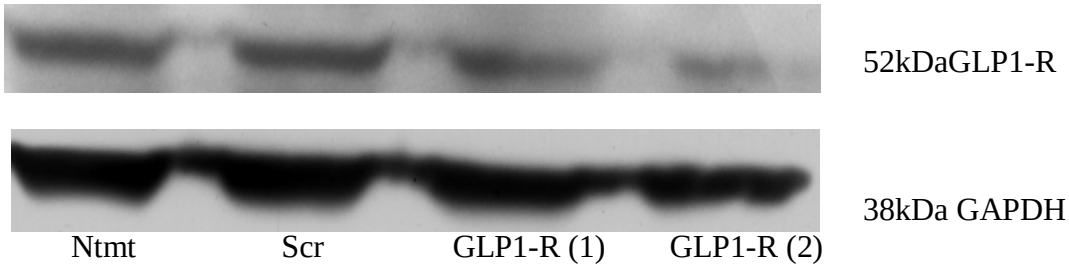

Figure 3.19.1A Western blot analysis of GLP1-R knockdown in siRNA-treated GLP1-R overexpressing DLKP cell line. Ntmt: No treatment, Scr: Scramble, GLP1-R(1): siRNA(1) and GLP1-R(2): siRNA (2).

3.19.2 To evaluate the effect of GLP1-R siRNA on proliferation in stable GLP1-R overexpressing DLKP 17 and DLKP 11 cell line

Stable overexpression of GLP1-R in DLKP 17 and 11 cells had a negative impact on cell proliferation. Both cell lines had decreased proliferation relative to their empty vector transfected counterparts. One would expect that if GLP1-R expression was knocked down, it should result in a rescue of the phenotype. Two GLP1-R specific siRNAs were used in the proliferation assay (section 2.9). 0.15µl of NeoFX transfection reagent per well of a 96-well plate was used to transfect 100nM of target siRNA into the cells (section 2.8.2). Figure 3.19.2A&B illustrates the impact of the siRNA treatment on DLKP 17 proliferation. GLP1-R siRNA treated cells showed a small rescue in the proliferation and especially siRNA (1) had significantly increased proliferation in both DLKP 17 and DLKP 11 cell lines. From western blot analysis it was evident that siRNA (2) was more effective than siRNA (1), though the rescue was more evident in DLKP 11 than DLKP 17 cell line. GLP1-R (1) siRNA showed a significant (4%) small increase in DLKP 17 and a significant (7%) small increase in DLKP 11.

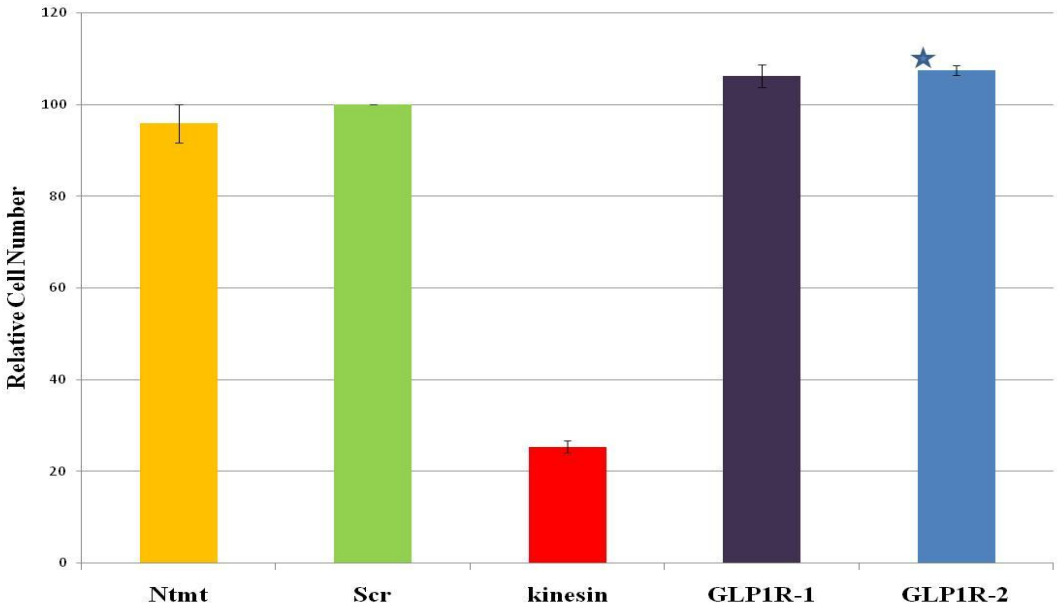

Figure 3.19.2A Effect of GLP1-R siRNA knockdown on proliferation in DLKP 17 GLP1-R overexpressing clone. Ntmt: no treatment, Scr: scramble control, Kinesin: control, GLP1-R-1: siRNA(1), GLP1-R-2: siRNA(2). A) DLKP 17: GLP1-R-1 siRNA treatment induced proliferation slightly higher than GLP1-R-2 treatment. *p-value (<0.05) and, error bar represents SEM. Kinesin was used as positive transfection control and N=3

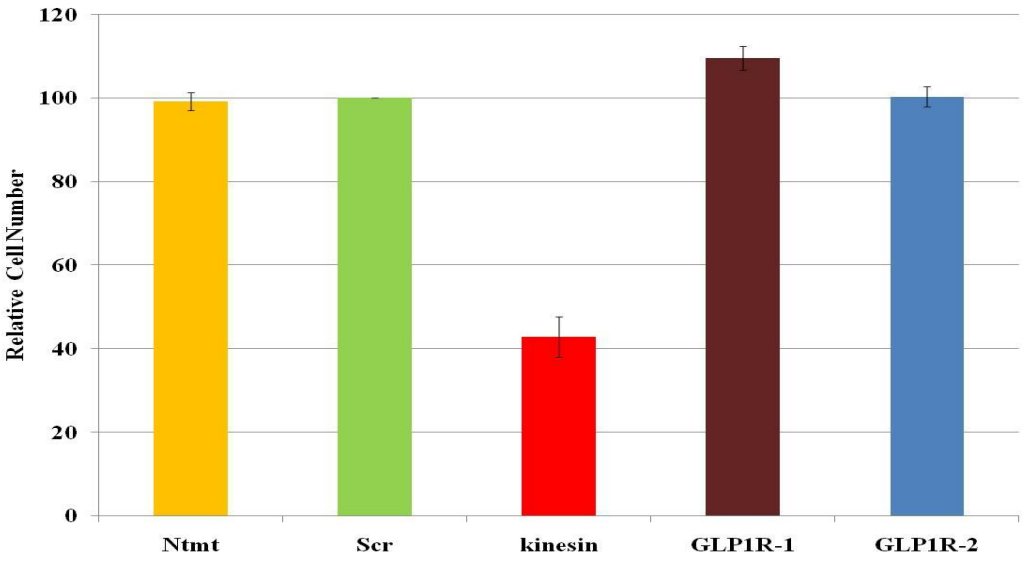

Figure 3.19.2B Effect of GLP1-R siRNA knockdown on proliferation in DLKP 11 GLP1-R overexpressing clone. Ntmt: no treatment, Scr: scramble control, Kinesin: control, GLP1-R-1: siRNA (1), GLP1-R-2: siRNA (2). B) DLKP 11: treatment with GLP1-R-1 and error bar represents SEM. Kinesin was used as positive transfection control. N=3.

.

3.19.3 To evaluate the effect of GLP1-R siRNA on the invasion phenotype in stable GLP1-R overexpressing DLKP 17 and DLKP 11 cell lines

We already established that stable GLP1-R overexpression in DLKP 17 (non invasive) targetable cell line resulted in an induced invasion phenotype. Furthermore to evaluate the effect of GLP1-R on invasion we performed knockdown of GLP1-R expression in both DLKP 17 and DLKP11 GLP1-R overexpressing cell lines. If the induced invasion is directly due to GLP1-R then knocking down its expression should result in a reversal of the invasive phenotype. GLP1-R siRNA treated DLKP 17 and DLKP 11 cell lines showed rescue in invasion phenotype relative to no treatment and scrambled controls. Though both GLP1-R siRNA 1 and 2 had significant impact on invasion phenotype, GLP1-R siRNA (2) impact was more intense (62% in DLKP-17 and 73% in DLKP-11). From our western blot confirmation it was evident that GLP1-R siRNA (2) resulted in greater knockdown at the protein level than siRNA (1).

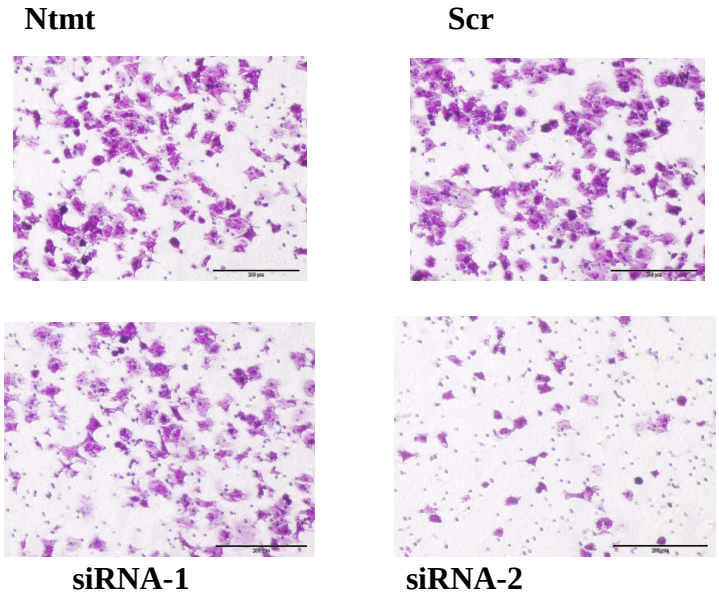

3.19.3A Effect of siRNA transfection on invasion in stable GLP1-R overexpressing DLKP 17 cell line. Ntmt: no treatment, Scr: scramble control, Kinesin: control, siRNA-1: GLP1-R-1, siRNA-2: GLP1-R-2.

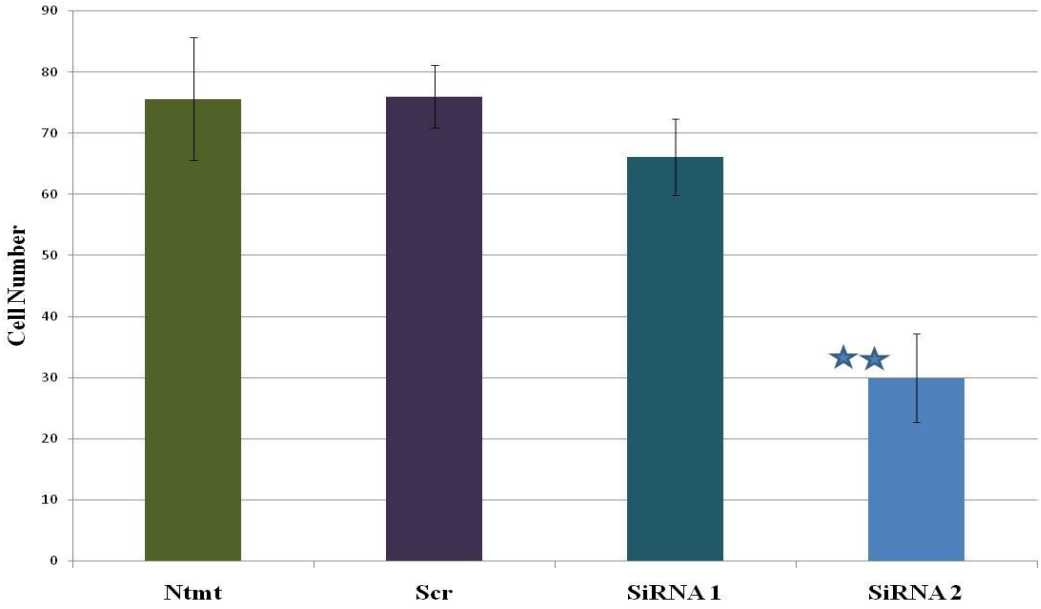

Figure 3.19.3B Graphical representation of invasion assay in DLKP 17 cells. Ntmt: no treatment, Scr: scramble control, Kinesin: control, siRNA(1): GLP1-R-1, siRNA(2): GLP1-R-2. Significant decrease was observed with p value **(<0.005), SEM ± 0.38% with GLP1-R (2) siRNA treatment and p-value **(<0.05), SEM ± 11.87% with GLP1-R (1) on invasion compared to scramble treatment and N=3.

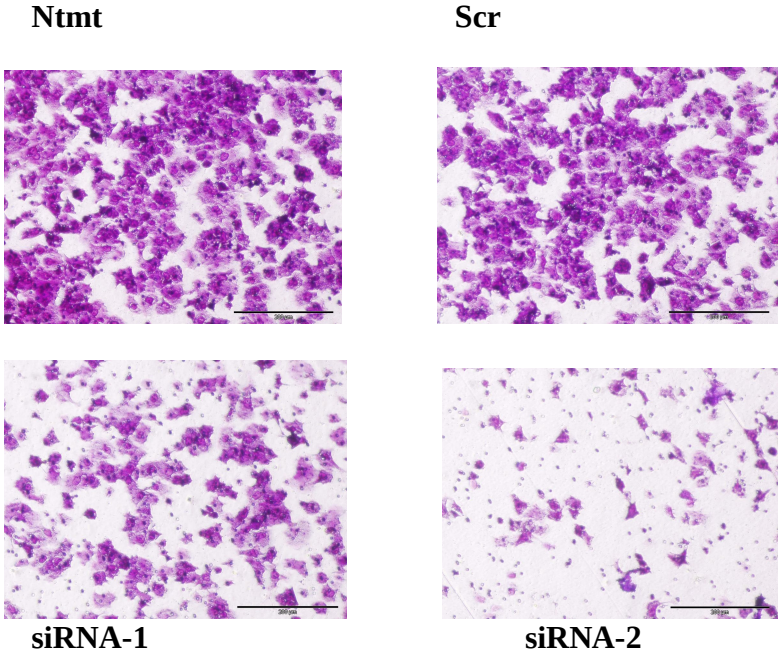

3.19.3C Effect of siRNA transfection on invasion in stable GLP1-R overexpressing DLKP 11 cell line Ntmt: no treatment, Scr: scramble control, Kinesin: control, siRNA(1): GLP1-R-1, siRNA(2): GLP1-R-2**.**

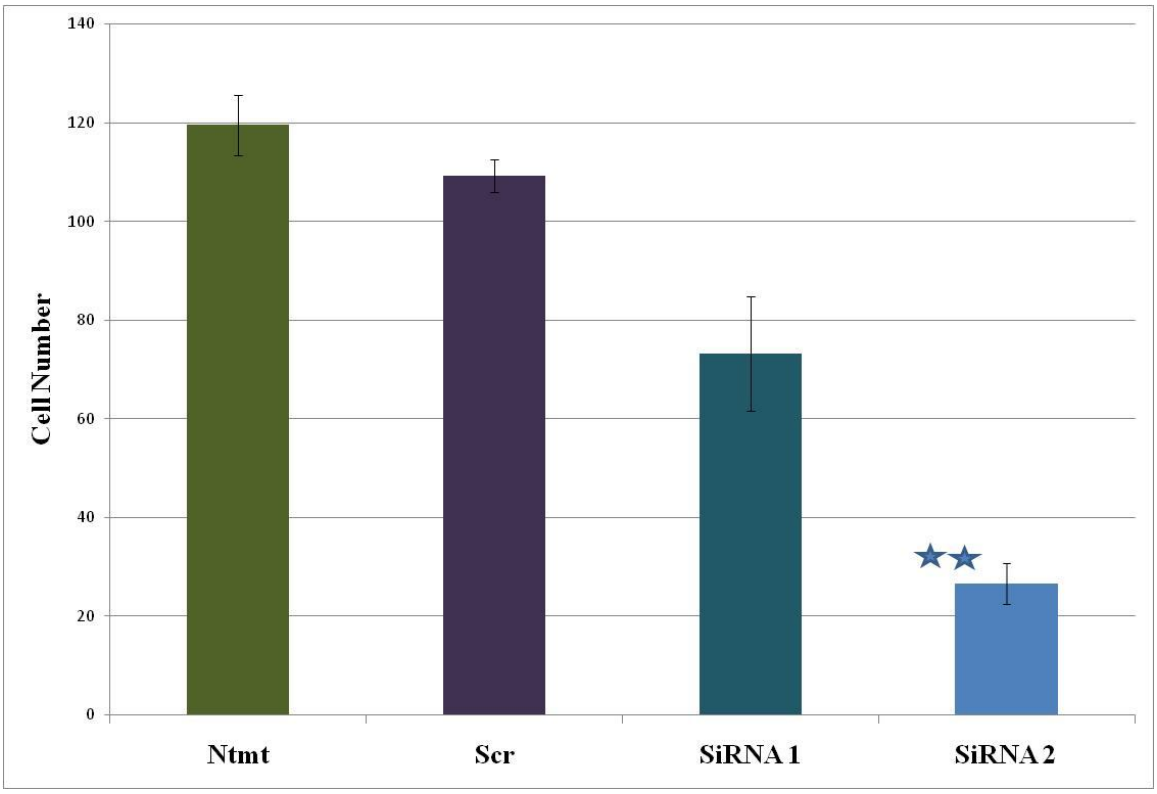

Figure 3.19.3D Graphical representation of invasion assay in DLKP 11 cells. Ntmt: no treatment, Scr: scramble control, Kinesin: control, siRNA (1): GLP1-R-1, siRNA(2): GLP1-R-2. Significant decrease was observed with p value ** (<0.005) with GLP1-R (2) siRNA treatment and with GLP1-R (2) siRNA a decrease was observed on invasion compared to scramble treatment. N=3.

3.20 Investigation of the effect of stable KCNJ8 overexpression in DLKP 17 and DLKP 11 cell lines

Inagaki *et al.*, (1995) identified a K_{ATP} channel, uK_{ATP}-1 (KCNJ8/Kir6.1), which represented a new subfamily of the inwardly rectifying K^+ channel family. This gene was identified in the microarray-based screening in our lab (A. Pierce, PhD 2006 thesis) as correlating with invasiveness in DLKP variant cell lines. To investigate any potential role in this phenotype, KCNJ8 cDNA was cloned in pShuttle-Ins targeting vector and co-transfected with pCre into DLKP 17 and DLKP 11 targetable cell lines. The transfected cells were selected for G418 resistance and limiting dilution and single cell cloning was performed to obtain individual cell line clones. Clones overexpressing KCNJ8 in both cell lines were selected as well as control clones transfected with empty vector. The effect of KCNJ8 on non invasive DLKP 17 and invasive DLKP 11 was investigated, including confirmatory analyses by qRT-PCR and western blot. The functional impact was monitored by proliferation and invasion assays.

Initial overexpression of KCNJ8 at transcript level was monitored by qRT-PCR (section 2.11.4). Figure 3.20A illustrates relative expression of KCNJ8 in a stable DLKP 17 clone compared to the empty vector control. DLKP 17 had a high level of transcription from the targetable locus region. However, we observed only a 2.6 fold increase (SD ± 0.31%) in KCNJ8 expression. It could be that the endogenous KNCJ8 concentration was already at its maximum tolerable level. Similarly figure 3.20B illustrates the degree of KCNJ8 overexpression in the DLKP 11 cell line, confirmed through qRT-PCR analysis. It was already established that DLKP 11 had a low level of transcription from its targetable locus. This was reflected in the levels of KCNJ8 expressed in the re-targeted DLKP11, where a 1.2 fold (SD ± 0.06%) increase was observed in mRNA. Though the magnitude of transgene up-regulation was lower than expected in both cell lines, the relative levels compared to each other were consistent with the known activity of their targetable loci.

A) DLKP-17

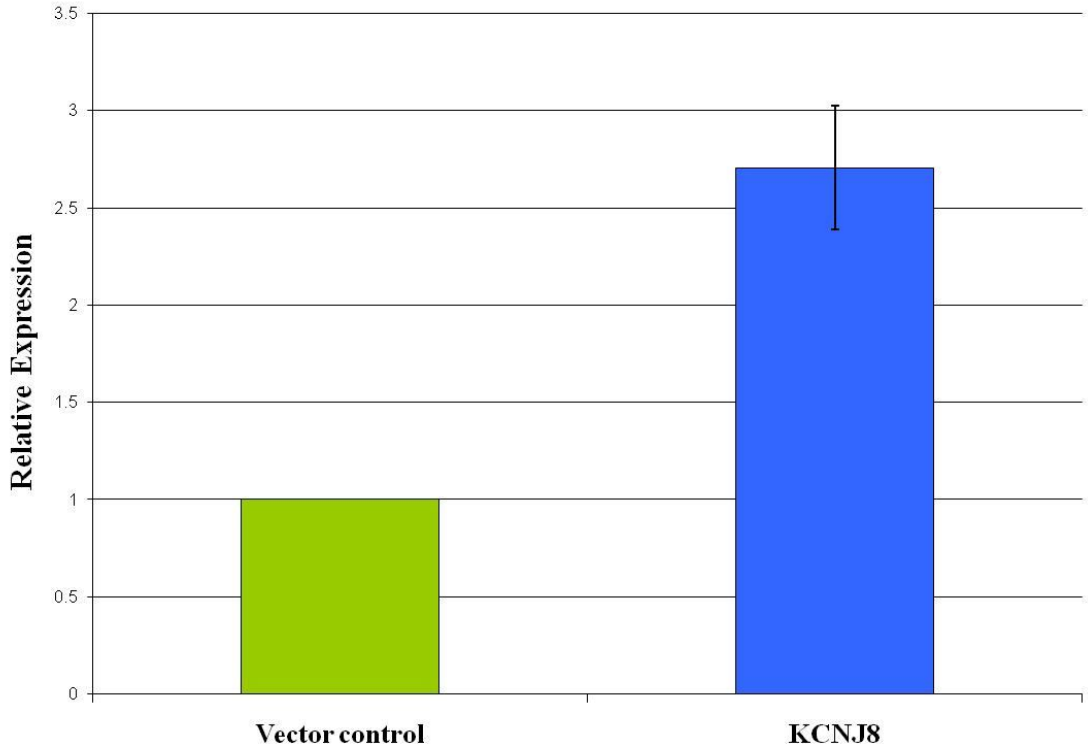

B) DLKP-11

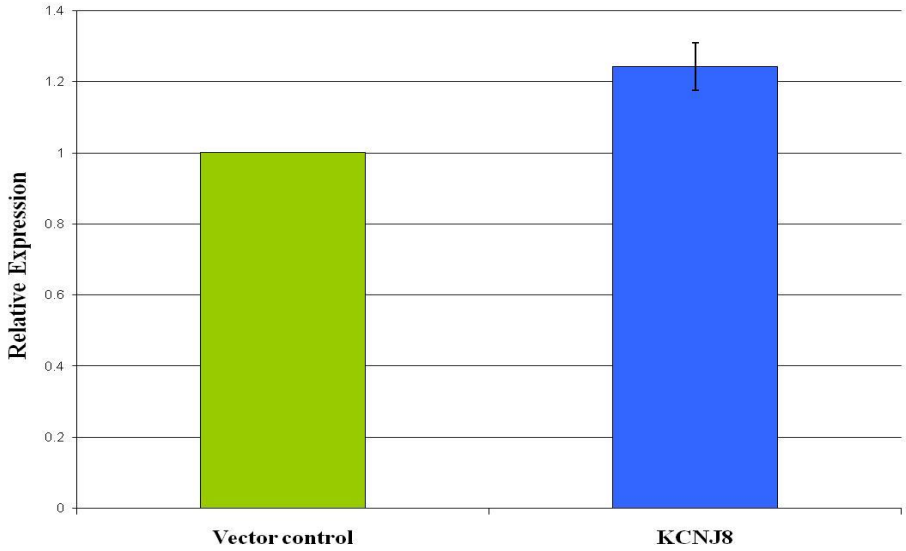

Figure 3.20A&B qRT-PCR confirmation of stable KCNJ8 transgene overexpression in DLKP 17 and DLKP 11 cell lines. A) DLKP 17: KCNJ8 2.25 fold relatively overexpressed and B) DLKP 11: KCNJ8 1.2 fold overexpression compared to vector control and N=3.

3.20.1 Western blot analysis confirmation of KCNJ8 stable overexpression in DLKP 17 and DLKP 11 cell lines.

Cells were transfected with a pShuttleKNCJ8 targetable vector and empty vector as a control to ensure that the transfection process did not affect target protein expression. The polyclonal anti-kir6.1 (KCNJ8) CAF-1 antibody used in these experiments was a gift from Prof. William A. Coetzee (NYU School of Medicine). Western blot analysis was performed as described previously, which identified a 44kDa band specific to KCNJ8. GAPDH was used as a loading control.

Immunoblot analysis revealed that there was no difference in KCNJ8 overexpression in both DLKP 17 and DLKP 11 cell lines relative to their empty vector control samples.

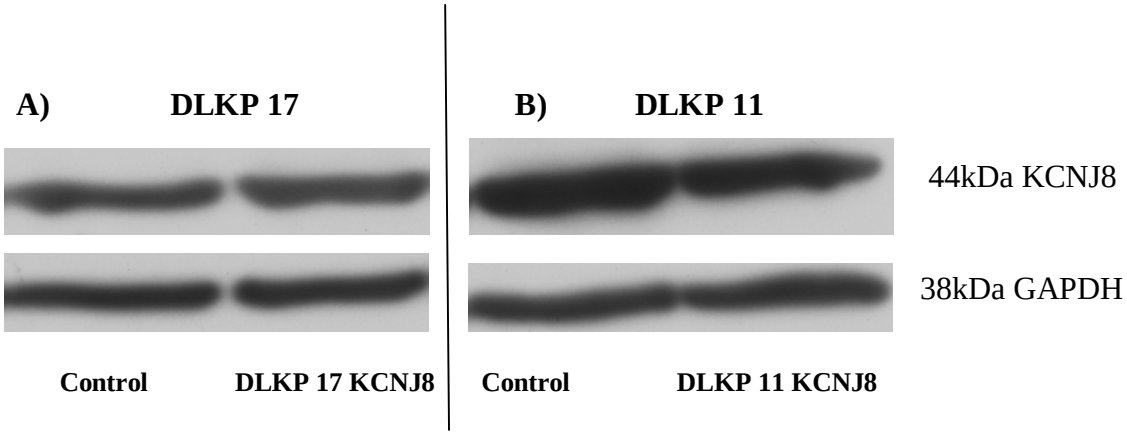

Figure 3.20.1A Western blot analysis of KCNJ8 overexpression in DLKP 17 and DLKP 11 cell lines. Polyclonal anti KCNJ8 antibody was used at 1/1000 dilution and generates a 44kDa band specific to KCNJ8

3.20.2 To evaluate the effect of stable KCNJ8 on proliferation in DLKP 17 and DLKP 11 cell lines

To determine if there was any impact on proliferation due to KCNJ8 stable overexpression, we performed a proliferation assay (section 2.9). The effect on proliferation was investigated by seeding in 96 well cell culture plates, 100µl of $3x10^4$ cells per ml of KCNJ8 overexpressing DLKP 17 and 11 cell lines and their empty vector controls. 48hrs after seeding the plate was assayed using the acid phosphatase assay as described in section 2.9

Stable overexpression of KCNJ8 in DLKP 17 had reduced proliferation relative to empty vector transfected cells. Conversely an increase in cell proliferation was observed in KCNJ8 overexpressing DLKP 11 cell line. Figure 3.20.2 A&B illustrates the impact of stable KCNJ8 transgene overexpression on DLKP proliferation. A 15% decrease proliferation was observed compared to control vector in DLKP 17. With DLKP 11 samples, relative to empty vector transfected DLKP 11, KCNJ8 overexpressing DLKP 11 clone displayed a 45% increase in cell proliferation compared to empty vector control.

A) DLKP-17

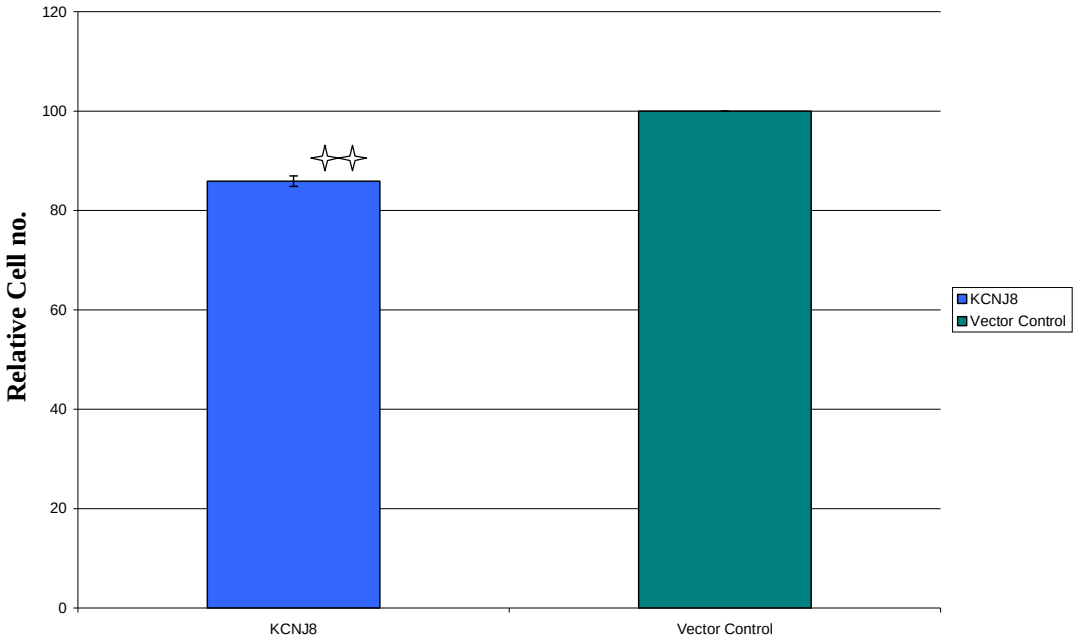

B) DLKP-11

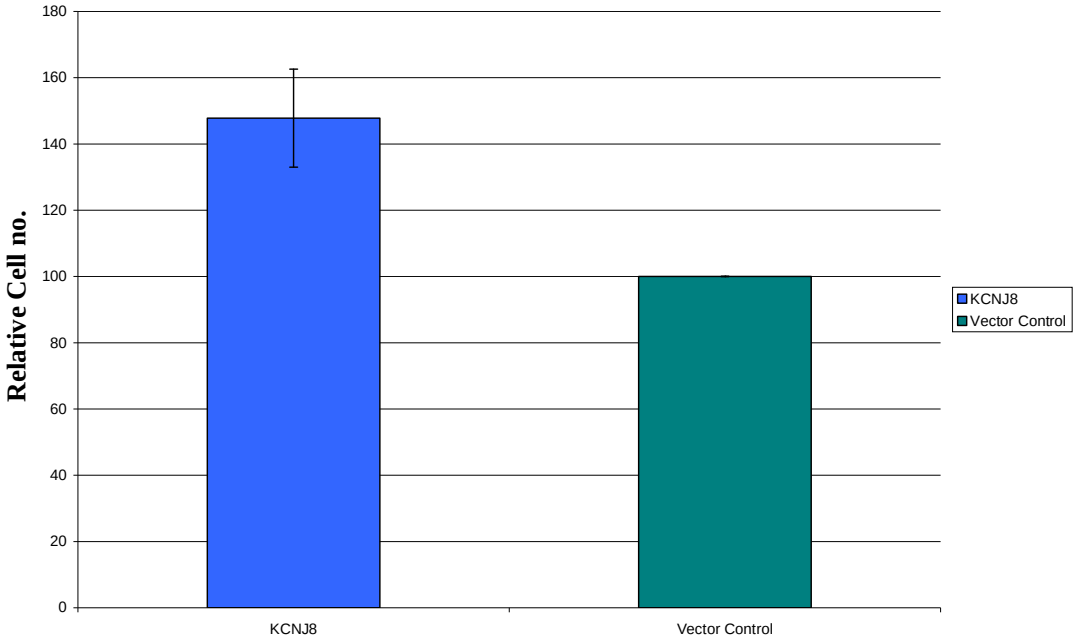

Figure 3.20.2 A&B Effect of stable KCNJ8 overexpression on proliferation assay in DLKP 17 and DLKP 11 cell lines. A) DLKP 17: significant effect on proliferation with p-value ** (<0.005). B) DLKP 11: no significant increase in proliferation compared to vector control and N=3.

3.20.3 Investigation of effect of stable KCNJ8 overexpression on invasion in DLKP 17 and DLKP 11 cell lines.

From our previous experiment to establish the baseline invasive phenotype of DLKP 17 and DLKP 11 cell lines it was observed that DLKP 17 was non invasive and DLKP 11 was highly invasive. To evaluate the effect of KCNJ8 overexpression on DLKP 17 and DLKP 11 invasion we performed an in vitro invasion assay. The invasion assays were performed over 48 hours using commercial invasion assay kit containing inserts pre-coated with Matrigel (ECM) without a serum gradient. The cells were seeded at 10^5 cells per insert. They were incubated at 37^oC for 48 hours after which the undersides of the inserts were stained; ten fields of view were counted per insert at 20X magnification and averaged. At least two inserts were used for the analysis of each condition.

The effect of KCNJ8 stable overexpression on DLKP 17 was dramatic (50 fold), i.e. a significant induction of non invasive to invasive phenotype was observed both visually as well as by cell counts in DLKP17 KCNJ8 overexpressing cells. Similarly in DLKP 11, which was already invasive, there was a further 18% increase in invasion.

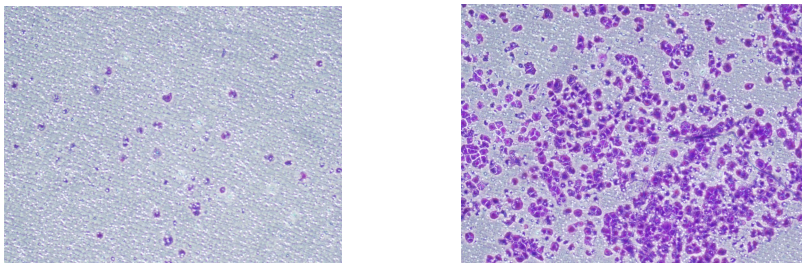

DLKP 17 Vector control DLKP 17 KCNJ8

Figure 3.20.3A Crystal violet stained representation of KCNJ8 overexpressing DLKP 17 cell line invasion assay.

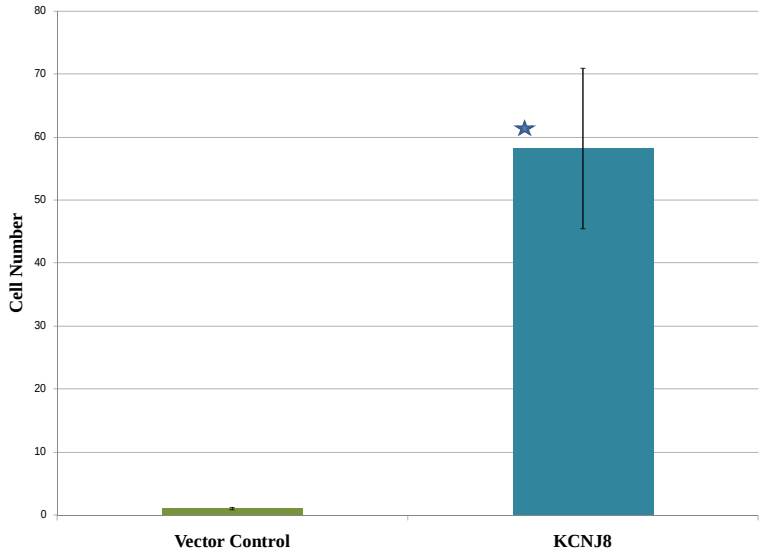

Figure 3.20.3B Graphical representation of invasion assay in DLKP 17 cells

Significant increase in invasion, was observed relative to DLKP 17 vector control with * [p-value (<0.02)] and N=3.

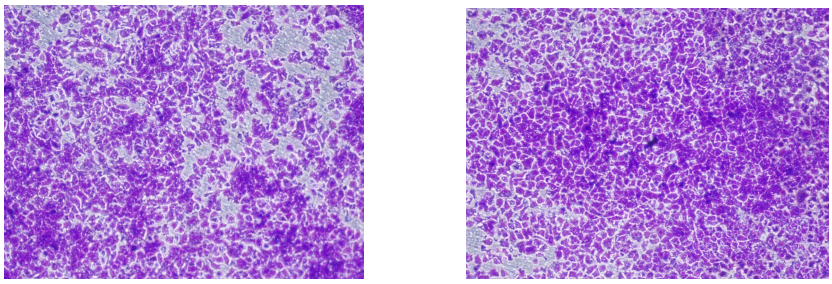

DLKP 11 vector control DLKP 11 KCNJ8

Figure 3.20.3C Crystal violet stained representation of KCNJ8 overexpressing DLKP 11 cell invasion assay.

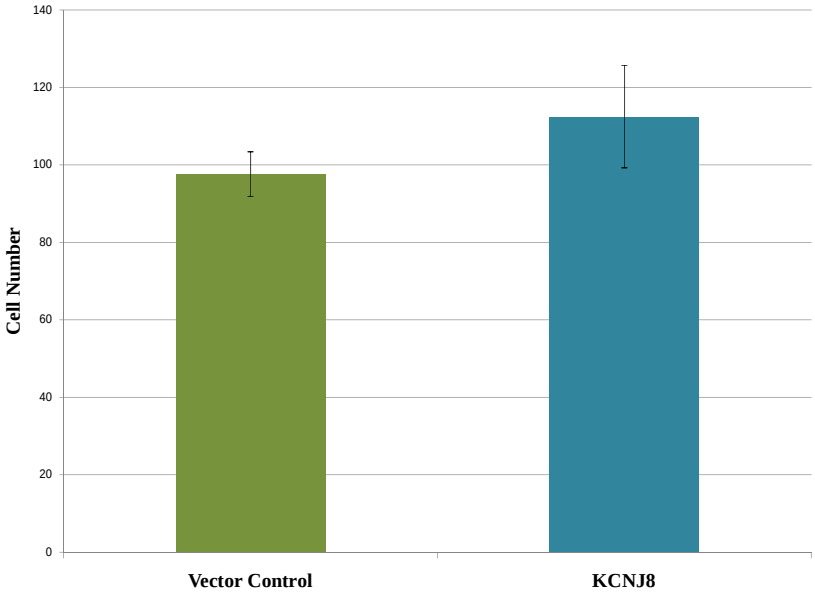

Figure 3.20.3D Graphical representation of invasion assay in DLKP 11 cells.

An increase in invasion was observed relative to DLKP 11 vector control and N=3.

3.21 Investigation of the effect of stable TFPI2 overexpression in DLKP 17 and DLKP 11 cell lines

TFPI2 is a 32kDa serine protease inhibitor that is associated with the ECM. This gene was identified in the microarray-based screening in our lab (Pierce A. PhD thesis 2006) as correlating with invasiveness in DLKP variant cell lines. TFPI2 cDNA was cloned in pShuttle-Ins targeting vector and co-transfected with pCre into DLKP 17 and DLKP 11 targetable cell lines. The transfected cells were selected for G418 resistance and limited dilution single cell cloning was performed to obtain cell line clone. Clones overexpressing TFPI2 in both DLKP 17 and 11 cells were selected as well as pShuttle control cells. The effect of TFPI2 on non invasive DLKP 17 and invasive DLKP 11 was investigated, including confirmatory analyses by qRT-PCR and western blot. Initial overexpression of TFPI2 at the transcript level was monitored by qRT-PCR (section 2.11.4). An 80 fold increase (Fig. 3.21A) in TFPI2 expression in DLKP 17 and a 1.3 fold increase (Fig. 3.21B) in DLKP11 cells was observed compared to empty vector control. Protein was extracted from these cell lines and western blot was performed (section 2.14). The antibody used did not detect TFPI2 protein either in parental or TFPI2 overexpressing cells.

A) DLKP-17

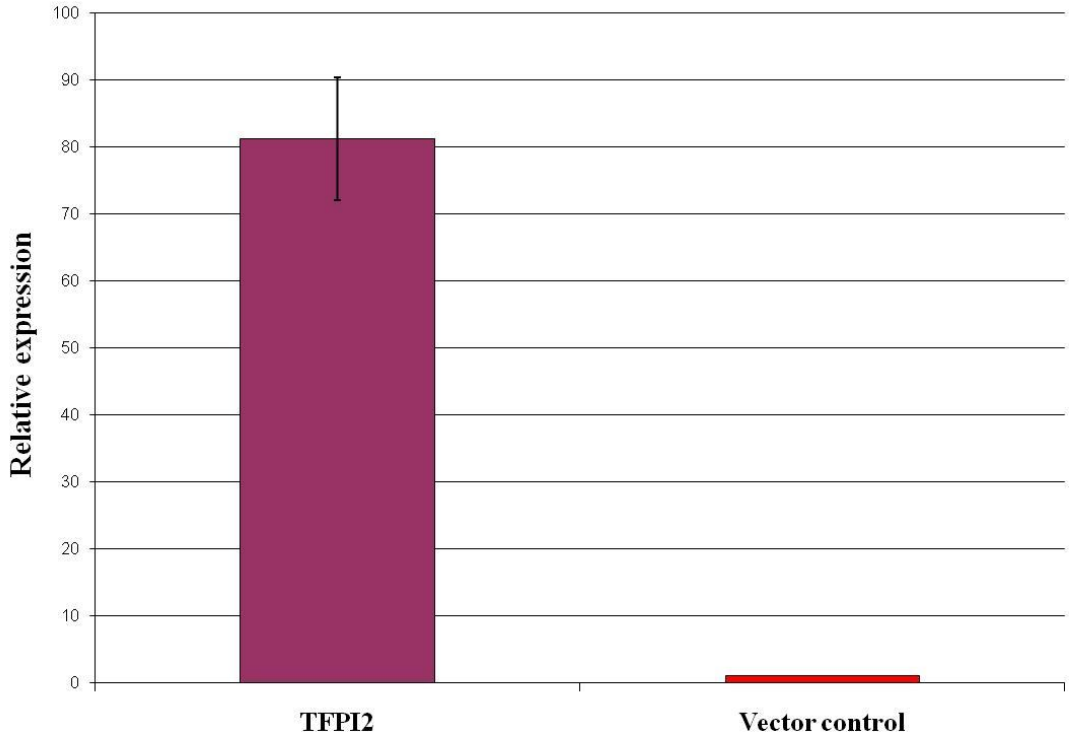

B) DLKP-11

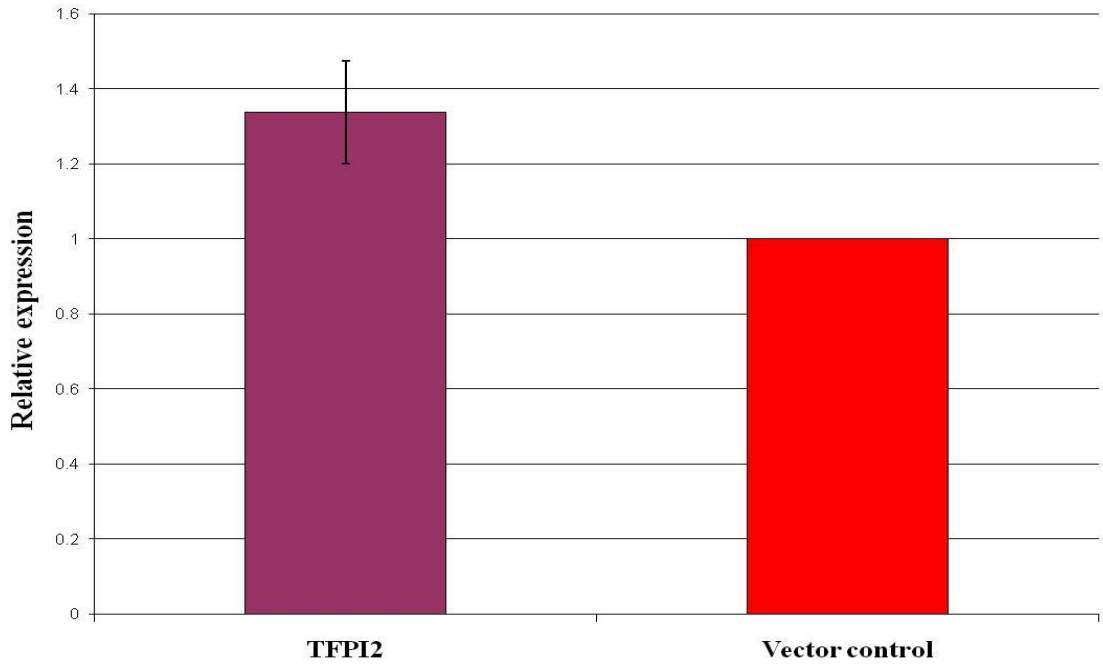

Figure 3.21A&B qRT-PCR confirmation of stable transgene TFPI2, overexpression in DLKP 17 DLKP and 11 cell lines. A) DLKP 17: TFPI2 overexpression compared to control B) DLKP 11: TFPI2 expression relative to control and N=3.

3.21.1 To evaluate the effect of stable TFPI2 expression on proliferation in DLKP 17 and 11 cell lines.

To determine if there was any impact on proliferation due to TFPI2 stable overexpression, we performed a proliferation assay (section 2.9). The effect on proliferation was investigated by seeding in 96 well cell culture plates. A seed density of TFPI2 overexpressing DLKP 17 and 11 cells at $3x10^3$ cells per well of a 96 well cell culture plate was used. 48 hrs after seeding each well the plate was assayed using the acid phosphatase assay as described in section 2.9. A significant decrease (24%) in cell proliferation was observed compared to control vector in DLKP 17 as represented in fig 3.21.1(A). Similarly relative to empty vector transfected DLKP 11 the TFPI2 stable overexpressing DLKP 11 clones had a significant 31% increase in rate of proliferation as

represented in fig 3.21.1(B) with compared to vector control. Suggesting role of TFPI2 in proliferation is cell line specific.

A) DLKP-17

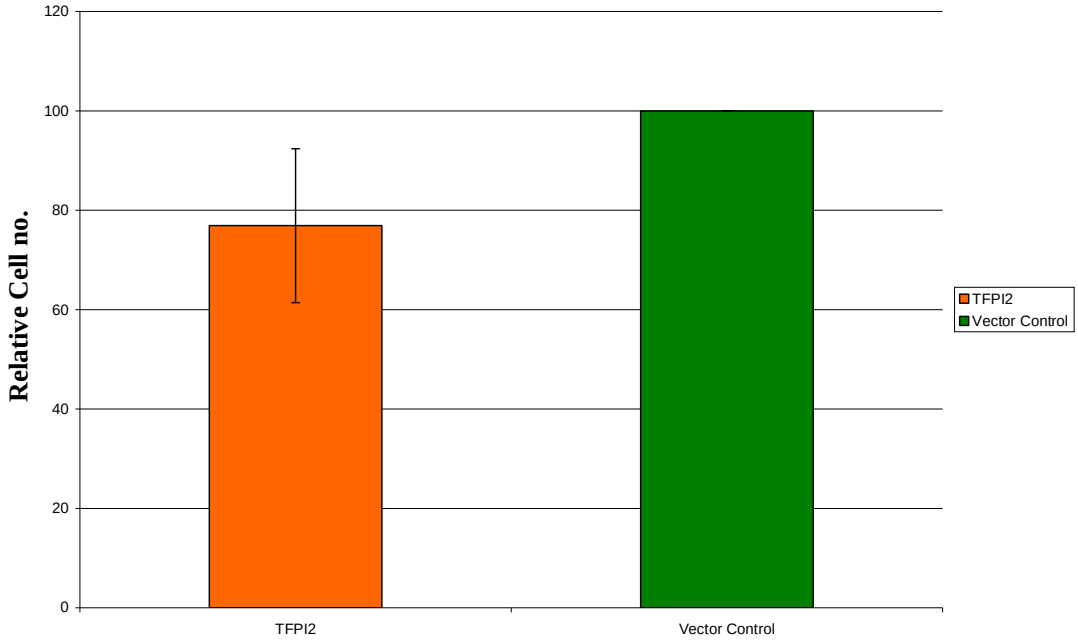

B) DLKP-11

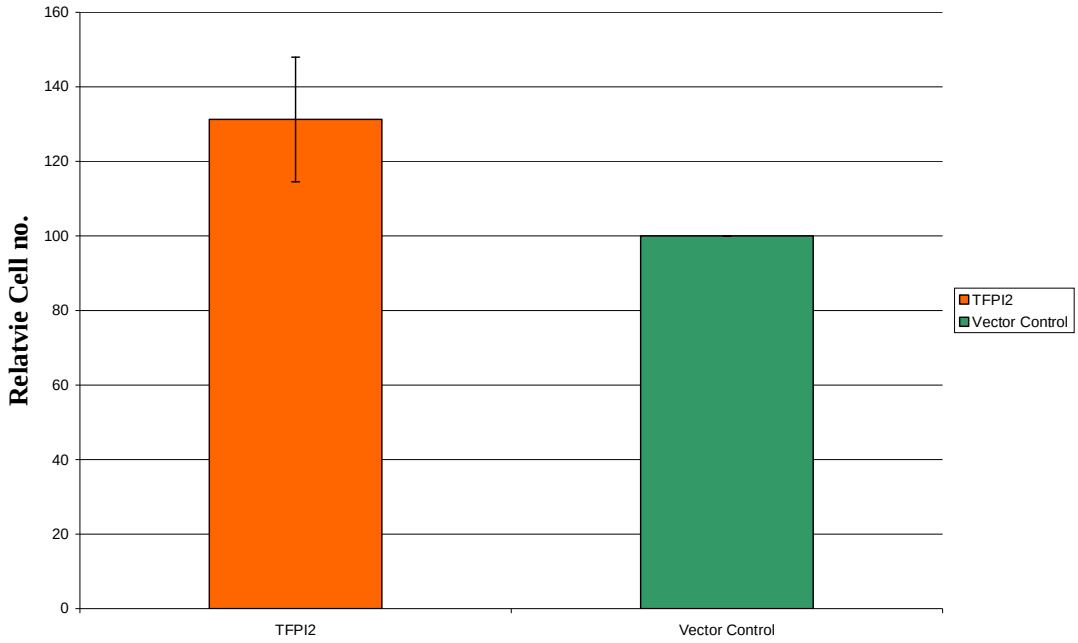

Figure 3.21.1 A&B Effect of stable TFPI2 expression on proliferation in DLKP 17 and DLKP 11 cell lines. A) DLKP 17: decrease in cell proliferation was observed B) DLKP 11: increase in proliferation observed and N=3.

3.21.2 Investigation of effect of stable TFPI2 expression on invasion in DLKP 17 and DLKP 11 cell lines.

To evaluate the effect of TFPI2 overexpression on DLKP 17 and DLKP 11 invasion we performed an in vitro invasion assay. The invasion assays were performed over 48 hours using a commercial invasion assay kit containing inserts pre-coated with Matrigel (ECM) without a serum gradient. The cells were seeded at 10^5 cells per insert. They were incubated at 37^{o}C for 48 hours after which the undersides of the inserts were stained; ten fields of view were counted per insert at 20X magnification and averaged. At least two inserts were used for the analysis of each condition.

The effect of TFPI2 stable overexpression on DLKP 17 was dramatic (25 fold), i.e. a significant induction from a non invasive to an invasive phenotype was observed both visually as well as by cell counts in DLKP17 TFPI2 overexpressing cells. Conversely in DLKP 11, invasiveness was observed to be decreased by ~12%.

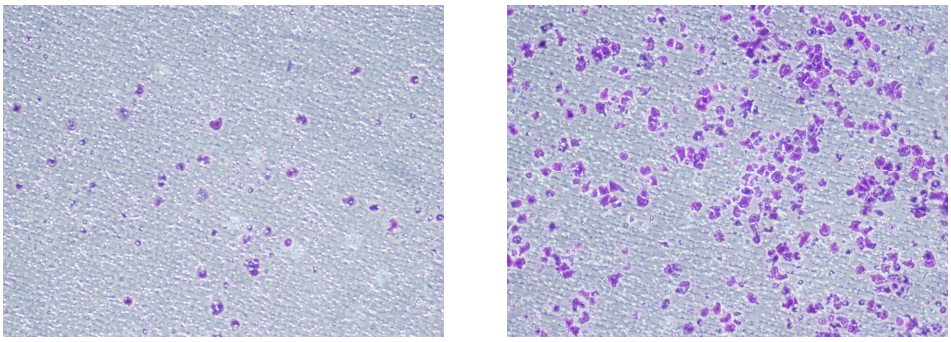

DLKP 17 vector control **DLKP 17 TFPI2**

3.21.2A Crystal violet stained representation of TFPI2 overexpressing DLKP 17 cell invasion assay.

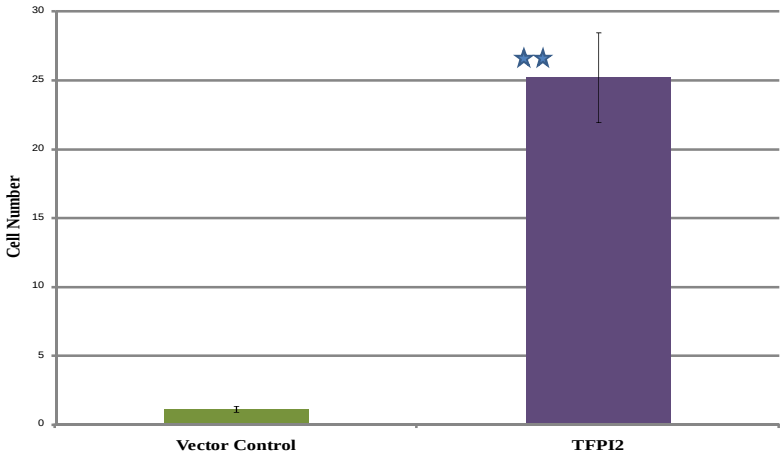

3.21.2B Graphical representation of invasion assay results.

Significant increase in invasion observed with stable TFPI2 expression compared to vector control with **p-value (≤0.004) N=3.

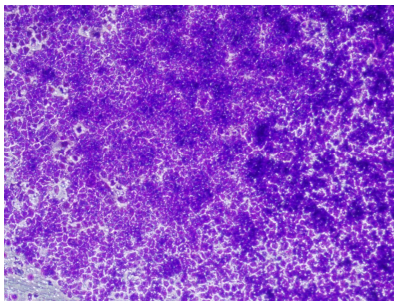

DLKP 11

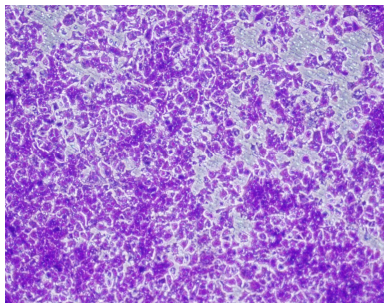

DLKP 11 TFPI2

3.21.2C Crystal violet stained representation of TFPI2 overexpressing DLKP 11 cell invasion assay.

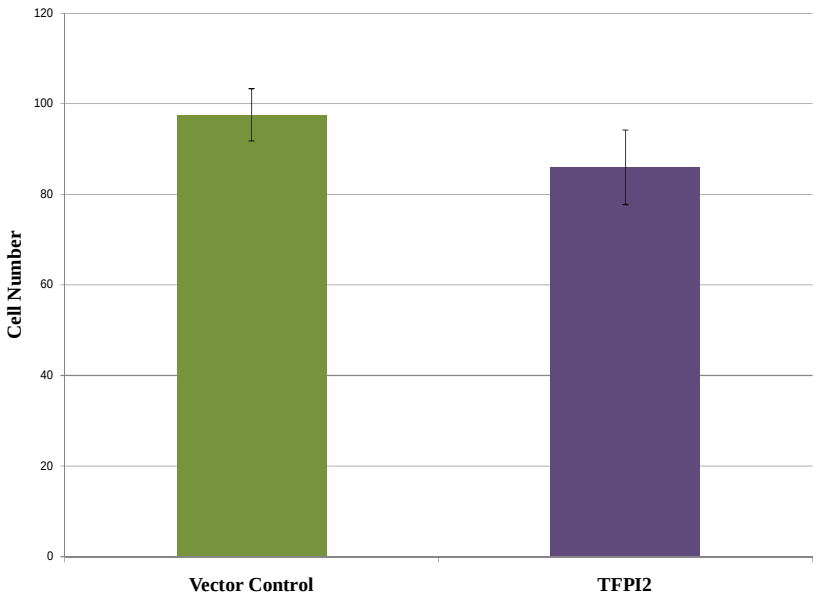

3.21.2D Graphical representation of invasion assay results. A decrease in invasion was observed due to TFPI2 overexpression, N=3.

In conclusion the opposing invasive and proliferative effects of TFPI2 in DLKP17 and 11 clones suggested the gene dosage and/or existing phenotype may dictate the impact of TFPI2 overexpression.

3.22 Investigation of the effect of stable S100A13 overexpression in DLKP 17 and DLKP 11 cell lines

S100 proteins are small EF hand Ca^{2+} binding proteins of variable length and sequence. There are a number of functions associated with S100 proteins, many associated with tumour development. In 1996, Wicki *et al*. identified a new S100 member termed S100A13 by screening expressed sequence tag (EST) databases. It was found to have a novel role in invasion by Pierce, et.al, (2008). Initial overexpression of S100A13 at the transcript level was monitored by qRT PCR (section 2.11.4). After several attempts we were not able to generate a stable S100A13 overexpressing DLKP cell line.

A) DLKP-17

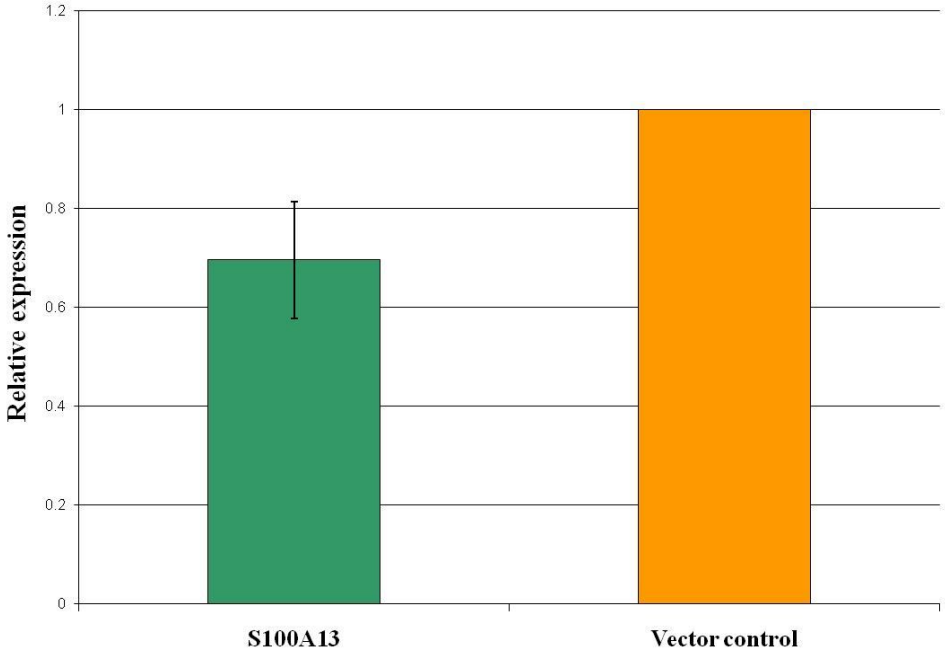

B) DLKP-11

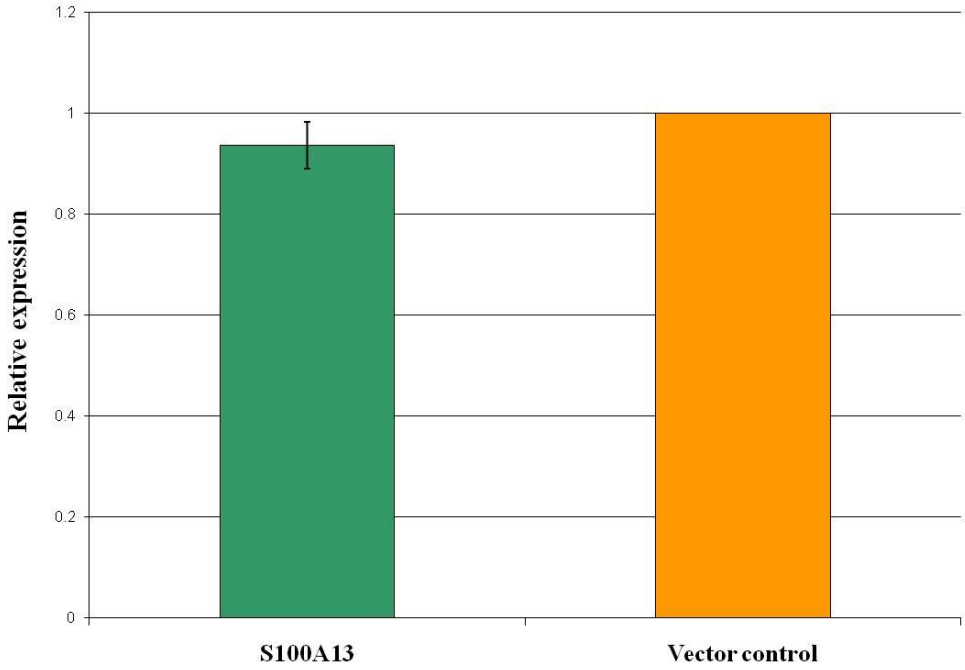

Figure 3.22A&B qRT-PCR analysis of S100A13 expression in DLKP 17 and DLKP11 cell lines. Figure illustrates that there was no S100A13 overexpression in DLKP 17 clone compared to empty vector control. Similarly figure 3.22.1B illustrates no stable S100A13 overexpression in DLKP 11 cell line.

In conclusion, even after several attempts it was not possible to overexpress S100A13 in either DLKP 17 or 11 cell lines. This was not expected, as the targetable overexpression system worked with three other transgenes GLP1-R, KCNJ8 and TFPI2. Also, transient overexpression worked before as shown by Pierce et.al (2008). A possible reason could be that DLKP cells may not tolerate stable S100A13 overexpression.

SECTION: D

3.23.0 MicroRNAs

3.23.1 Overview of approach and key results

MicroRNAs (miRNAs) are a class of small endogenous non coding RNA molecules whose normal function involves the regulation of gene expression post-transcriptionally. It is estimated that 3% of the genome encodes miRNAs and approximately 30% of human protein coding genes are predicted to be regulated by miRNAs. Several studies suggest that uncontrolled expression of miRNAs or clusters of miRNAs may lead to abnormal cellular functions including proliferation, differentiation and apoptosis resulting in human diseases. Recently much attention has been focused on the role of miRNAs in cancer.

The focus of this study was to investigate the potential role of miRNAs in lung cancer invasion. In collaboration with Ambion, we performed miRNA bioarray profiling of DLKP (parent, non invasive) Vs DLKP-A (Adriamycin drug resistant, highly invasive) human lung cancer cell lines. As a result, there were several differentially expressed miRNAs identified. Among them we selected five miRNAs for PCR validation. The five miRNAs were mir-21, mir-27a, mir-29a, mir-30a5p and mir-30c. From PCR validation (section 2.12.2) we selected three miRNAs for further functional validation: mir-21, mir-27a and mir-29a.

Table 3.23A Endogenous miRNA levels in DLKP-A relative to DLKP

MiRNAs	Bioarray results Relative expression	qRT-PCR results Relative expression
Hsa-mir-21	**Up**	**Up**
Hsa-mir-27a	**Up**	**No change**
Hsa-mir-29a	**Up**	**Down**
Hsa-mir-30c	**Up**	**Down**
Hsa-mir-30a5p	**Up**	**No change**

As these miRNAs were differentially regulated in DLKPA compared to DLKP (Table 3.23A), we suspected they may play a role in cancer invasion mechanism. The role of mir-21 in lung cancer was already known from several studies. Hence, we used it as our experimental control. Mature sense (pre-miRNAs: Pre-mir sequence is a double stranded 21-mer identical to the mature form of the miRNA, so transfecting these is like overexpression) and antisense sequences (anti-miRNAs: Anti-mir is a single stranded nucleotide sequence complementary to target miRNA which inhibits miRNA activity) were transiently transfected in DLKP and DLKP-A cell lines (Section 2.8.2).To make sure the transfection worked we used kinesin as a transfection control and 72hrs post transfection the cells were harvested for miRNA isolation (section 2.12). qRT-PCR was then performed (fig. 3.25A).

To assess if these miRNAs had any effect on cell proliferation, we subjected both anti and pre miRNA treated cells to proliferation assay (section 2.9). The results confirmed that transient overexpression of these miRNAs did not have a significant impact on DLKP or DLKPA cell proliferation (fig.3.25B& C). We also checked for effects on drug sensitivity due to overexpression or knockdown of these miRNAs to investigate the role of miRNAs in chemotherapeutic drug resistance (CDRs). No significant impact was observed (fig. 3.25.1A&B).

Our main aim was to investigate if any of these chosen target miRNAs had any impact on the invasion phenotype. Hence, anti-mir and pre-mir treated DLKP and DLKPA cells were subjected to invasion assay (section 2.10). The mir-21 and 27a miRNAs were found to be pro- invasive and mir-29a was found to be anti-invasive (fig. 3.26A, 3.26B, 3.26C). The experiment was repeated in biological triplicate to confirm the observation. From the literature it was already known that mir-21 and mir-27a are involved in cancer invasion/metastasis related pathways, which was in agreement with our observations too. But there was no previous evidence of mir-29a as an anti-invasiomer**;** therefore we further proceeded to delineate the role and effect of mir-29a in cancer cell invasion.

To establish that the anti invasive effect of mir-29a expression was not only lung cancer cell line specific we included another cell line in our study PANC-1, which is a pancreatic

cancer cell line with a highly invasive phenotype. We transiently transfected pre-mir-29a or control sequence into PANC-1 cells. qRT-PCR analysis of extracted RNA samples confirmed mir-29a to be overexpressed by 2.3 fold (refer fig. 3.27A). A significant decrease of about 55% in PANC-1 invasion phenotype was observed relative to control transfected cells (Figure 3.27B).

Further we asked the question, what would be the phenotypic impact of stable mir-29a overexpressed in DLKPA cell line? To address this we PCR amplified endogenous pre mir-29a from DLKP genomic DNA and subcloned in p4.1CMV-Neo plasmid vector (Ambion) (fig. 3.28A). A negative sequence was also cloned in p4.1CMV-Neo vector which was used as control during stable overexpression studies. The p4.1CMV-Neo-mir-29a plasmid vector was transfected into DLKPA and stable clones were generated. The clones were checked for mir-29a expression by qRT-PCR (fig. 3.28D). The DLKPA clones displaying mir-29a overexpression were subjected to invasion and proliferation assay (section 3.29 and 3.30), and it was observed that the clones had significantly reduced invasion and cellular proliferation. Genes that are predicted to be regulated by miRNAs are usually based on in silico analysis. When this study was undertaken only one publication reported proteomic data on miRNA expression (Zhu et al., 2007. To identify possible gene targets being regulated by mir-29a we performed a comprehensive proteomic profiling of anti and pre-mir-29a treated DLKPA cells using 2D-DIGE (section 2.14.6) followed by MALDI-TOF and/or LC-MS for identification of differentially regulated protein spots (Table 3.43.i).

From the proteomic analysis we selected four gene targets for functional validation studies by siRNA knockdown. These were downregulated due to pre-mir-29a treatment (which reduces invasion) in the DLKPA cell line. The rationale behind this selection was that if they mediated the mir-29a effect then knockdown of these genes should reduce cancer cell invasion. The target genes RAN, GRB2, MIF and ANX2 were all previously identified in studies on mechanisms of cancer invasion/metastasis. SiRNA knockdown of these targets was confirmed by qRT-PCR analysis (fig. 3.34.1A, 3.35A, 3.36A, 3.37A). The siRNA treated cells were subjected to invasion assay (section 2.10). Only RAN knockdown had any significant impact on the invasive phenotype of DLKPA (fig. 3.38.2A&B). Investigation of the effect of siRNA treatment on proliferation (section 2.9) confirmed that RAN knockdown reduced proliferation (fig. 3.38.1A) as well. No other

target had any significant impact on proliferation in DLKPA (fig. 3.34.2A, 3.35.1A, 3.36.1A). RAN knockdown was confirmed by western blot analysis (fig. 3.38A).

The siRNA target knockdown studies suggested that RAN could be a direct target of mir-29a regulation. To investigate this further we performed a 3'RAN UTR reporter assay. The rationale behind this experiment was that we know that miRNAs target the 3'UTR region of target genes to regulate translation. So by cloning the 3'RAN UTR sequence at the 3' end of GFP, and co-expressing mir-29a, knockdown of GFP expression would provide evidence of interaction between the mir-29a and RAN-UTR. RAN 3'UTR was PCR amplified and cloned downstream of GFP in a reporter vector (fig. 3.39A, B, C), the pEGFP RAN 3'UTR plasmid was transfected in DLKPA cell line and a mixed stable cell line was developed. Pre-mir-29a was then transiently overexpressed in DLKPA-GFP-RAN 3'UTR and monitored for GFP knockdown by qRT-PCR analysis (fig. 3.39.D) as well as by flow-cytometry (fig. 3.39E). There was a reduction in both GFP mRNA level as well as at the protein level. Although the protein reduction was statistically significant it was small (5-6%), suggesting RAN could be a secondary rather than a primary target of mir-29a though further work would be required to establish this.

3.24 qRT-PCR Validation of selected differentially regulated miRNAs.

In collaboration with Ambion, we performed miRNA microarray studies comparing DLKP with DLKPA. The RNA samples were sent to Ambion for hybridization, scanning and data normalization. This data was sent to us and from the list we chose 5 differentially expressed miRNAs. They were mir-21, mir-27a, mir-29a, mir-30a5p and mir-30c. To confirm these findings we performed Sybr green based qRT-PCR analysis. Total RNA was isolated from both cell lines in biological triplicate (n=3) using mirVana RNA isolation kit. 1µl (25ng) of total RNA sample was used for each RT reaction. 5s RNA was used as the endogenous control. The PCR was performed and analyzed with Applied Biosystems 7500 SDS software programme.

From the qRT-PCR analysis it was confirmed that 3 target miRNAs were differentially regulated. The mir-30a5p and mir-27a were not found to be differentially regulated. The mir-21 was ~2 fold upregulated in DLKPA relatively; mir-29a was ~0.3 fold and hsa-mir-30c was ~0.5 fold downregulated in DLKPA compared to DLKP. Figure 3.25A illustrates qRT- PCR validation of the five chosen miRNAs.

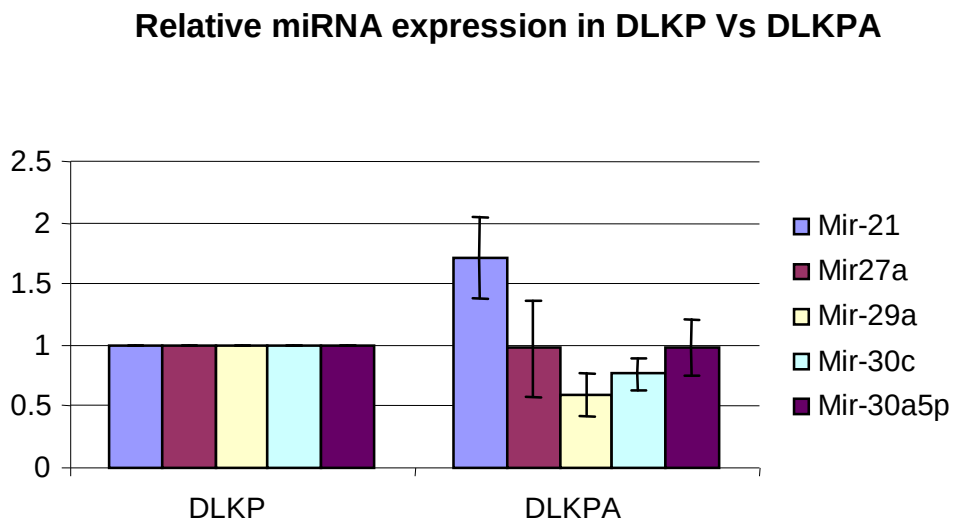

Figure 3.24A qRT-PCR validation of miRNA genes, in DLKP Vs DLKPA.

The graph represents the miRNA expression trend which was observed over several biological and technical repeats. It is evident that mir-21 is upregulated and mir-29a and mir-30c are downregulated. But mir-27a and mir-30a-5p were unchanged. Error bar represents at least n=3

3.25 Effect of transient overexpression and knockdown of chosen miRNAs on cell proliferation.

Based on qRT-PCR results three miRNA targets were chosen, hsa-mir-21, hsa-mir-27a and hsa-mir-29a, to determine if there was any impact on proliferation due to their transient overexpression and/or knockdown. NeoFX was used to transfect 50nM of target pre-mir and anti-mir sequences into the cells (section 2.8.2). Pre-mir sequence is a double stranded 21-mer identical to the mature form of the miRNA (so transfecting these is like overexpression) and anti-mir is a single stranded nucleotide sequence complementary to target miRNA which behaves as siRNA or antisense to miRNA. To control for non specific effects of the transfection process on phenotype, we also used negative pre and anti miRNA sequence, which are random 21-mer sequences. NeoFX transfection agent alone was also included as control. Finally to ensure transfection efficiency we used Kinesin specific siRNA.

The effect on proliferation was investigated by seeding 100µl of $3x10^4$ cells per ml in a 96 well plate. The cells were seeded on top of the already pipetted NeoFX: miRNA complex. This facilitates efficient 'reverse' transfection. 72 hrs post incubation each well on the plate was assayed using the acid phosphatase method. Before proceeding further we wanted to confirm the actual level of transfected miRNA sequence. We performed miRNA qRT-PCR analysis on pre and anti mir transfected cells. 72hrs later total RNA was isolated and qRT-PCR analysis was done.

From the qRT-PCR analysis it was confirmed that pre-mirRNAs were upregulated (23 fold) in the transfected cells relatively. An example of mir-29a overexpression is represented in figure 3.25A. However, we were not able to detect knockdown. This was probably due to the fact that anti-mir, unlike siRNAs, does not catalyse degradation of the target miRNA, but merely binds to target miRNA. During extraction of miRNAs or PCR reaction, they get dissociated hence, no knockdown is observed in the miRNA level.

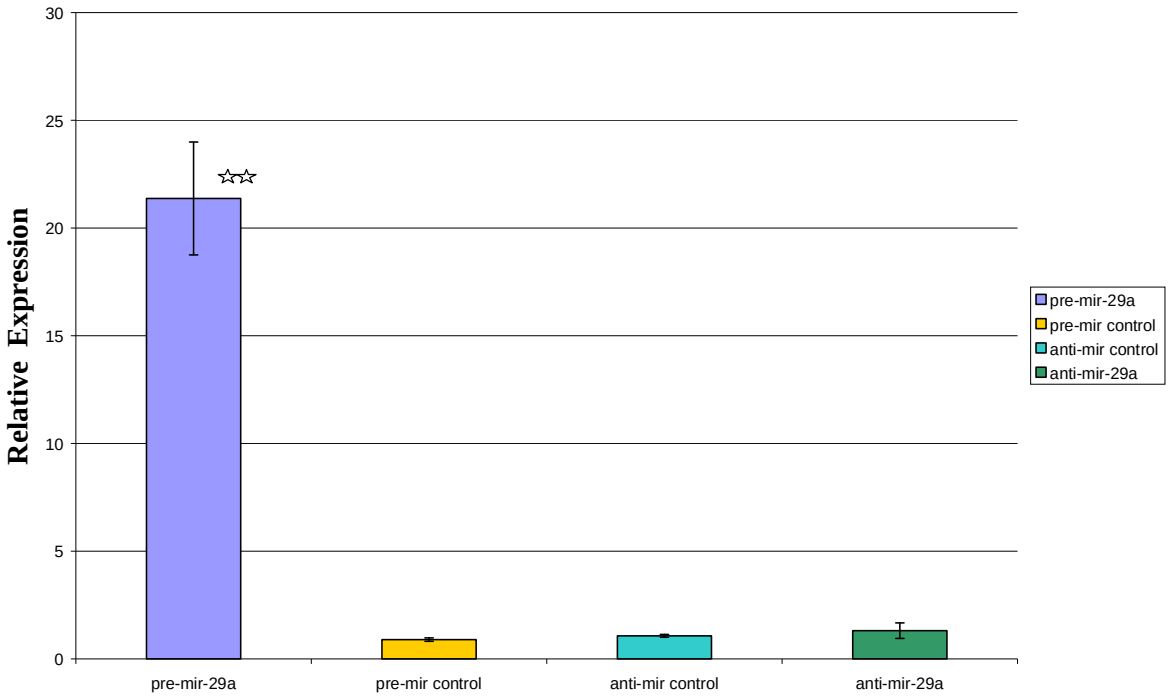

3.25A qRT-PCR analysis of pre and anti-mir-29a transfected DLKPA cell line.

A significant increase in mir-29a levels was observed, error bar represents (SEM ± 1.51), with ** (<0.005) *p*-Value,

From figure 3.25B&C a small but significant (12% in DLKP and 7% in DLKPA) increase due to pre-mir-21 treatment was observed in proliferation and there was no impact on proliferation by mir-27a or 29a treatments, though kinesin control confirmed the efficient transfection.

B) DLKP

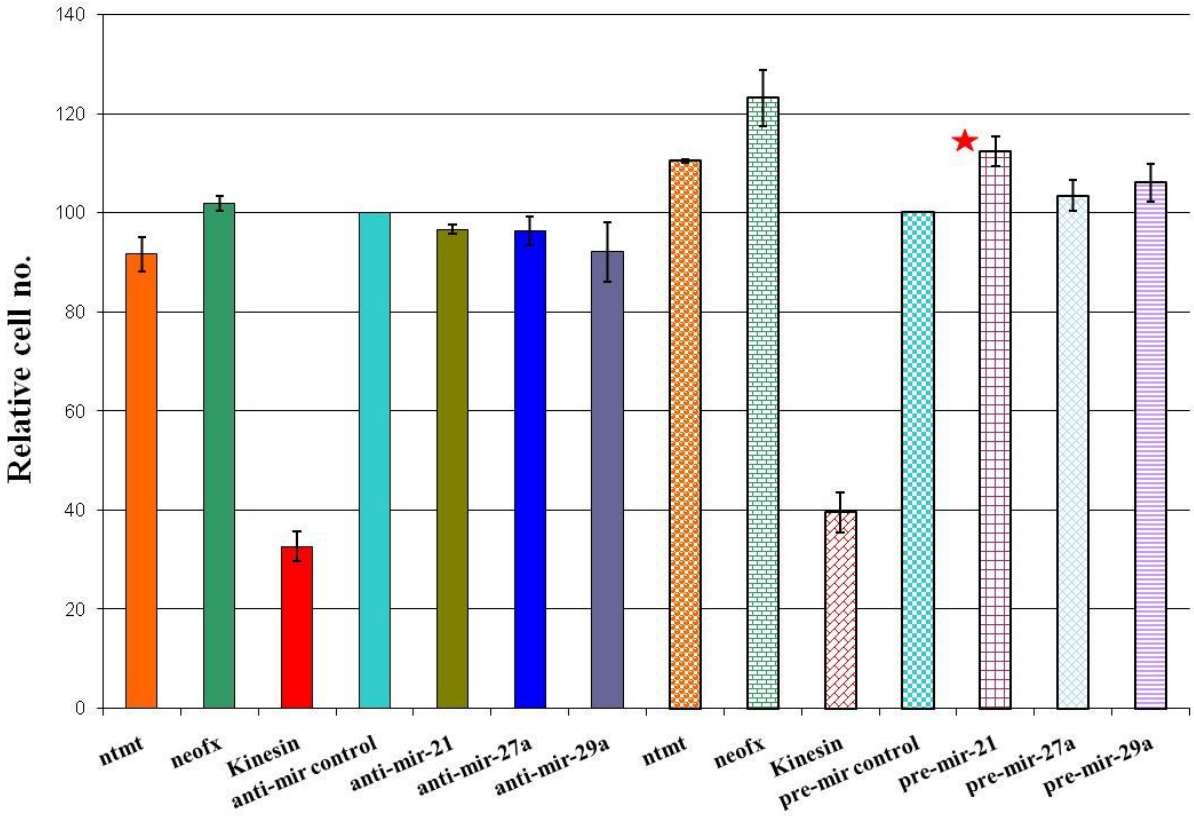

Figure 3.25B Effect on proliferation due to Anti and Pre miRNA treatment in DLKP cell line. Ntmt; no treatment, neofx; NeoFX transfection agent control, Kinesin; positive control, anti-mir-control; control for miRNA sequence, anti-mir-21, 27a and 29a, pre-mir-21, 27a and 29a. The effect of anti and pre-miRNA treatments were normalized with anti-miRNA controls and pre-miRNA control treated samples. Figure represents anti and pre miRNA treatments in DLKP with * p-value (<0.05) seen only with pre-mir-21 treatment relative to control treatment. The error bar represent SD and n=3.

C) DLKPA

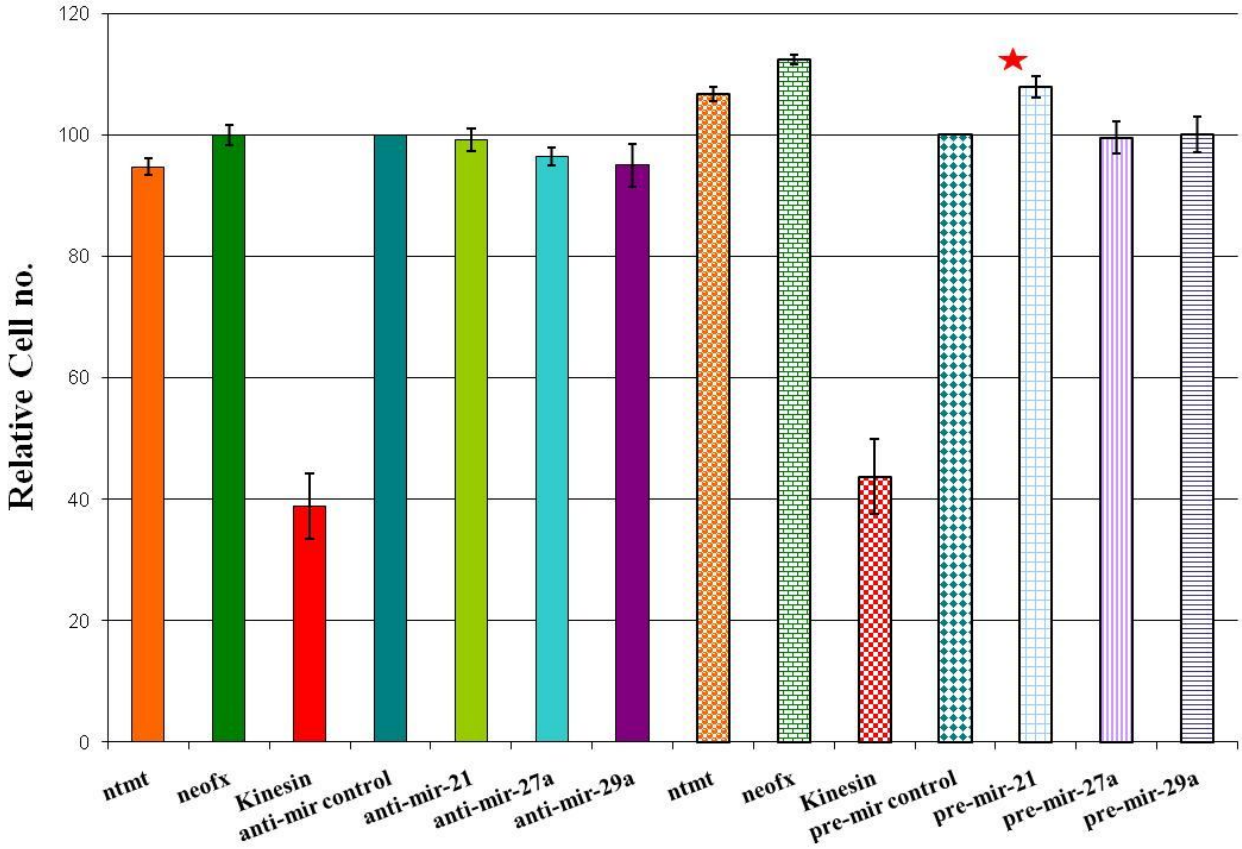

Figure 3.25C Effect on proliferation due to Anti and Pre miRNA treatment in DLKPA cell line. Ntmt; no treatment, NeoFX; NeoFX transfection agent control, Kinesin; positive control, anti-mir-control; control for miRNA sequence, anti-mir-21, 27a and 29a, pre-mir-21,27a and 29a. Figure represents anti and pre miRNA treatments in DLKPA with * p-value (<0.05) seen only with pre-mir-21 treatment relative to control treatment. The error bar represent SD and n=3.

3.25.1 To evaluate the effect of Adriamycin sensitivity in miRNA treated DLKP and DLKPA cell lines.

One of the model cell lines used in this study DLKPA, was an Adriamycin resistant cell line, developed in the NICB (Heenan et al., 1997). Adriamycin, an active medicine against many cancers, is one of the older chemotherapy drugs, having been in use for decades. Like most chemotherapeutics, there is always the chance of tumours developing drug resistance. To study this phenomenon the lung cancer cell line DLKP (mildly invasive) was pulse treated with Adriamycin, resulting in the selection and isolation of a drug-resistant, highly invasive variant cell line, referred to as DLKPA.

For this reason the targets chosen from our miRNA profiling of DLKP Vs DLKPA, may be associated with either the resistance to drug and/or the invasive phenotype. We decided to perform drug sensitivity assay (by monitoring proliferation phenotype) post miRNA treatment and drug treatment. 50nM of pre-mir and anti-mirs were transfected into the cells (section 2.8.2). 72hrs later the media from the 96 wells was replaced with drug containing media (122μg/ml of Adriamycin, previously established to represent IC50 for DLKPA cell line) and incubated for a further 24hrs. Each well on the plate was measured by acid phosphatase assay. Though our effort was to determine the impact drug sensitivity in DLKPA, we also used DLKP in the same experiment to with IC50 similar to DLKPA to check whether it had any impact due to miRNAs inhibition and overexpression. From the results it was evident that DLKP cells were 7-8% more sensitive to drug after anti-mir treatments of 21, 27a and 29a (Fig. 3.25.1A). Conversely a 12-18% increase in resistance was observed due to miRNA overexpression. No effect in the DLKPA cell line was observed (Fig 3.25.1B).

A)DLKP

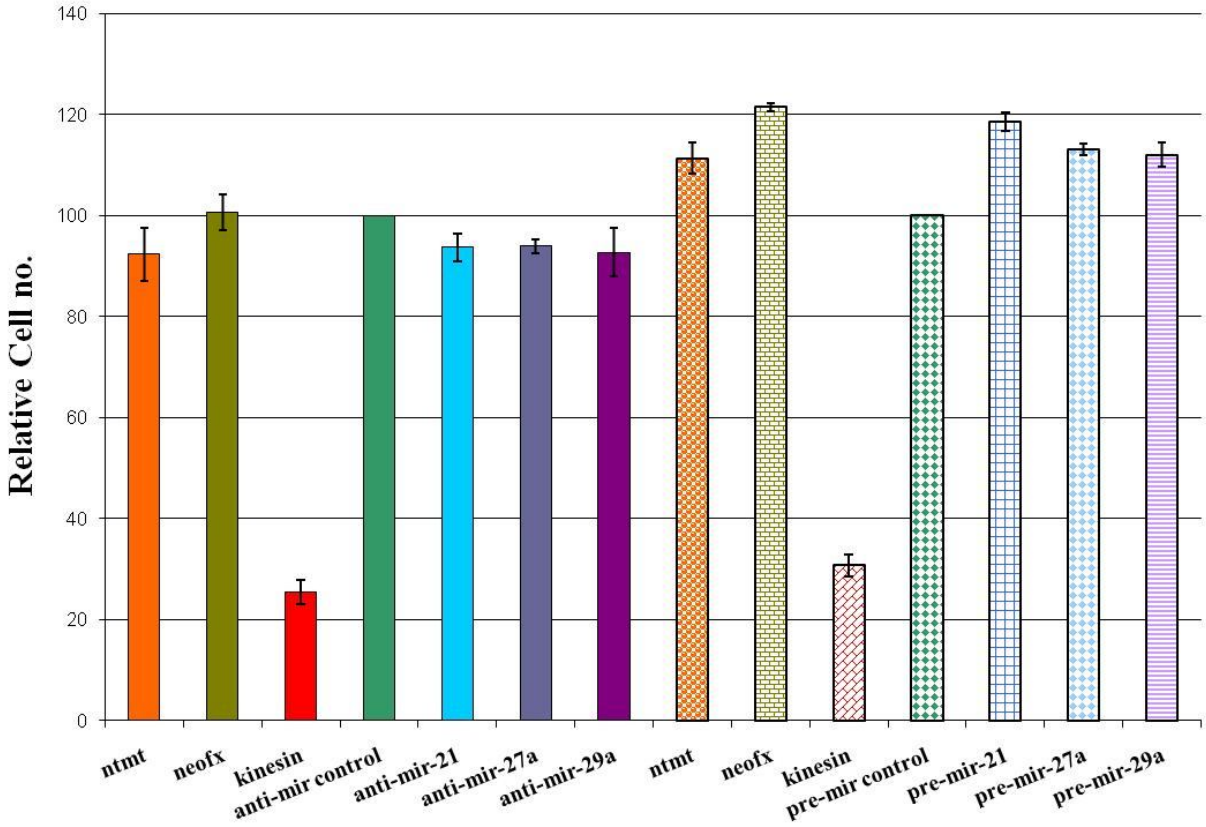

Figure 3.25.1A Anti and Pre miRNA treatment and 24 hrs Adriamycin drug treated proliferation assay in DLKP cell lines. Ntmt; no treatment, NeoFX; NeoFX transfection agent control, Kinesin; positive control, anti-mir-control; control for miRNA sequence, anti-mir-21,27a and29a, pre-mir-21,27a and 29a. Adriamycin pulsing (IC50=122μg/ml). Error bar represents ± SEM. The effect of anti and pre-miRNA treatments were normalized with anti-miRNA controls and pre-miRNA control treated samples.

B) DLKPA

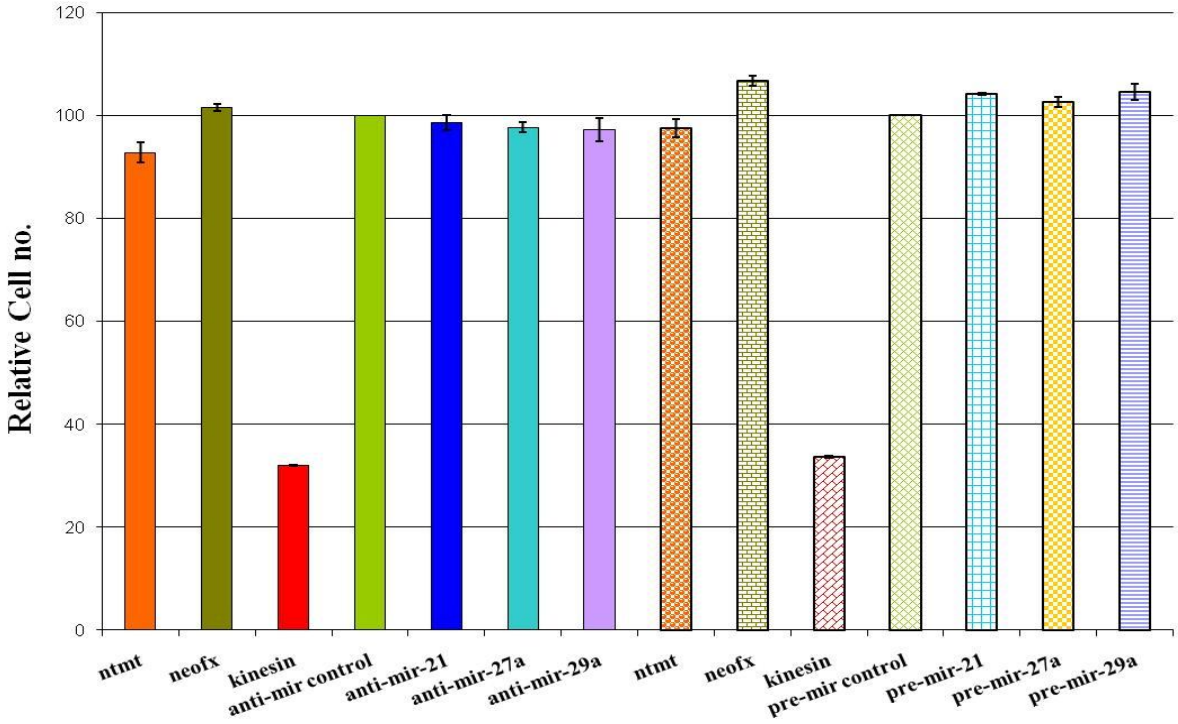

Figure 3.25.1B Anti and Pre miRNA treatment and 24 hrs Adriamycin drug treated proliferation assay in DLKPA cell lines. Ntmt; no treatment, NeoFX; NeoFX transfection agent control, Kinesin; positive control, anti-mir-control; control for miRNA sequence, anti-mir-21,27a and29a, pre-mir-21,27a and29a. Adriamycin pulsing (IC50=122µg/ml).Error bar represents ± SEM. The effect of anti and pre-miRNA treatments were normalized with anti-miRNA controls and pre-miRNA control treated samples.

3.26 Investigation of the effect on invasion due to miRNA treatment in DLKP and DLKPA cell lines.

The aim of this study was to investigate the potential role of miRNAs in controlling or influencing the invasive phenotype in lung cancer cells. We performed a miRNA microarray study to identify differentially regulated miRNAs. The DLKP parent cell line in these subsequent validation experiments was found to be more invasive. This frozen culture came from a separate stock to that which was profiled originally. And the nature of DLKP being a poorly differentiated cell line could have caused this difference. From microarray studies we chose three miRNAs which we suspected to have a role in cancer

cell invasion. We performed an in vitro invasion assay with DLKP and DLKPA cell lines to evaluate the impact if any on the invasive phenotype in these cell lines. 50nM of target pre-mir and anti-mirs were transfected into the cells (section 2.8.2). To control for non-specific effects of the transfection process we used negative pre and anti miRNA sequences, which are random 21-mer sequences. To ensure transfection efficiency we used Kinesin specific siRNA (figure.3.26A, 3.26B and 3.26C).

The effect on invasion was investigated by seeding 24 well cell culture plates with 1ml of $2x10^5$ cells per ml cell suspension of DLKP and DLKPA cell lines. The cells were seeded on top of the NeoFX: miRNA solution mixtures which facilitate efficient reverse transfection. 72hrs later invasion assay analysis was performed using commercial invasion assay kits containing inserts pre-coated with matrigel without a serum gradient. The cells were seeded in a 100µl volume at 10^6 cells per ml. The cells were incubated at 37^oC for 48 hours after which, at least two inserts were used for the analysis of each condition.

The anti-mir-21 treated DLKP and DLKPA cell lines were observed to have impact on invasion with 51% and 37% reduction respectively. Similarly anti-mir-27a treated DLKP with 36%) and DLKPA (40%) cell lines showed significant impact on invasion. Conversely increased invasion due to anti-mir-29a in DLKP (38%) was observed and no effect on DLKPA invasion phenotype was observed as shown in (figure.3.26D, and 3.26F).

The pre-mir21 treated DLKP (41%) and DLKPA (38%) cells were observed to have increased invasion. A similar impact due to pre-mir-27a treated DLKP (38%) and DLKPA (26%) was observed, as shown in (figure.3.26E). Conversely decreased invasion due to pre-mir-29a treatment (21% in DLKP and 29% in DLKPA) was observed as shown in (figure.3.26.G). These results indicated that mir-21 and 27a were proinvasive and mir-29a was an anti invasive miRNA species.

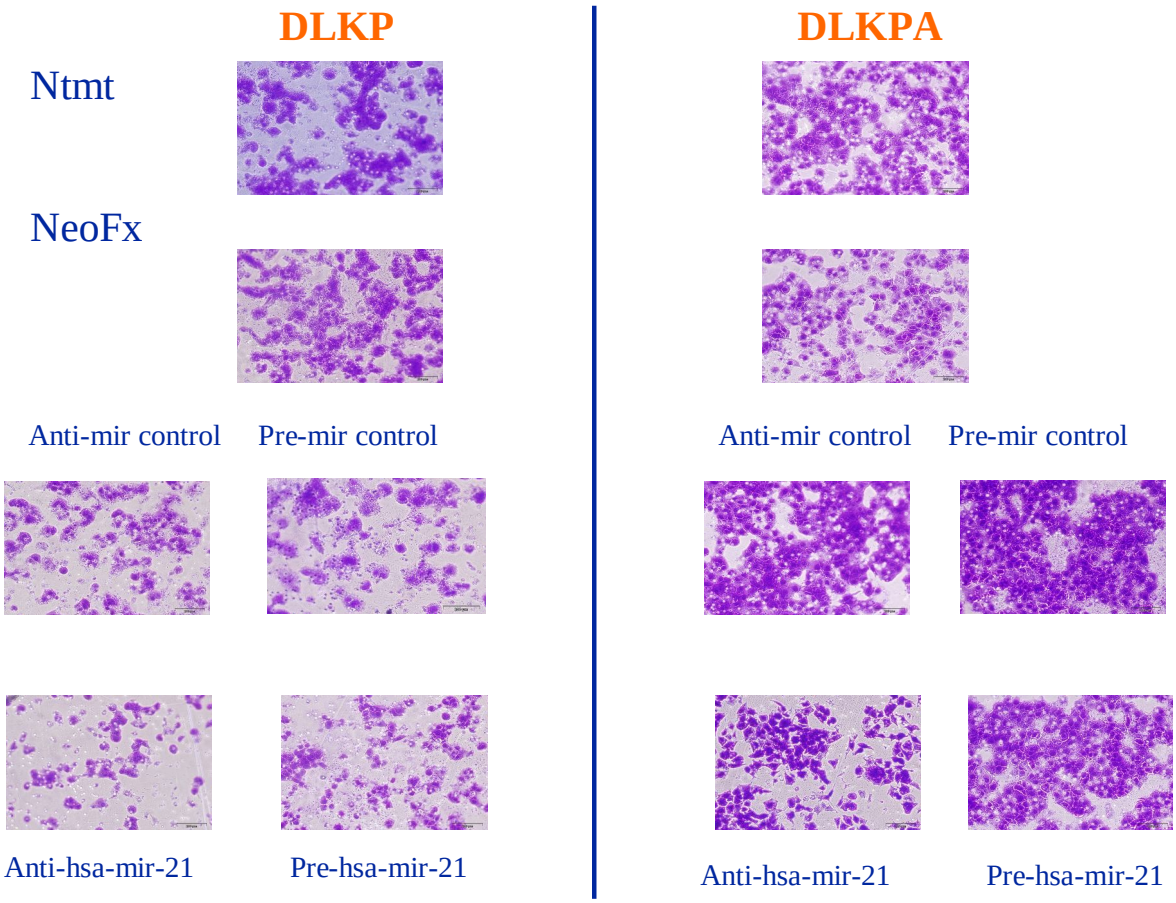

Figure 3.26A Impact of transient transfection of pre and anti-mir-21 on the in vitro invasiveness of DLKP and DLKPA cells.

Ntmt: No treatment; NeoFX: cell treated with transfection agent only; Anti-mir and Pre-mir control: transfection with non-specific pre and anti-mir molecules; Pre- and anti-mir21: cells treated with mir-21 specific anti-and pre-mir sequences. Matrigel inserts were stained and counted for invasive cells 48hrs after seeding. Cells were transfected 72hrs before seeding. Magnification =20X.

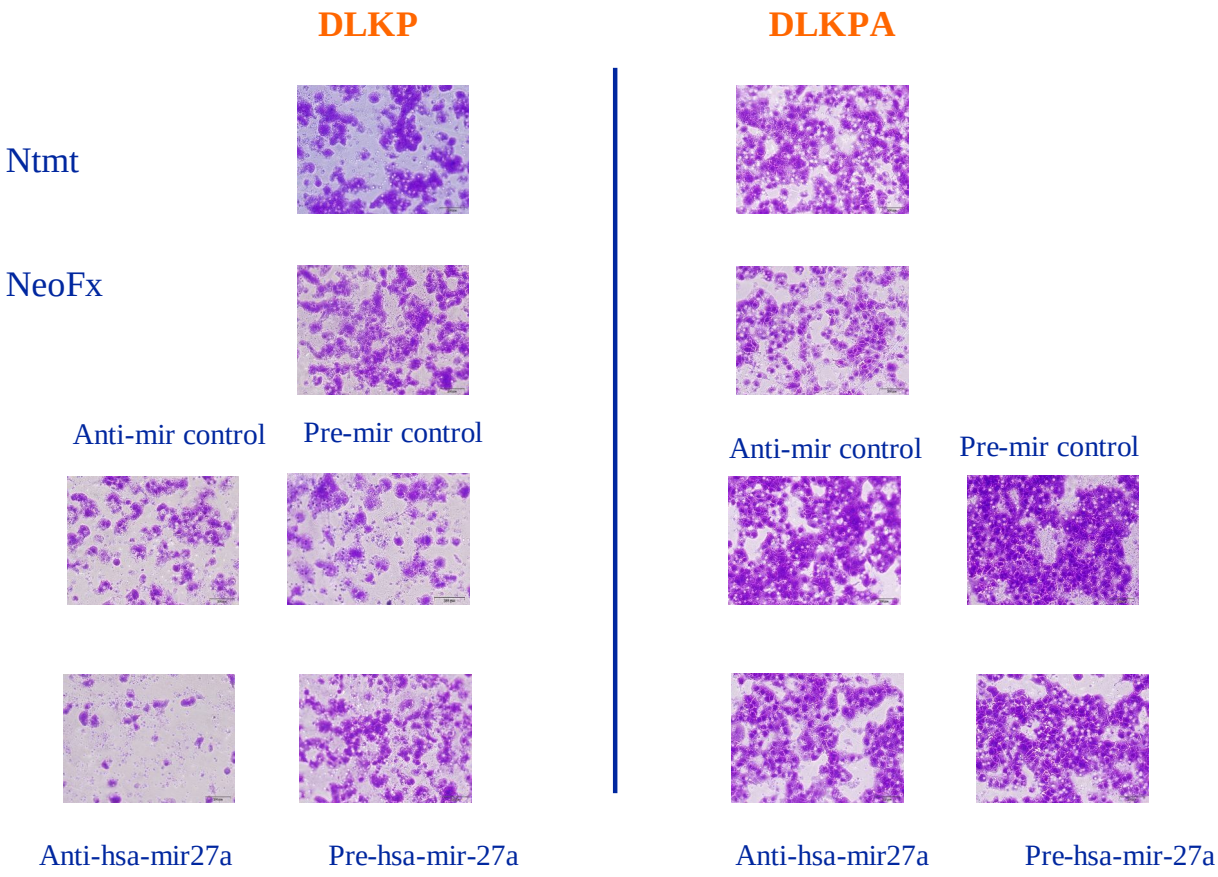

Figure 3.26B Impact of transient transfection of pre and anti-mir-27a on the in vitro invasiveness of DLKP and DLKPA cells.

Ntmt: No treatment; NeoFX: cell treated with transfection agent only; Anti-mir and Pre-mir control: transfection with non-specific pre and anti-mir molecules; Pre- and anti-mir27a: cells treated with mir-27a specific anti-and pre-mir sequences. Matrigel inserts were stained and counted for invasive cells 48hrs after seeding. Cells were transfected 72hrs before seeding. Magnification =20X.

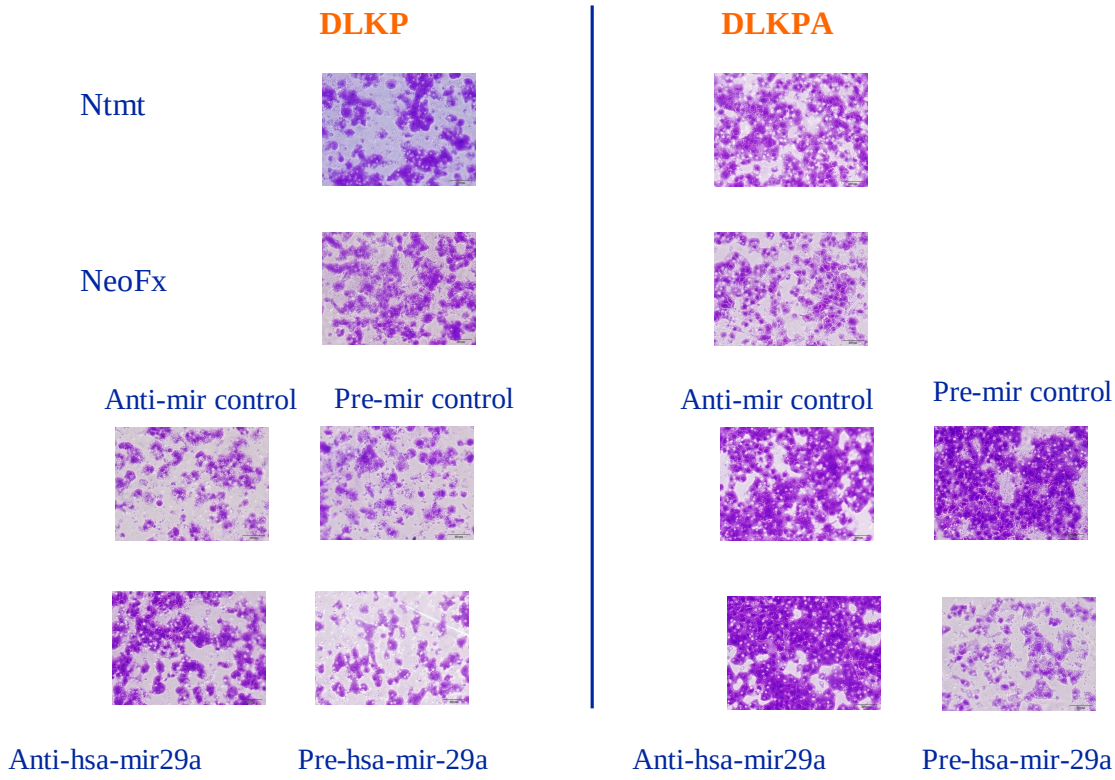

Figure 3.26C Impact of transient transfection of pre and anti-mir-29a on the in vitro invasiveness of DLKP and DLKPA cells.

Ntmt: No treatment; NeoFX: cell treated with transfection agent only; Anti-mir and Pre-mir control: transfection with non-specific pre and anti-mir molecules; Pre- and anti-mir29a: cells treated with mir-29a specific anti-and pre-mir sequences. Matrigel inserts were stained and counted for invasive cells 48hrs after seeding. Cells were transfected 72hrs before seeding. Magnification =20X.

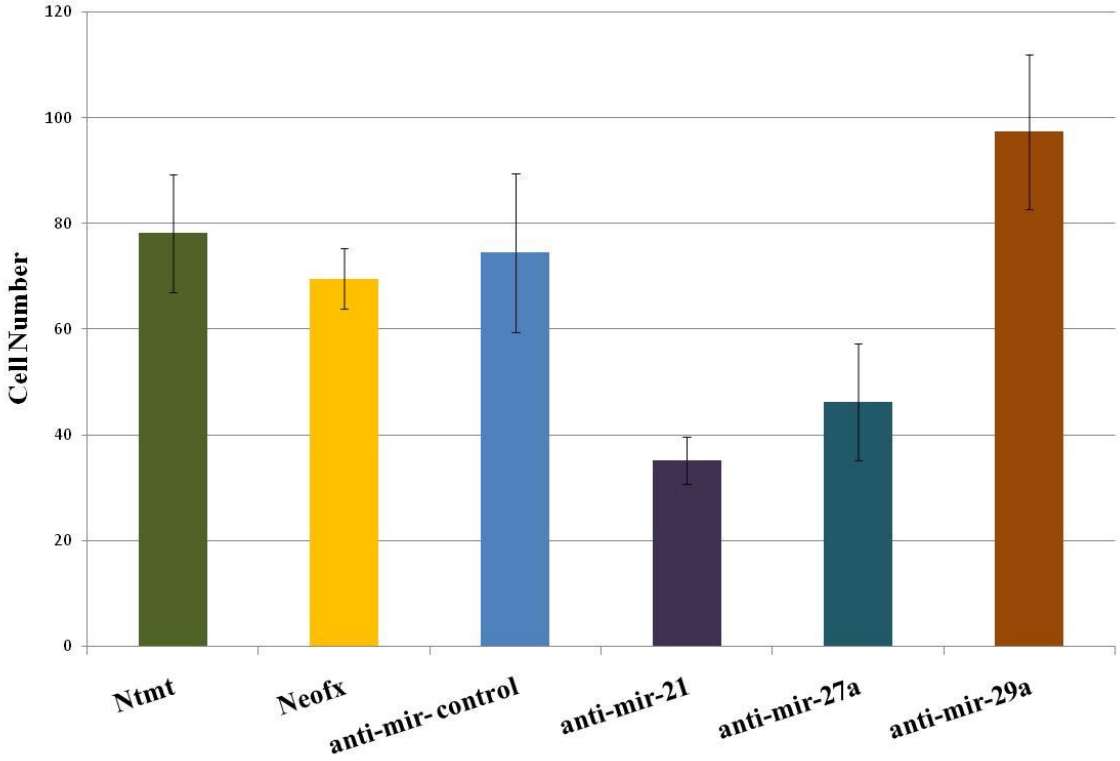

Figure 3.26D Graphical representation of invasion assay post anti-mir-21, mir-27a and mir-29a treatment in DLKP cell line. Ntmt: No treatment; NeoFX: cell treated with transfection agent only; Anti-mir control: transfection with non-specific anti-mir molecules; Anti-mir21, 27a and mir29a: cells treated with mir-21,27a and 29a specific anti-mir sequences. Figure represents anti miRNA treatments in DLKP. The error bar represent ±SEM and n=3.

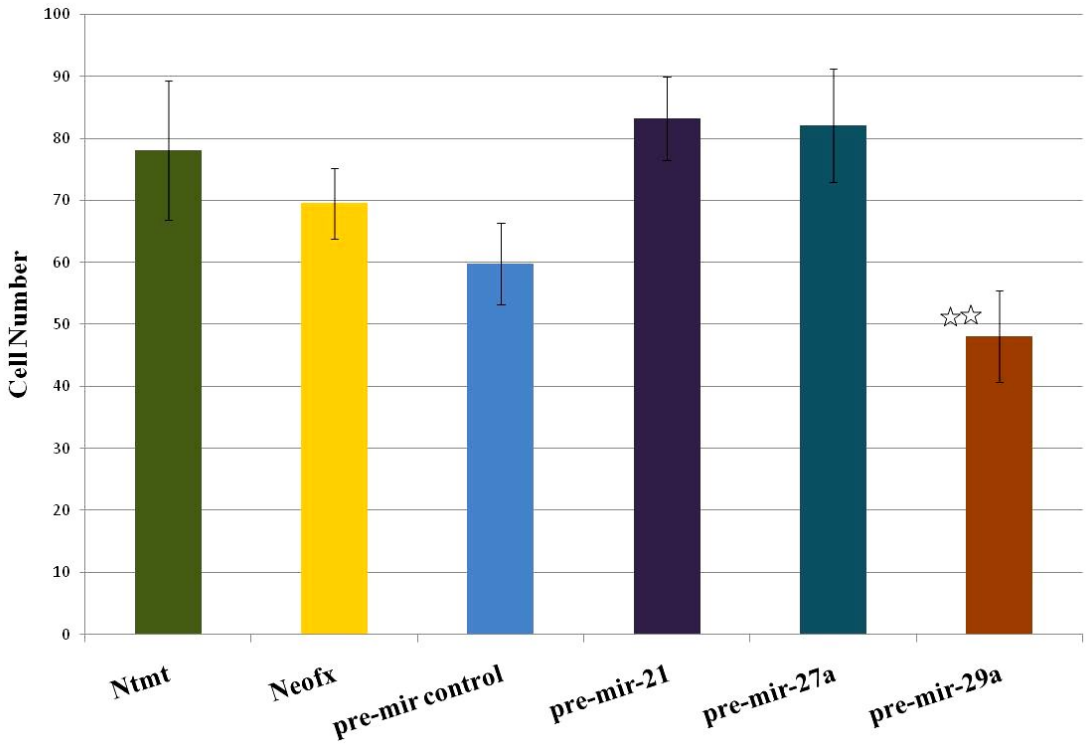

Figure 3.26E Graphical representation of invasion assay post pre-mir-21, mir-27a and mir-29a treatment in DLKP cell line. Ntmt: No treatment; NeoFX: cell treated with transfection agent only; Anti-mir control: transfection with non-specific anti-mir molecules; Pre-mir21, 27a and mir29a: cells treated with mir-21,27a and 29a specific pre-mir sequences. Figure represents anti and pre miRNA treatments in DLKP with * p-value (<0.05) seen only with pre-mir-29a treatment relative to control treatment. The error bar represent ±SEM and n=3

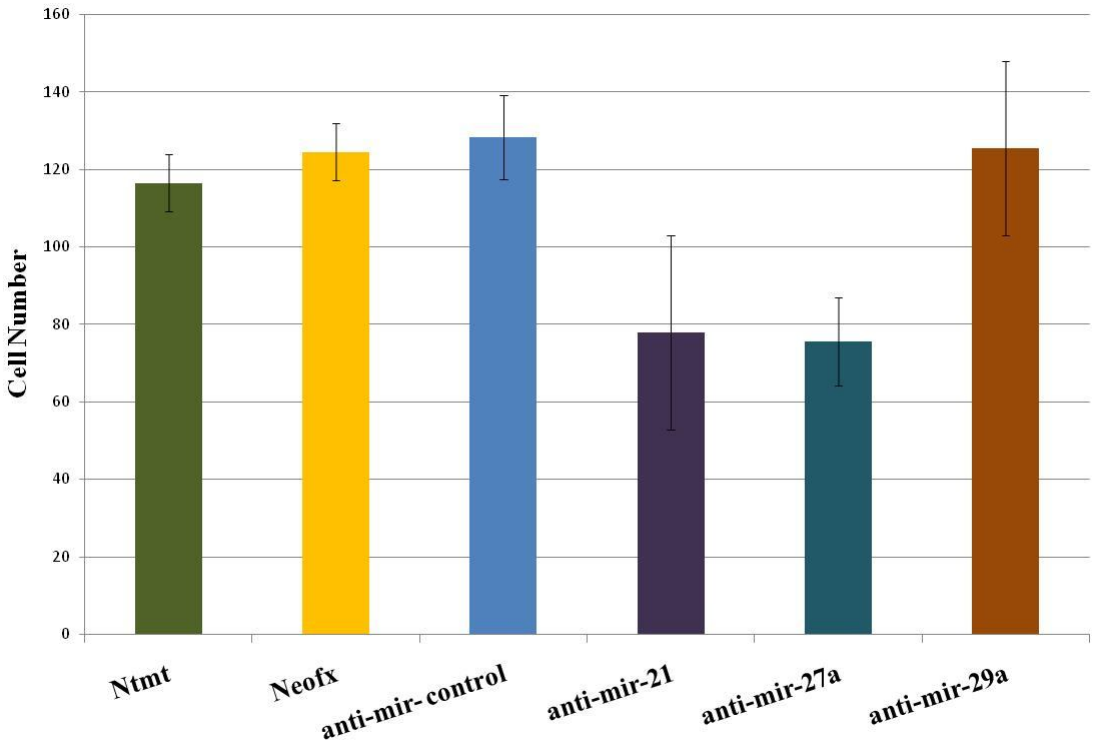

Figure 3.26F Graphical representation of invasion assay post anti-mir-21, mir-27a and mir-29a treatment in DLKPA cell line. Ntmt: No treatment; NeoFX: cell treated with transfection agent only; Anti-mir control: transfection with non-specific anti-mir molecules; Anti-mir21, 27a and mir29a: cells treated with mir-21,27a and 29a specific anti-mir sequences. Figure represents anti and pre miRNA treatments in DLKPA The error bar represent ±SEM and n=3.

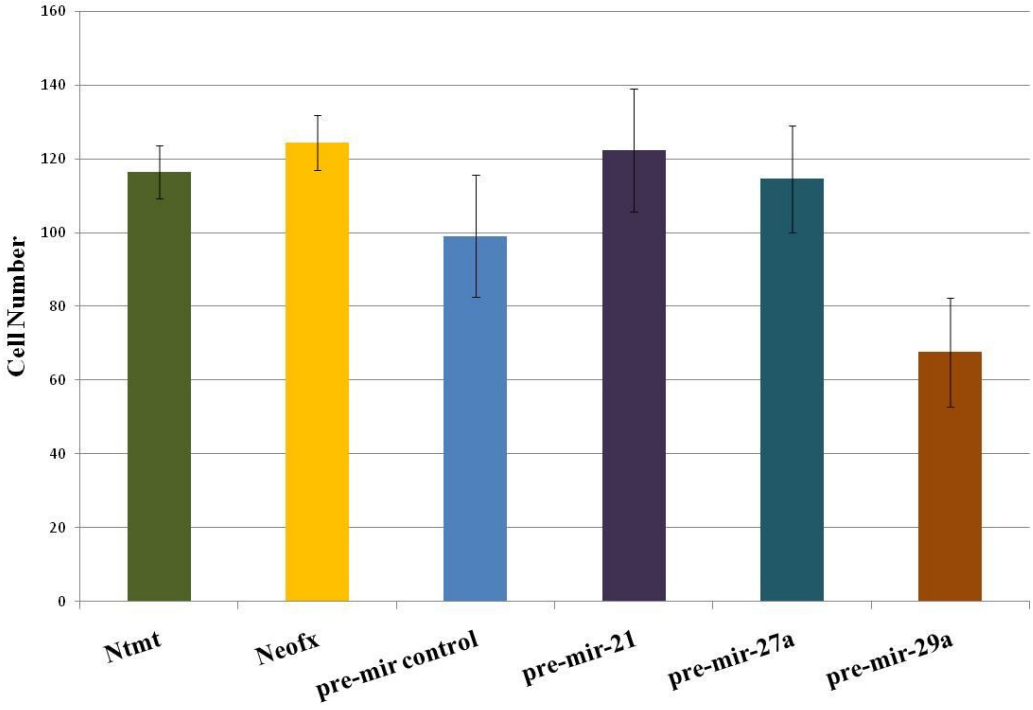

Figure 3.26G Graphical representation of invasion assay post pre-mir-21, mir-27a and mir-29a treatment in DLKPA cell line. Ntmt: No treatment; NeoFX: cell treated with transfection agent only; Anti-mir control: transfection with non-specific anti-mir molecules; Pre-mir21, 27a and mir29a: cells treated with mir-21,27a and 29a specific pre-mir sequences. Figure represents anti and pre miRNA treatments in DLKPA. The error bar represent SD and n=3.

3.27 Investigation of the effect of mir-29a transient overexpression on PANC-1 cell line (pancreatic carcinoma) invasion phenotype

To establish that the anti invasive effect of mir-29a expression was not only lung cancer cell line specific we included another cell line in our study, PANC-1 which is a pancreatic cancer cell line with a highly invasive phenotype. We transiently transfected pre-mir-29a and control sequence into PANC-1 cells in 24-well cell culture plates. TaqMan based qRT-PCR was performed to confirm mir-29a overexpression. The qRT-PCR analysis of RNA samples confirmed mir-29a overexpression of 2.3 fold relatively (Fig. 3.27A).

Briefly, 50nM of target pre-mir-29a was transfected into cells (section 2.8.2). 72hrs later invasion assay analysis was performed with 48 hours incubation. The cells were seeded in 100µl volume at 10^6 cells per ml and cells were incubated at 37^oC for 48 hours after which the underside of the inserts were stained with crystal violet and counted per insert at 20X magnification. At least two inserts were used for the analysis of each condition.

The invasion assay results further confirmed the impact of mir-29a as an anti invasive miRNA. A significant decrease of about 55% in PANC-1 invasion phenotype was observed relative to control transfected cells. Figure 3.27 A&B illustrates post mir-29a transient overexpression with PANC-1 in vitro invasion assay. This illustrated that the impact of mir-29a on invasion was not necessarily tissue specific but may play a more general role in the control of cellular invasiveness.

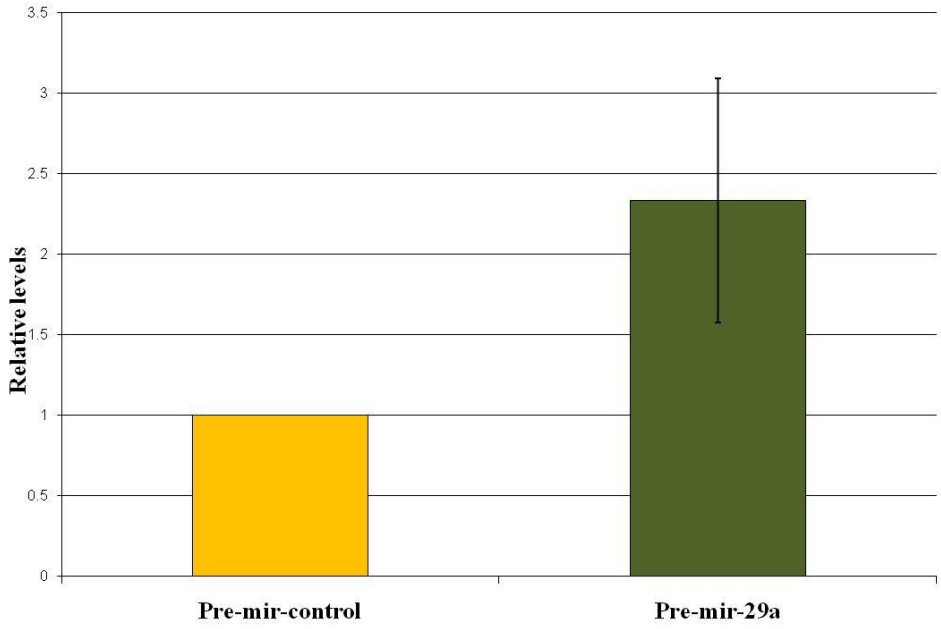

Figure 3.27A qRT-PCR confirmation of transient mir-29a overexpression.

Pre-mir-control: pre-mir control sequence transfected as control; Pre-mir-29a: pre-mir-29a mature sequence transfected; error bar represents SEM ± 0.26.

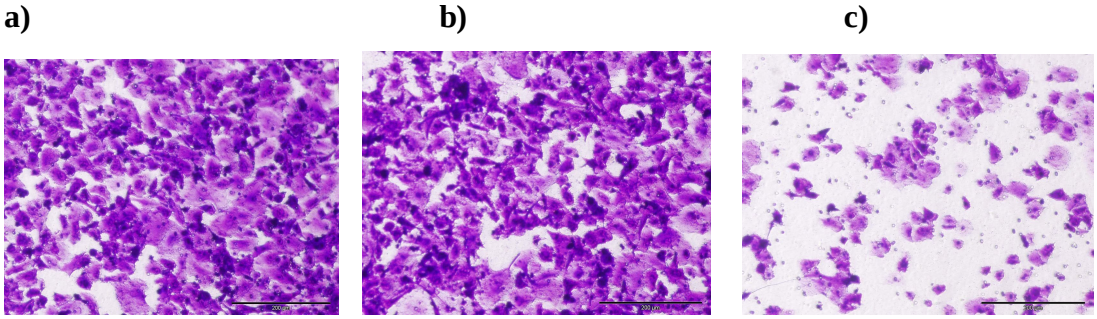

PANC-1 Ntmt Pre-mir control Pre-mir-29a

Figure 3.27B Effect of mir-29a transient overexpression on invasion in PANC-1 cell line. a) Ntmt: no treatment control; b) Pre-mir control; transient overexpression of Pre-mir- control, c) Pre-mir-29a: pre-mir-29a treated, magnifications 20X.

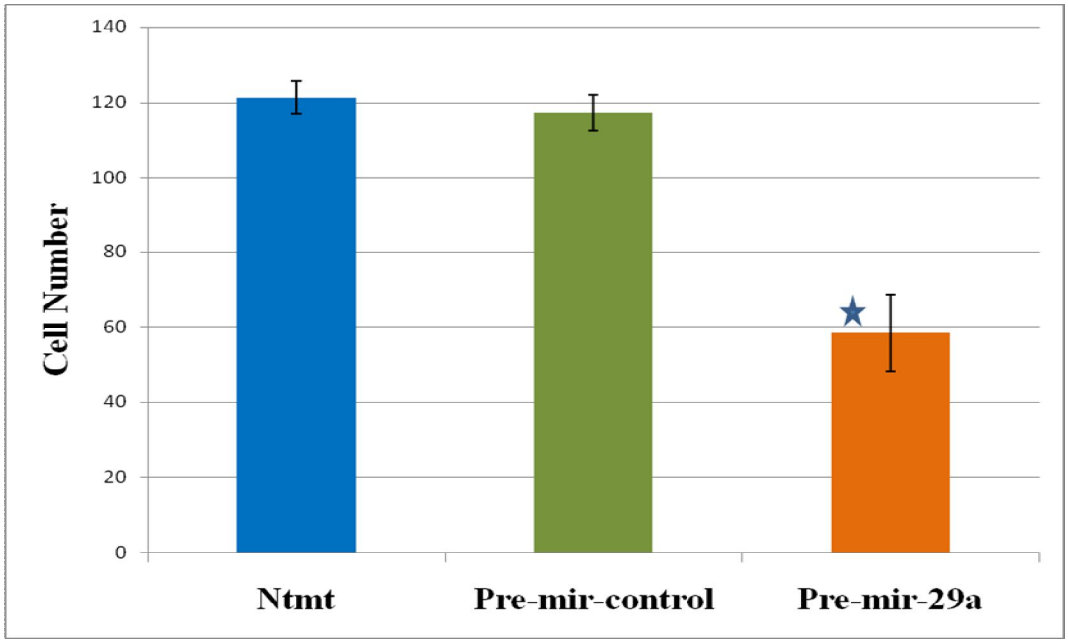

Figure 3.27C Impact of transient mir-29a overexpression.

Ntmt: no treatment; Pre-mir-control: pre-mir control sequence treated; Pre-mir-29a: pre-mir-29a mature sequence treated. Invasion assay counts represents SEM ± with * (≤0.05) *p*-Value and n=3.

3.28 Effect of stable overexpression of mir-29a on invasion and proliferation of DLKPA cell line

Transient overexpression of hsa-mir-29a was observed to have an anti-invasive effect on DLKPA cells with a 40% decrease in invasion observed. But, no significant impact on proliferation was observed. To further investigate this we designed primers to amplify pre-mir-29a (228nt in length) from DLKP genomic DNA and clone the amplicon in a mammalian expression vector for stable overexpression in DLKPA to generate cells that stably overexpressed the mir-29a transcript. The **p*Silencer*™** 4.1-CMV plasmid vector was purchased from Ambion. This is a mammalian expression vector designed for long-term gene silencing experiments in a broad range of cell lines. The vector carries an RNA polymerase II-type CMV promoter (human cytomegalovirus immediate-early promoter) and an optimized SV40 polyadenylation signal to drive high-level expression of hairpin siRNA/miRNA. Endogenously miRNAs are expressed as longer hairpin molecules. These primary transcripts (pri-miRNAs) are then cleaved in the nucleus by the Drosha protein to release 60-70nt pre-miRNA hairpins. We designed primers to amplify the endogenous pri-mir-29a in such a way that the amplified region contained at least 70-90nt flanking the 64nt pri-mir-29a; this would facilitate processing by Drosha to a functional pre-mir-29a sequence (Fig.3.28A). Pre-mir-29a is exported to the cytoplasm by an Exportin 5-dependent mechanism where it is processed by Dicer to generate mature 21-24 nt miRNAs (Lee et al., 2003). The cloning of mir-29a was successful (Fig. 3.28B) and was sent for sequence confirmation (MWG sequencing facility in Germany). A negative control vector was also used to generate stable DLKPA cell lines. The sequencing results confirmed the mir-29a sequence, when blasted against human genomic DNA database. A perfect match of 228nt hit was observed (refer Fig.3.28C).

The mir-29a plasmid was transfected in DLKPA cells and stable cell lines were generated. To confirm mir-29a specific overexpression, total RNA was isolated and quantified. TaqMan based qRT-PCR was performed to confirm stable mir-29a overexpression. The qRT-PCR analysis of RNA samples identified at least three DLKPA cell lines with confirmed mir-29a overexpression, ranging from 2-4 fold relatively (Fig.3.28D).

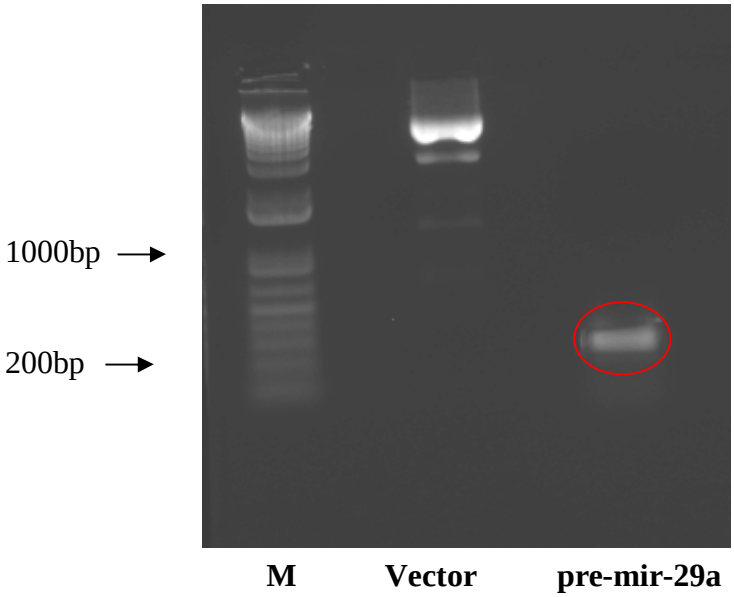

Figure 3.28A Restriction enzyme digestion of p*Silencer*™ 4.1-CMV-Neo vector.
M: 1kb plus DNA ladder; Vector: digested vector backbone; pre-mir-29a: ~250 bp pri-mir-29a amplicon digested with *BamHI* and *HindIII*.

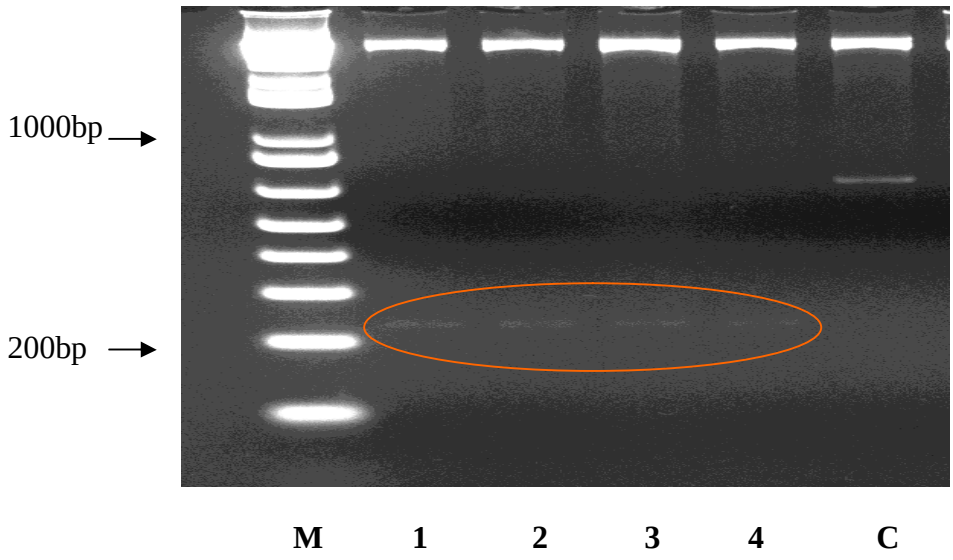

Figure 3.28B Restriction enzyme digestion analysis to check cloning of pre-mir-29a.
Lanes M: 1kb plus DNA ladder; 1, 2, 3, 4: *BamHI* and *HindIII* digestion release expected product ~ 250 bp confirming insert cloning; C: negative control.

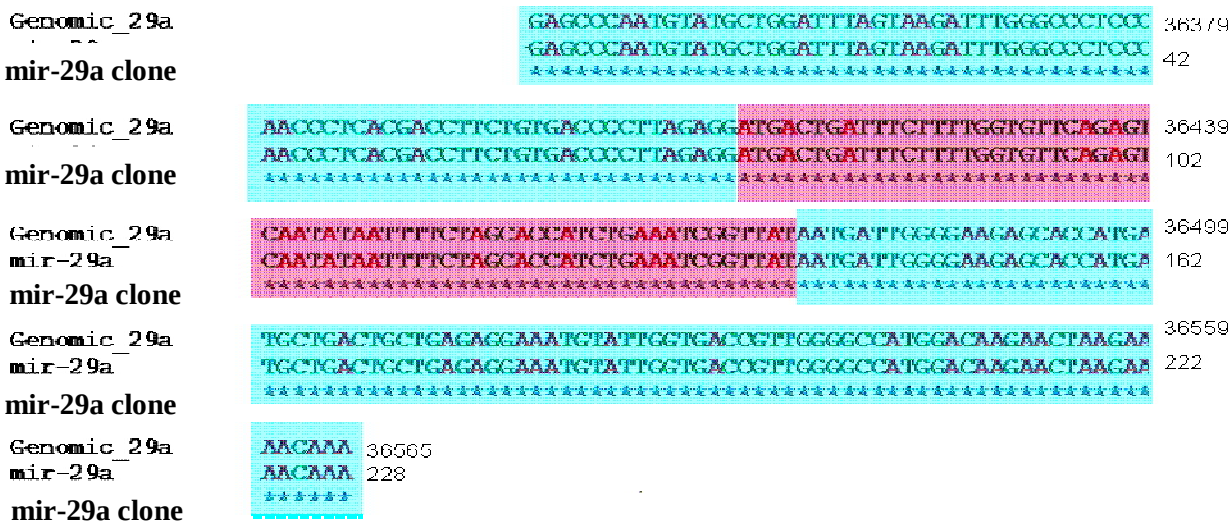

Figure 3.28C ClustalW alignment of cloned hsa-mir-29a sequence. Confirmation of mir-29a sequence compared to genomic sequence. The region showed in pink represents the exact match of pri-mir-29a sequence (64nt) and blue regions represent flanking sequences on either side of pri-mir-29a.

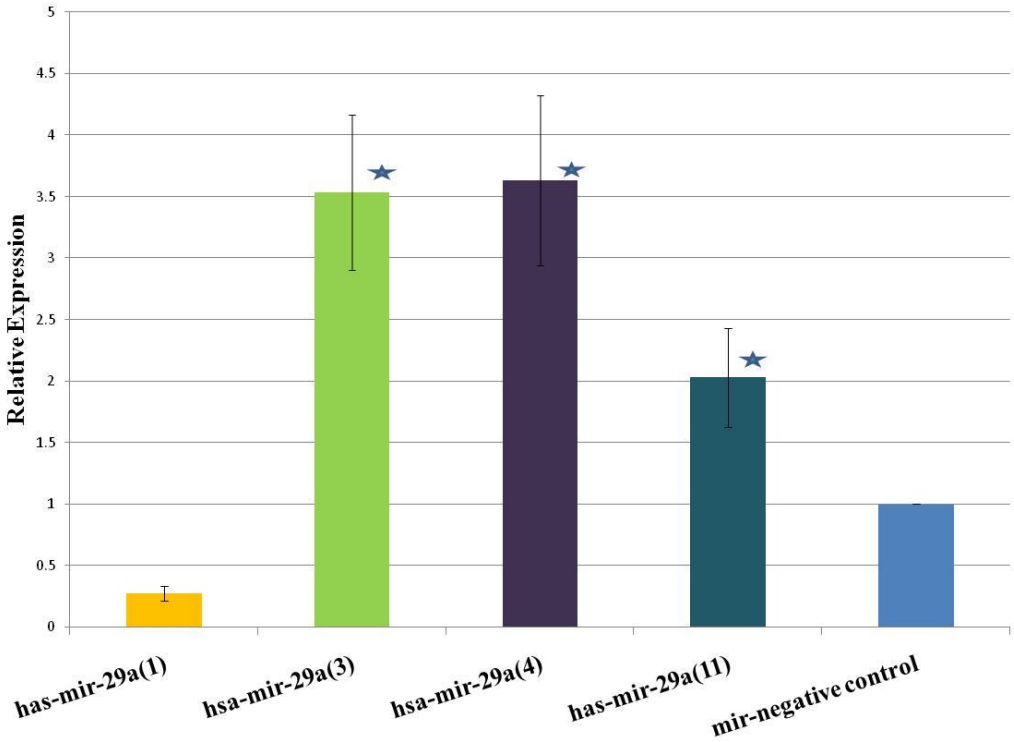

Figure 3.28D qRT-PCR confirmation of stable mir-29a overexpression in DLKPA cell line. Three DLKPA clones (3,4 and 11) had confirmed hsa-mir-29a stable overexpression with a 2-3.5 fold up regulation compared to control, and clone 1 demonstrated mir-29a downregulation where * (< 0.05) *p*-value. The values were normalized to mir-negative control treatment and (n=3).

3.29 Investigation of effect of mir-29a stable overexpression on DLKPA Proliferation

72hrs after transient mir-29a overexpression in DLKPA cells there was no significant impact on proliferation. But, we did see decreased invasive phenotype in these cells. Once we established the stable mir-29a overexpressing DLKPA clones we decided to investigate if there was any effect on proliferation. This was investigated by seeding the stable clones in 100µl volume at $3x10^4$ cells per ml in a 96 well plate. 48 hrs after seeding each well on the plate was assayed using the acid phosphatase assay as described in (Section 2.9). An impact on proliferation was observed due to mir-29a stable overexpression. DLKPA clone 3 was observed to have reduced proliferation by [36%], Clone 4 reduced by [25%] and Clone 11 by [44%].

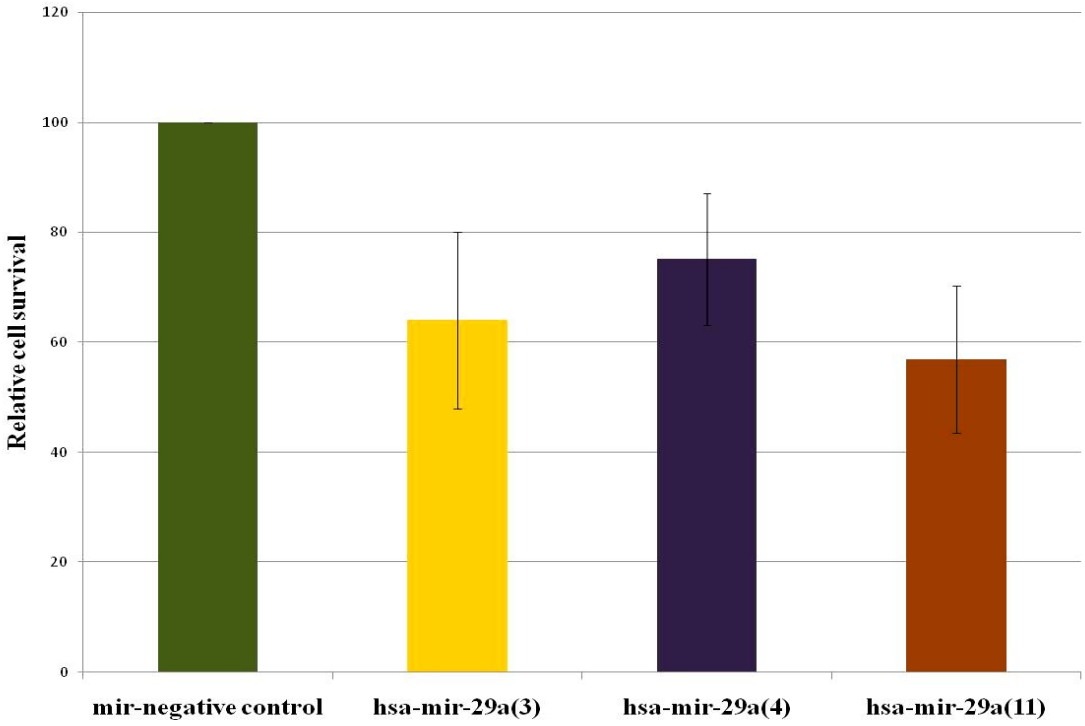

Figure 3.29A Effect of stable mir-29a overexpression on DLKPA proliferation.
Mir-negative control: miRNA sequence as negative control for mature sequence; mir-29a(3); mir-29a(4) and mir-29a(11): stable overexpressing mir-29a DLKPA clone 3,4 and 11, (N=3).

3.30 Investigation of effect of mir-29a stable overexpression on DLKPA invasive phenotype

Transient pre-mir-29a overexpression reduced invasiveness of DLKPA by 40%, suggesting that mir-29a may be actively involved in cancer cell invasion. But was this just due to the transient effect of a synthetic mir-29a sequence? To address this we developed stable overexpressing DLKPA cell lines. This was achieved through transfecting mir-29a plasmid (mir-29a, PCR amplified from endogenous genomic DNA and cloned in pSilencer mammalian expression vector) in DLKPA and applied selection pressure to generate mir-29a stable expression cell lines. Stable overexpression was confirmed through qRT-PCR analysis. These stable clones were used for evaluation of the effect on the invasion phenotype in DLKPA. The cells were seeded on Matrigel^{TM} inserts in 100µl volume at 10^6 cells per ml and incubated at 37^oC for 48 hours after which the underside of the inserts were stained and counted at 20X magnification. At least two inserts were used for the analysis of each condition.

There was a significant reduction in invasion of mir-29a stable overexpressing DLKPA cell lines compared to negative control expressing DLKPA. Three DLKPA cell lines mir-29a (3), 58%, mir-29a (4) 44% and mir-29a (11) 47%. The degree of reduction in invasion correlated closely with the level of overexpression detected by qPCR.

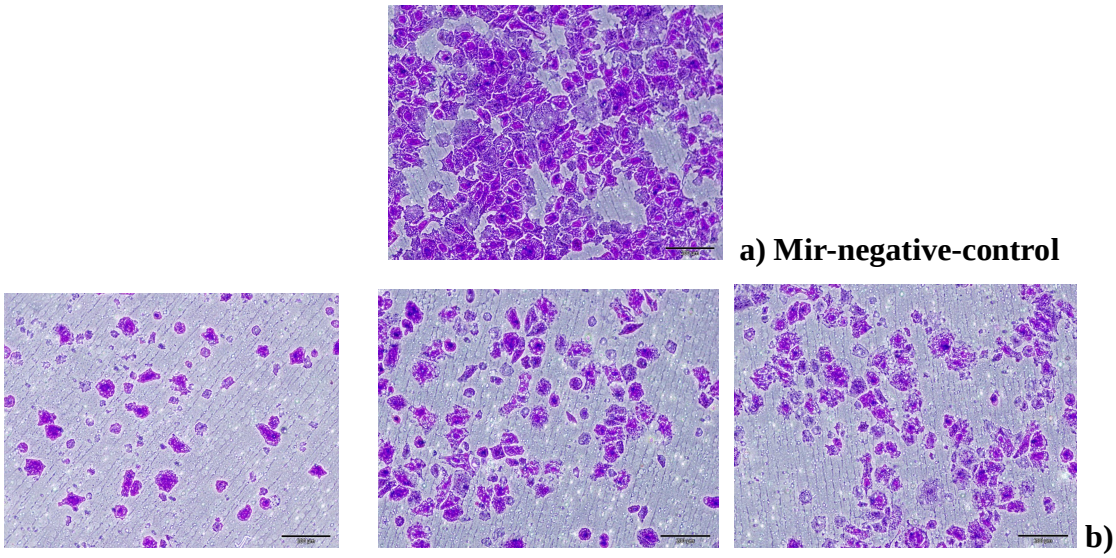

a) Mir-negative-control

b) Mir-29a (3) **c) Mir-29a (4)** **d) Mir-29a (11)**

Figure 3.30A In vitro invasion of stable mir-29a overexpression in DLKPA through matrigel. a) Mir-negative control; negative sequence expressing cells, b) Mir-29a(3); clone (3) expression mir-29a, c) Mir-29a(4); clone(4) expressing mir-29a and d) Mir-29a (11); clone (11) expressing mir-29a. Magnifications at 20X.

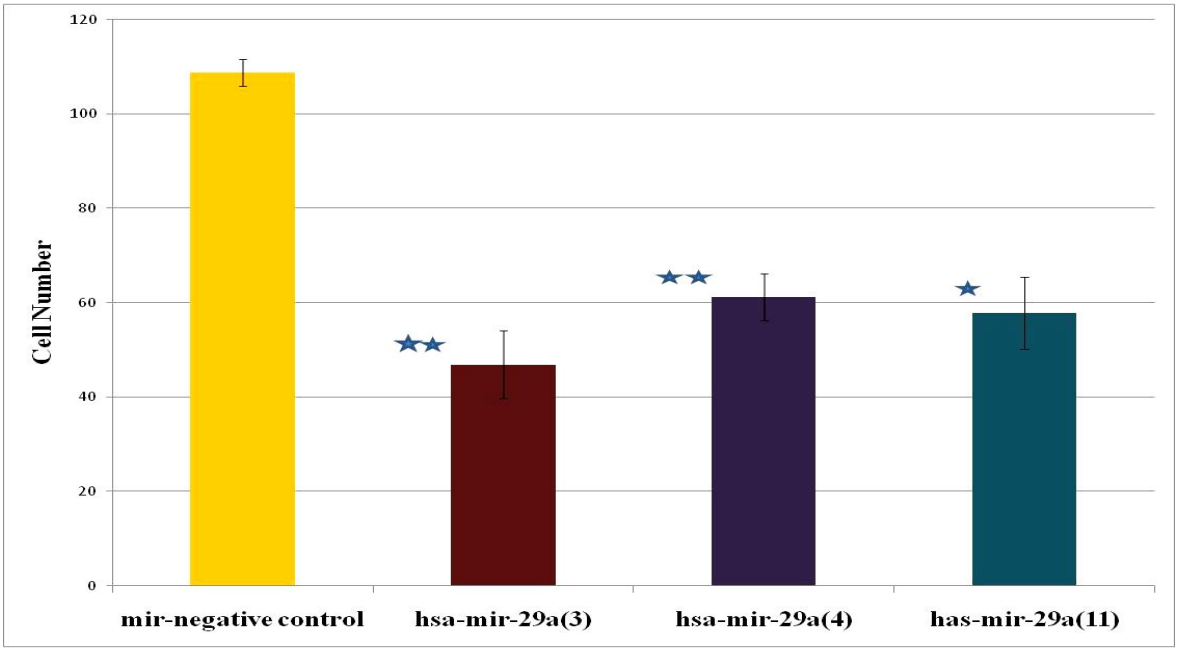

Figure 3.30B Impact of stable mir-29a overexpression.

Mir-negative control; negative sequence expressing cells, Mir-29a (3); clone (3) expression mir-29a, Mir-29a (4); clone (4) expressing mir-29a and Mir-29a (11); clone (11) expressing mir-29a, with ** (≤ 0.005) and * (≤ 0.05) *p*-value where (n=3).

3.31 To evaluate the expression of c-Myc in a panel of cell lines, differing in their invasive phenotype

C-Myc a well studied oncogene has been reported to be involved in regulating the expression of mir-29a. Myc is known to directly upregulate a pro-tumorigenic group of miRNAs known as the miR-17–92 cluster (Tsung-Cheng et.al, 2008). From our qRT-PCR analysis of the relative mir-29a levels in DLKP versus DLKPA, it was evident that mir-29a was downregulated in DLKPA. DLKPA is a highly invasive cell line. We theorised based on previous studies and our functional results that mir-29a expression in our model cell lines might reflect c-Myc expression which is upstream of mir-29a and regulates mir-29a transcription. We decided to evaluate the endogenous c-Myc levels in our panel of cancer lines, DLKP (mildly invasive), DLKPA and PANC-1 (both highly invasive). A c-Myc specific primer pair was designed to analyse endogenous c-Myc transcript levels by qRT PCR. RNA was isolated from cell lines and used to generate cDNA for quantitative PCR.

The qRTPCR data represents (fig.3.31A) technical replicates and relative c-Myc levels. The initial qRT-PCR data suggested there was no significant increase in c-Myc in the more invasive cell lines compared to mildly invasive cell line DLKP, though this was a first observation with technical replicates. Further confirmation would be required to evaluate the impact of c-Myc regulation via mir-29a.

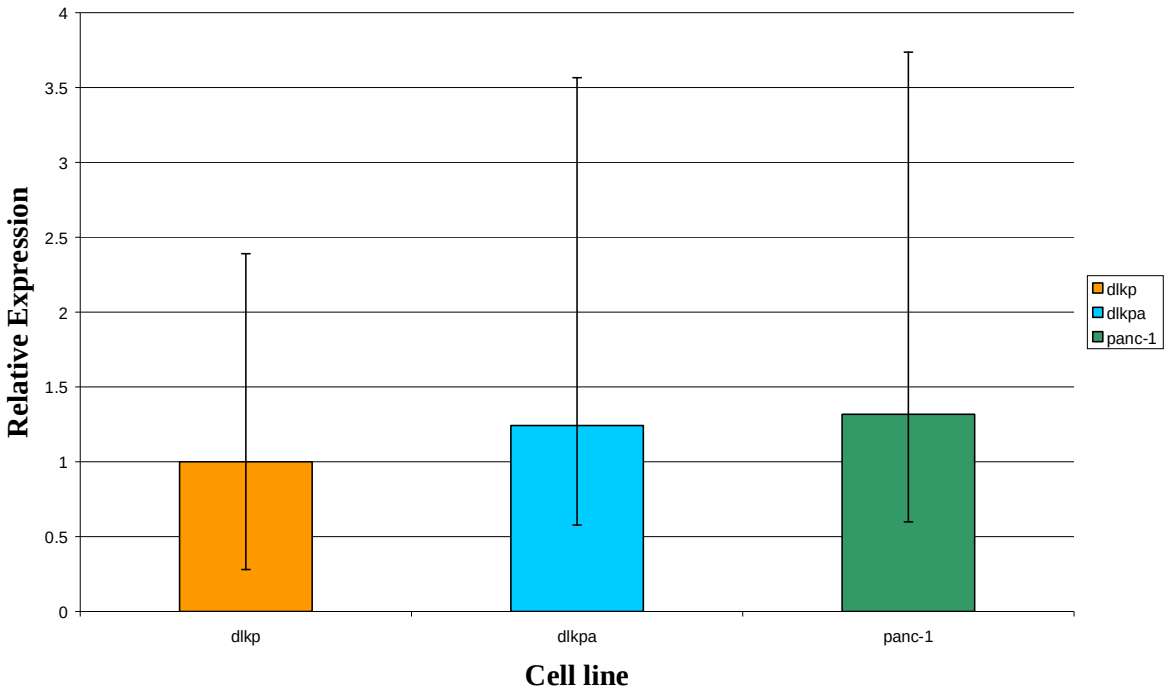

Figure 3.31A Graphical representation of relative endogenous c-Myc levels.

DLKP: mildly invasive lung cancer line; DLKPA: highly invasive drug resistant cell line; PANC-1: highly invasive pancreatic carcinoma cell line. The error bar represents technical replicates (n=4), minimum and maximum values as derived from the software analysis.

3.32 2-Dimensional difference in gel electrophoresis analysis of DLKPA cells transfected with pre-mir-29a

The transient overexpression of pre-mir-29a in DLKP and DLKPA was found to reduce invasion by between 20-30% and conversely anti-mir treatment increased invasion by 36% in DLKP. During the time of this study there were no reports in the literature on mir-29a being anti invasive in cancer cells. We decided to perform proteomic profiling to discover potential targets of mir29a. Pre and anti mir-29a transfection were performed as before. 72hrs later cells were trypsinised (multiple samples for each treatment to ensure enough protein extract for the proteomic study), and protein was extracted. 50μg of protein from each sample was used in this study. 2D-DIGE proteomic analysis was performed as described (sections 2.14.6).

3.32 .1 Experimental outline for 2-D DIGE analysis of the samples

Proteins that were differentially regulated due to pre and anti-mir-29a overexpression in DLKPA were analysed by 2-D DIGE. Triplicate biological repeats with duplicate technical repeats were reverse labelled with Cy3 and Cy5. All samples used in the experiment were pooled and labelled with the internal dye Cy2. Each sample was compared internally to the same standard, to account for any gel-to-gel variation.

3.32.2 DeCyder analysis

Differential protein expression between Pre-mir-29a versus Pre-mir-control and Anti-mir-29a versus anti-mir-control was detected using 2D-DIGE. DeCyder image analysis merged the Cy2, Cy3 and Cy5 images for each gel and detected spot boundaries for the calculation of normalised protein abundance. All paired images were then matched to generate comparative cross-gel statistical analysis. DeCyder^{TM} software revealed confirmed protein spots as represented in the Table 3.32.2i

Table 3.32.2i

Comparisons	Up	Down	Total Spots	Identified Proteins
Pre-mir-29a	11	110	121	60
Anti-mir-29a	21	64	85	29

Spot identification was based on BVA (Biological variation analysis) of the spots showing greater ±1.2 fold change in expression with 1 WAY ANOVA score of ≤ 0.05. A representative 2D-DIGE protein map is shown in Fig. 3.32.2A including the master spot numbers.

A)

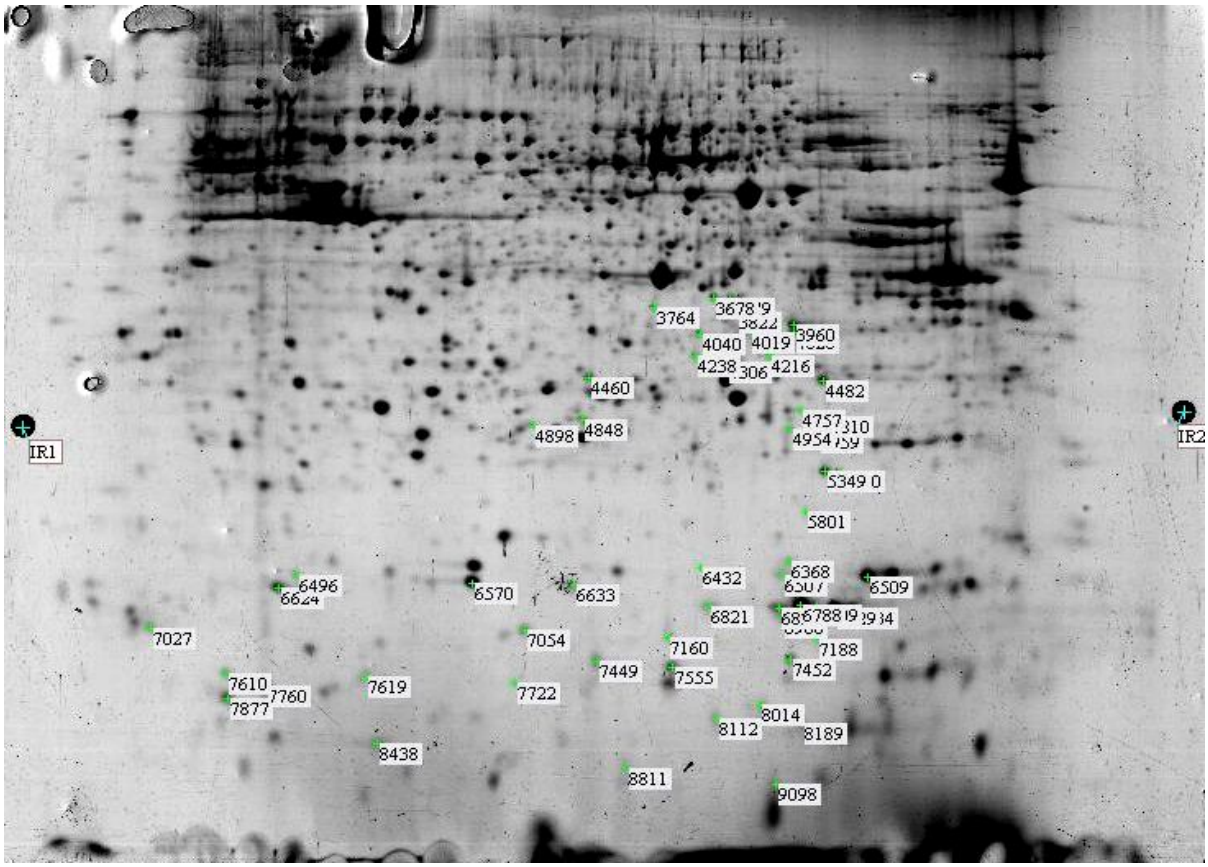

Figure 3.32.2A 2D DIGE scan of protein gel from pre-mir-29a transfected DLKPA. The protein spots (green spots with software generated ID numbers) were picked for identification using MALDI-TOF and LC-MS.

3.32.3 Protein identification and Generation of Differentially regulated protein lists

For protein identification, all proteins were digested and identified at least twice from separate gels with MALDI-TOF MS. An expectation value of <0.02 was used for all reported identifications, which indicates 0.2% of the identifications would occur by chance. It is broadly accepted that miRNAs regulate gene expression at the post transcriptional level, resulting in down regulation of target proteins. Previous studies have shown that miRNAs target at the posttranscriptional level by binding to the 3'UTR region of an mRNA and as a result protein translation is downregulated. In theory if we overexpress a miRNA we would expect genuine target genes to be downregulated at the protein level. Conversely to block a particular miRNA with anti miRNA, then its target proteins should be upregulated. In our experiment we observed proteins upregulated and downregulated in both pre-mir and anti-mir treated DLKPA cells.

Accordingly we generated two lists of proteins as represented in Table 3.32.3i (down regulated proteins due to Pre-mir-29a), and Table 3.32.3ii (up regulated proteins due to Anti-mir-29a). In addition we also observed sets of proteins that were up-regulated due to pre-mir-29a treatment and downregulated due to anti-mir-29a treatment. These probably represent proteins downstream of mir-29a target proteins, i.e. secondary targets of mir-29a action.

The differential expressed protein spots were identified by either MALDI-TOF and/or LC-MS and were analyzed with different bioinformatics software programs including PATHWAY STUDIO, PANTHER, and PUBMATRIX to predict biological functions affected and the importance of the protein targets. RNAhybrid, a widely used programme to identify predicted miRNA gene targets was also employed. This programme applies seed match criteria, i.e. Watson-Crick seed matches that are conserved in the UTR regions of whole-genome alignments to assign target prediction.

Master Spot	Gene symbol	Gene Name	GI Accession	Ref.seq.mRNA Accession	Mass[Da]	Av Ratio	1-ANOVA(p-value)	Matched peptide
1428	ALDOA	ALDOLASE A, FRUCTOSE-BISPHOSPHATE	gi|113606|	NM_184041	39395.3	-1.23	0.061	6
1437	NDUFA10	SUPEROXIDE DISMUTASE 1, SOLUBLE (AMYOTROPHIC LATERAL SCLEROSIS 1 (ADULT))	gi|13097333|	NM_004544	41070	-1.25	0.0013	6
1443	HIBCH	3-HYDROXYISOBUTYRYL-COENZYME A HYDROLASE	gi|146324905|	NM_014362	43454.4	-1.42	0.005	4
1499	GALE	UDP-GALACTOSE-4-EPIMERASE	gi|68056598|	NM_001008216	38257.3	-1.21	0.037	2
1520	ANXA1	ANNEXIN A1	gi|113944|	NM_000700	38690	-1.24	0.006	2
1548	ANXA2	ANNEXIN A2	gi|56967119|	NM_001002858	36640	-1.21	0.0059	17
1691	SFRS1	SPLICING FACTOR, ARGININE/SERINE-RICH 1 (SPLICING FACTOR 2, ALTERNATE SPLICING FACTOR	gi|45708738|	NM_006924	22560	-1.29	0.042	7
1706	ESD	ESTERASE D/FORMYLGLUTATHIONE HYDROLASE	gi|12654663|	NM_001984	32020	-1.25	0.0013	7
1711	GNB2L1	GUANINE NUCLEOTIDE BINDING PROTEIN (G PROTEIN), BETA POLYPEPTIDE 2-LIKE 1	gi|54037164|	NM_006098	35054.6	-1.32	0.048	2
1721	ATP6V1E1	ATPASE, H+ TRANSPORTING, LYSOSOMAL 31KDA, V1 SUBUNIT E1	gi|549207|	NM_001696	26128.8	-1.34	0.013	2
1748	HIBADH	3-HYDROXYISOBUTYRATE DEHYDROGENASE	gi|12643395|	NM_152740	35305.8	-1.2	0.0074	2
1782	CACYBP	CALCYCLIN BINDING PROTEIN	gi|46576651|	NM_014412	26193.7	-1.2	0.036	5
1816	PAFAH1B2	PLATELET-ACTIVATING FACTOR ACETYLHYDROLASE IB SUBUNIT BETA	gi|55977293|	NM_002572	25553.1	-1.21	0.0043	3
1819	PGAM1	PHOSPHOGLYCERATE MUTASE 1 (BRAIN)	gi|67464305|	NM_002629	29970	-1.22	0.0021	8
1827	FKBP3	PEPTIDYL-PROLYL CIS-TRANS ISOMERASE	gi|232096|	NM_002013	25161.3	-1.24	0.03	3
1839	CLPP	ATP DEPENDENT CLP PROTEOLYTIC SUBUNIT	gi|3023512|	NM_006012	30160.6	-1.42	0.03	2
1848	ERP29	ENDOPLASMIC RETICULUM PROTEIN 29	gi|6015110|	NM_006817	28975.2	-1.29	0.0027	3
1872	HSPB1	HEAT SHOCK 27KDA PROTEIN 1	gi|19855073|	NM_001540	22768.5	-1.24	0.03	2
1892	PRDX6	PEROXIREDOXIN 6	gi|1718024|	NM_004905	25019.2	-1.22	0.041	5
1902	Psma6	PROTEASOME (PROSOME, MACROPAIN) SUBUNIT, ALPHA TYPE, 6	gi|46397655|	NM_002791	27381.8	-1.28	0.017	2
1908	HPRT	HYPOXANTHINE PHOSPHORIBOSYLTRANSFERASE 1 (LESCH-NYHAN SYNDROME)	gi|459815|	NM_000194	24730	-1.27	0.0046	7
1922	1RRP	RAN, MEMBER RAS ONCOGENE FAMILY	gi|5107684|	NM_006325	23300	-1.35	0.00024	5
1924	GRB2	GROWTH FACTOR RECEPTOR-BOUND PROTEIN 2	gi|28876|	NM_002086	18620	-1.25	0.0059	8
1925	PSMA2	PROTEASOME (PROSOME, MACROPAIN) SUBUNIT, ALPHA TYPE, 2	gi|39644890|	NM_002787	24970	-1.23	0.0096	5
1935	SLMO2	CHROMOSOME 20 OPEN READING FRAME 45	gi|26392626|	NM_016045	21481	-1.28	0.019	7
1936	LYPLA2	LYSOPHOSPHOLIPASE II	gi|41017276|	NM_007260	24720.7	-1.25	0.0003	2
1938	GSTK1	GLUTATHIONE S-TRANSFERASE SUBUNIT 13 HOMOLOG	gi|12643338|	NM_015917	25480.3	-1.39	0.0015	1
1959	VBP1	VON HIPPEL-LINDAU BINDING PROTEIN 1	gi|1465751|	NM_003372	19520	-1.27	0.015	5

(Cont'd)

Master Spot	Gene symbol	Gene Name	GI Accession	Ref.seq.mRNA	Mass[Da]	Av Ratio	1-ANOVA(p-value)	Matched Peptides
1961	PRDX3	PEROXIREDOXIN 3	gi|32483377|	NM_006793	26110	-1.32	0.0031	1
1966	PRDX1*	PEROXIREDOXIN 1	gi|55959887|	NM_002574	19130	-1.304	0.0249	6
1976	PSMB4	PROTEASOME (PROSOME, MACROPAIN) SUBUNIT, BETA TYPE, 4	gi|116242733|	NM_002796	29185.5	-1.41	0.0024	3
1998	PSMB2	PROTEASOME (PROSOME, MACROPAIN) SUBUNIT, BETA TYPE, 2	gi|1709762|	NM_002794	22821.7	-1.21	0.029	1
2004	PARK7	PARKINSON DISEASE (AUTOSOMAL RECESSIVE, EARLY ONSET) 7	gi|42543006|	NM_007262	20060	-1.26	0.00072	10
2006	Sfrs3	SPLICING FACTOR, ARGININE/SERINE-RICH 3	gi|51338673|	NM_003017	19317.9	-1.26	0.011	3
2008	CMPK1	CYTIDYLATE KINASE	gi|12644008|	NM_016308	22208.3	-1.29	0.00039	15
2018	TPx-B	PEROXIREDOXIN 2	gi|9955016|	NM_005809	21680	-1.36	0.0011	9
2029	ARL3	ADP-RIBOSYLATION FACTOR-LIKE PROTEIN 3	gi|543851	NM_004311	20442.8	-1.31	0.046	1
2031	APRT	ADENINE PHOSPHORIBOSYLTRANSFERASE	gi|114074|	NM_000485	19595.4	-1.35	0.015	2
2047	PEBP1	PHOSPHATIDYLETHANOLAMINE BINDING PROTEIN 1	gi|1352726|	NM_002567	21043.7	-1.53	0.0004	13
2075	PPIB	PEPTIDYLPROLYL ISOMERASE B (CYCLOPHILIN B)	gi|1310882|	NM_000942	19700	-1.41	0.027	8
2083	NME1	NON-METASTATIC CELLS 1, PROTEIN (NM23A) EXPRESSED IN	gi|127981|	NM_198175	17137.7	-1.28	8.40E-05	16
2085	RPL11	RIBOSOMAL PROTEIN L11	gi|51701767|	NM_000975	20239.7	-1.45	0.0005	3
2103	CFL1*	COFILIN 1 (NON-MUSCLE)	gi|116848|	NM_005507	18490.7	-1.53	0.0019	6
2104	BTF3L4	BASIC TRANSCRIPTION FACTOR 3-LIKE 4	gi|75042131|	NM_152265	17260	-1.43	0.0019	2
2136	SOD1	SUPEROXIDE DISMUTASE 1, SOLUBLE (AMYOTROPHIC LATERAL SCLEROSIS 1 (ADULT))	gi|134611|	NM_000454	15925.9	-1.39	0.043	3
2149	PPIA*	PEPTIDYLPROLYL ISOMERASE A (CYCLOPHILIN A)	gi|75766275|	NM_021130	180300	-1.355	0.010125	9
2169	IGH2bM35a	IMMUNOGLOBIN HEAVY CHAIN	gi|7161037|	AJ253041	10600	-1.35	0.004	4
2182	ISG15	INTERFERON, ALPHA-INDUCIBLE PROTEIN (CLONE IFI-15K)	gi|386837|	NM_005101	17910	-1.63	0.0026	4
2186	FABP5	FATTY ACID BINDING PROTEIN 5 (PSORIASIS-ASSOCIATED)	gi|232081|	NM_001444	15154.6	-1.42	0.005	8
2188	GMFB	GLIA MATURATION FACTOR, BETA	gi|46577593|	NM_004124	16702.5	-1.43	0.0021	3
2199	RPS12	RIBOSOMAL PROTEIN S12	gi|133742|	NM_001016	14516.5	-1.43	0.012	2
2205	SH3BGRL	SH3 DOMAIN BINDING GLUTAMIC ACID-RICH PROTEIN LIKE	gi|75042673|	NM_003022	12766.4	-1.22	0.012	4
2207	HIST4H4*	Histone H4	gi|75061938|	NM_175054	11360.4	-1.55	0.0011	2
2210	HINT1	HISTIDINE TRIAD NUCLEOTIDE-BINDING PROTEIN 1	gi|1708543|	NM_005340	13793.1	-1.33	0.0048	4
2213	LGALS1	GALECTIN-1	gi|42542978|	NM_002305	14910	-1.45	0.0005	6
2232	MIF	MACROPHAGE MIGRATION INHIBITORY FACTOR (GLYCOSYLATION-INHIBITING FACTOR)	gi|1170955|	NM_002415	12468.2	-1.63	0.035	3

Table 3.32.3i List of differentially downregulated proteins due to pre-mir29a treatment compared to negative control. Cut off value of ≤ -1.2 fold and 95% confidence in 1 way ANOVA was applied for screening differentially regulated proteins, the list bears mRNA reference sequence and gi sequence recognition IDs for each identified protein spot. * represents proteins identified more than once i.e. in more than one spot position.

Gene symbol	Gene Name	Protein ID	Ref.Seq.ID	Mass [Da]	Av Ratio	1-ANOVA (p-value)	Matched peptide
DDT	D-dopachrome decarboxylase	gi|2828192|	NM_001355	12703.7	1.35	0.039	1
ACTC1	Alpha-actin-1	gi|55976646|	NM_005159	42023.9	1.22	0.036	3
SHOT1	Shootin-1	gi|156637366|	NM_018330	71595.7	1.21	0.034	3
ALDH1A1	Aldehyde dehydrogenase 1	gi|2183299|	NM_000689	55.44	1.28	0.047	8
CCT3	T-complex protein 1 subunit gamma	gi|66774185|	NM_005998	60495.4	1.24	0.024	4
LOC652797	Pyruvate kinase isozymes M1/M2	gi|20178296|	XM_001719890	57900.2	1.27	0.024	8
ATP5A1	ATP synthase subunit alpha, mitochondrial precursor	gi|158514235|	NM_001001937	59713.7	1.22	0.013	6
SERBP1	Plasminogen activator inhibitor 1 RNA-binding protein	gi|52783206|	NM_001018067	44938.5	1.24	0.0036	3
TRXR1	Thioredoxin reductase 1	gi|50403780|	NM_003330	55.49	1.25	0.02	5
EEF1A1	Eukaryotic translation elongation factor 1 alpha 1	gi|31092|	NM_001402	50.45	1.23	0.022	7
PTBP1	Polypyrimidine tract-binding protein 1	gi|131528|	NM_002819	57185.8	1.29	0.0074	3
ENO1	Alpha-enolase	gi|31873302|	NM_001428	47.42	1.24	0.055	12
PGK1*	Phosphoglycerate kinase 1	gi|48145549|	NM_000291	44.98	1.24	0.034	5
RuvB-like 2	48 kDa TATA box-binding protein-interacting protein	gi|28201890|	NM_006666	51124.6	1.22	0.049	1

Table 3.32.3ii List of differentially upregulated proteins in DLKPA due to anti-mir29a expression compared to negative control. Cut off value of $\geq +1.2$ fold and 95% confidence in 1 way ANOVA was applied for identification. The list bears mRNA reference sequence and gi sequence recognition IDs for each identified protein spots. * represents proteins being identified more than once i.e. in more than one spot position.

3.33 Bioinformatics analysis of differentially regulated protein ID's

3.33.1 *PANTHER* (Protein Analysis through Evolutionary Relationships)

In the genomic era, one of the fundamental goals is to characterize the function of proteins on a large scale. Computational algorithms and databases for comparing protein sequences have reached a relatively mature stage of development. PANTHER is a freely available, comprehensive software system for relating protein sequence evolution to the evolution of specific protein functions and biological roles. The PANTHER classification system is a unique resource that classifies genes by their function (Thomas et al., 2003) using published scientific experimental evidence and evolutionary relationships to predict function even in the absence of direct experimental evidence (http://www.pantherdb.org/) . PANTHER is designed to be structured such that absolute depths in different parts of the ontology correspond to roughly equivalent levels of functional specificity. Protein family trees are constructed computationally from sequence data and roles in biological processes and pathways, based on experiments performed. The proteomic profiling of mir-29a treated DLKPA cell line identified several possible gene targets. To identify the global distribution of these genes in terms of their biological process, molecular function and biological pathways, we used the PANTHER programme. The genes were found to be involved in a wide range of molecular functions (fig. 3.33.1A), biological process (fig. 3.33.1B) and biological pathways (fig. 3.33.1C). Briefly, under molecular functions, categories such as nucleic acid binding (14%) and oxidoreductase (11%) were observed to have relatively significant representation of target proteins. Similarly, in biological process, two main categories were found to have relatively large numbers of protein targets represented i.e. Protein Metabolism and Modification (18%) and Immunity and Defence (16%). Conversely under biological pathways (fig. 3.33.1C) a wide spread among the pathways was observed with no particular pathway overly represented possibly due to the limited size of the dataset.

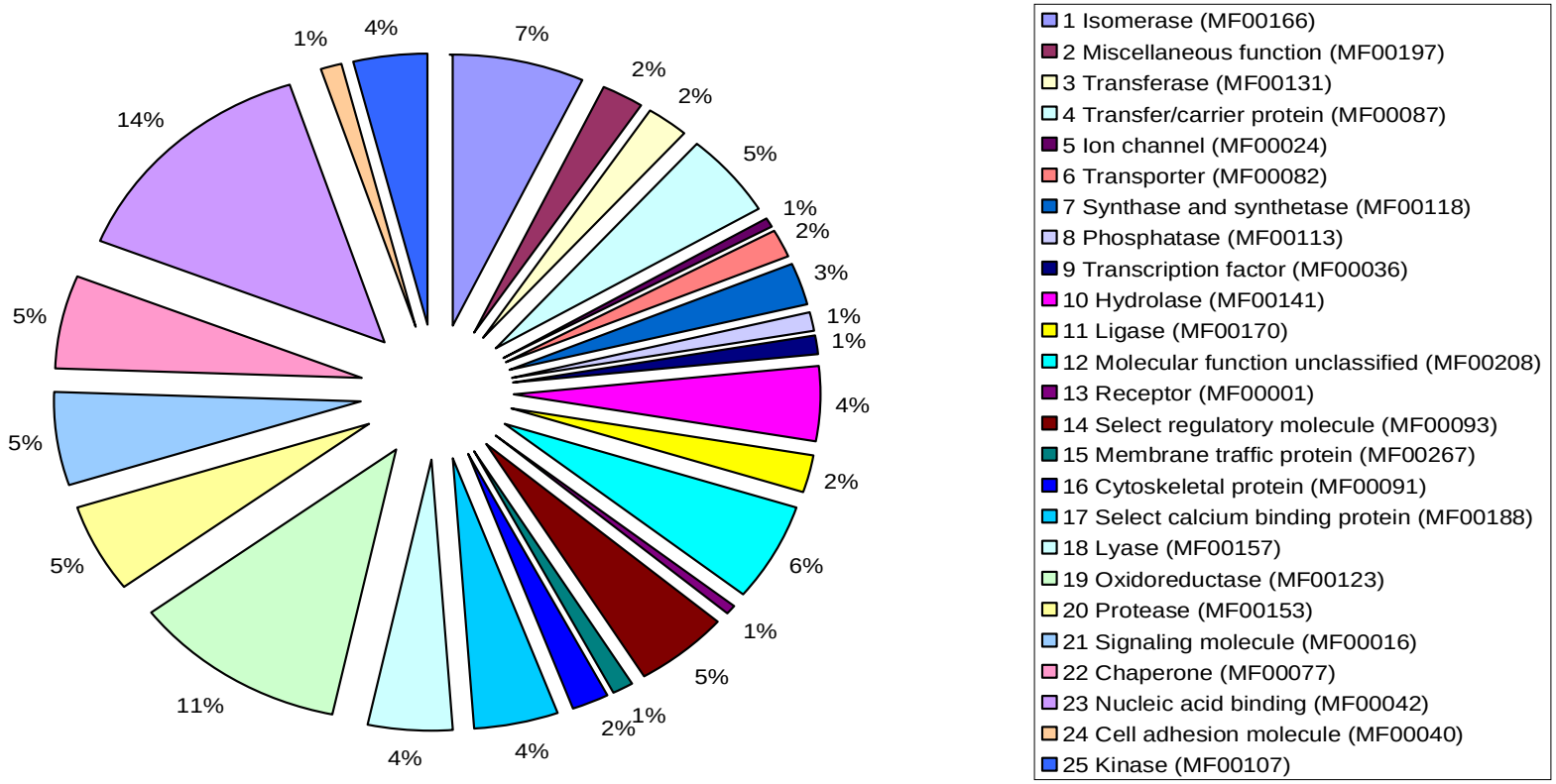

Figure 3.33.1A PANTHER based classification of all identified protein targets based on Molecular function.

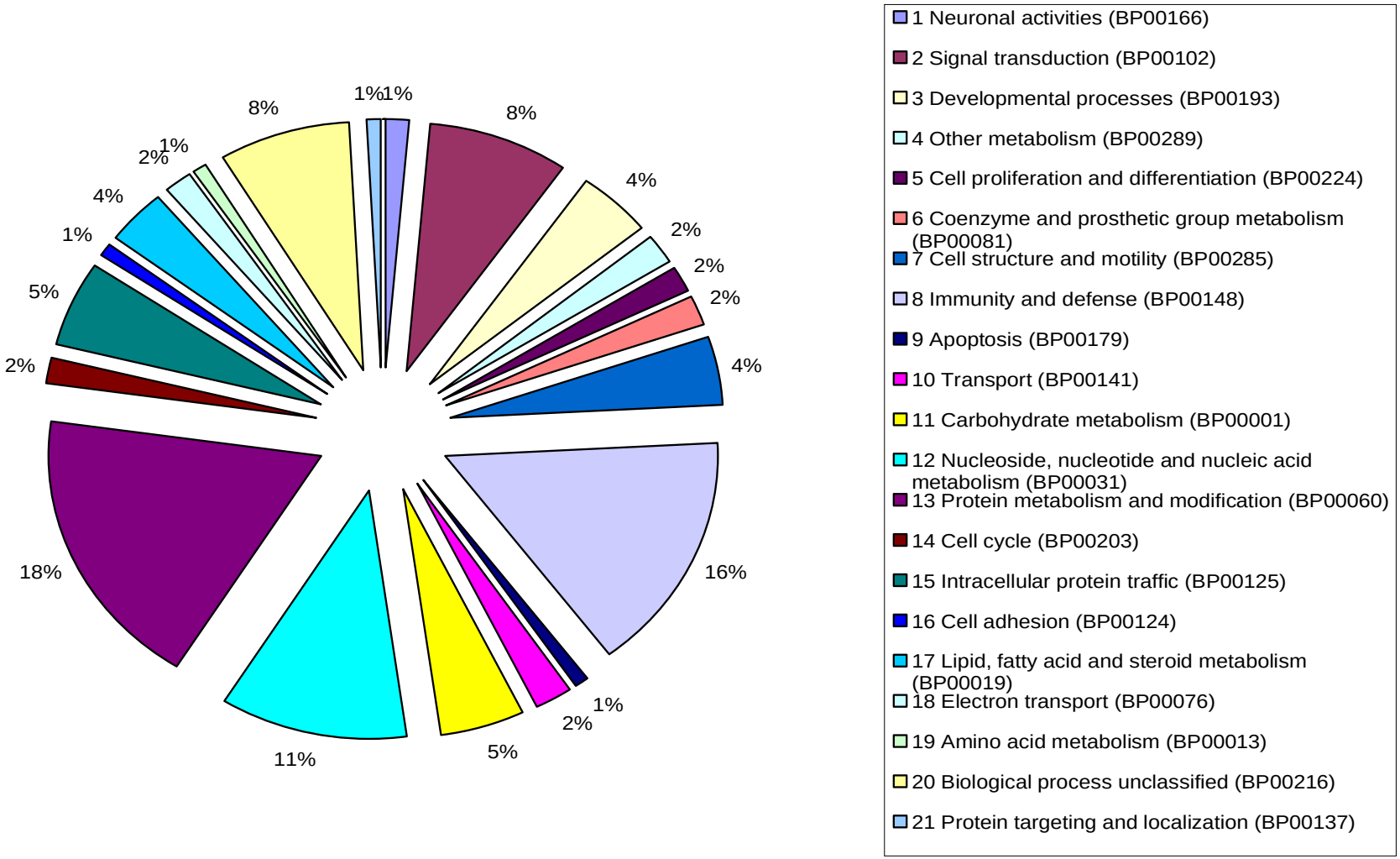

Figure 3.33.1B PANTHER classification based on Biological Process.

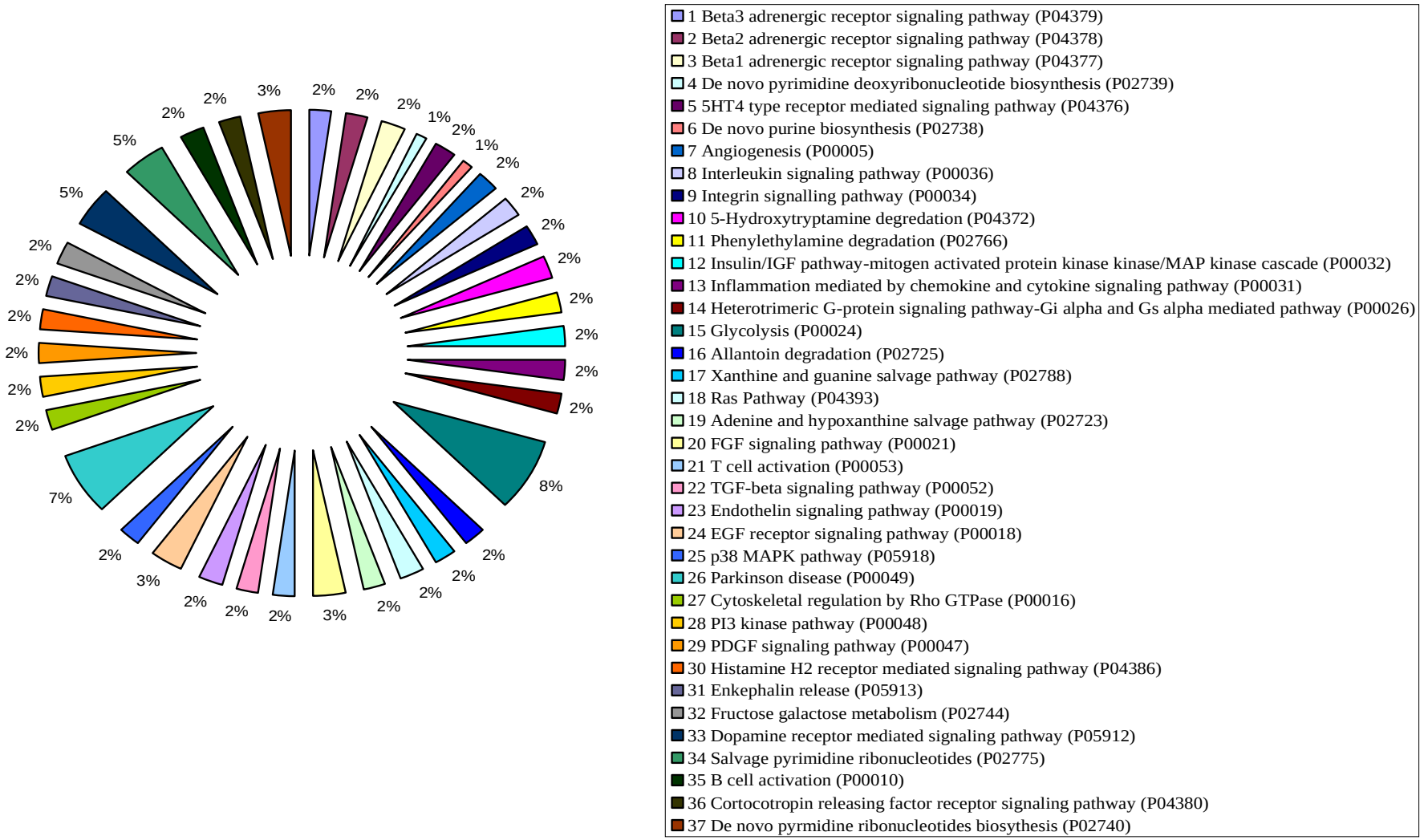

Figure 3.33.1C PANTHER classification based on Biological Pathway.

3.33.2 Pathway Studio Analysis of identified proteins

Pathway Studio permits the identification of biological interactions among genes and proteins of interest from the published literature, and provides links to the supporting sentences in the matching journal article citations (for articles available online in Pub Med). The software can also connect two genes/proteins with the shortest possible path; import a list of genes/proteins, which can then be arranged into a pathway. We used the programme to interrogate the list of proteins identified in our study. Apoptosis, motility, proliferation, differentiation and mutagenesis, were the most frequent cellular processes impacted by the proteins on our list.

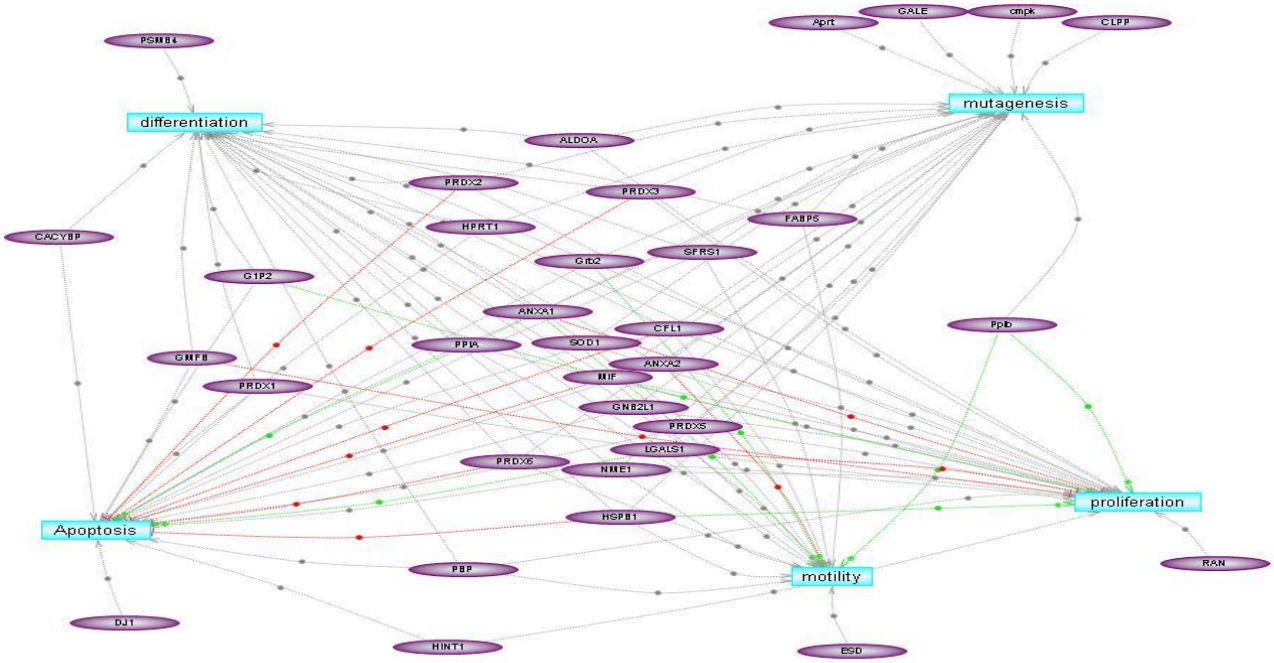

Figure 3.33.2A Pathway Studio analysis of protein targets. The rectangular boxes represent key biological process and ovals represent genes. The red lines connected between and among the genes and processes are known to have negative impact and similarly green lines depict known positive regulation. The grey lines denote unknown impact.

3.33.3 Insilco based 3'UTR seed match of mir-29a and its targets

Vertebrate mRNAs are targeted for post-transcriptional repression by miRNAs through mechanisms involving pairing of 3′ UTR seed matches to bases at the 5′ end of miRNAs (Nielsen, 2007). Potential miRNA targets may be predicted by finding perfect Watson-Crick seed matches (fig. 3.33.3A) that are conserved in the UTR regions of whole-genome alignments. Moreover, the requirement of a 7-nt match to the seed region of the miRNA (nucleotides 2–8) could be relaxed to require a 6-nt match to a reduced seed comprising nucleotides 2–7 of the miRNA while still retaining specificity (Lewis et al., 2005). To elucidate the microRNA regulatory network, it is important to have prior knowledge of potential targets. Among existing target prediction methods RNA-hybrid predicts multiple potential binding sites of miRNAs in large target RNAs (Rehmsmeier et al., 2004). The analysis of seed match regions between mir-29a and 3'UTR sequences of the gene targets was done with RNAhybrid. We uploaded our target sequences and mir-29a reference sequence and ran the programme.

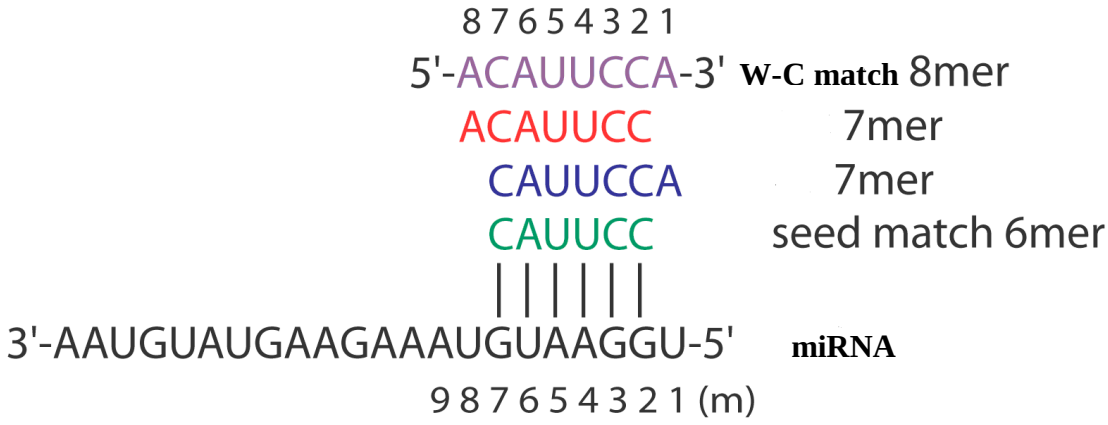

Adopted from http://hollywood.mit.edu/targetrank/seedMatchTypes.html

---

Figure 3.33.3A Seed match criteria. Segments have Watson-Crick (WC) complementarity ("matching") to positions 2-7 ("seed") of a miRNA.

From the target prediction programme we were able to identify 14 protein targets from both down regulated as well up regulated list of identified proteins, which had satisfactory W-C match and/or 2-7 mer match between 3'UTR mRNA and 5'seed region of mir-29a sequence.

TARGET : PRDX6
length: 989
MIRNA : hsa-miR-29a
length: 22

mfe: -20.2 kcal/mol

position 6
```
target 5'   U G  GA    C        U 3'
             U GA    AG UGGUGCUG
             G CU    UC ACCACGAU
miRNA  3' AUU G  AAAG  U          5'
```

TARGET : CMPK1
length: 2119
MIRNA : hsa-miR-29a
length: 22

mfe: -23.8 kcal/mol

position 1738
```
target 5' A       G     CUA      U 3'
           GACUGAU   AGA   GGUGCU
           UUGGCUA   UCU   CCACGA
miRNA  3' A       AAG   A        U 5'
```

TARGET : PEBP1
length: 2119
MIRNA : hsa-miR-29a
length: 22

mfe: -23.8 kcal/mol

position 1738
```
target 5' A       G     CUA      U 3'
           GACUGAU   AGA   GGUGCU
           UUGGCUA   UCU   CCACGA
```

```
miRNA  3' A       AAG   A        U 5'
```

TARGET : ANX2
length: 488
MIRNA : hsa-miR-29a
length: 22

mfe: -25.1 kcal/mol

position 10
```
target 5' C    U  GCGUC    AA       C 3'
           GGCC GA     CAGA  UGGUGCU
           UUGG CU     GUCU  ACCACGA
miRNA  3' A       AAA              U 5'
```

TARGET : CNN2
length: 1185
MIRNA : hsa-miR-29a
length: 22

mfe: -18.1 kcal/mol

position 796
```
target 5'   C    GUAGCUA   CUGCA      C 3'
             CUGA       GGA     GGUGCU
             GGCU       UCU     CCACGA
miRNA  3' AUU    AAAG       A          U 5'
```

TARGET : SFRS1
length: 4512
MIRNA : hsa-miR-29a
length: 22

mfe: -20.9 kcal/mol

position 2948
```
target 5' A    UUAAC     CCUUG       A 3'
           GACU     AUUUC     GGUGCUA
           UUGG     UAAAG     CCACGAU
miRNA  3' A    C         UCUA          5'
```

TARGET : PSMA2
length: 713
MIRNA : hsa-miR-29a
length: 22

mfe: -19.5 kcal/mol

position 463
```
target 5'  U           UGAAAUCCUAG      C 3'
            AUUGA  UCAG           GGUGCU
            UGGCU  AGUC           CCACGA
miRNA  3' AU     AA    UA               U 5'
```

TARGET : ARL3
length: 3184
MIRNA : hsa-miR-29a
length: 22

mfe: -22.13 kcal/mol

position 2402
```
target 5' G      AGGG    CAAGGCCUGGGG      C 3'
           GGCCGG    CAGG            GGUGCU
           UUGGCU    GUCU            CCACGA
miRNA  3' A      AAA     A                U 5'
```

TARGET : PPIB
length: 225
MIRNA : hsa-miR-29a
length: 22

mfe: -19.1 kcal/mol

position 65
```
target 5' G     CACUGGCCCC       G 3'
           AGCUG          GGUGCUG
           UUGGC          CCACGAU
miRNA  3' A     UAAAGUCUA          5'
```

TARGET : PPIA
length: 1695
MIRNA : hsa-miR-29a
length: 22

mfe: -21.9 kcal/mol

position 1152
```
target 5' A    A   ACU           C 3'
           AGCC GGU      UGGUGCUA
           UUGG CUA      ACCACGAU
miRNA  3' A        AAGUCU          5'
```

TARGET : GMFB
length: 3597
MIRNA : hsa-miR-29a
length: 22

mfe: -19.3 kcal/mol

position 3542
```
target 5' G   AGUC    GUUA  C        U 3'
           GAC    UUUU    AG AUGGUGCU
           UUG    AAAG    UC UACCACGA
miRNA  3' A   GCU                    U 5'
```

TARGET : ACTC1
length: 1956
MIRNA : hsa-miR-29a
length: 22

mfe: -21.3 kcal/mol

position 760
```
target 5' A   A   GG     CUGGUA       A 3'
           GAC UGG   CAGG      GGUGCUG
           UUG GCU   GUCU      CCACGAU
miRNA  3' A       AAA    A             5'
```

TARGET : KIAA1598
length: 1767
MIRNA : hsa-miR-29a
length: 22

mfe: -20.6 kcal/mol

position 547
```
target 5'  U     AAG  U         U 3'
            GCUGA   UU GA GGUGCU
            UGGCU   AG CU CCACGA
miRNA  3' AU     AA   U  A      U 5'
```

TARGET : SERBP1
length: 5397
MIRNA : hsa-miR-29a
length: 22

mfe: -24.2 kcal/mol

position 1679
```
target 5'  U     GCAUG   U CAC        A 3'
            GCUGA     UUC G   UGGUGCUA
            UGGCU     AAG C   ACCACGAU
miRNA  3' AU     A       U U            5'
```

SECTION: E

3.34 Functional validation of selected gene targets from proteomics study using siRNA

From the proteomic profiling of possible mir-29a targets we generated two lists of differentially regulated proteins. These were further put through bioinformatic analysis to delineate their relevance in biological pathways. Pubmatrix based literature mining with relevance to cancer cell invasion, proliferation, metastasis and drug resistance was performed. From these studies we selected four gene targets with established roles in cancer cell invasion/metastasis for functional validation. The targets chosen were all downregulated due to pre-mir-29a overexpression. Having identified that mir-29a had an anti-invasive effect and having identified several differentially regulated genes upon mir-29a overexpression we wanted to establish whether modifying some of these proteins individually would mediate the same effect on phenotype. Therefore, specific gene targets were knocked down to investigate the effect on cancer cell invasion and/or proliferation. The target genes RAN, GRB2, MIF and ANX2 were chosen from literature searches due to an established role in cancer invasion/metastasis. Two separate siRNA sequences for each target were used in our experiments.

To summarize this section, knockdown of these targets was confirmed by qRT-PCR analysis (fig. 3.34.1A, 3.35A, 3.36A, 3.37A). 72hrs post siRNA treatment; cells were subjected to invasion assay. Of the 4 genes chosen, only RAN had any significant impact on the invasion phenotype of DLKPA. RAN knockdown was observed to reduce invasion significantly in DLKPA (Section 3.37). 72hrs post siRNA treatment; a proliferation assay confirmed that RAN knockdown significantly reduced cellular proliferation as well. Knockdown of the other three targets did not show any significant impact on either phenotype in DLKPA (Section 3.34, 3.35, 3.36).

3.34.1 MIF Specific siRNA knockdown at mRNA levels in DLKPA cell line

Proteomics study indicated that MIF expression was downregulated due to pre-mir-29a transient overexpression in DLKPA, which also reduced the DLKPA invasive phenotype. Thus it was decided to specifically knockdown MIF expression using two independent siRNA sequences in the invasive DLKPA cell lines to determine any functional effect on invasion or proliferation. 2µl of NeoFX transfection reagent per well of a 24-well plate was used to transfect 50nM of target siRNA into the cells. MIF-specific knockdown was confirmed by qRT-PCR and the effect of MIF knockdown on proliferation and invasion investigated.

MIF knockdown was examined using RT-PCR (Figures 3.34.1A). The RT negative control consisted of PCR master mix with RNA that was not reverse transcribed. A no template control (NTC), and no primer control was also used. The control was observed to have no amplification. MIF specific PCR primers were used to accurately measure relative MIF mRNA expression. The data was normalised using β-actin as an endogenous control. The results confirmed that MIF knockdown was achieved at the mRNA level.

As shown in figure 3.34.1A qRT PCR analysis demonstrate MIF specific knockdown at mRNA level. The graph is a composite of three biological repeats and relative to scrambled siRNA treated sample. The siRNA-MIF 2 was observed to have higher knockdown efficiency (60%) than siRNA-MIF 1 (40%) compared to the scramble control.

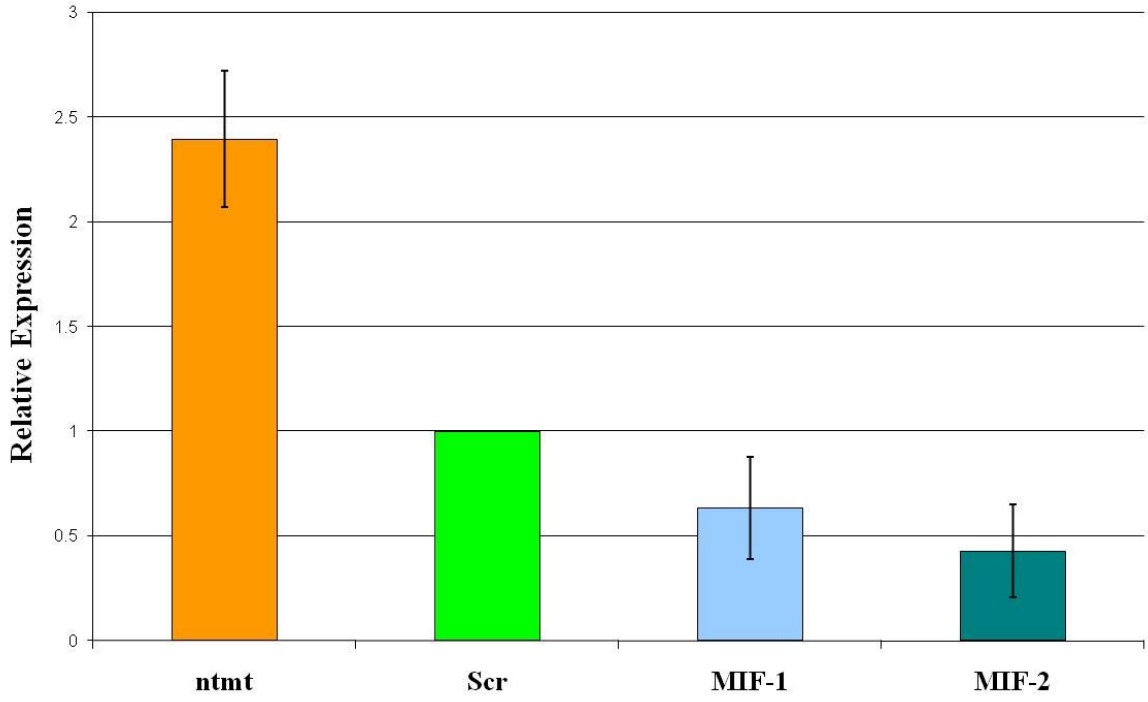

Figure 3.34.1A Relative qRT-PCR analysis of MIF siRNA knockdown.

Ntmt: No treatment; Scr: Scramble sequence negative control; MIF-1: MIF specific siRNA 1; MIF-2: MIF specific siRNA2 , compared to scramble control and n=3.

3.34.2 Evaluation of MIF knockdown on DLKPA proliferation

The effect of transfecting MIF siRNA on proliferation of DLKPA was investigated. Cells were seeded at 2 x 10^3 cells/well of a 96-well plate (Figure 3.34.2A), which was the same density used to seed all the siRNA transfections in six-well plates. Relative cell number was determined using the acid phosphatase assay at 72hrs post transfection. Transfection with any of the siRNA sequences did not have a significant affect on proliferation compared to non-treated and scrambled siRNA transfected cells. Kinesin was used as transfection positive control and a significant decrease (62%) in cellular proliferation was observed (Fig. 3.34.2A).

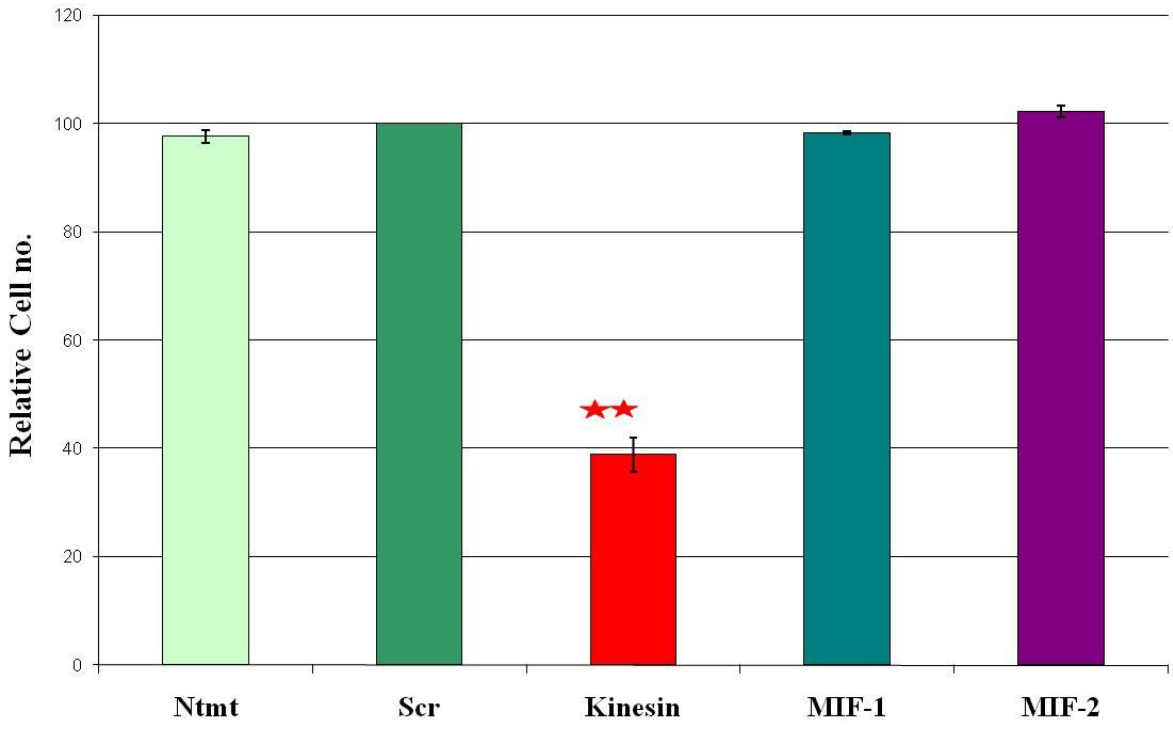

Figure 3.34.2A Effect on proliferation of DLKPA cells transfected with MIF specific siRNAs. Ntmt: No treatment; Scr: Scramble sequence negative control; Kinesin: kinesin specific siRNA used as positive control; MIF-1: MIF specific siRNA 1; MIF-2: MIF specific siRNA2. Kinesin observed to have significant impact, and ** p-value (<0.01) and n=3.

3.34.3 Evaluation of MIF siRNA effect on DLKPA invasion

The effect of decreasing MIF expression on DLKPA invasion was investigated. Invasion assay analysis was performed 72 hours after transfection, to allow the cells to recover from the transfection procedure. At least two inserts were used for the analysis of each condition. The counts per number of inserts used were then also averaged and this figure was used to generate graphs of relative invasive capacity.

From the figure 3.34.3A&B it's evident that MIF knockdown had no impact on invasion phenotype of the DLKPA cell line.

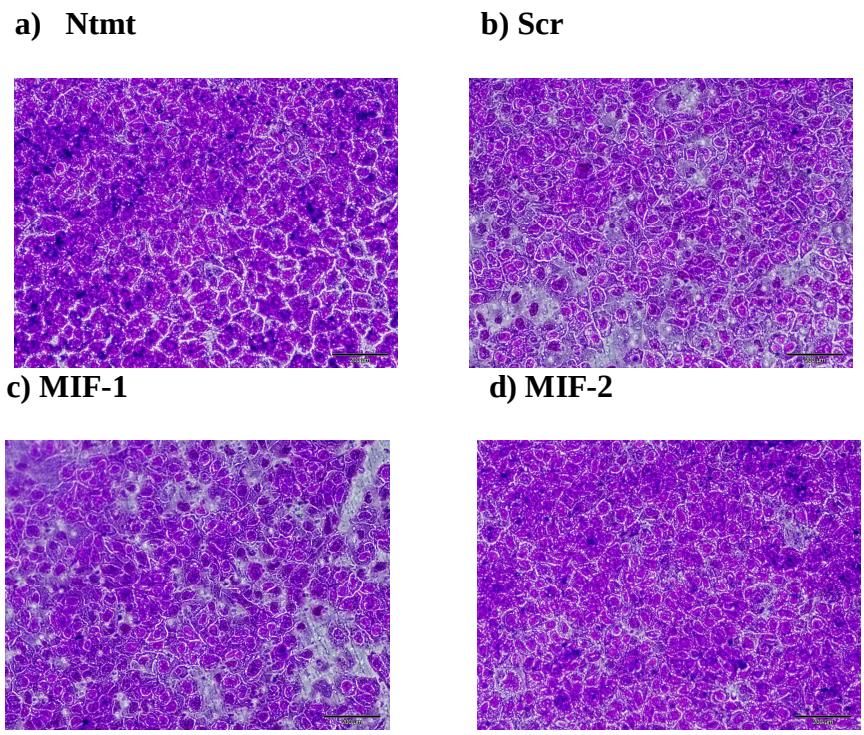

Figure 3.34.3A Crystal violet staining representation of in vitro invasion assay of MIF siRNA treated DLKPA cell line. Ntmt: No treatment; Scr: Scramble sequence negative control; Kinesin: kinesin specific siRNA used as positive control; MIF-1: MIF specific siRNA 1; MIF-2: MIF specific siRNA2; Magnification 20X.

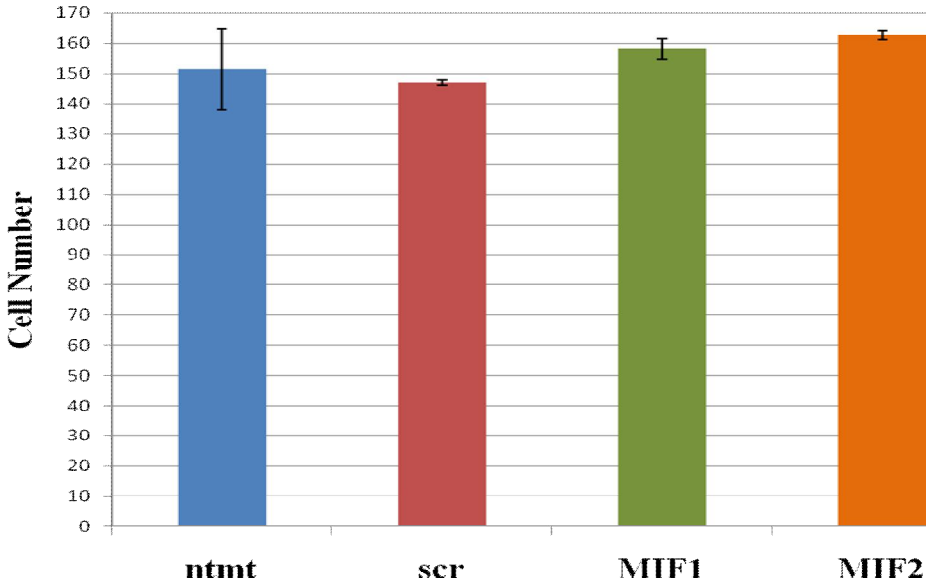

Figure 3.34.3B Graphical representation of in vitro invasion assay counts, post 72 hrs MIF siRNA treatments in DLKPA cell line. Ntmt: No treatment; Scr: Scramble sequence negative control; Kinesin: kinesin specific siRNA used as positive control; MIF-1: MIF specific siRNA 1; MIF-2: MIF specific siRNA2.

3.35 ANX2 specific siRNA knockdown at mRNA levels in DLKPA cell line

Annexin A2 (ANX2) is a $Ca2^{+}$ dependent phospholipid-binding protein. Proteomics study indicated that ANX2 expression was downregulated due to pre-mir-29a transient overexpression in DLKPA, which could account for the reduced DLKPA invasion phenotype. Hence, it was decided to knockdown ANX2 expression using two independent siRNA sequences in the invasive DLKPA cell lines to determine any functional effect on invasion or proliferation. 2µl of NeoFX transfection reagent per well of a 24-well plate was used to transfect 50nM of target siRNA into the cells. ANX2-specific knockdown was confirmed by qRT-PCR.

ANX2 knockdown was examined using RT-PCR (Figures 3.35A). The RT negative control consisted of PCR master mix with RNA that was not reverse transcribed. A no template control (NTC), and no primer control was also used. The control was observed to have no amplification. ANX2 specific PCR primers were used to accurately measure relative MIF mRNA expression. The data was normalised using

β-actin as an endogenous control. The results confirmed that ANX2 knockdown was achieved at the mRNA level. The graph is a composite of three biological repeats and relative to scrambled siRNA treated sample. The siRNA-ANX2-2 observed to have higher knockdown efficiency of 83% fold, SE ± 0.02) than siRNA-ANX2-1 which also was observed to have 70% knockdown SE ± 0.13) compared to scramble control.

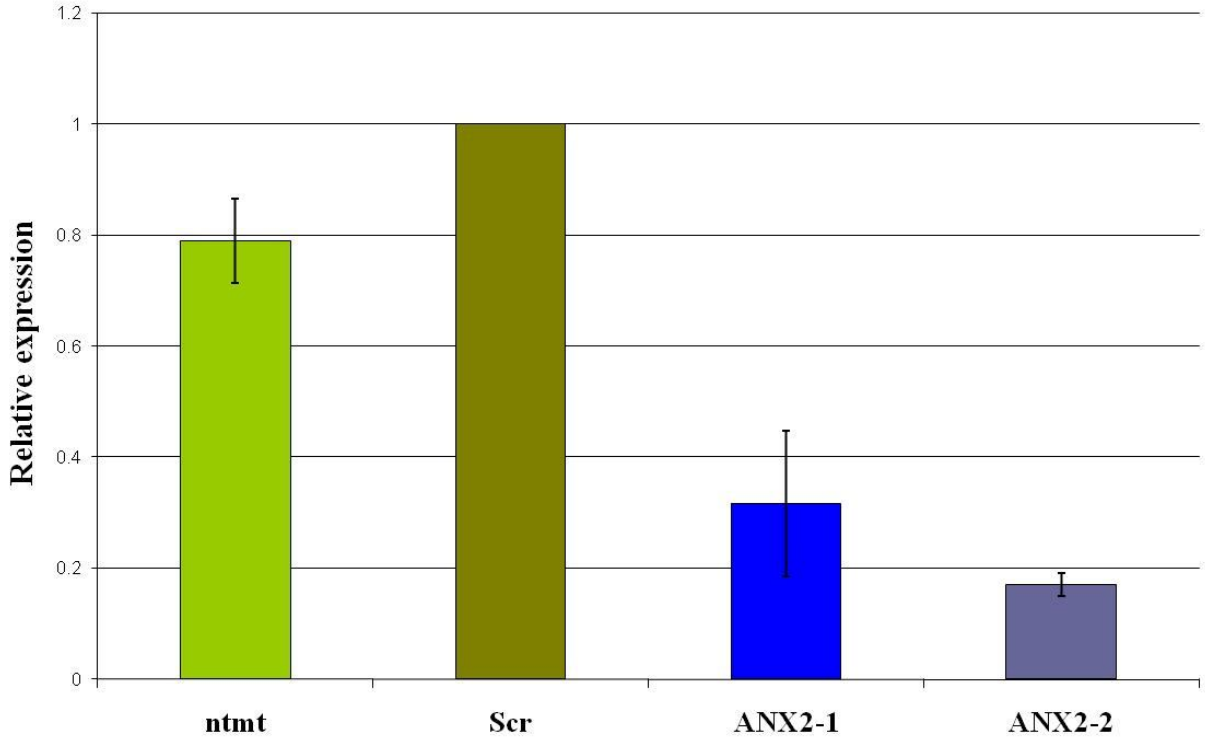

Figure 3.35A Relative qRT-PCR analysis of ANX2 siRNA knockdown.

Ntmt: No treatment; Scr: Scramble sequence negative control; ANX2-1: ANX2 specific siRNA 1; ANX2-2: ANX2 specific siRNA2. The error represents SEM ± 0.02 for ANX2-2, and SEM ± 0.13 for ANX2-1 relatively.

3.35.1 Evaluation of ANX2 siRNA effect on DLKPA proliferation

The effect of transfecting ANX2 siRNA on proliferation of DLKPA was investigated. Cells were seeded at 2 x 10^3 cells/well of a 96-well plate (Figure 3.35.1A), which was the same density used to seed all the siRNA transfections in six-well plates. Relative cell number was determined using the acid phosphatase assay at 72hrs post transfection. No significant effect was observed due to ANX2 knockdown compared to scramble control; kinesin was used as transfection positive control and a significant decrease in cellular proliferation was observed (62%)

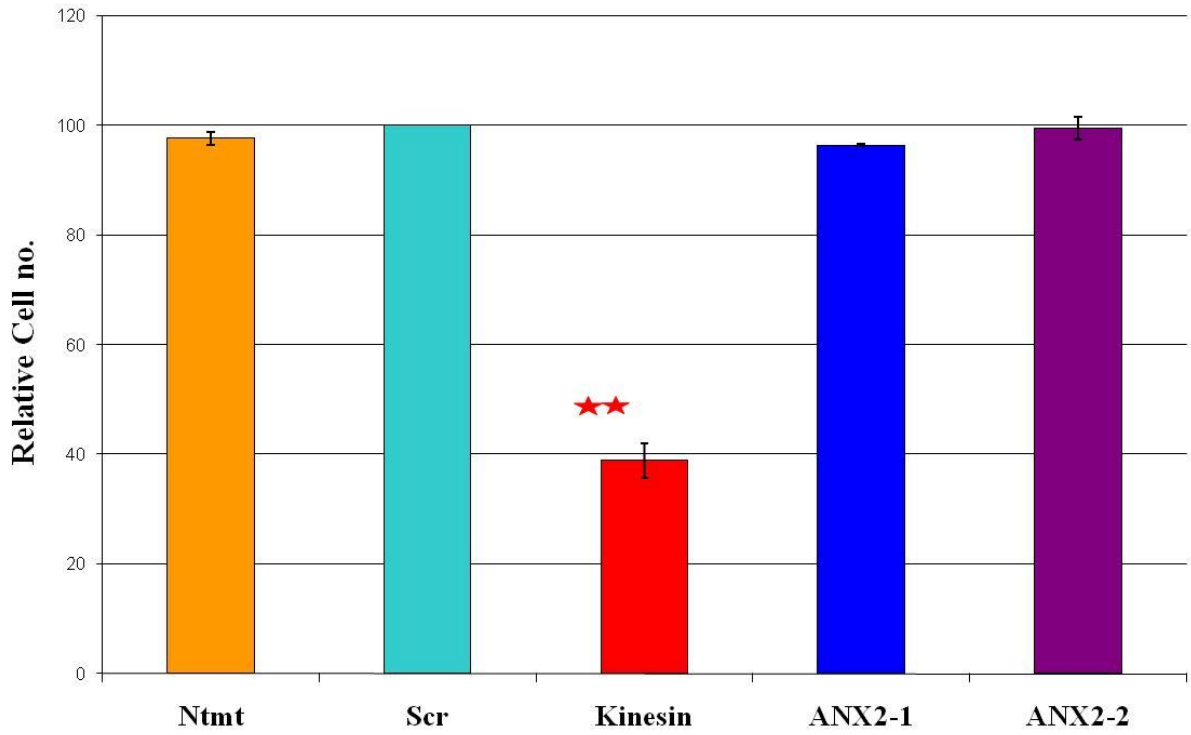

Figure 3.35.1A Effect on proliferation of DLKPA cells transfected with ANX2 specific siRNAs. Ntmt: No treatment; Scr: Scramble sequence negative control; Kinesin: kinesin specific siRNA used as positive control; ANX2-1: ANX2 specific siRNA 1; ANX2-2: ANX2 specific siRNA2. Kinesin observed to have significant ** p-value (<0.01) and n=3.

3.35.2 Evaluation of ANX2 siRNA effect on DLKPA invasion

The effect of decreasing ANX2 expression on DLKPA invasion was investigated. Invasion assay analysis was performed 72 hours post transfection, to allow the cells to recover from the transfection procedure, using commercial invasion assay kits containing inserts pre-coated with matrigel. At least two inserts were used for the analysis of each condition. The counts per number of inserts used were then also averaged and this figure was used to generate graphs of relative invasive capacity.

From the graph (Fig. 3.35.2B) it is evident that ANX2 knockdown has no impact on the invasive phenotype of DLKPA cell line. No significant effect was observed on the invasive phenotype due to siRNA knockdown compared to scrambled treatment.

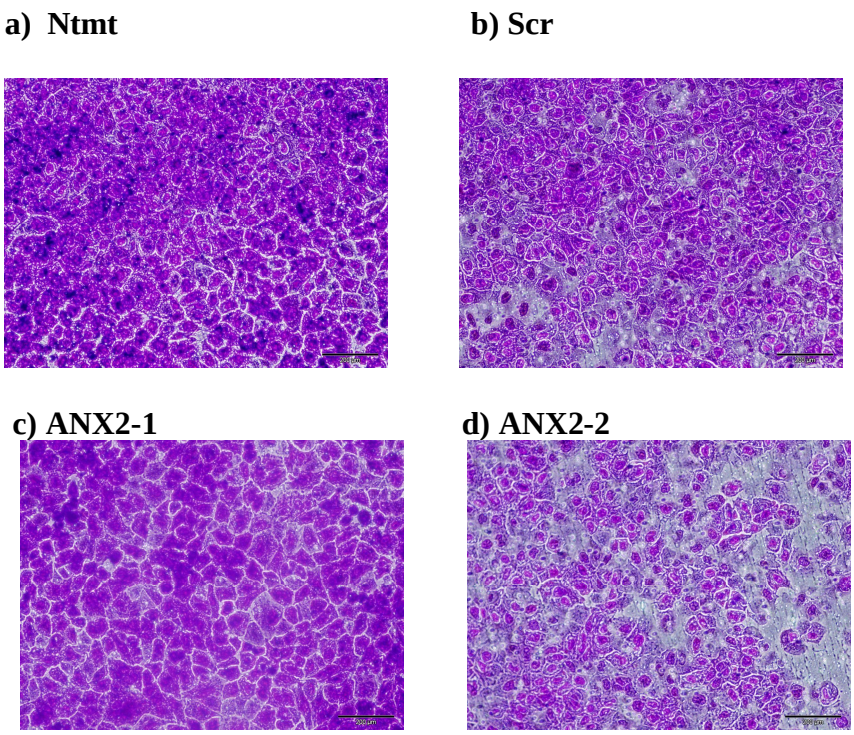

Figure 3.35.2A Crystal violet staining representation of in vitro invasion assay of ANX2 siRNA treated in DLKPA cell line. Ntmt: No treatment; Scr: Scramble sequence negative control; ANX2-1: ANX2 specific siRNA 1; ANX2-2: ANX2 specific siRNA2; Magnification 20X.

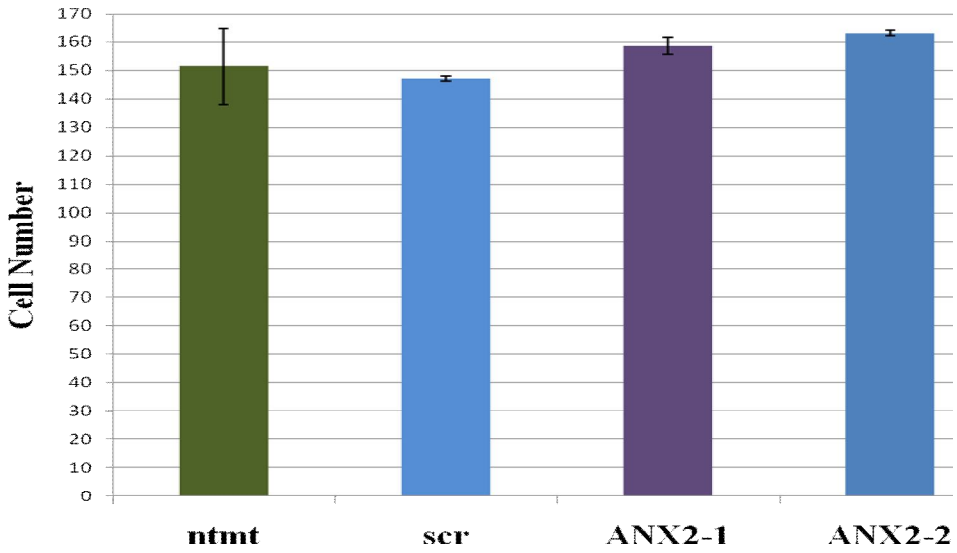

Figure 3.35.2B ANX2 siRNA in vitro invasion assay in DLKPA cell line. Ntmt: No treatment; Scr: Scramble sequence negative control; ANX2-1: ANX2 specific siRNA 1; ANX2-2: ANX2 specific siRNA2;

3.36 GRB2 specific siRNA knockdown at mRNA levels in DLKPA cell line

Proteomics study indicated that GRB2 expression was downregulated due to pre-mir-29a transient overexpression in DLKPA, which could account for the reduced DLKPA invasion phenotype. Hence, it was decided to knockdown GRB2 expression using two independent siRNA sequences in the invasive DLKPA cell lines to determine any functional effect on invasion or proliferation. 2µl of NeoFX transfection reagent per well of a 24-well plate was used to transfect 50nM of target siRNA into the cells. GRB2-specific knockdown was confirmed by qRT-PCR. GRB2 knockdown was examined using RT-PCR (Figures 3.36A). The RT negative control consisted of PCR master mix with RNA that was not reverse transcribed. A no template control (NTC), and no primer control was also used. The control was observed to have no amplification. GRB2 specific PCR primers were used to accurately measure relative GRB2 mRNA expression. The data was normalised using β-actin as an endogenous control.

The graph (Fig. 3.36A) is a composite of biological repeats and relative to scrambled siRNA treated sample, which was set to 1 for the analysis. The siRNA-GRB2-1 was observed to have a higher knockdown efficiency (65%) than siRNA-GRB2-2 (14%), compared to the scramble control.

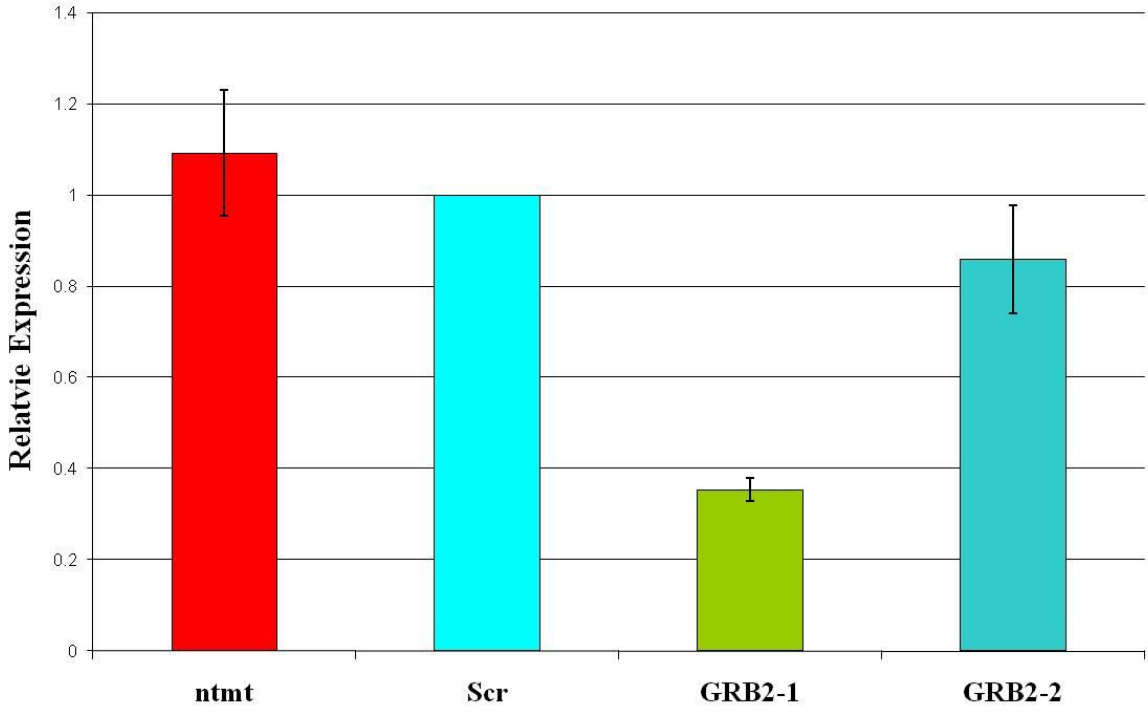

Figure 3.36A Relative qRT-PCR analysis of GRB2 siRNA knockdown. Ntmt: No treatment; Scr: Scramble sequence negative control; GRB2-1: GRB2 specific siRNA 1; GRB2-2: GRB2 specific siRNA2 relatively and n=3.

3.36.1 Evaluation of GRB2 siRNA effect on DLKPA proliferation

The effect of transfecting GRB2 siRNA on proliferation of DLKPA was investigated. Cells were seeded at 2 x 10^3 cells/well of a 96-well plate (Figure 3.36.1A), which was the same density used to seed all the siRNA transfections in six-well plates. Relative cell number was determined using the acid phosphatase assay at 72hrs after transfection. Transfection with either of the siRNA sequences did not have a significant effect on proliferation compared to non-treated and scrambled siRNA transfected cells. Kinesin was used as transfection positive control and a significant decrease in cellular proliferation was observed (62%) compared to scramble treatment.

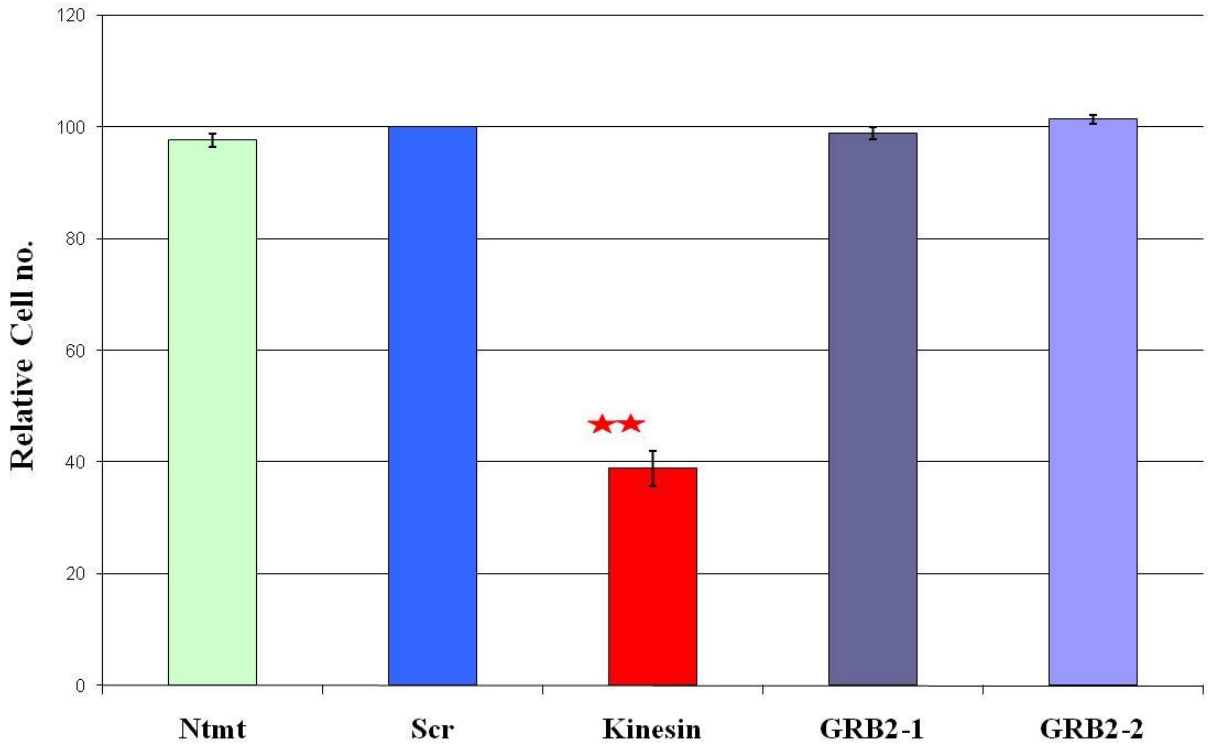

Figure 3.36.1A Effect on proliferation of DLKPA cells transfected with GRB2 specific siRNAs. Ntmt: No treatment; Scr: Scramble sequence negative control; Kinesin: kinesin specific siRNA used as positive control; GRB2-1: GRB2 specific siRNA 1; GRB2-2: GRB2 specific siRNA2. Kinesin observed to have significant impact with ** p-value (<0.01) and n=3.

3.36.2 Evaluation of GRB2 siRNA effect on DLKPA invasion

The effect of decreasing GRB2 expression on DLKPA invasion was investigated. Invasion assay analysis was performed 72 hours post transfection, to allow the cells to recover from the transfection procedure, using commercial invasion assay kits containing inserts pre-coated with matrigel. At least two inserts were used for the analysis of each condition. The counts per number of inserts used were then also averaged and this figure was used to generate graphs of relative invasive capacity. From the graph (Fig. 3.36.2B) it is evident that GRB2 knockdown has no impact on the invasive phenotype of the DLKPA cell line compared to scrambled treatment.

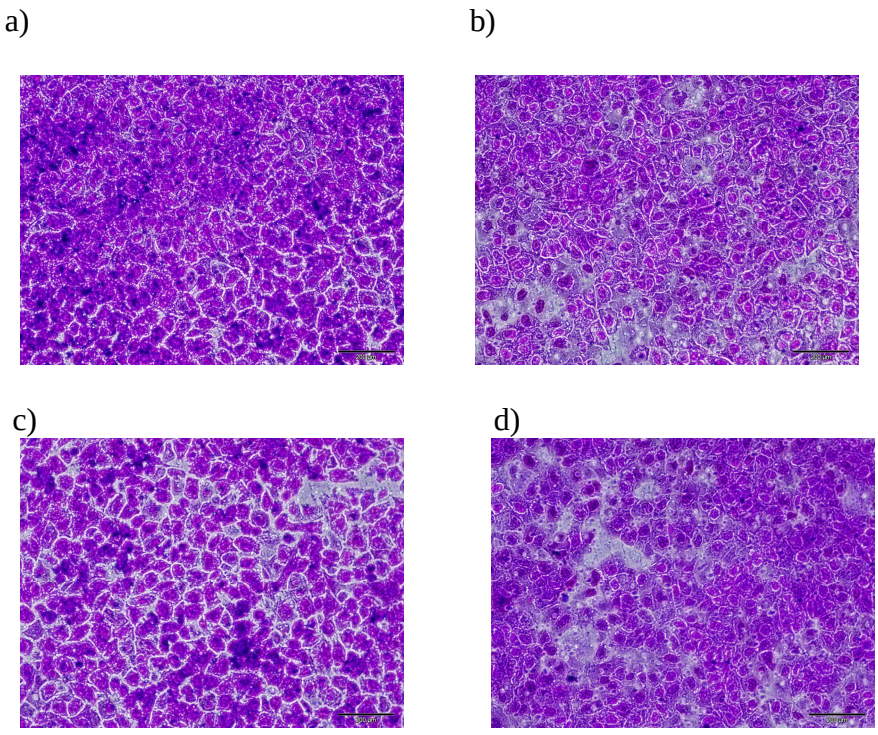

Figure 3.36.2A Crystal violet staining representation of in vitro invasion assay of GRB2 siRNA treated DLKPA cell line. Ntmt: No treatment; Scr: Scramble sequence negative control; GRB2-1: GRB2 specific siRNA 1; GRB2-2: GRB2 specific siRNA2; Magnification 20X.

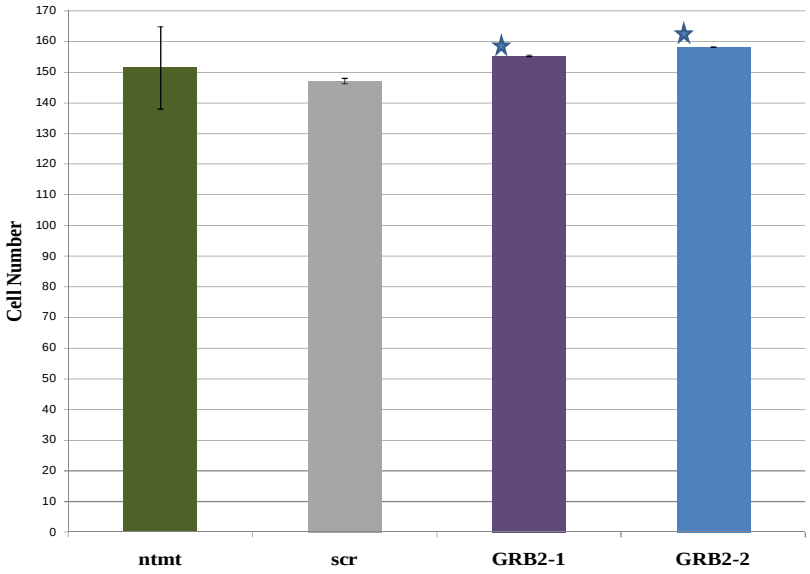

Figure 3.36.2B GRB2 siRNA in vitro invasion assay in DLKPA cell line. Ntmt: No treatment; Scr: Scramble sequence negative control; GRB2-1: GRB2 specific siRNA 1; GRB2-2: GRB2 specific siRNA2.

3.37 RAN specific siRNA knockdown at mRNA levels in DLKPA cell line

RAN (RAS-related nuclear protein) was identified by MALDI-TOF as 1RRP-C chain of the RAN-GPPNHP-RANBD1 complex and found to be decreased by 1.35 fold in mir-29a treated DLKPA cells. Vetter et al., 1999 showed the complex has four chains A, B, C, D. Chain A and C are composed of RAN and chain B and C composed of 'Nuclear Pore Complex Protein' NUP358 (RBP2). In order to investigate if RAN specifically played a role in the concomitant reduction in invasion we decided to specifically knockdown RAN expression using two independent siRNA sequences in the invasive DLKPA cell line. The siRNA transfection was performed as described previously. RAN-specific knockdown was confirmed by qRT-PCR and the effect of RAN knockdown on proliferation and invasion investigated.

RAN knockdown was examined using RT-PCR (Figures 3.37A). The RT negative control consisted of PCR master mix with RNA that was not reverse transcribed. A no template control (NTC), and no primer control was also used. RAN specific PCR primers were used to accurately measure relative RAN mRNA expression. The data was normalised using β-actin as an endogenous control. As shown in figure 3.38A RAN specific decrease in mRNA, was observed for samples at 72hrs. The siRNA-RAN-2 was observed to have higher knockdown efficiency (48%) than siRNA-RAN-1 (35%) compared to scramble control.

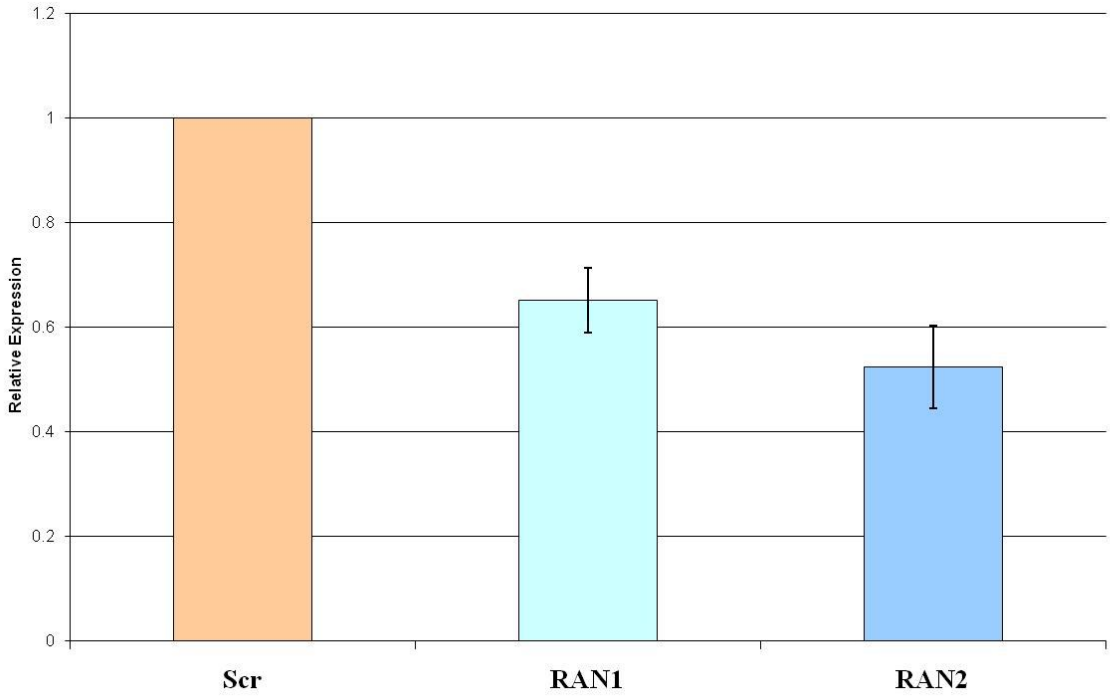

Figure 3.37A qRT-PCR analysis of siRNA mediated RAN knockdown in DLKPA cell line. Ntmt: No treatment; Scr: Scramble sequence negative control; RAN-1: RAN specific siRNA 1; RAN-2: RAN specific siRNA2. The siRNA-RAN-2 was observed to have higher knockdown efficiency compared to scramble control.

3.38 Western blot analysis of RAN siRNA knockdown

Two independent siRNAs specific to RAN were transfected in DLKPA cell line and the protein level was analysed by western blot (section 2.14). 72hrs after treatments the cells were trypsinised; protein was extracted, and used for western blot analysis. From figure 3.38.1A it is evident that both siRNAs mediated RAN knockdown and more precisely RAN-2 was observed to have a higher knockdown efficiency than RAN1 compared to scramble control, which agrees with the transcriptional quantification (fig.3.38A).

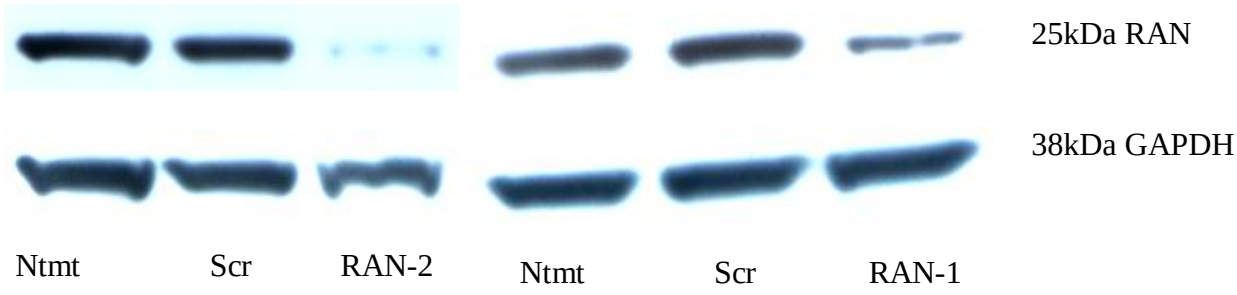

Figure 3.38A western blot analysis of RAN siRNA knockdown in DLKPA.
Ntmt: No treatment; Scr: Scramble sequence negative control; RAN-1: RAN specific siRNA 1; RAN-2: RAN specific siRNA2. The polyclonal anti RAN antibody generates approximately 25kDa band specific to RAN. Anti GAPDH antibody was used as loading control and generated a 38 kDa GAPDH specific band.

3.38.1 Evaluation of RAN siRNA knockdown effect on DLKPA cell proliferation

The effect of transfecting RAN siRNA sequences on proliferation was investigated. Figure 3.38.1A represents the results of the proliferation assay. A significant effect was observed due to RAN knockdown compared to scramble control i.e. 49% decrease with RAN-2 and 44% decrease with RAN-1 siRNA. Again this correlated with the level of protein knockdown. Kinesin was used as a transfection positive control and a significant decrease in cellular proliferation was observed (62%).

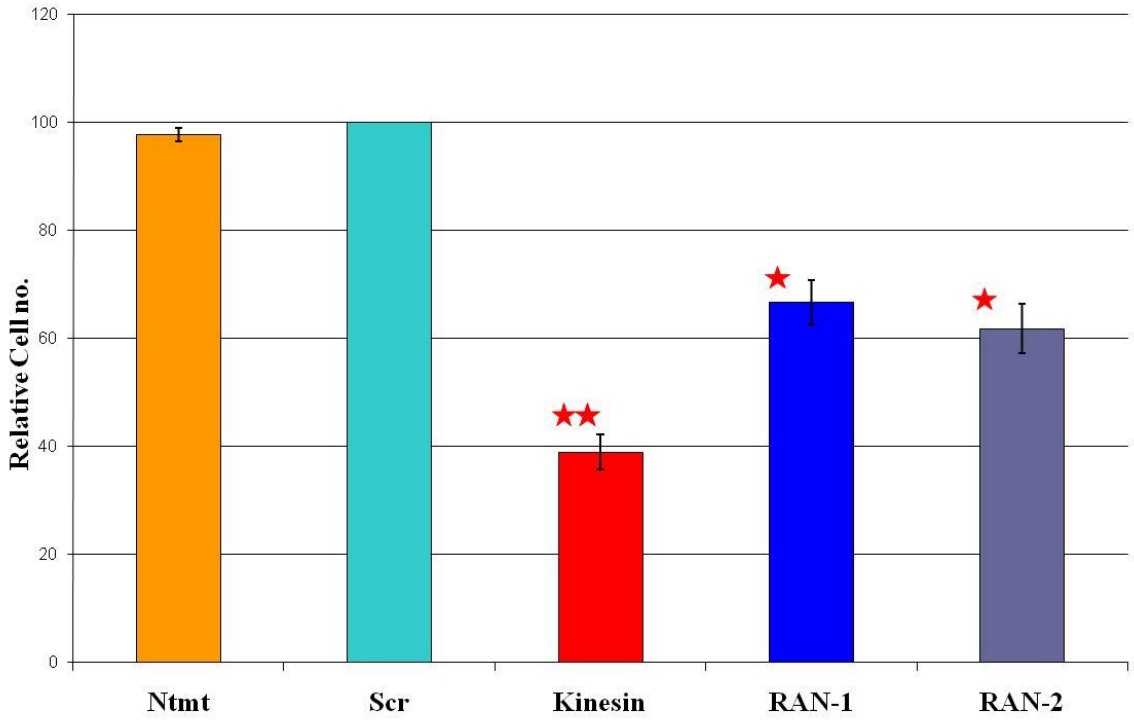

Figure 3.38.1A Effect on proliferation of DLKPA cells transfected with RAN specific siRNAs. Ntmt: No treatment; Scr: Scramble sequence negative control; Kinesin: kinesin specific siRNA used as positive control; RAN-1: RAN specific siRNA 1; RAN-2: RAN specific siRNA2. Kinesin was used as transfection positive control and a significant decrease in cellular proliferation was observed, for kinesin with ** p-value (<0.01). RAN-2 and RAN-1 with * p-value (<0.05) and N=3.

3.38.2 Evaluation of RAN siRNA effect on DLKPA invasion

The effect of decreasing RAN expression on DLKPA invasion was investigated. Invasion assay analysis was performed 72 hours post transfection, to allow the cells to recover from the transfection procedure. At least two inserts were used for the analysis of each condition. The counts per number of inserts used were then also averaged and this figure was used to generate graphs of relative invasive capacity.

The effect of RAN siRNA on DLKPA invasion phenotype was observed to be dramatic, i.e. a significant 42% reduction due to RAN-1 siRNA treatment and 80% reduction due to RAN-2 siRNA treatment were observed in DLKPA cells compared to scramble treatment (Fig. 3.38.2B).

a) Ntmt **b) Scr**

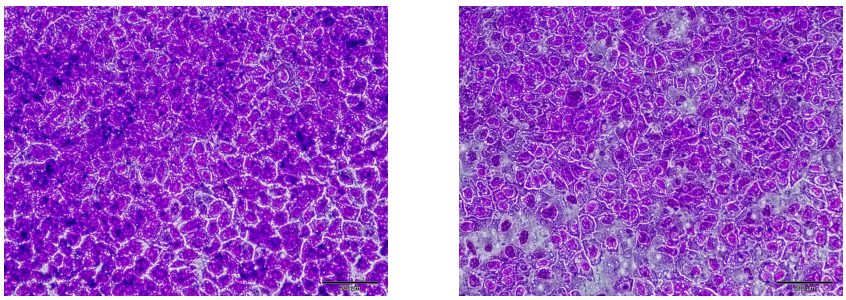

c) RAN-1 **d) RAN-2**

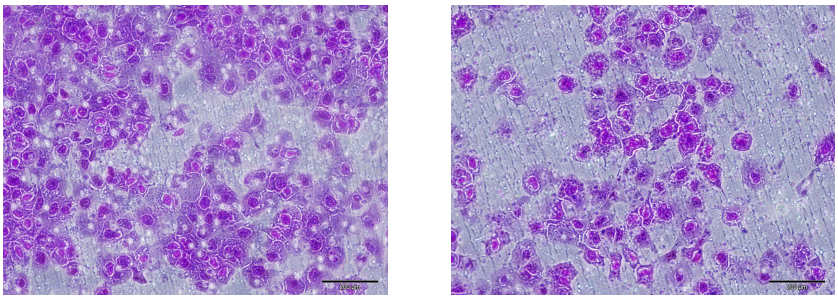

Figure 3.38.2A Crystal violet staining of in vitro invasion assay of RAN siRNA treated DLKPA cell line. Ntmt: No treatment; Scr: Scramble sequence negative control; Kinesin: kinesin specific siRNA used as positive control; RAN-1: RAN specific siRNA 1; RAN-2: RAN specific siRNA2; Magnification 20X.

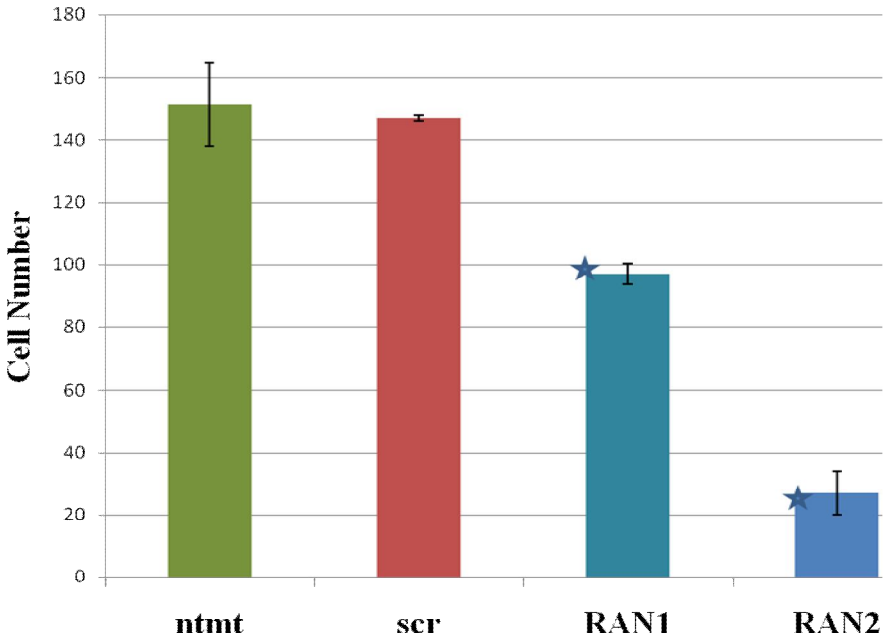

Figure 3.38.2B 72hrs post RAN siRNA in vitro invasion assay in DLKPA cell line. Ntmt: No treatment; Scr: Scramble sequence negative control; Kinesin: kinesin specific siRNA used as positive control; RAN-1: RAN specific siRNA 1; RAN-2: RAN specific siRNA2 with p-value *(<0.05) and N=3.

3.39 Investigation of whether RAN may be a direct target of mir-29a

From the siRNA knockdown studies it was evident that the effect of RAN on invasion was similar to mir-29a overexpression in the DLKPA cell line. To further evaluate whether RAN may be a direct target of mir-29a we amplified the 3'UTR region of RAN and cloned it downstream of GFP in a reporter plasmid. The rationale behind this relied on the fact that miRNAs target 3'UTR region of mRNAs. Accordingly, cell lines expressing 3'UTR sequence of RAN cloned downstream of a reporter gene, upon treatment with pre-mir-29a, would be expected to display reduced reporter protein expression if RAN was a direct target. Hence, RNA was isolated from DLKPA cell line and using random primers; we reverse transcribed cDNA. The cDNA thus amplified was further used to PCR amplify RAN using specific primers with restriction enzymes overhangs at the both 5' and 3' ends. The BamHI/HindIII digested 3'UTR of RAN was cloned downstream of GFP coding sequence in pEGFP-

C1. The GFP-RANUTR plasmid was transfected and a mixed stable DLKPA cell population was generated. Furthermore this stable cell line was transiently transfected with pre-mir-29a and pre-mir-control (100nM), and 72hrs later cells were harvested for RNA and protein analysis. We used a flowcytometer to measure GFP expression levels in live cells. The initial flowcytometer experiments were done at 48, 72 and 96hrs. This analysis revealed that at 72hrs there was a shift in the GFP expressing cell population. Numerous biological replicates were conducted at 72hrs. Similarly the RNA extracted from these samples was subjected to qRT-PCR to evaluate the knockdown in GFP mRNA levels.

The RAN 3'UTR cloning was successful as represented in figures (3.39A, 3.39B, 3.39C), the qRT-PCR analysis of GFP expression due to pre-mir-29a treatment revealed that there was knockdown at the mRNA level in mir-29a transfected cells (figure 3.39D).

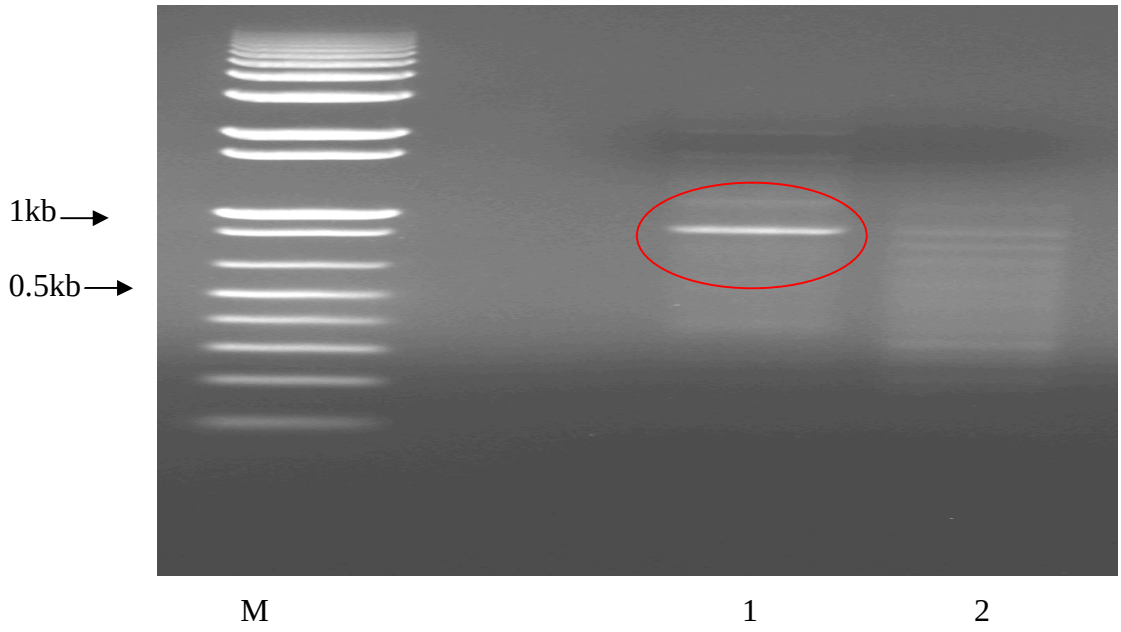

Figure 3.39A PCR amplification of Ran 3'UTR using RNA as template for cDNA preparation from DLKP cell line. The cDNA generated with 1) Random primer, 2) sequence specific primer, M- 1Kb plus DNA ladder.

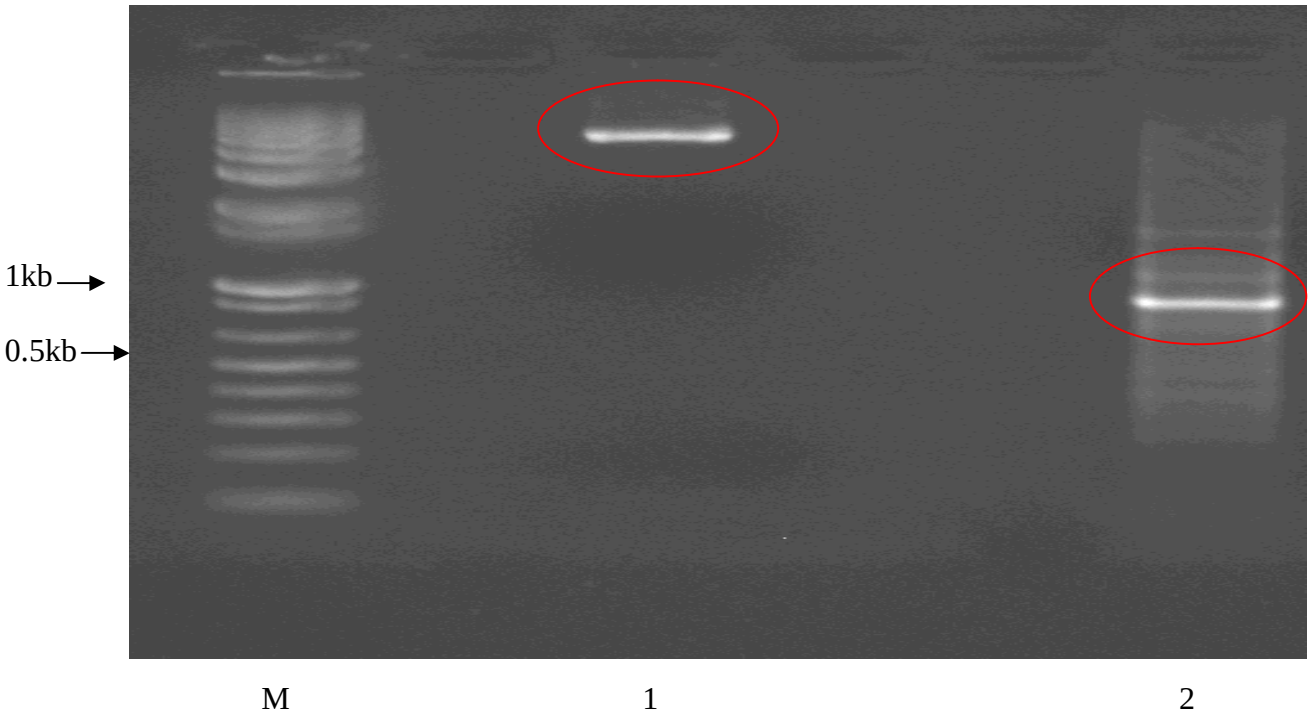

Figure 3.39B DNA agarose gel confirmation, of BamHI and HindIII digestion. PEGFP-C1 (lane 1) and pcr amplified 3'RAN UTR (lane 2), lane M: 1kbplus DNA ladder.

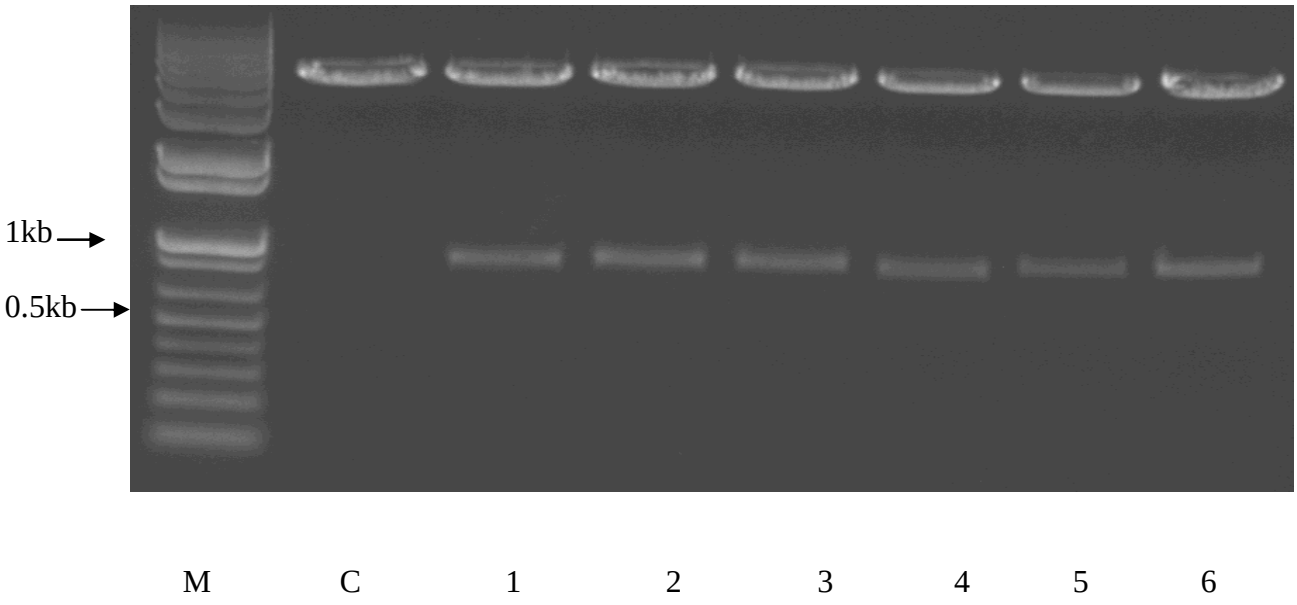

Figure 3.39C RAN 3'UTR cloning restriction enzyme digestion reaction to check for GFP-C1-RAN-3'UTR clone. M- 1kb plus DNA ladder, C- Uncut control, 1-6 plasmid prepped samples, all the samples released expected ~950bp size product.

In the figure 3.39E the rationale behind plotting segments of total population was to determine whether a decrease in GFP expression was observed due to data collected at a single point or is it a genuine decrease within the population as a whole. So if that is true then we should expect a shift towards more low expressing cells and less high expressing cells in mir-29a transfected cells. From the graph it is evident that the decrease in GFP expression was across the population in pre-mir-29a treated cells which is represented in red line, relative to blue line (control) in figure 3.39E.

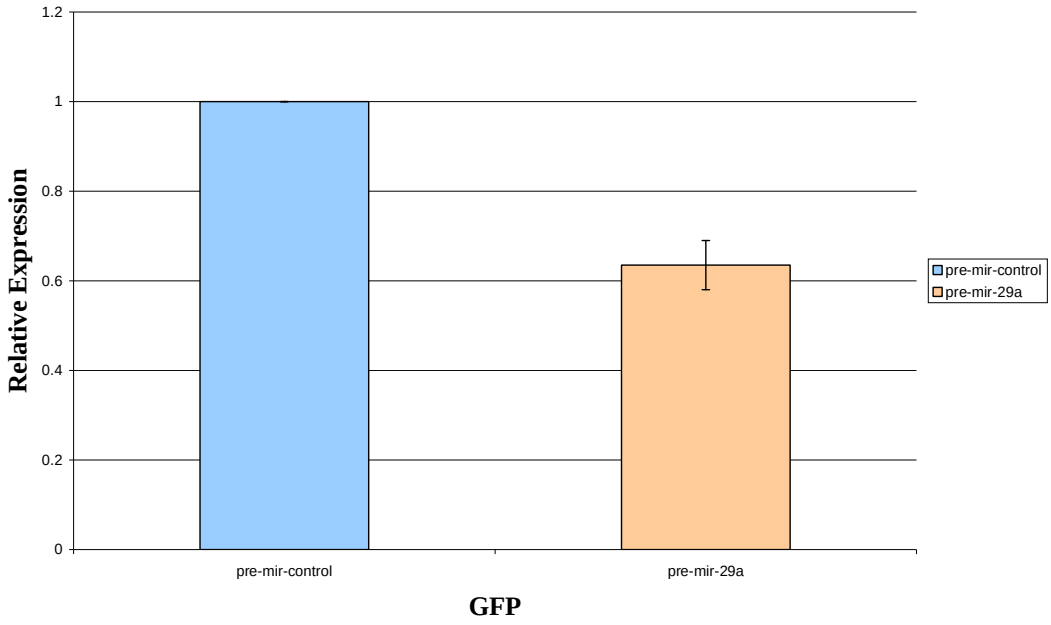

Figure 3.39D qRT-PCR analysis 72 hrs after pre-mir-29a treatment.

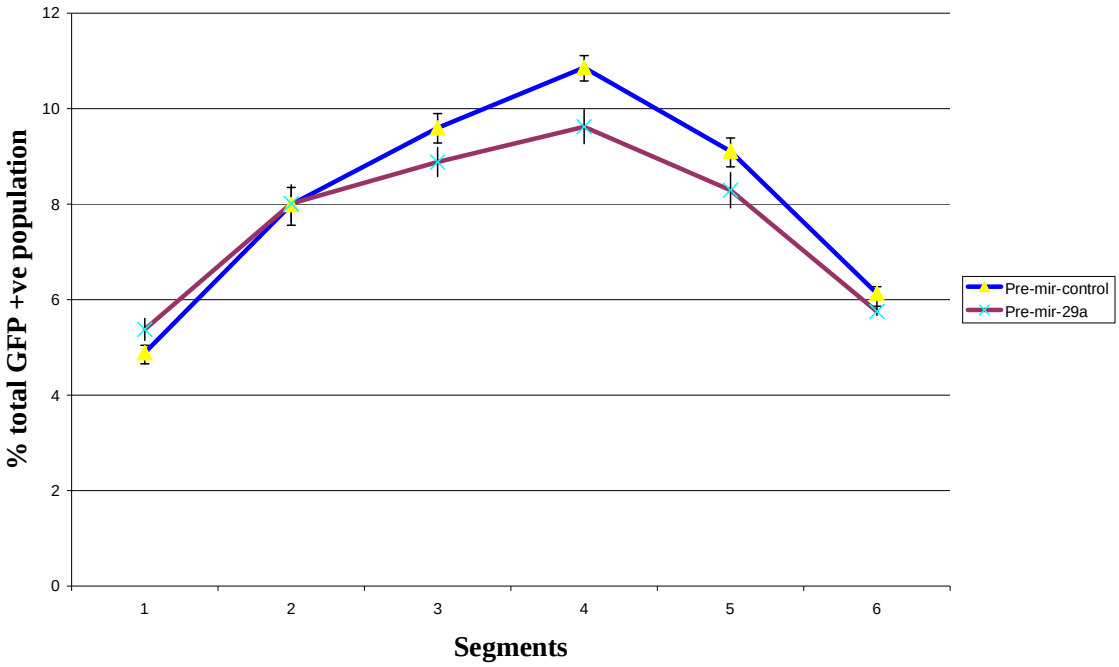

Figure 3.39E Flowcytometer analysis of GFP expression. Post mir-29a transfected DLKPA cell line expressing stable GFP-RAN 3'UTR. X-axis represents individual segments of a mixed GFP expressing DLKPA population where some cells are low expressers (segment 2-3), some are medium (3-4) and so on. Some have expression levels below the detectable 'threshold (1). The Y-axis represents the amount of cells in that segment as % of whole population. And the shift was significant with p –value (<0.05), error bar represents (n=10).

3.40 GLP1-R a possible mir-29a target

During our in silico analysis of predicted mir-29a targets, we discovered Glucagon like Peptide 1 Receptor (GFLP1R) was predicted as a possible target of mir-29a using miRBase miRNA target prediction programme from the Sanger Institute (http://microrna.sanger.ac.uk/sequences/). From our stable transgene overexpression studies it was confirmed that GLP1-R was a potential mediator of invasion in our model cell lines. This was also further confirmed with siRNA based knockdown studies (refer section 3.17, 3.18 and 3.19). From our mir-29a experiments it was evident that mir-29a is anti invasive, so we decided to check the levels of GLP1-R in mir-29a stable overexpressing cell line to investigate whether there might be a common regulation pathway involving both molecules.

Initially we checked the endogenous mRNA levels of GLP1-R by qRT-PCR analysis in mir-29a DLKPA stable clones, mir-29a (3) and mir-29a (4) relative to mir-negative sequence expressing clone. GLP1-R mRNA levels were decreased (70%) in mir-29a DLKPA clone (3) and a significant (81%) decrease in mir-29a clone (4). From the first set of results (Fig. 3.40D) it was observed that pre-mir-29a treatment had decreased GLP1-R levels compared to pre-mir-negative treatment. No difference was observed with anti-mir-29a treatment. Further work would be required to confirm the observation.

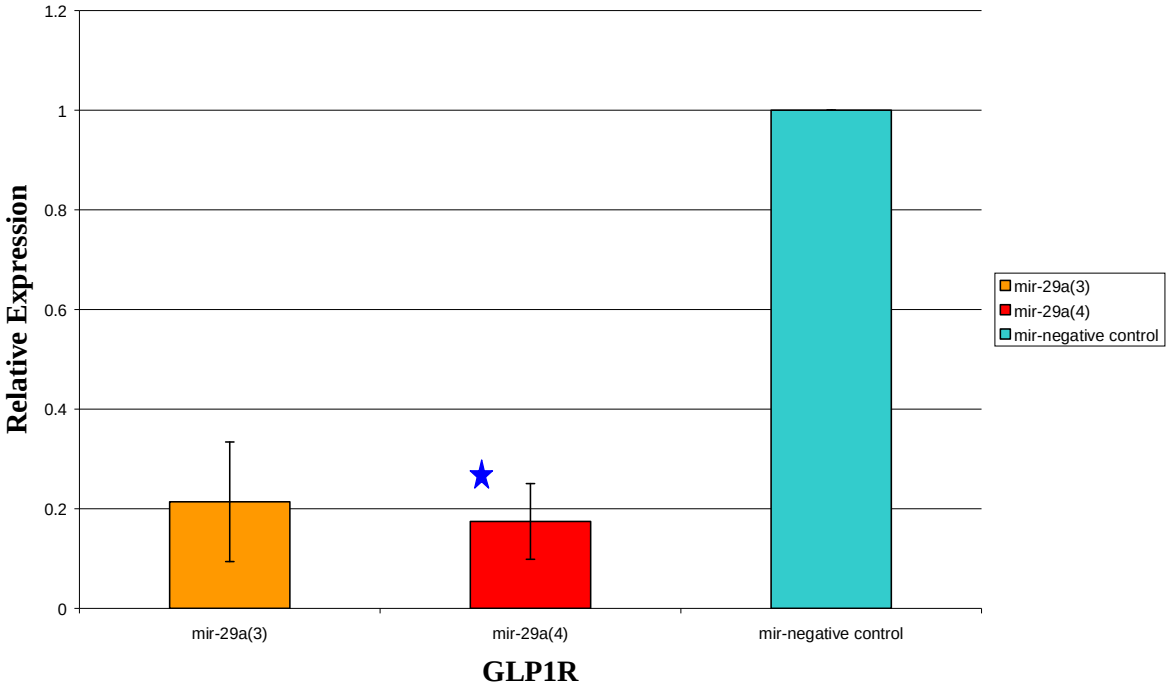

Figure 3.40C qRT-PCR analysis endogenous GLP1-R in mir-29a stable overexpressing DLKPA cell line. Mir-29a (3): DLKPA mir-29a expressing clone 3; mir-29a(4): DLKPA mir-29a expressing clone 4; mir-negative control: DLKPA expressing negative sequence as control and for mir-29a(4) clone with a significant p-value (≤0.05) and N=3.

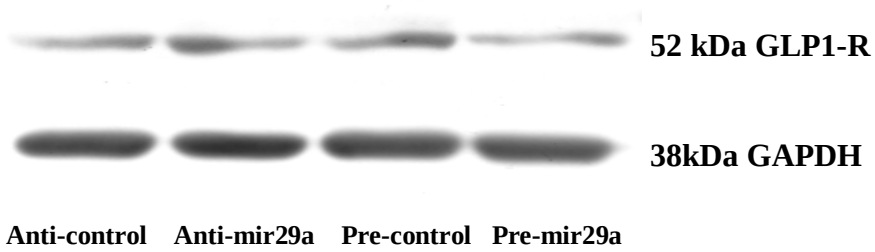

Figure 3.40D Representative western blot analysis of GLP1-R in pre and anti mir-29a transiently transfected DLKPA cell line. Anti-control: anti-mir sequence control; Anti-mir-29a; anti-mir29a sequence treated sample; Pre-control: pre-mir sequence treated; Pre-mir-29a: pre-mir-29a sequence treated sample. Pre-mir-29a treated samples appeared to have reduced GLP1-R expression. GLP1-R antibody developed 52kDa bands and GAPDH was used as loading control with 38 kDa bands.

4.0 DISCUSSION

4.1 Overview

Lung cancer is the most lethal and prevalent of malignancies in the world with deaths exceeding those from breast, colon and prostate cancer combined (Akehurst et al, 2002; Danesi et al, 2003). The use of chemotherapy in the treatment of non-small cell lung cancer (NSCLC) patients has greatly increased over the last twenty years, with agents being used in combination more effectively than alone. The most commonly used drugs for the treatment of NSCLC are the taxanes and platinum drugs with platinum-based doublets remaining the preferred option (Socinski, 2004). However, the development of resistance to these drugs is frequent and a major obstacle in lung cancer treatment.
(Akehurst et al, 2002)

The purpose of this research thesis was to study molecular mechanisms of invasion/metastasis in lung cancer cell lines. In particular, we investigated the impact of expression of four specific genes on invasion in lung cancer cell lines; and the role of specific microRNAs in regulation of the invasion phenotype in lung cancer cell lines. In order to have optimal cell lines with which to approach the questions, we also attempted to generate stable targetable cell lines.

Invasion is a prerequisite step in cancer metastasis. Invading tumour cells appear to have lost the control mechanism that prevents normal cells from invading neighbouring tissue at inappropriate times and places (Friedl and Wolf, 2003b). Metastasis is the spread of cancer from a primary tumour to distant sites in the body. A distinguishing feature of malignant cells is their capacity to invade surrounding normal tissues and metastasise through the blood and lymphatic systems to distant organs. This process of metastasis is the most devastating aspect of cancer. The loss of tight regulatory mechanisms is mainly due to gene mutations resulting in genetic instability (Friedl and Wolf, 2003a). The difference must lie in the proteins that start, stop or maintain the invasion programme at times and places that are inappropriate for non-malignant cells. A major goal is to understand what signals and signal transduction pathways are

perpetually activated or deregulated in malignant invasion (Kohn et al, 1997). Microarrays have been utilised to identify gene signatures that would differentiate between various primary and metastatic adenocarcinoma (Deutsch, 2003). This group reported a metastasis-associated gene signature that contained eight up regulated and nine down-regulated genes.

The lung cancer cell lines models used in our study were DLKP (non invasive) and DLKPA (invasive) carcinoma cell lines. DLKP was isolated from a tumor histologically diagnosed as a poorly differentiated lung carcinoma (Law et al, 1992) in the National Institute for Cellular Biotechnology (NICB). The DLKPA variant is resistant to Adriamycin, a chemotherapeutic drug, and was also generated in the NICB (Heenan, 1997). The research work carried out in this thesis can be divided into two main sections.

- **Development of genetic tools for stable, targetable transgene overexpression.**

The impact of dysregulated expression of a particular gene is often studied by generating cell lines that overexpress the gene after random insertion in the genome. The problem with random transgene integration is variation in stable gene expression in the resulting clones and is usually due to chromosomal position effects and/or copy number variation between different clones. This often results in genetic instability, loss of observed phenotype in real time and as a result, cell lines with unpredictable behaviour. To address this variation, we attempted to design and construct two different Cre-LoxP based mammalian expression systems to generate targetable lung cancer cell lines. A GFP based reporter system was used initially to generate stable cell lines and used to monitor the expression and stability characteristics of the cell lines.

- **Investigation into the role of differential expression of a group of genes including miRNAs, in cancer invasion.**

As mentioned above, in order to investigate the mode of action and function of a gene product it is often useful to alter the expression of the gene either by overexpression or specific knockdown. Microarray profiling studies done in this lab (Pierce A. PhD thesis 2005) on a panel of lung cancer cell lines with various invasive phenotypes identified a list of differentially expressed genes. It was also demonstrated that transiently altering the expression of several of these genes could modulate the invasive capacity of these cell lines (Pierce et al, 2008). Based on this microarray data and subsequent qRT-PCR analysis we selected 4 genes (KCNJ8, TFPI2, S100A13, GLP1-R) for evaluation of the effect on proliferation and invasion of stable over expression in targetable DLKP cell lines.

MiRNAs (miRNAs) are noncoding, small regulatory RNAs. Recent studies have revealed their involvement in cell development and various cellular processes. We investigated miRNAs potentially involved in cancer invasion in DLKP Vs DLKPA cell lines. In particular we followed up our studies with one miRNA (mir-29a) which was observed to have an anti-invasive impact in our model cell lines. To identify possible gene targets being dysregulated due to reduced or increased expression of mir-29a we performed proteomics analysis and functional investigation of selected targets.

Section I:

4.2 Development of targetable lung cancer cell lines for stable transgene overexpression

The possibility of stably integrating genes into the genome of mammalian cells has an important impact on many biomedical research areas as well as for the development of pharmaceutical products. While transient transfection is advantageous for fast analysis of genes, it is frequently desirable to observe the effect of stable long-term,

reproducible, as well as defined, gene expression. Major applications of stable transfection are the analysis of gene function and regulation (Grimm et al, 2004) large scale protein production (Wurm, 2004), drug discovery and gene therapy (Glover et al, 2005).

The major drawback of generating transgenic cell lines by random integration of plasmid DNA is the unpredictability in expression between clones. Other problems associated with non-targeted, random insertion of exogenous transgenes include:

- Loss of expression due to instability or silencing at the epigenetic level, at particular chromosomal loci.
- Prolonged screening process for sub clones suitable for experimentation.
- Risk of possible disruption of important endogenous sequences or genes

4.3 How the targeting system works

A review by Sherratt et al (1995) showed that the DNA rearrangements catalyzed by site-specific recombinases from the tyrosine recombinase family are used in a variety of important gene recombination events. In addition to the integration and excision of viral genomes into and out of host chromosomes, site-specific recombinases recognize specific DNA sequences and catalyze DNA rearrangements only between those sequences (Sherratt et al, 1995). Based on sequence similarity, over 100 tyrosine recombinases were identified (Nunes-Duby et al, 1998). The most well-studied examples include the integrase protein from bacteriophage λ (Sarkar et al, 2002), the bacterial XerC and XerD recombinases (Aussel et al, 2002), the Cre recombinase from bacteriophage P1 (Hoess et al, 1984), and the Flp recombinase from the *Saccharomyces cerevisiae* 2 micron circle plasmid (Sadowski, 1995). Craig (1988) and others showed that these proteins catalyse site-specific recombination between DNA substrates in a stepwise manner, exchanging one pair of DNA strands to form a Holiday junction (HJ) intermediate and then resolving the HJ intermediate to produce an exchange of the second pair of strands (refer to figure 1.13) (Craig, 1988).

The Cre gene which encodes a site specific DNA recombinase can catalyse recombination between specific sites in a DNA sequence (Ray et al, 2000). These sites are known as LoxP (locus of X-over P1) sequences, which are 34 base pairs long and bear binding region for the Cre to recombine the DNA surrounding them (fig. 4.3A). Two Cre subunits bind to each loxP site and the sites associate to form a complex. As a result, the DNA in between the *LoxP* sites is excised and subsequently degraded.

Figure 4.3A Mechanism of Cre recombination. Cre specifically recognizes and binds to the recombinase binding elements (RBEs), which are arranged as inverted repeats surrounding a central 8-bp crossover region **(in bold)**

4.3.1 Why Cre/LoxP excision of DNA is so useful

The LoxP sequence originally comes from the P1 bacteriophage, which is a bacterial virus that contains DNA that is not found in animals or plants. Since LoxP sequences are 34 base pairs long there is virtually no chance that one would randomly find them in a genome. Therefore, LoxP sequences can be artificially inserted into animals or plants and used for the precise excision of DNA. In our study system, since we have flanked the geo gene with LoxP sites, after inserting in the genome of the host would act as targets for Cre. Cre recombinase represents one of the simple tyrosine recombinase. Studies reported by Lin et al, (1985), confirmed that Cre will recombine essentially any DNA substrates which contain the LoxP sites, with no requirements for

accessory proteins. The mode of action is dependent on the orientation of the LoxP sites (fig. 4.3B). Any sequence in-between forward directed LoxP sites **(>->)** will be removed by Cre enzyme, and sequence in between LoxP sites facing each other **(>-<)** would be inverted and re ligated. In our study we are using the forward orientation as we are interested in targeting strategies.

4.4 Stability assessment of stable DLKPgeo clones

Before generating the clones for stability assessment there was a need to optimize the transfection conditions for the cell lines. This was found to be 1:3 ratio of DNA to Lipofectamine 2000 with minimal cell toxicity and maximum transfection efficiency.

More importantly we wanted to ensure that the GFP-Neo fusion that was constructed in the pBKS-geo plasmid retained its dual functionality. Fusion proteins such as this have been used by other groups to minimise the use of extra promoters or IRES sequences in plasmids in order to reduce plasmid size. These have included LacZ-neo fusions (Baker, 1997) and similar GFP-neo fusions (Hansen, 2002). The construct assembled in this work was shown to retain both its fluorescent GFP properties (Fig. 3.1.6) though to a slightly lesser extent than wild type GFP, and an active neomycin phosphotransferase capable of conferring G418 resistance on transfected cells (Fig. 3.1.6).

To generate a panel of targetable DLKP clones, cells were transfected with pBKS-geo. The plasmid carried a recombination cassette and contained the following elements a) A reporter fusion gene Geo [GFP fused with Neo *(*neomycin resistance gene)] both driven by a strong CMV promoter (Constien et al, 2001), b*)* LoxP sequences placed on either side of the Geo cassette which would eventually be knocked out by transient expression of Cre recombinase (Stec and Sigmund, 1998) to generate LoxP based targetable cell line**.** GFP positive and G418 resistant cells were selected by single cell cloning. Each well containing a single cell was identified and expanded before stocks of each were frozen. These stable DLKPgeo clones were thawed back in 24 well cell culture plates. Of the 50 clones thawed back only 33 clones survived the initial freeze thaw. This was not surprising as we know either due to freezing processes involved or

the ability of clones to recover back, one would always experience this. These 33 clones were passaged regularly with constant monitoring visually under fluorescent microscope. In addition GFP expression was recorded by flowcytometer measurements.

During this process, which lasted for four and a half months, we observed clones with various Geo expression levels. It is evident from our results that clones with a range of expression levels (monitored through flow cytometer) were observed (Section 3.2). In addition, though they were all single cell clonal populations, there were what appeared to be non-fluorescing, G418 resistant cells as well as cells with different levels of GFP expression. An in vitro study in mammalian cellular systems shows that the spontaneous emergence of phenotypic heterogeneity is a rule rather than an exception (Stockholm et al, 2007). Transcriptional heterogeneity has been observed in cultures of various lines of genetically identical cells even in controlled environments (Rubin, 1993). These different expression phenotypes can be strikingly different; for example, non malignant cells can spontaneously produce neoplastic sub-clones at a frequency dependent on the culture conditions (Rubin, 2001). Conversely, cells in isogenic (from same parental clone) populations of malignant cell lines in culture can spontaneously revert to stable non-malignant phenotypes (Lavrovsky et al, 1992 and Sun et al, 1996). Snapka et al, (1997) reported that cells with higher levels of transgene amplification displayed a low rate of G1/S transition suggesting that amplified sequences may activate a cell cycle checkpoint. It has also been shown that extinction of expression is caused not just by transgene elimination but by transcriptional silencing and that this in turn, is influenced by the nature of the transgene itself (Migliaccio et al, 2000). Besides copy number, another factor influencing the stability of transgenic cell lines is the genomic location of the integration event(s). Neildez-Nguyen et al, (2008) observed in their studies that a) factors acting on the promoter account mainly for the generation of variability and, consequently, the phenotypic diversification of the cell population, b) epigenetic mechanisms act to increase the robustness of the cellular state by stabilizing the gene transcription levels or by reinforcing the silenced state. We suspected the appearance of GFP negative population in our model studies could be a cell cycle effect.

4.5 Cell cycle analysis

In order to investigate the differences in cell cycle phase which we thought contributed to differences in DLKP-geo clonal expression we used propidium iodide (DNA binding dye) based cell cycle analysis. The comparison between DLKP parent and several DLKP-geo clones revealed that at each time point there was a higher percentage of cells in G0/G1 phase in the DLKP-geo clone and less in G2/M compared to the parent. In both cell lines there was a decrease in the percentage of cells in G0/G1 with increasing time after serum activation as expected. However, more importantly there was no fluctuation in the level of fluorescence measured in the DLKP-geo clone after the initial burst of translation associated with the addition of serum. This observation eliminated the possibility of transgene expression levels varying due to cell cycle stage. The most likely explanation and one for which more evidence was seen subsequently in the studies with several transgenes, is that the fluorescence data captured during the guava analysis was somewhat misleading. During flowcytometer analysis, the cut off setting that the user applies to define the positive and negative population is based on non-transfected control. In the case of clones with low transgene expression i.e. low fluorescence, there is a greater chance of a cell falling below this line. This results in it being 'recorded' as GFP negative. The cell that passes through laser and amount of signal detected will depend on shape of cell, GFP localisation and the way the cell is facing.

Therefore even though the output data is represented in percentage GFP positive cells in the population, it most probably reflects the level of GFP expression in the clone in general. That is in a clonal population of strongly positive cells the majority will fall above the cut off. In a clone that has low GFP expression there is a greater likelihood of a cell falling below the cut off. Therefore a higher percentage appears negative. In reality this just indicates a clonal population with a low level of transgene expression.

4.6 Proof of concept of targeting tool

To prove the targeting tool worked we constructed a shuttle vector that consisted of a promoterless neo, downstream of a single LoxP site, and a CMV promoter to drive transgene expression. Neo confers resistance to G418 drug therefore; if the promoterless Neo transfected cells had not undergone recombination at LoxP locus in the DLKP genome then the cells should lack resistance to G418 and die. Conversely, if targeted recombination occurs then the CMV already present at the targetable locus would drive neo expression and in turn, the cells would survive G418 that confirms targeted integration. A LacZ reporter gene was cloned into the shuttle vector pShuttle (Fig.3.7.3, 3.7.4) and co-transfected with Cre. The cells were subjected to G418 selection for 5-6 days (DLKP parent cell line base level threshold for G418 selection) the surviving cells were fixed and stained with X-gal; pSVGal plasmid was used as a positive control (section 2.7.2). Cells expressing β-gal were stained blue (Fig 3.7.4). In the cultures transfected with pShuttle without Cre there was large number of surviving cells, many of which were not LacZ positive.

Possible reasons for this could be A) Random insertion of the pShuttle plasmid near an endogenous enhancer/promoter element resulting in activation of neo. This would result in G418 resistant cells. These random insertion events often include degradation of part of the exogenous sequence by intracellular nucleases potentially resulting in inactivation of the LacZ gene in some cases.

B) Re-arrangements of the exogenous sequence prior to random integration in the genome resulting in activation of neo, by the plasmid-encoded CMV sequence.
C) Chromatin silencing events that only affect the LacZ sequence. Keeping in mind that the selection process enriches for clones that express neo therefore cells that had silenced neo transcription (but not those that had silenced LacZ) would die.

It has been reported that the silencing effect can be avoided by the inclusion of chromatin insulators proximal to the transgene (Felsenfeld et al, 1996). Insulators are DNA sequences that can function as directional blocking elements either by interfering with promoter/enhancer interactions when positioned in the intervening sequence or by

reducing position effects imparted on transgenes when flanking the integrated transcription units (Rivella, 2000).

An insulator sequence (kind gift from Prof. Gary Felsenfeld) was cloned between the CMV and promoterless neo to try to minimise the observed phenomenon. As a result, there was a dramatic difference i.e. there were much fewer surviving cells after G418 selection and most stained positive for X-gal. However the system was still not 100% effective i.e. we did find a small population of cells which were X-gal negative and G418 positive (section 3.11). Despite the slight "leakiness" observed in the targeting system we have demonstrated the development of a panel of DLKP clones with various transgene expression levels from a re-targetable genetic locus. Though the re-targeting procedure resulted in some background, non-targeted clones it was sufficiently robust to provide a useful tool for subsequent gene studies.

Section II:

4.7 LINE-1 (Long Interspersed Nuclear Element 1) Specific Targeting

Homologous recombination (HR) refers to any process in which two similar DNA sequences interact and exchange genetic information. Cells have the inherent ability of performing HR. The most obvious natural occurrence of HR is in meiotic recombination (Smith, 2001).

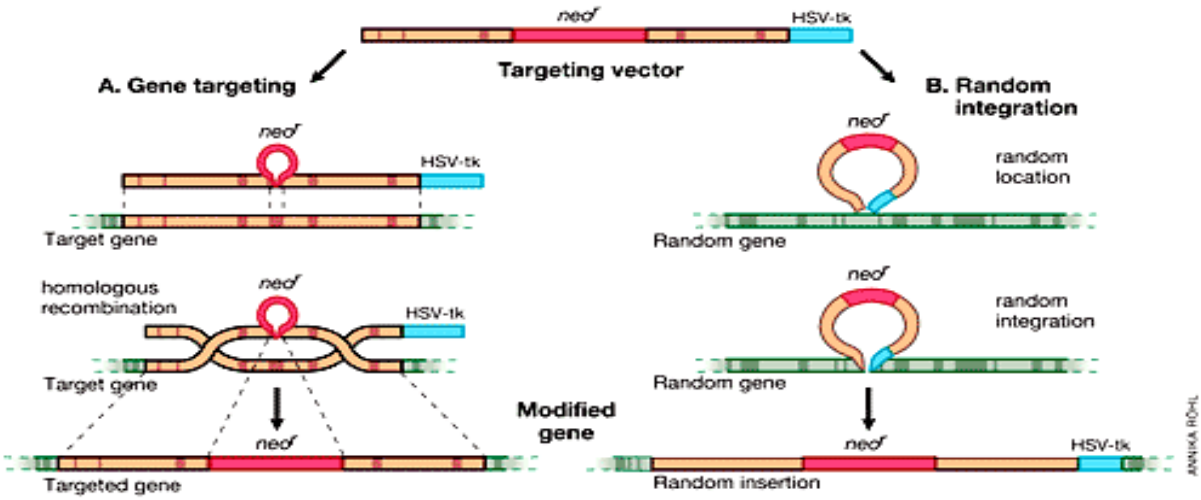

Adopted from http://nobelprize.org/nobel_prizes/medicine/laureates/2007/adv.html

---

Figure 4.7A represents specific targeted as well as random targeted gene recombination mechanisms. Figure illustrates an example of mechanism of specific and random integration of target gene recombination in genomic DNA environment. In both gene targeting (A) and random integration (B), the upper line shows the targeting vector, the middle one the chromosomal gene, and the lower one the modified gene. The type of vector used for stable integration defines the integration mechanism, the regulation of transgene expression and the selection conditions for stably expressing cells. After integration the level and time of expression of the gene of interest depends on the promoter cloned upstream on the expression vector and on the particular integration site.

Studies involving gene targeting of artificially introduced defective genes by Lin et al. reported a ratio of random integration to gene targeting of 100000:1. This indicated a high frequency of random integration events (Lin et al, 1985). An overview study concluded that absolute frequencies of gene targeting in mammalian cells remain low, and the ratio of targeted to random integration is still heavily weighted in favour of the latter (Smith, 2001). Until the frequencies are improved, the potential use of gene targeting in non-selective systems will be limited. Such improvement is likely to depend upon a more detailed understanding of gene targeting. The random integration effect could be eliminated by generating a targeting locus in the system prior to transgene introduction.

Our first approach relied on initially introducing the LoxP site into the genome in a random manner followed by assessment of a panel of resulting clones for their level of transgene expression. The second approach we took was to introduce the re-targetable LoxP site into the genome in a more controlled, directed manner. This relied on the phenomenon of homologous recombination (HR). In mitotic eukaryotic cells, the primary use of homologous recombination is to repair DNA double-strand breaks (DSBs). In meiotic eukaryotic cells, homologous recombination is the way cells exchange genetic material between homologous chromosomes to create genetic diversity and is the way that cells synapse homologous chromosomes to allow proper chromosomal segregation (Porteus, 2007). This phenomenon has been taken advantage of to study gene function in mice and other model organisms by generating gene deletion mutants. Typically a selective marker is flanked by sequences homologous to the target locus and is introduced into embryonic stem cells. In cells where homologous recombination occurs, these flanking arms replace the endogenous allelic sequence and place the selection marker at the locus simultaneously disrupting the exon/intron structure, and 'breaking up' the gene. We chose this method to place the LoxP site in the DLKP genome in a directed manner. However, HR occurs at very low frequency even in germ cells and its frequency is extremely low in somatic cells. Gene targeting frequencies of 10^{-2} (one homologous integration event per hundred random integration events) or higher typically occur in ES cells depending on numerous criteria (Jasin et al, 1996).

An attempt was made to generate stable, targetable cell lines, using human Long Interspersed Nuclear Elements or LINE-1or L1 element as the targetable locus. L1 elements are ubiquitous human transposons which replicate through an RNA intermediate mechanism. L1's are the most common family of non-LTR retrotransposons in the human genome. There are approximately 80-100 retrotransposition competent active copies of this element in the human genome. The full length mammalian L1 is ~6000 bp long and is composed of the 5' UTR region bearing an internal promoter, two open reading frames ORF1 and ORF2 separated by intergenic region and 3'UTR containing a poly(A) tail. The ORF1 is non-sequence-specific RNA binding protein and the ORF2 harbours three domains involved in L1 retrotransposition activity: endonuclease, reverse transcriptase and a 3' terminal Zn finger-like domain (Dombroski, 1991). Studies done by Feng et al, (1996) have shown that the transposition of engineered L1s in cultured human cells occurs at reasonable frequency. The human genome is estimated to be comprised of ~17-20% of L1 elements (Lander et al, 2001), the majority of which are inactive. We knew that the frequency of homologous recombination is very low in somatic cells compared to stem cells (Yamane-Ohnuki et al, 2004). To increase the possibility of encountering a HR event we deliberately selected an abundant target sequence in the genome. Using human L1 element as target would also help avoid targeting endogenous genes, and possibly shed light on homologous recombination efficiency in somatic cells which hasn't yet been completely explored.

The complete human L1 sequence was a kind gift from Dr. Olga Piskareva (NICB). The plasmid that we designed and constructed contained the following elements, a reporter fusion gene [Geo (GFP+Neo)] and LoxP sequences flanked by split 5' and 3' ORF-2 sequence of human L1 element. An external CMV promoter was cloned in-between 5' arm and *LoxP* sequence. Herpes Simplex Virus *thymidine kinase* expression cassette was cloned upstream of the 5' L1 flanking sequence to negatively select for random integration events (Fig. 3.9.3.2).

600 stably transfected single cell clones were screened by PCR to try to identify homologous targeting events. Several pairs of primers were designed and used in our screen with the sense primer designed outside the 5' arm but still within the L1 element

(in-between ORF1 and ORF2) and antisense primer in the Geo region. In the event of HR these would amplify ~2kb product (fig. 3.10.2). Since, we did not have a perfect positive control we used sP52 plasmid which had ORF1 and ORF2 regions of L1 element and pBKS 5'-3' L1 targeting plasmid to make sure the primers were capable of binding to their sequence. Unfortunately we were not able to find even a single positive clone which displayd a LINE-1 homologous recombination event, suggesting that the homologous recombination frequency was at least less than one in six hundred, compared to random integration.

Considering the factors that improved gene targeting in mouse, various attempts have been undertaken in the following years to improve the ratio of homologous to illegitimate recombination. However, in plants neither extending the length of homology in the transferred DNA to up to 22 kb (Thykjaer et al, 1997) nor including negative selectable markers outside of the homology of the targeting vector to be able to select against random integration (Risseeuw et al, 1997, and Gallego et al, 1999) did not result in a significantly higher frequency of gene targeting. Yamane-ohnuki et al (2004) reported screening over 70,000 clones to identify just one clone with the desired homologous recombination event, i.e. establishment of *fut8* knockout in Chinese hamster ovary cells.

This work demonstrates that even when targeting an extremely abundant genetic element in the genome, homologous recombination rates remain very low. Transfection efficiency plays an important role in recombination events. Maximum efficiency is directly proportional to increased frequency of homologous recombination. Vectors based on adeno-associated virus (AAV) can efficiently modify homologous chromosomal target sequences (Russell and Hirata, 1998). *In vivo* analysis of retroviral gene transfer to chondrocytes within collagen scaffolds for the treatment of osteochondral defects showed that far higher transfection rates (up to 100%) can be achieved with AAV viral transfection methods (Ueblacker et al, 2007). A replication-defective adenovirus can be used for high transfection efficiency as already been extensively used in recent past (Fujita et al, 1995). Therefore future work was considered to improve transfection efficiency by viral based methods.

Section III:

4.8 Stable Transgene Overexpression studies

The main focus of this thesis was to investigate genes that may have a potential role in cancer cell invasion/proliferation and potentially result in downstream metastasis of cancer. Previously in the lab a comparative gene expression profiling between highly invasive (DLKP-1, DLKP-2 and TXT-2) and less invasive (TXT-1 and VCR) lung cancer variant lines was performed. This work identified many differentially regulated genes some of which may potentially serve as molecular 'signatures' for invasiveness in lung cancer cell lines. These types of signatures may help provide earlier diagnosis and influence and individualise the therapies prescribed to cancer patients thereby improving prognosis. The results in the thesis identified transcripts associated with a more aggressive invasive phenotype and demonstrate that transiently altering the expression of some of these mRNAs can modulate the invasive capacity of these lung cancer cells (Pierce et al, 2008).

The gene targets GLP1R, KCNJ8, TFPI2 and S100A13 were differentially upregulated in DLKP-1, DLKP-2 and TXT-2 invasive cell lines. Except GLP1R the other 3 gene targets, of which functional relevance had been transiently validated in the lab previously and were predicted to be of potential therapeutic importance.

- KCNJ8 knockdown reduced invasion and proliferation in invasive cell lines but transient cDNA overexpression in non-invasive cell lines did not have any impact on invasion. It was therefore an interesting target to validate in our stable overexpression system, because as we know from the previous study that transient overexpression did not have any significant impact on in vitro invasion.
- TFPI2 knockdown increased invasion and proliferation in non invasive cell lines but transient overexpression did not have any impact on the invasive phenotype in invasive cell lines. Therefore stable overexpression to further investigate its role in cancer invasion was necessary.
- Similarly it was found that S100A13 was differentially expressed in the panel of cell lines studied, correlating with qPCR data. Decreasing S100A13

expression had no effect on proliferation but did decrease invasion. However transiently increasing S100A13 expression had no effect on invasion in the less/non-invasive cell lines, despite a measurable increase in protein expression following transient transfection (Pierce et al, 2008). S100A13 was therefore chosen to determine whether stable overexpression in our targetable system would impact on this phenotype in the cell line models.

Furthermore to investigate the stable overexpression of these chosen gene targets in our model cell lines and to monitor the impact of gene dosage effect on cell invasion in our stable overexpression studies we also included GLP1-R (Glucagon like peptide 1 receptor) which was found to be differentially up-regulated in invasive compared to mildly invasive cell lines.

These genes were subcloned into pShuttle vector (Section 3.11) co-transfected with Cre individually into two selected master targetable DLKP cell lines. DLKP targetable clones 17 and 11 were selected from our stability studies (section 3.2), which were different in their transgene expression levels as illustrated in figure 4.8A. The rationale behind selecting these two targetable clones was to investigate the dosage effect of transgene expression. They were *Cre* treated to remove *geo* leaving a LoxP site as an endogenous, targetable locus. Subsequent co-transfections were carried out (section 2.8.1), with constructed transgene shuttle vectors and Cre.

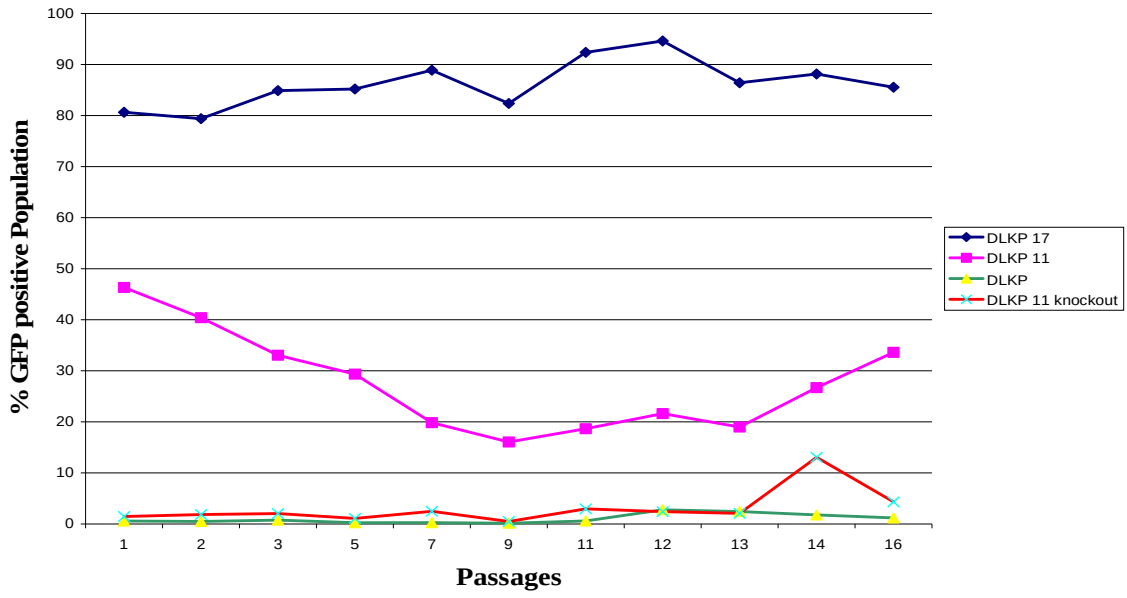

Figure 4.8A GFP expressing DLKP clones 17 (high expresser) and 11 (low expresser) compared to DLKP parent and DLKP geo knock out clone.

4.8.1 Targeted stable GLP1-R transgene overexpression in DLKP 17 and 11 cell lines

Glucagon like peptide 1 receptor (GLP1-R) is a 463 amino-acid member of the G protein coupled receptor (GPCR) superfamily which is highly expressed in islet β-cells. It has been recently reported that it is differentially expressed in several tumor types, but its role in cancer cell invasion has not been reported (Korner et al, 2007).
A study involving screening of GLP1-R expression by northern blot analysis revealed the constitutive expression of GLP1-R in stomach, islets and lungs (Thorens, 1992).

A 50% decrease in proliferation was observed in DLKP 17 GLP1-R and an ~18-20% decrease in DLKP 11 GLP1-R overexpressing cells relative to empty vector transfected stable cells. In vitro invasion assay of DLKP 17 and 11 GLP1-R overexpressing cells revealed that non-invasive DLKP 17 became invasive due to GLP1-R overexpression but there was no significant effect on the invasive DLKP 11 cell line was observed (Section 3.17.2). In order to investigate whether the GLP1-R effect was cell line specific or not we transiently overexpressed GLP1-R in non invasive MCF-7 breast carcinoma cell line. GLP1-R overexpression induced invasion in vitro in this cell line suggesting a more general role for GLP1-R in invasion.

To investigate whether we could reverse the effect of GLP1-R overexpression on invasion and proliferation we performed GLP1-R siRNA functional knockdown in GLP1-R stably overexpressing cell lines. We observed a significant rescue in the proliferation (~15%) in both DLKP 17 and 11 GLP1-R overexpressing clones. Similarly a significant reversal (40-60%) in the invasion phenotype was observed in both DLKP 17 and 11 GLP1-R overexpressing clones. This provided further evidence that the observed induction in invasion in GLP1-R transfected cells was specifically due to elevated expression of this protein.

4.8.2 Assigning role for GLP1-R in cancer cell invasion

This work suggests a previously unreported role for GLP1-R in invasion and proliferation. Drucker et al, (1987) reported that stimulation of GLP1-R and GLP2R in islet cells via GLP1 or GLP2 induces proliferation, differentiation and inhibits apoptosis. Multiple G-protein coupled receptors act through the cAMP/PKA signal transduction pathway. These receptors are coupled to G-proteins which either stimulate (G_s) or inhibit (G_i) (Kamp, 2000). Normally activation of GLP1-R leads to activation of Adenylate cyclase (AC) which catalyses the conversion of ATP to cAMP which then activates Protein kinase A (PKA) (Thorens, 1992). Our experimental observations definitely suggest an important role of GLP1-R in cancer cell invasion which may be independent of proliferation. This was evident from our results that the stable overexpression of GLP1-R in non invasive DLKP 17 cell line induced invasion but decreased proliferation. DLKP 11 which is already an invasive cell line did not appear to any impact on invasion due to GLP1-R overexpression but reduced proliferation. Korner et al, (2007) surveyed the expression pattern of GLP1-R in a wide spectrum of human tumours (n=149) and nonneoplastic human tissues (n=209) using receptor autoradiography. Their study concluded that GLP1-R is expressed at relatively high levels in tumor tissues. Therefore.
, it could be used as novel molecular target for identification and targeted therapy. The mechanism by which GLP1-R specifically induces the invasive phenotype remains unclear at present and further investigation is required to delineate its role.

4.9 Targeted stable KCNJ8 transgene overexpression in DLKP 17 and 11 cell lines

This work was done with previous knowledge of a role for KCNJ8 in cancer cell invasion previously observed in our laboratory (Pierce, A PhD (2006 NICB). KCNJ8 was identified as a gene potentially involved in invasion in microarray studies involving DLKP and its drug variants with altered invasion phenotype. KCNJ8 expression was increased in the more invasive cell lines compared to less invasive cell lines. A study of KCNJ8 mRNA expression by qRT-PCR confirmed increased

expression in the invasive cell lines DLKP-1, DLKP-2 and TXT-2 compared with the less invasive cell lines TXT-1 and VCR (Pierce A, PhD thesis 2005).
The observations were limited to transient overexpression and siRNA knockdown studies. Therefore we wanted to evaluate the role of KCNJ8 using our targetable stable overexpression model. Following cDNA transfections stable overexpression was confirmed in both DLKP 17 and DLKP 11 cell lines by qRT-PCR but western blot analysis did not indicate any difference at the protein level relative to empty vector transfected cell lines. Because KCNJ8 levels in the DLKP 17 and 11 cells was already at high levels any small increase may not have been detected by western blot analysis. We examined DLKP 17 and DLKP 11 KCNJ8 in an in vitro invasion assay and found that non invasive DLKP 17 had become invasive and invasive DLKP 11 was 15% more invasive. However an inverse effect on proliferation was observed in the two cell lines.

4.9.1 Assigning a function for KCNJ8

KCNJ8 mRNA levels were 2.5 fold in upregulated in DLKP 17 compared to vector control and 1.2 fold in upregulated DLKP 11 compared to vector control. Our results indicate that KCNJ8 contributes to the induction of invasion in both DLKP 17 and 11. However, a 20% decrease in proliferation in DLKP 17 and a 45% increase in proliferation in DLKP11 suggested that the increased invasion in DLKP 17 is independent of proliferation but were not same with already invasive DLKP 11. It may be that the phenotype observed was cell line specific.

Potassium channel (KCh) is composed of two main sub-families of channels 1) KCh voltage dependent (Kv) 2) Inward-rectifier KCh (Kir) family. Kv1.3 the most documented of the Kv1 family and it is overexpressed in breast, colon and prostate cancer. Kv1.1 and Kv1.5 show impaired expression in breast and glioma malignant cell lines, respectively. KCNJ8 belongs to the Kir family. Besides the role of potassium channel (KCh) during cell growth, it is also found to be de-regulated in highly proliferating cancer cells. Furthermore, the expression of KCh is impaired in several types of tumours. Studies suggest that a certain grade of malignancy correlates with the

expression of KCh. Although several types of KCh have been associated with a highly proliferative state only a few types have clearly oncogenic effects such as Kv10.1 and K2p9.1 that generate oncogenic phenotypes when introduced in healthy animals. Altered expression of members from all groups of KCh has been found in different types of tumours and cancer cells (Pei et al, 2003 and Pardo et al, 1999).

The qPCR results from (Pierce A. PhD 2005) indicated that KCNJ8 was differentially expressed in the panel of cell lines studied, in agreement with array data. Decreasing KCNJ8 expression had no effect on proliferation, but did increase invasion. Increasing KCNJ8 expression had no effect on invasion in the non-invasive cell lines. However, western blots for KCNJ8 overexpression were not conclusive. Our western blots were not suggestive of any differential expression at protein levels. Conclusion is that the impact on invasion and proliferation may not be as a direct impact of KCNJ8 overexpression, but could be due to off-target effects. Studies by Felipe et al, (2006) show increase of Kir proteins in breast and lung cancers. Further they have also noticed that the expression of KCa1.1, Ca^{2+}-activated K^+ (BK) and KCa3.1 Intermediate K conductance (IK) is also abundant in neuroblastoma and prostate cancer and correlated malignancy in breast and lung cancer cell lines due to altered expression of K2p9.1 (Felipe et al, 2006).

There is also increasing interest in the potential implications of K^+ channels as pharmacological targets for cancer therapy and for use as biomarkers to aid diagnosis (Wang, 2004). Binggeli and Weinstein (1986) proposed that altered signalling of plasma membrane electric potential of cancer cells could contribute to tumour growth. Bianchi et al, (1998) showed that plasma membrane electric potential in tumour cells is often modulated by the activity of K^+ channels. Though our experiments are inconclusive in terms of a function for KCNJ8 in the regulation of proliferation, there is a strong indication for a role in cancer cell invasion, independent of proliferation.

4.10 Targeted stable TFPI2 transgene overexpression in DLKP 17 and 11 cell lines

The observations in our laboratory previously concerning the effect of TFPI2 on the invasive phenotype with transient overexpression and siRNA induced knockdown. Hence, we decided to use this gene in our stable overexpression model cell line system. We had two cell lines with inverse invasive phenotype, i.e. DLKP 17 (non-invasive) and DLKP 11(invasive). Investigation of the effect of prolonged expression of TFPI2 in these cells with different transgene expression as well as invasive characteristics was considered of interest.

TFPI2 is an ECM-associated serine protease inhibitor with a role in ECM degradation during tumour cell invasion and metastasis, wound healing and angiogenesis (Konduri et al, 2001). An early study by Sawaya et al, (1998) reported that recombinant TFPI2 inhibits plasmin that is bound to HT-1080 cells, preventing matrix degradation and invasion. Increasing TFPI2 expression, thereby inhibiting plasmin may be of therapeutic benefit in cancer therapy. Decreased TFPI2 mRNA expression was observed in our lab in the invasive cell lines, particularly in TXT-2, compared with the poorly invasive cell lines TXT-1 and VCR (Pierce A, PhD thesis 2005).

From qRT-PCR analysis in both DLKP 17 and 11 clones it was evident that the two clones had distinctively different TFPI2 stable overexpression in accordance with their parental expression levels. Unfortunately the antibody used was not able to detect TFPI2 protein in western blot analysis. In vitro invasion assay of TFPI2 overexpressing DLKP 17 and 11 cells revealed that non invasive DLKP 17 became invasive and invasive DLKP 11 was less, but it was not a significant decrease (refer fig. 3.21.2A&B). A proliferation assay showed decreased cell growth in DLKP 17 and increased in DLKP 11 (fig. 3.21.1A&B). TFPI2 expression exogenously by transient cDNA transfection had no effect on proliferation, but did decrease invasion dramatically (Pierce A, PhD 2005).

4.10.1 Assigning a function for TFPI2

The anti-invasive and increased proliferation phenotype of TFPI2 overexpression in invasive DLKP 11 was in agreement with previous studies. Konduri et al, (2001), stably transfected a vector expressing TFPI2 in the melanoma cell line C-32 and observed a decrease in invasion in TFPI2 over expressing clones. Sense and antisense vectors to TFPI2 were also used to examine the role of TFPI2 in human glioma invasiveness. Sense clones were much less invasive compared to antisense clones in vitro and formed smaller tumours in vivo. A study revealed that TFPI2 expression inhibited the invasive, but not the migratory capability of ovarian tumour cells in vitro (Zhong et al, 2003). Tanaka, (2003) reported that REF-1 (Retinal pigment epithelial cell factor) which is similar to TFPI2, showed growth promoting activity when overexpressed in Chinese hamster ovary (CHO) cells. The same effect was not observed in human fibroblasts.

From our work we found TFP12 stable overexpression increased invasion and decreased proliferation in DLKP 17 TFPI2 stable overexpressing cell line. Possible reasons why TFPI2 overexpression in non invasive DLKP 17 induced invasion could be a) DLKP is a poorly differentiated cell line (McBride et al, 1998). It can be subcloned into three different types i) Mesenchymal (M) ii) Squamous (S) and iii) Intermediate (I). DLKP 17 cell line appeared to resemble the squamous epithelial type. In addition, when it was analysed for its basal invasion ability it was found to be non-invasive. Conversely, the DLKP 11 cell line was invasive and appeared morphologically to resemble the mesenchymal type. B) Our model cell lines were DLKP 17(high expresser) and DLKP 11 (low expresser) in which TFPI2 was stably overexpressed. The gene dosages cold have impacted on invasion in DLKP 17; a non-invasive cell line has become invasive due to TFPI2 stable overexpression. Compared to DLKP 11 the overexpression of TFP12 in DLKP 17 was high. It appears to be that after a certain threshold of TFP12 levels in non-invasive DLKP 17 has induced invasion. As reported from other studies (Zhong et al, 2003). Tanaka, (2003), the TFPI2 effect may be cell type specific and could be dosage related as well.

4.11 Stable S100A13 transgene overexpression in DLKP 17 and 11 cell lines

In 1996 a new S100 member termed S100A13 was identified by screening expressed sequence tag (EST) databases (Wicki et al, 1996). Smirnov et al, (2005) identified S100A13 as a novel predictor of metastasis following its detection in circulating tumour cells in blood. Pierce et al, (2008) show that decreasing S100A13 expression in invasive cell lines can reduce their invasive capacity by as much as 84%. This is the first study to provide causal evidence for a role of S100A13 in invasion. Conversely, overexpression of exogenous S100A13 in less invasive cell lines (DLKP-1, DLKP-2 and TXT-2) was not sufficient to stimulate invasion. This may have been due to the transient nature of the experiment.

Therefore we decided to investigate S100A13 in our stable overexpression model system. After several attempts we were not able to isolate a stable S100A13 overexpressing DLKP cell line. The qRT-PCR screening of several clones confirmed no overexpression in both DLKP 17 and 11 clones. In our study we found that three out of four genes could be overexpressed but not S100A13. This was despite the presence of a strong viral promoter (CMV) and the generation of G418 resistant clones. A possible reason could be that DLKP cells may not tolerate stable S100A13 overexpression.

4.12 Summary

The qRT-PCR and western blot analysis revealed overexpression of GLP1-R as well as differences in the level of expression between two targetable DLKP (17 and 11) clones. A novel in vitro role of GLP1-R in cancer cell invasion was identified and we propose that GLP1-R may be sufficient to induce invasion. GLP1-R was anti-proliferative in our cell lines and the proinvasive effect was independent of proliferation.

qRT-PCR confirmed KCNJ8 overexpression but no distinct overexpression at the protein level was detectable. The pro invasive effect of KCNJ8 on non invasive cell

line was interesting. The proliferation assay results were inconclusive and suggested that it could be cell line specific.

Though there was differential up regulation of TFPI2 at the transcript level, there were issues with the antibody for western blot analysis. TFPI2 overexpression in non-invasive cell line background would not be expected to induce invasion and/or proliferation, but it did in our cell line model. On the other hand, overexpression in the invasive cell line reduced invasion and proliferation in agreement with other reports and confirming the observations in the transient experiments.

After several attempts we were unable to stably overexpress S100A13. It is not uncommon for cells to remain recalcitrant to overexpression of certain proteins due to detrimental physiological effects, and it may be that S100A13 is one such molecule.

Section IV:

4.13 MiRNAs in Invasion

MicroRNAs (miRNAs) are a class of small endogenous non coding RNA molecules whose normal function involves the regulation of gene expression post-transcriptionally. It is estimated that 3% of the genome encodes for miRNAs and roughly around 30% human protein coding genes are regulated by miRNAs (Barbarotto et al, 2008). Several studies have shown that uncontrolled variation in the expression levels of miRNAs or cluster of miRNAs may lead to abnormal cellular functions such as proliferation, differentiation and apoptosis. This can result in altered physiological homeostasis leading to disease and in particular there is evidence of a role in cancer. Although much effort is focussed on functional identification of the role of miRNAs and their related target genes in human physiology very few studies have concentrated on identifying translational targets of a particular miRNA. Target prediction has been performed using computational algorithms, comparing complementary 3'UTR sequence of target mRNAs to mature miRNA sequence. Several miRNA-target prediction software packages are currently available based on criteria such as a) Orthologous phylogenetic conservation of complementary 3'UTR target sequences, b) binding energy of duplex between miRNA-target, c) sequence complementarity between miRNA-target of 6-8bp of continuous pairing in the 5' half of the miRNA.

A single miRNA has the potential to bind to multiple mRNAs making it a key regulator of expression of several mRNAs simultaneously, unlike siRNAs which are target specific. Hsu et al, (2008) suggested that miRNAs regulate protein-protein interacting networks. However, it still remains a challenging task for proper identification of physiologically relevant miRNA-target interactions. The main focus of this project was to investigate miRNAs involved in cancer invasion/proliferation in an in vitro model system as well as to identify potential gene targets through proteomic profiling and comparing it with available insilico target predicting programmes.

4.13.1 MiRNAs Bioarray

In collaboration with Ambion, we performed miRNA bioarray studies comprising DLKP (parent, mildly invasive) Vs DLKPA (Adriamycin resistant, highly invasive) human lung cancer cell lines. Among several differentially regulated miRNAs we selected five miRNAs for PCR validation. The five miRNAs were mir-21, mir-27a, mir-29a, mir-30a5p and mir-30c. Based on miRNA qRT-PCR validation we selected three miRNAs for functional validation (fig. 3.25A). The selected miRNAs were mir-21, mir-27a and mir-29a**.** Functional validation, including effect on proliferation, drug toxicity, and invasion phenotype of DLKP and DLKPA was monitored. We investigated the effect due to overexpression and inhibition of miRNA activity in both cell lines. As these miRNAs were differentially regulated in DLKPA compared to DLKP, we suspected a role in cancer cell invasion.

4.13.2 Impact of transient overexpression of mir-21, mir-27a and mir-29a on invasion and proliferation phenotype in DLKP and DLKPA cell lines

Commercially available synthetic miRNA (anti and pre miRNAs) were transfected in DLKP and DLKPA cells and subjected to invasion and proliferation assay. Transient overexpression of mir-21 resulted in a small but significant increase in cellular proliferation. Mir-27a and mir-29a did not have any significant impact on DLKP and DLKPA proliferation (fig. 3.25.1 A&B). Mir-21 has previously been shown to act as an oncogene by down-regulating a tumor suppressor (Zhu et al, 2007). They found mir-21 is overexpressed in tumor tissues compared to their normal counterparts. Similarly Liu et al, (2008) showed mir-27a is an oncogene, whereby suppression of mir-27a inhibits gastric cancer cell growth. Therefore, we used mir-21 and mir-27a as biological controls in our experiments.

Both mir-21 and mir-27a miRNAs were pro invasive (refer to Section 3.26). Mertens-Talcott et al, (2007) studies in breast carcinoma cell lines, showed that mir-27a downregulates the expression of *Myt-1*. MYT1 inhibits cell cycle through enhanced

phosphorylation and inactivation of Cdc2 and transcription repressor ZBTB10. This further leads to overexpression of Sp1, Sp3, and Sp4 transcription factors which happens to promote tumor growth and angiogenesis. In addition, prohibitin has been identified as a direct target of mir-27a from a 3'UTR reporter assay and target specific knockdown of prohibitin (a DNA synthesis inhibitor) which decreased cancer cell growth (Scott et al. 2006). Our results also showed a decrease in cancer cell invasion but do not have any impact on proliferation, suggesting a transient effect of mir-27a may not have any impact on growth in our cell line models. Conversely mir-29a was anti invasive (refer fig. 3.26.A, B, C and D). A very interesting study by Fabbri M, (2007) revealed that enforced expression of mir-29a (as well as other family members mir-29b and mir-29c) in lung cancer cell lines rescued normal patterns of DNA methylation and induced re-expression of methylation-silenced tumor suppressor genes FHIT and WWOX. Although there were very few studies relating mir-29a with cancer from our initial results and the existing literature it is evident that the mir-29 family is a very important miRNA in cancer therapeutics.

4.13.3 Effect of Transient overexpression of mir-21, mir-27a and mir-29a on drug sensitivity in DLKP and DLKPA cell lines

One of the model cell lines used in this study DLKPA was an Adriamycin resistant cell line, developed in the NICB (Heenan et al, 1997). Adriamycin, an active medicine against many cancers, is one of the older chemotherapy drugs, having been in use for decades. The fact that we had identified miRNAs that were differentially expressed between DLKP and DLKPA meant that these could be related to either (or both) the invasive phenotype or the drug resistance phenotype. In light of this we wished to discover if any of the chosen targets impacted on the sensitivity of DLKPA to Adriamycin when dysregulated. Our proliferation assay results showed no significant impact on cell survival due to transient overexpression of target miRNAs in our model cell line (fig. 3.26.3A&B). A study involving a panel of paclitaxel-(A2780TAX, A2780TC1 and A2780TC3) and cisplatin-resistant (A2780CIS) cells was assessed by microarray analysis (Sorrentino et al, 2008). They found a target in miR-130a, whose down regulation was linked to the translational activation of the M-CSF gene, a known

resistance factor for ovarian cancer. Other studies with doxorubicin-resistant MCF-7 cells (MCF-7/DOX) show considerable dysregulation of the miRNAome profile (Kovalchuk et al, 2008). Transfection of the MCF-7/DOX-resistant cells with mir-451 resulted in increased sensitivity of cells to DOX, indicating that correction of altered expression of miRNA may have significant implications for therapeutic strategies aimed at cancer drug resistance. So far there are no known reports involving mir-21, mir-27a and mir-29a with respect to drug sensitivity studies in cancer. Our experiments based on impact on proliferation showed no significant effect of miRNA expression on drug sensitivity. Based on this it would appear that the differential expression of these particular miRNAs in DLKPA is not related to or at least not the cause of the drug resistant phenotype.

4.14 Stable overexpression of mir-29a in DLKPA cell line

When we first observed mir-29a as differentially expressed in our system, there was no previous evidence of mir-29a having an anti-invasive role. Therefore we proceeded to investigate the role and effect of mir-29a in cancer cell invasion. We cloned mir-29a in p4.1CMV-Neo plasmid vector (fig. 3.28A&B). A negative sequence was also cloned in p4.1CMV-Neo vector which was used as a control during stable overexpression studies. The qRT-PCR analysis confirmed clones were overexpressing mir-29a (fig. 3.28D). The clones were subjected to invasion and proliferation assay (fig. 3.29A, 3.30A&B). A significant decrease in cellular proliferation was observed due to mir-29a stable overexpression. A very interesting study by Fabbri M, (2007) revealed that enforced expression of mir-29a (as well as other family members mir-29b and mir-29c) in lung cancer cell lines rescued normal patterns of DNA methylation and induced re-expression of methylation-silenced tumor suppressor genes FHIT and WWOX. Mott et al, (2007) showed that mir-29 family members are involved in Mcl-1(anti-apoptotic Bcl2 family member) protein regulation and apoptosis. This might explain the observed impact on proliferation in DLKPA. Furthermore we demonstrate this effect is not cell type specific. Transiently transfected mir-29a in pancreatic cancer cell line PANC-1(highly invasive) considerably reduced invasion.

C-Myc, a well studied oncogene, has been reported to be involved in regulating the expression of mir-29a. From our qRT-PCR analysis of the relative mir-29a levels in DLKP versus DLKPA, it was evident that mir-29a was downregulated in DLKPA. We theorised based on previous studies and our functional results, that mir-29a-promoter activity in our model cell lines might reflect c-Myc expression which is upstream of mir-29a and represses mir-29a transcription. We decided to evaluate the endogenous c-Myc levels in our panel of cancer lines, DLKP (mildly invasive), DLKPA and PANC-1 (both highly invasive). The initial qRT-PCR data suggested there was no significant increase in c-Myc in the more invasive cell lines compared to mildly invasive cell line DLKP, though this was a first observation with technical replicates. Tsung-Cheng et.al (2008) reported that Myc directly up- regulates a pro-tumorigenic group of miRNAs known as the miR-17–92 cluster. This suggested that the reduced endogenous concentration of mir-29a in invasive cells may be in part due to increased c-Myc expression resulting in repression of mir-29a transcription. Further analysis including the impact of c-Myc dysregulation on mir-29a expression in our cell lines would be required to show this effect.

Recent literature revealed that not only mir-29a but its other two family members mir-29b and mir-29c are also involved in regulation of tumor progression. Overexpression of mir-29b reduced Mcl-1 protein expression in KMCH cholangiocarcinoma cell lines. This effect was direct, as mir-29b negatively regulated the expression of a reporter construct (Mcl-1 3' untranslated region UTR-based). Enforced mir-29b expression reduced Mcl-1 cellular protein levels and sensitized the cancer cells to tumor necrosis factor-related apoptosis-inducing ligand (TRAIL) cytotoxicity (Mott, 2007). A study in nasopharyngeal carcinomas (NPCs) showed miRNA mir-29c was expressed at one-fifth the levels in tumours as in normal epithelium (Sengupta et al, 2008). In NPC tumours, the lower mir-29c levels correlated with higher levels of multiple proteins whose 3′ UTRs can bind mir-29c at target sequences conserved across many vertebrates. Most of the mir-29c targeted genes identified encode extracellular matrix proteins, including multiple collagens and laminin γ1 that are associated with tumor cell invasiveness and metastatic potential, prominent characteristics of NPC. So from the existing literature it is evident that mir-29 family might prove to be important targets in cancer therapeutics.

4.15 Proteomic profiling of anti and pre-mir-29a treated DLKPA cell line

The transient overexpression of pre and anti mir-29a in our cell line model was found to modulate invasion by reducing it by 40% with pre-mir treatment and conversely increases invasion by 36% with anti-mir treatment. At the time this work was performed most of the genes that were predicted to be regulated by miRNAs were based on insilico analysis. Only one study involving mir-21 where the miRNAs targets were identified based on 2D-DIGE based proteomic analysis has been reported (Zhu et al, 2007). More recent emerging reports on mir-29 family members being involved in cancer and our initial experimental observation relating to effect on cancer cell invasion in vitro prompted us to proceed further with 2D-DIGE proteomic profiling of cells with dysregulated expression of mir-29a to identify and functionally evaluate possible gene targets.

4.16 Identification of Differentially Expressed Proteins

To identify possible gene targets being regulated by mir-29a in DLKPA cells we performed proteomic profiling of anti and pre-mir-29a treated DLKPA cell line by 2D-DIGE. The differentially regulated spot identification was based on BVA (Biological variation analysis). Spots representing ±1.2-fold change in expression and with a 1-WAY ANOVA score of ≤ 0.05 were considered for further identification. The differentially regulated protein list was normalized for control treatments. Identification of differentially regulated protein spots was performed (Table 3.33.i & ii) by MALDI-TOF or LC-MS. Recent studies involving stable isotope labelling of amino acids (SILAC) in cell culture based work to investigate the effect of specific miRNAs dysregulation on the cell proteome have provided greater insight (Vinther, 2006). A study involving mir-1 expression in HeLa cells revealed that 12 out of 504 investigated proteins were repressed by mir-1 transfection. This repressed set of genes significantly overlaps with mir-1 regulated genes that have been identified with DNA array technology and are predicted by computational methods (Vinther, 2006). Their findings demonstrate that SILAC can be used for miRNA target identification and

highly expressed miRNA can regulate the levels of many different proteins. In our study we show 121 spots being downregulated due to pre-mir-29a treatment and 85 spots upregulated by inhibiting mir-29a. Out of 121 spots 60 were identified and out of 85, 29 spots were identified. The unidentified spots tended to be low abundant protein spots which are always a challenge to identify. Bioinformatic analysis (PANTHER, Pathway studio and Pubmatrix) was applied to the list of differentially regulated proteins. Pathway Studio assigned possible functional roles of these proteins with the majority of the proteins biased towards apoptosis, differentiation, proliferation, and mutagenesis. PANTHER classified the differentially regulated proteins into ontological categories. Genes involved in a wide range of molecular functions (fig. 3.33.1A), biological processes (fig. 3.33.1B) and biological pathways (fig. 3.33.1C), were identified. Several genes which were interesting in relation to cancer cell invasion and metastasis and were downregulated due to pre-mir-29a overexpression were **PRDX6, ANX2, CMPK1, PEBP1, CNN2, SFRS1, PSMA2, ARL3, PPIB, PPIA and GMFB. ACTC1, SHOT1 and SERBP1** were upregulated due to anti-mir-29a treatment in the DLKPA cell line. Vertebrate mRNAs are targeted for post-transcriptional repression by miRNAs through mechanisms involving pairing of 3′ UTR seed matches to bases at the 5′ end of miRNAs (refer to Fig. 3.33.3A) (Nielsen, 2007). The above target mRNAs were also identified as possible mir-29a targets, based on in silico RNAhybrid prediction program that predicts seed match regions between a 5'miRNA and 3'UTR sequences of gene targets (Rehmsmeier, 2004).

4.17 Overview of Protein targets involved in different cellular processes

The proteomic profiling of possible targets of mir-29a left us with a valuable target gene list which was subjected to bioinformatics analysis to gain further insight into their potential role in cancer cell invasion. We used Pathway Studio 5.0, a bioinformatic programme aimed at the visualisation and analysis of biological pathways, gene regulation networks and protein interaction maps. It has an inbuilt database which connects to the available PubMed information. Pathway Studio works

by identifying relationships among genes, small molecules, cell objects and processes and builds pathways based on these relationships. The other important aspect of this software programme is that it allows a focussed search on pathways and cell signalling networks. We uploaded the list of differentially regulated protein targets and from the out put it was evident that majority of proteins were implicated in cellular process like proliferation, differentiation, motility, apoptosis, and mutagenesis. The first three would be in keeping with our observed effect on invasion and cell growth. However, it is important to note that the knowledge that more commonly studied process are more likely to score 'hits' in this type of database. At the same time, it is a useful way to subgroup the targets in order to consider their importance in the context of this study. LGALS1 (Horie, 1999) and PPIA (Jin, 2004) were known to positively regulate apoptosis. HSPB1 (Dias, 2002), PRDX6 (Chen, 2003), MIF (Amin, 2003), CFL1 (Seike, 2003), PRDX3 (Young, 2004), and PRDX2 (Lin, 2003) were reported to be negative regulators of apoptosis. PPIB (Rycyzyn, 2000), HSPB1 (Cornford, 2000) were positive regulators of cell proliferation while GMFB (Lim, 1990), and ANXA1 (Rhee, 2000) were negative regulators. Similarly PPIB (Vanpouille, 2004), GRB2 (Atabey, 2001) and ANXA1 (Ernst, 2004) had known positive impact on motility and ANXA2 (Barwe, 2005) was a negative regulator of this process.

4.17.1 Apoptosis

LGALS1 and PPIA were known to positively regulate apoptosis. HSPB1, PRDX6, MIF, CFL1, PRDX3, and PRDX2 are negative regulators of apoptosis. All these targets were found to be downregulated due to mir-29a overexpression. There are different apoptotic pathways in high and low metastatic ability lung cancer cells. Apoptosis involves a series of biochemical events that lead to a variety of morphological changes, including blebbing, changes to the cell membrane such as loss of symmetry and attachment, chromatin condensation, cell shrinkage (Kerr et al, 1972; Wyllie et al, 1980). Several studies categorically substantiated that the cells that escape programmed cell death result in malignancy. HSPB1 (HSP27) is reported to negatively regulate apoptosis and also reported to have positive impact on proliferation. Peptidoprolyl isomerase A or PPIA or Cyclophillin A, the protein encoded by this gene

is a member of the peptidyl-prolyl cis-trans isomerase (PPIase) family (Yurchenko et al, 2002). Studies by Li et al, (2006) with pancreatic cancer cells showed that PPIA was significantly overexpressed as a result of increased proliferation and growth. Bostwick et al, (2000) proposed that HSP27 expression is associated with poor prognosis in gastric, liver, and prostate carcinoma. LGALS1 is a positive regulator of apoptosis and has been reported to have a negative role in cell proliferation. Galectins constitute a gene family of β-galactoside-specific lectins that show high homology in their carbohydrate-binding site. Barondes et al, (1994) showed lectins are involved in many biological events and Galectin-1 is a laminin binding protein that recognizes poly N-acetyllactosamine chains on the basement membrane. Basement membrane proteins have a major influence on cell adhesion, migration, proliferation and also in tumor invasion and metastasis (Barsky et al, 1983). Van den Brule et al, (1995) examined in vitro galectin 1 mediated adhesion assay in melanoma, and results suggest that galectin-1 might participate in melanoma cell adhesion to laminin and therefore constitutes a possible modulator of invasion and metastasis. Low galectin-1 expression in tumours is associated with unusually long survival periods in patients. Conversely, high levels of galectin-1 expression have been observed for highly invasive tumours in the case of human surgical samples and of animal models (Camby et al, 2005). Camby et al, (2005) categorically showed that in U87 human glioblastoma cells that stable inhibition of galectin-1 expression alters the expression of a number of genes like cullin-2, p53, ADAM-15, and MAP-2 that either directly or indirectly influence adhesion, motility and invasion of human glioblastoma cells. A recent study involving both stable knockdown and transient-targeted knockdown by siRNA treatment induced an intracellular accumulation of integrin-beta1 suggesting galectin-1 uses an integrin mediated pathway in glioma malignancy (Fortin et al, 2008).

Shichi and Demar, (1990) proposed PRDX6 as a bifunctional 25 kDa protein with both GSH (Glutathione) peroxidase and phospholipase A_2 activities. Also PRDX6 is expressed in many organs, with a particularly high level of expression in the lungs. Chen et al, (2002) and Newcomb et al, (2004) showed oxidants play an important role in the modulation of cell proliferation, apoptosis, and synthesis of growth factors associated with tumor growth and invasion. Kinnula et al, (2004) suggested the unbalanced activation of antioxidant enzymes can induce carcinogenesis and malignant transformation by intracellular redox imbalance or exaggeration of oxidative stress.

Manevich and Fisher, (2005) showed that stable PRDX6 expression in cells protected against oxidative stress, whereas antisense treatment resulted in oxidant stress and apoptosis. Chang et al, (2007) did proteomic profiling between the MDA-MB-435HM cells and their parental counterparts MDA-MB-435 cells, and found that PRDX6 was highly overexpressed. Conversely, siRNA knockdown of specific PRDX6 expression decreased the invasive potential of breast cancer cells, partially through regulation of uPAR, Ets-1, MMP-9, RhoC and TIMP-2 expression. Odreman et al, (2005) compared the protein pattern of low-grade fibrillary astrocytomas to that of glioblastoma multiforme by 2D electrophoresis and mass spectrometry analysis. Their result showed peroxiredoxin 1 and 6, the transcription factor BTF3, and alpha-B-crystallin were more highly expressed in glioblastoma multiforme whereas protein disulfide isomerase A3, the catalytic subunit of the cAMP-dependent protein kinase, and the glial fibrillary acidic protein were increased in low-grade astrocytomas. From the recent research it is confirmed that PRDX6 is a relatively new target for cancer gene therapy. Furthermore it being regulated by mir-29a to reduce invasion from our results makes it a very interesting target to look further at its role in cancer treatment in detail.

4.17.2 Motility

Directed migration of cells to inappropriate locations can result in life threatening consequences such as the congenital defects prominent in the brain. It contributes to pathologies including vascular disease, chronic inflammatory diseases, and tumor formation and metastasis (Horwitz and Webb, 2003). Understanding cell migration is also becoming important to emerging areas of biotechnology which focus on cellular transplantation and the manufacture of artificial tissues. Down regulated protein targets PPIB, GRB2, PRDX5 and ANXA1 are known to have positive impacts on motility and this is in keeping with our observation that increased mir-29a decreases invasion. ANXA2 and SFRS1 have been shown to be negative regulators of this process. A study was performed to investigate the role of AnxA1 in the invasion of a model epithelial cell line, SKCO-15, derived from colorectal adenocarcinoma (Babbin, 2006). Small interfering RNA-mediated knockdown of AnxA1 expression resulted in a significant reduction in invasion through Matrigel-coated filters. Localization studies

revealed a translocation of AnxA1 to the cell surface upon the induction of cell migration, and functional inhibition of cell surface AnxA1 using antiserum (LCO1) significantly reduced cell invasion. SFRS1 (splicing factor, arginine/serine-rich 1) was found to be decreased in Herceptin treated ErbB2-overexpressing cell lines and was also shown to affect cellular motility (Mukherji *et al,* 2006; Ghigna *et al,* 2005) Our analysis also reveals a predicted miR-29a binding site in the 3'UTR of SFRS1.

4.17.3 Cell proliferation

PPIB, HSPB1, GRB2, LGALS1, GMFB, and ANXA1 were identified as being downregulated due to mir-29a overexpression suggesting they might be direct targets of mir-29a action. PPIB, HSPB1 and GRB2 are known to positively regulate cell proliferation whereas LGALS1, GMFB, and ANXA1 are negative regulators. Heat shock proteins (HSPs) are overexpressed in a wide range of human cancers and have been implicated in tumour cell proliferation, differentiation, invasion, metastasis, death and recognition by the immune system. Calderwood et al, (2006) proposed two main strategies, based on heat shock proteins in tumour progression and response to therapy. Firstly, pharmacological modification of HSP expression or molecular chaperone activity and secondly, their use in anticancer vaccines exploiting their ability to act as immunological adjuvants. Ciocca and Calderwood, (2005) show they are useful biomarkers for carcinogenesis in some tissues and signal the degree of differentiation and the aggressiveness of some cancers including hyperplastic endometrium, uterine cervix, colon and hepatocellular carcinoma. Circulating levels of HSP and anti-HSP antibodies in cancer patients could be useful in tumour diagnosis.

Lee et al, (2008) examined NIH3T3 cells overexpressing HSP27, which were observed to have a retarded cell migration and invasion phenotype in wound-healing assays. Later they identified that FAK phosphorylation was affected and also reduced matrix metalloproteinase-2 (MMP-2) expression and hence that the FAK/STAT3/MMP-2 signalling pathway was being altered. In contrast from our proteomics study, HSP27 was found to be downregulated due to mir-29a treatment, which in turn reduced the invasive phenotype in our model cell lines.

Annexins belong to a family of the calcium-dependent phospholipid binding proteins. They are also substrates of receptor tyrosine kinases. Overexpression of Annexin II, which has been reported in various carcinomas, is thought to be associated with cell proliferation, differentiation and cell-cell adhesion in the pathogenesis of carcinoma (Emoto, 2001). In this study involving Annexin II and c-erbB-2 by using, immunohistochemistry in 153 primary gastric carcinomas revealed that Annexin II was expressed in 8 human gastric carcinoma cell lines (Emoto, 2001). It was more strongly expressed in the cell membrane than in the cytoplasm of tumor cells in primary gastric carcinoma tissues. Annexin II and c-erbB-2 overexpression were significantly correlated $p = 0.0002$) and patients with Annexin II had poorer prognoses ($p = 0.0066$). In our study mir-29a overexpression downregulates Annexin II and in turn reduced invasion in our cell line models. From literature it is clear that overexpression of AnnexinII indeed relating to tumor growth. Therefore AnnexinII could form a key regulator molecule in cancer therapeutics.

Section V:

4.18 Protein targets chosen for siRNA functional validation

From our proteomic profiling and bioinformatic analysis we selected four cancer cell invasion/metastasis related gene targets for specific siRNA knockdown studies. These target genes were differentially downregulated due to pre-mir-29a treatment in DLKPA cells. The rationale behind selection of specific gene targets was that knockdown of these genes had previously been associated with cancer cell invasion and/or proliferation. The target genes RAN, GRB2, MIF and ANX2 were chosen based on a literature search which revealed them to be involved in mechanisms of cancer cell invasion/metastasis.

Only RAN had any significant impact on the invasive phenotype of DLKPA. RAN knockdown was observed to result in significantly reduced invasion in DLKPA (fig. 3.38.2A&B). RAN knockdown at the protein level was confirmed with western blot analysis (fig. 3.38A). RAN knockdown also significantly reduced DLKPA proliferations refer fig. 3.37.1A). Knockdown of the other targets did not show any significant impact on invasion or proliferation in DLKPA. This was not surprising due to nature of miRNA regulation which involves group of genes being deregulated to effectively modulate any process i.e. a highly tuned regulation.

RAN (RAS-related nuclear protein) was identified as 1RRP-C chain of the RAN-GPPNHP-RANBD1 complex with -1.35 fold difference between pre-mir-control and pre-mir-29a treated DLKPA cell line. Vetter et al, (1999) showed the complex has four chains A, B, C, D. Chain A and C are composed of RAN and chain B and C are composed of NUCLEAR PORE COMPLEX PROTEIN NUP358 (RBP2). RAN is a small GTP binding protein involved in the control of DNA synthesis and cell cycle progression, and also is essential for the translocation of RNA and proteins through the nuclear pore complex (Sazer and Dasso, 2000). Esquela-Kerscher and Slack, (2006) revealed that RAN is also involved in exporting pre-miRNA in a complex with Exportin 5 from the nucleus to the cytoplasm. Kurisetty *et al* (2008) have recently demonstrated that RAN overexpression in a non-invasive rat mammary epithelial cell

line results in increased anchorage-independent growth, cell attachment, invasion through Matrigel™ in vitro and metastasis in rats. With all these intriguing literature relating RAN and its relevance in maintaining molecular balance as well as role in cancer invasion which was in agreement with our results led us to further investigate its link to mir-29a.

4.18.1 RAN 3' UTR reporter assay to evaluate target specificity of *mir-29a*

To further evaluate whether RAN may be a direct target of mir-29a we amplified the 3'UTR region of RAN and cloned downstream of GFP in a reporter plasmid. The rationale behind this was that miRNAs target 3'UTR region of mRNAs. Accordingly, cell lines expressing 3'UTR sequence of RAN cloned downstream of a reporter gene upon treatment with pre-mir-29a, would be expected to display reduced reporter protein expression if RAN was a direct target. We developed a mixed stable RAN 3'UTR GFP expressing DLKPA cell line by transfecting with the reporter plasmid (fig. 3.39A, B, C). Pre-mir-29a and negative-pre-mir-control were transiently transfected into the cells and they were monitored for GFP expression. At 72hrs there was a significant drop in GFP levels. The observation that the average fluorescence signal in cells stably expressing a GFP reporter gene fused to the RAN 3'UTR was reduced by only 5-6% suggests that the impact on endogenous RAN protein expression (35% down-regulated in proteomics analysis) might be secondary to the effect of miR-29a. However, the presence of a predicted miR-29a target site in the RAN 3'UTR using current algorithms (5nt match at 5' end of mir-29a) doesn't discount the possibility of some interaction between miR-29a and the mRNA transcript. Another consideration relates to a recent report demonstrating the combined action of miR-29 and miR-181 on Tcl1 to modulate its expression in CLL (Pekarsky *et al,* 2006). Like Tcl1, RAN is a strongly predicted target for *miR-181* binding. It may be that increased expression of both miRNAs is required for significant reduction in protein expression. On the other hand, RAN is a critical protein and the concentration range at which it is tolerated in cells is probably narrow. It has been demonstrated recently that non-canonical seed matches result in less extreme modulation of expression (Baek *et al,* 2008). Studies

reporting differential expression of several thousand genes in cells overexpressing particular miRNAs demonstrate that the degree of down-regulation of a target protein may be quite low (Baek *et al*, 2008; Selbach *et al,* 2008). This is consistent with the theory that miRNAs act more as modulators of protein expression – smoothing out more dramatic influences such as transcriptional activation or repression.

4.19 Effect of MIF siRNA knockdown on invasion and proliferation phenotype in DLKPA

Several studies relating to Macrophage Migration Inhibitory factor (MIF) in cancer invasion/metastasis/proliferation led us to look at its functional impact in our invasive cell line models. Since, MIF was downregulated in mir-29a (-1.63 fold) overexpressing cells, we hypothesized that siRNA induced knockdown of MIF might decrease the invasion phenotype in DLKPA cells. Downregulation of MIF was confirmed from qRT-PCR analysis (fig. 3.34.1A). Bloom and Bennett (1970) identified a product produced by T lymphocytes inhibited the random migration of cultured macrophages as Macrophage migration inhibitory factor (MIF). Li et al, (2004) studies reveal that MIF induced invasion through activation of MMP-9 and IL-8 in nasopharyngeal carcinoma cells (NPC). A recent study by Rendon BE et al (2007) reported that siRNA knockdown of MIF results in a >90% loss of both the migratory and invasive potential of human lung adenocarcinoma cells. They also found that reduction of Rac1 member of Rho GTPase family in MIF deficient cells. The functional impact of MIF knockdown was observed to have no significant impact on either invasion (fig. 3.34.3A&B) or proliferation (fig. 3.34.2A) phenotype in DLKPA cell line. Shimizu et al, (1999) for the first time reported that human melanocytes and melanoma cells express MIF and found that anti-MIF antibody injected into mouse drastically reduced tumor induced angiogenesis. Ren et al, (2003) observed that increased MIF serum levels correlated with increased IL-8 levels in hepatocellular carcinoma (HCC) patients compared to normal. A very well studied molecule in cancer progression did not seem to have any effect on our model cell line.

4.20 Effect of ANX2 siRNA knockdown on invasion and proliferation in DLKPA

Annexin A2 (ANX2) a Ca2+ -dependent phospholipid-binding protein, was found to be -1.21 downregulated in pre-mir-29a treated cells. Recent studies linking Annexin A2 to tumor invasion/metastasis (refer. Page 302) led us to select this gene target for siRNA specific knockdown studies in our cell line models. Knockdown was confirmed thorough qRT-PCR analysis. There was no significant impact on either the invasive or the proliferation phenotype of the DLKPA cell line. Emoto et al, (2001) compared annexin 2 levels in 8 gastric carcinoma cell lines to c-erb-2 overexpression. They found that annexin A2 overexpression is confined to the cell membrane rather than the cytoplasm of tumor tissues and upregulation of annexin A2 in patients had poor prognoses. Huang et al, (2008) show ANX2 is involved in p53-mediated apoptosis in lung cancer cell line. Overexpression of p53 decreased annexin 2 levels in highly metastatic Anip973 lung cancer cells. ANX2 specific siRNA knockdown inhibited proliferation, suggesting ANX2 is involved in p53 mediated apoptosis and cell growth.

Recent studies by Hastie et al, (2008) found that treatment of human prostrate cancer cell line 1542CP3TX with interferon gamma decreased ANX2 and its binding partner p11 by 4 fold. A decrease in invasion of the cells was observed due to IFNgamma and/or anti annexin 2 antibody treatment but not in LNCap2, which is an annexin 2 negative prostrate cancer cell line. From our results it is clear that, though increasing mir-29a expression results in decreased invasion of DLKPA cells and decreased expression of ANX2, reducing ANX2 alone was insufficient to replicate the phenotype. Indeed annexin A2 has a predicted seed 6nt seed match in its 3'UTR for mir-29a. This doesn't rule out ANX2 as having a role in mediating the mir-29a dependent effect in conjunction with many other proteins also. On the other hand the differential expression of ANX2 in these cells may have no causal role in the phenotype but merely be a result of it.

4.21 Effect of GRB2 siRNA knockdown on invasion and proliferation phenotype in DLKPA

From our proteomics studies GRB2 was -1.25 fold downregulated in mir-29a overexpressing DLKPA cells. The qRT-PCR analysis of endogenous GRB2 RNA levels was found to be very low in the DLKPA cell line. Further siRNA specific knockdown was confirmed from qRT-PCR analysis (fig. 3.36A). Lowenstein et al, (1992) showed that Growth factor receptor-binding protein 2 (GRB2) is an adapter protein critical in bridging signal transduction between the activated protein receptor tyrosine kinase (RPTK) and the RAS-mediated MAP kinase cascade. Dharmawardana et al, (2006) described a role for GRB2 in the oncogenesis of human malignancies, cell motility and angiogenesis processes contributing to tumor growth, invasiveness and metastasis. Studies by Jelovac et al, (2004) showed that an increase in tumour size due to letrazole treated in mouse bearing MCF-7 breast tumour. Further investigation led the to conclusion that overexpression of GRB2 activated Ras or MAP kinase signalling and possible cross talk with estrogen receptor (ER) in breast cancer cell lines treated with letrazole. In our invasive cell line model we did not observe any impact of GRB2 siRNA knockdown on invasion or proliferation. As our observation were based on transient knockdown of GRB2, and the fact that GRB2 key important growth related gene it may require a stable or prolonged knockdown to see any impact. Further work needs to be done to establish a le of mir-29a regulation of GRB2.

4.22 Summary

In summary this section discusses the role of miRNAs in cancer cell in vitro invasion and proliferation. Anti-mir29a increased and pre-mir29a decreased invasion in both DLKP and DLKPA (more evident in DLKPA). Conversely miRNA 21 and 27a treatment were observed to have the opposite effect on invasion. DLKPA cells were transfected with anti or pre-mir-29a and used for proteomic profiling. The 2D DIGE study identified more than 100 differentially regulated proteins. Two Lists were created, list 1 contained proteins downregulated due to pre-mir-29a treatment and list2

with proteins up regulated due to anti-miRNA treatment. Four gene targets were chosen for further siRNA specific functional validation.

The qRT-PCR analysis confirmed knockdown of all the targets. In vitro invasion and proliferation assays were performed. MIF, ANX2 and GRB2 did not have any effect on the invasive or proliferation phenotype. RAN knockdown resulted in dramatically decreased invasion and proliferation in DLKPA cell line. Flow-cytometer analysis revealed a 5-6% reduction in GFP-RAN-UTR reporter expression when transfected with mir-29a, implying that RAN might be a weak or downstream target of mir-29a.

We confirmed the effect of mir-29a on cancer cell invasion was not tissue specific by transfecting pre-mir-29a in PANC-1 and developed stable mir-29a overexpressing DLKPA cell lines. These cell lines had a dramatic reduction in invasion which correlated with the level of mir-29a expression. In conclusion we provide convincing evidence that mir-29a is an anti-invasive microRNA.

5.0 Conclusion and Future Work

5.1 Targetable DLKP cell Line

We describe the successful development of stable Cre-LoxP based targetable DLKP cell lines. Furthermore we demonstrated by using an insulator element that we could improve the specificity of the genetic construct used. We concluded that this system was suitable for the generation of clones for the study of overexpression of several genes which correlated with lung cancer cell invasion in vitro.

5.1.2 Stability assessment

In stable transgene overexpression in vitro, clonal variability in gene expression levels or sudden loss in transgene expression is a major hurdle in gene functional studies. To investigate the stability of transgene overexpression we performed a time course assessment by using thirty three stable DLKP clones expressing the fusion protein geo. These clones were subjected to regular passaging and freeze thaw for over four and a half months, with monitoring of the GFP expression by fluorescent microscopy and as well using flow-cytometer based evaluation of expression. From the stability assessment of a panel of DLKP geo overexpression clones we learned that, although the clones are from an isogenic population they had very different stability profiles, which may be due to different genomic integration sites demonstrating clearly the problems with random integration. In addition we were able to choose clones with different levels of transgene expression based on the results of this experiment.

5.1.3 Stable Transgene overexpression studies

DLKP 17 (high expression) and DLKP 11(low expression) were chosen. DLKP 17 was non invasive and DLKP 11 was highly invasive. Four transgenes (GLP1-R, TFPI2, KCNJ8, and S100A13) were selected, cloned in a shuttle vector and co-transfected with Cre. qRT-PCR and western blot analysis of GLP1-R overexpressing cells revealed difference in level of expression in the targetable DLKP (17 and 11) clones in keeping with the levels expected in these clones. A possible role for GLP1-R in promoting cancer cell invasion was established. The proliferation assay suggested that GLP1-R

was anti-proliferative in our cell lines and that the proinvasive effect was independent of cell proliferation.

qRT-PCR analysis confirmed KCNJ8 overexpression but western blot analysis revealed no obvious increase compared to control. The pro invasive effect of KCNJ8 on the non invasive cell line was interesting. The proliferation assay results were inconclusive. TFPI2 overexpression in the non invasive cell line increased invasion and proliferation. Overexpression in the invasive cell line reduced invasion and proliferation. cDNA transfection did not result in S100A13 overexpression.

5.2 LINE-1 element site specific targeting

An attempt was made to generate stable, targetable cell lines, using human Long Interspersed Nuclear Elements or LINE-1or L1 element as the targetable locus transposition of engineered L1s in cultured human cells occurs at reasonable frequency. The human genome is estimated to be comprised of ~17-20% of L1 elements. The Frequency of homologous recombination (HR) is very low (Yamane-Ohnuki et al., 2004) in cells other than stem cells. To increase the possibility of encountering a HR event we deliberately selected an abundant sequence target in the genome. Using human L1 element as target should help avoid targeting endogenous genes. This work demonstrates that even when targeting an extremely abundant genetic element in the genome, homologous recombination rates remain very low. 600 stably transfected single cell clones were screened by PCR without identifying a LINE-1 specific homologous targeting event.

5.3 MicroRNA and Proteomic studies

MirRNA expression profiling of invasive and anti invasive lung cancer cell lines identified several differentially regulated gene. Five of which were chosen for validation. Of these mir-21 and 27a were found to be down regulated in invasive cells and when their expression was modified exogenously both were found to be pro-invasive. Mir-29a upregulation caused a reduction in cell invasion as well as proliferation when stably overexpressed. Comprehensive proteomic profiling by 2D

DIGE of mir-29a treated DLKPA cells revealed more than 100 differentially regulated protein spots; (± 1.2 fold and 95% confidence in p-value as cut off criteria).

Four gene targets which were differentially downregulated due to mir-29a overexpression were chosen for further functional validation using siRNA mediated knockdown. qRT-PCR analysis confirmed the knockdown of all the targets. Knockdown of MIF, ANX2 and GRB2 did not have any effect on invasion or proliferation phenotype. However, RAN knockdown decreased invasion in DLKPA cells. We have shown that mir-29a may be involved in tuning RAN expression as well as hundreds of other genes.

Transfection of pre-mir-29a into PANC-1 (invasive pancreatic cancer cell line) also resulted in decreased invasion. This result suggested that anti-invasive effect of mir-29a was more general. We also performed stable overexpression of pre-mir-29a by cloning the endogenous mir-29a into a mammalian overexpression vector and developed a stable mir-29a overexpressing DLKPA cell line. These cells exhibited a dramatic reduction in invasion and proliferation. In conclusion, the data provides convincing evidence that mir-29a is an anti-invasive miRNA.

5.4 Future Work

5.4.1 Developing Stable Cell lines and Transgene Overexpression

Future work would involve selecting clones with similar invasiveness but with different transgene expression levels to further investigate dosage effect of transgenes on invasion and proliferation phenotype. In addition it would be interesting to select clones with similar transgene expression levels but different invasion phenotypes to investigate the impact of transgenes on invasion phenotype.

5.4.1.1 GLP1-R

Glucagon like Peptide 1 Receptor (GLP1-R) stable overexpression revealed a novel in vitro role in cancer cell invasion. This observation was not only confirmed in DLKP

but also in non-invasive breast carcinoma cell line MCF-7 which displayed induction of invasion following GLP1-R overexpression. The siRNA induced knockdown of GLP1-R rescued the non-invasive phenotype in DLKP 17 and 11 invasive cell lines.

It would be interesting to gain further insight into possible pathway involved in this regulation. One could utilize GLP1-R specific blocking agents. Exendin 9-39 is a GLP1-R antagonist (a mutant of Exendin-4, agonist of GLP1-R and analog of GLP1) ligand which functions as blocking agent for GLP1-R. Future work could involve blocking GLP1-R in DLKP 17 and 11 overexpressing cell lines and investigate impact on the invasion phenotype.

GLP1-R belongs to G-Protein coupled receptor family. G protein-coupled receptors are involved in many diseases, and are also the target of around half of all modern medicinal drugs (Pierce, 2002). It is also known that phosphorylation of GPCRs by several other kinases, such as protein kinases A and C (PKA and PKC) (Benovic et al., 1985; Roth et al., 1991) can result in receptor desensitization. Pro-angiogenic GPCRs activate a network of small GTPases, Akt and mitogen-activated protein kinase (MAPK) signalling that promotes the migration, survival and growth of endothelial cells (Dorsam, 2007). Future work involves in investigation of the downstream targets (signal transduction) of GLP1-R in relevance to cancer cell invasion.

5.4.2 To improve frequency of Homologous Recombination with LINE-1 element targeting

Our screen for LINE-1 specific HR events from 600 single cell DLKP clones indicated that the frequency was at least less than 1 in 600. The application of recombinant adeno associated virus (rAAV) transduction to improve frequency of homologous recombination is already underway. Therefore future work would involve using these vectors to try to improve the efficiency of HR at LINE1 loci in these cells.

5.4.3 MicroRNAs

So far there is no literature concentrating on the effects of mir-21, mir-27a and mir-29a in chemo therapeutic drug resistant models. Although from our transient overexpression or blocking experiments we did not observe any significant impact on drug sensitivity, it would interesting to investigate the impact of stable expression or blocking of these miRNAs on chemo therapeutic drug sensitivity. NICB harbours several different CDR related cancer cell lines, therefore a good opportunity to investigate the effect on invasion, proliferation due to altered drug sensitivity with miRNAs treatment.

Comprehensive proteomic profiling of possible mir-29a targets led us to several interesting candidate gene targets. Fourteen genes were predicted by RNAhybrid to be possessing mir-29a binding seed region in their 3'UTR. In this thesis only a few targets were functionally validated.

C-Myc, a well studied oncogene, has been reported to be involved in regulating the expression of mir-29a. The qRT-PCR data suggested a increased levels of c-Myc trend in invasive cell lines compared to mildly invasive cell line DLKP. Reports suggest that Myc directly up- regulates a pro-tumorigenic group of miRNAs known as the miR-17–92 cluster. This was also confirmed in our study that the reduced endogenous concentration of mir-29a in invasive cells may be in part due to increased c-Myc expression resulting in repression of mir-29a transcription. Further analysis including the impact of c-Myc dysregulation on mir-29a expression in these cell lines would be required to prove this, as well as confirming the observed increase in c-Myc mRNA at the protein level. Future work could also involve delineating the *c-Myc/mir-29a* associated gene regulation pathway in cancer cell invasion.

We also found that mir-29a has a predicted binding site for GLP1-R. mRNA qRT-PCR analysis of stable mir-29a overexpressing DLKPA clones showed decreased GLP1-R at mRNA level, although western blot results were inconclusive. It is already established through several studies that miRNA targets the 3'UTR region of mRNA to

dysregulate protein synthesis. So accordingly if we can mutate the predicted seed region (miRNA:3'UTR mRNA binding site) in 3'UTR of GLP1-R and further check for rescue on the impact of mir-29a expression, then that would be convincing enough to establish mir-29a-GLP1-R target specificity. Future work might involve GLP1-R 3'UTR mutation studies. In addition it would also be interesting to do similar 3'UTR mutation studies to validate the fourteen RNAhybrid predicted mir-29a target proteins by either using luciferase or GFP based reporter assays.

6.0 Bibliography

AGGARWAL, K., LEILA, H., CHOE & LEE, K. H. (2006) Shotgun proteomics using the iTRAQ isobaric tags Briefings in Functional Genomics and Proteomics 5(2):112-120.

AKEHURST, R. L., BRAZIER, J. E., MATHERS, N., O'KEEFE, C., KALTENTHALER, E., MORGAN, A., PLATTS, M. & WALTERS, S. J. (2002) Health-related quality of life and cost impact of irritable bowel syndrome in a UK primary care setting. Pharmacoeconomics, 20, 455-62.

AMIN, M. A., VOLPERT, O. V., WOODS, J. M., KUMAR, P., HARLOW, L. A. & KOCH, A. E. (2003) Migration inhibitory factor mediates angiogenesis via mitogen-activated protein kinase and phosphatidylinositol kinase. Circ Res, 93, 321-9.

ANDERSON, K. D., SENGUPTA, J., MORIN, M., NEVE, R. L., VALENZUELA, C. F. & PERRONE-BIZZOZERO, N. I. (2001) Overexpression of HuD accelerates neurite outgrowth and increases GAP-43 mRNA expression in cortical neurons and retinoic acid-induced embryonic stem cells in vitro. Exp Neurol, 168, 250-8.

ANDERSON, L. & SEILHAMER, J. (1997) A comparison of selected mRNA and protein abundances in human liver. Electrophoresis, 18, 533-7.

ANDREASEN, P. A., KJOLLER, L., CHRISTENSEN, L. & DUFFY, M. J. (1997) The urokinase-type plasminogen activator system in cancer metastasis: a review. Int J Cancer, 72, 1-22.

ATABEY, N., GAO, Y., YAO, Z. J., BRECKENRIDGE, D., SOON, L., SORIANO, J. V., BURKE, T. R., JR. & BOTTARO, D. P. (2001) Potent blockade of hepatocyte growth factor-stimulated cell motility, matrix invasion and branching morphogenesis by antagonists of Grb2 Src homology 2 domain interactions. J Biol Chem, 276, 14308-14.

ARGILES, J. M. (2005) Cancer-associated malnutrition. Eur J Oncol Nurs, 9 Suppl 2, S39-50.

AUSSEL, L., BARRE, F. X., AROYO, M., STASIAK, A., STASIAK, A. Z. & SHERRATT, D. (2002) FtsK Is a DNA motor protein that activates chromosome dimer resolution by switching the catalytic state of the XerC and XerD recombinases. Cell, 108, 195-205.

BABBIN, B. A., LEE, W. Y., PARKOS, C. A., WINFREE, L. M., AKYILDIZ, A., PERRETTI, M. & NUSRAT, A. (2006) Annexin I regulates SKCO-15 cell invasion by signaling through formyl peptide receptors. J Biol Chem, 281, 19588-99.

BAKER, R. K., HAENDEL, M. A., SWANSON, B. J., SHAMBAUGH, J. C., MICALES, B. K. & LYONS, G. E. (1997) In vitro preselection of gene-trapped embryonic stem cell clones for characterizing novel developmentally regulated genes in the mouse. Dev Biol, 185, 201-14.

BARBAROTTO, E., SCHMITTGEN, T. D. & CALIN, G. A. (2008) MicroRNAs and cancer: profile, profile, profile. Int J Cancer, 122, 969-77.

BAR-ELI, M. (1999) Role of interleukin-8 in tumor growth and metastasis of human melanoma. Pathobiology, 67, 12-8.

BARONDES, S. H., COOPER, D. N., GITT, M. A. & LEFFLER, H. (1994) Galectins. Structure and function of a large family of animal lectins. J Biol Chem, 269, 20807-10.

BARSKY, S. H., TOGO, S., GARBISA, S. & LIOTTA, L. A. (1983) Type IV collagenase immunoreactivity in invasive breast carcinoma. Lancet, 1, 296-7.

BARWE, S. P., ANILKUMAR, G., MOON, S. Y., ZHENG, Y., WHITELEGGE, J. P., RAJASEKARAN, S. A. & RAJASEKARAN, A. K. (2005) Novel role for Na,K-ATPase in phosphatidylinositol 3-kinase signaling and suppression of cell motility. Mol Biol Cell, 16, 1082-94.

BAYLIN, S. B. & HERMAN, J. G. (2000) DNA hypermethylation in tumorigenesis: epigenetics joins genetics. Trends Genet, 16, 168-74.

BENOVIC, J. L., PIKE, L. J., CERIONE, R. A., STANISZEWSKI, C., YOSHIMASA, T., CODINA, J., CARON, M. G. & LEFKOWITZ, R. J. (1985) Phosphorylation of the mammalian beta-adrenergic receptor by cyclic AMP-dependent protein kinase. Regulation of the rate of receptor phosphorylation and dephosphorylation by agonist occupancy and effects on coupling of the receptor to the stimulatory guanine nucleotide regulatory protein. J Biol Chem, 260, 7094-101.

BIANCHI, L., WIBLE, B., ARCANGELI, A., TAGLIALATELA, M., MORRA, F., CASTALDO, P., CROCIANI, O., ROSATI, B., FARAVELLI, L., OLIVOTTO, M. & WANKE, E. (1998) herg encodes a K+ current highly conserved in tumors of different histogenesis: a selective advantage for cancer cells? Cancer Res, 58, 815-22.

BINGGELI, R. & WEINSTEIN, R. C. (1986) Membrane potentials and sodium channels: hypotheses for growth regulation and cancer formation based on changes in sodium channels and gap junctions. J Theor Biol, 123, 377-401.

BIRD, A. (2002) DNA methylation patterns and epigenetic memory. Genes Dev, 16, 6-21.

BISHOP, J. O. & SMITH, P. (1989) Mechanism of chromosomal integration of microinjected DNA. Mol Biol Med, 6, 283-98.

BLAGOEV, B. & PANDEY, A. (2001) Microarrays go live--new prospects for proteomics. Trends Biochem Sci, 26, 639-41.

BLOOM, B. R. & BENNETT, B. (1970) Relation of the migration inhibitory factor (MIF) to delayed-type hypersensitivity reactions. Ann N Y Acad Sci, 169, 258-65.

BOSTWICK, D. G., NORLEN, B. J. & DENIS, L. (2000) Prostatic intraepithelial neoplasia: the preinvasive stage of prostate cancer. Overview of the prostate committee report. Scand J Urol Nephrol Suppl, 1-2.

BORGHAEI, R. C., RAWLINGS, P. L., JR. & MOCHAN, E. (1998) Interleukin-4 suppression of interleukin-1-induced transcription of collagenase (MMP-1) and stromelysin 1 (MMP-3) in human synovial fibroblasts. Arthritis Rheum, 41, 1398-406.

BRABLETZ, T., JUNG, A., DAG, S., HLUBEK, F. & KIRCHNER, T. (1999) beta-catenin regulates the expression of the matrix metalloproteinase-7 in human colorectal cancer. Am J Pathol, 155, 1033-8.

BROOKS, P. C., STROMBLAD, S., SANDERS, L. C., VON SCHALSCHA, T. L., AIMES, R. T., STETLER-STEVENSON, W. G., QUIGLEY, J. P. & CHERESH, D. A. (1996) Localization of matrix metalloproteinase MMP-2 to the surface of invasive cells by interaction with integrin alpha v beta 3. Cell, 85, 683-93.

BRUBAKER, P. L. & DRUCKER, D. J. (2002) Structure-function of the glucagon receptor family of G protein-coupled receptors: the glucagon, GIP, GLP-1, and GLP-2 receptors. Receptors Channels, 8, 179-88.

BUKRINSKY, M. (2002) Active site residues of cyclophilin A are crucial for its signaling activity via CD147. J Biol Chem, 277, 22959-65.

BURGESS-BEUSSE, B., FARRELL, C., GASZNER, M., LITT, M., MUTSKOV, V., RECILLAS-TARGA, F., SIMPSON, M., WEST, A. & FELSENFELD, G. (2002) The insulation of genes from external enhancers and silencing chromatin. Proc Natl Acad Sci U S A, 99 Suppl 4, 16433-7.

CAI, H. N. & SHEN, P. (2001) Effects of cis arrangement of chromatin insulators on enhancer-blocking activity. Science, 291, 493-5.

CAI, X., HAGEDORN, C. H. & CULLEN, B. R. (2004) Human microRNAs are processed from capped, polyadenylated transcripts that can also function as mRNAs. Rna, 10, 1957-66.

CAIRNS, R. A., KHOKHA, R. & HILL, R. P. (2003) Molecular mechanisms of tumor invasion and metastasis: an integrated view. Curr Mol Med, 3, 659-71.

CALIN, G. A., LIU, C. G., SEVIGNANI, C., FERRACIN, M., FELLI, N., DUMITRU, C. D., SHIMIZU, M., CIMMINO, A., ZUPO, S., DONO, M., DELL'AQUILA, M. L., ALDER, H., RASSENTI, L., KIPPS, T. J., BULLRICH, F., NEGRINI, M. & CROCE, C. M. (2004a) MicroRNA profiling reveals distinct signatures in B cell chronic lymphocytic leukemias. Proc Natl Acad Sci U S A, 101, 11755-60.

CALIN, G. A., SEVIGNANI, C., DUMITRU, C. D., HYSLOP, T., NOCH, E., YENDAMURI, S., SHIMIZU, M., RATTAN, S., BULLRICH, F., NEGRINI, M. & CROCE, C. M. (2004b) Human microRNA genes are frequently located at fragile sites and genomic regions involved in cancers. Proc Natl Acad Sci U S A, 101, 2999-3004.

CALDERWOOD, S. K., KHALEQUE, M. A., SAWYER, D. B. & CIOCCA, D. R. (2006) Heat shock proteins in cancer: chaperones of tumorigenesis. Trends Biochem Sci, 31, 164-72.

CALDERWOOD, S. K., THERIAULT, J. R. & GONG, J. (2005) How is the immune response affected by hyperthermia and heat shock proteins? Int J Hyperthermia, 21, 713-6.

CAMBY, I., DECAESTECKER, C., LEFRANC, F., KALTNER, H., GABIUS, H. J. & KISS, R. (2005) Galectin-1 knocking down in human U87 glioblastoma cells alters their gene expression pattern. Biochem Biophys Res Commun, 335, 27-35.

CAMPO, E., MUNOZ, J., MIQUEL, R., PALACIN, A., CARDESA, A., SLOANE, B. F. & EMMERT-BUCK, M. R. (1994) Cathepsin B expression in colorectal carcinomas correlates with tumor progression and shortened patient survival. Am J Pathol, 145, 301-9.

CHAMBERS, A. F., MACDONALD, I. C., SCHMIDT, E. E., KOOP, S., MORRIS, V. L., KHOKHA, R. & GROOM, A. C. (1995) Steps in tumor metastasis: new concepts from intravital videomicroscopy. Cancer Metastasis Rev, 14, 279-301.
CHAMBERS, A. F. & TUCK, A. B. (1993) Ras-responsive genes and tumor metastasis. Crit Rev Oncog, 4, 95-114.

CHAN, S. P. & SLACK, F. J. (2006) microRNA-mediated silencing inside P-bodies. RNA Biol, 3, 97-100.

CHANG, X. Z., LI, D. Q., HOU, Y. F., WU, J., LU, J. S., DI, G. H., JIN, W., OU, Z. L., SHEN, Z. Z. & SHAO, Z. M. (2007) Identification of the functional role of peroxiredoxin 6 in the progression of breast cancer. Breast Cancer Res, 9, R76.

CHEN, Y., CAI, J., MURPHY, T. J. & JONES, D. P. (2002) Overexpressed human mitochondrial thioredoxin confers resistance to oxidant-induced apoptosis in human osteosarcoma cells. J Biol Chem, 277, 33242-8.

CHEN, G. Q., ZHOU, L., STYBLO, M., WALTON, F., JING, Y., WEINBERG, R., CHEN, Z. & WAXMAN, S. (2003) Methylated metabolites of arsenic trioxide are more potent than arsenic trioxide as apoptotic but not differentiation inducers in leukemia and lymphoma cells. Cancer Res, 63, 1853-9.

Cho W.C.S., (2007) OncomiRs: the discovery and progress of microRNAs in cancers. Mol Cancer 6: 60.

CIOCCA, D. R. & CALDERWOOD, S. K. (2005) Heat shock proteins in cancer: diagnostic, prognostic, predictive, and treatment implications. Cell Stress Chaperones, 10, 86-103.

CORNFORD, P. A., DODSON, A. R., PARSONS, K. F., DESMOND, A. D., WOOLFENDEN, A., FORDHAM, M., NEOPTOLEMOS, J. P., KE, Y. & FOSTER, C. S. (2000) Heat shock protein expression independently predicts clinical outcome in prostate cancer. Cancer Res, 60, 7099-105.

COTTER, T. P., KEALY, N. P., DUGGAN, P. F., CURTAIN, A. & BREDIN, C. P. (1997) Elevated serum angiotensin converting enzyme levels in metastatic ovarian dysgerminoma. Respir Med, 91, 237-9.

CONDEELIS, J. (1993) Life at the leading edge: the formation of cell protrusions. Annu Rev Cell Biol, 9, 411-44.

CONSTIEN, R., FORDE, A., LILIENSIEK, B., GRONE, H. J., NAWROTH, P., HAMMERLING, G. & ARNOLD, B. (2001) Characterization of a novel EGFP reporter mouse to monitor Cre recombination as demonstrated by a Tie2 Cre mouse line. Genesis, 30, 36-44.

CRAIG, N. L. (1988) The mechanism of conservative site-specific recombination. Annu Rev Genet, 22, 77-105.

CRAWFORD, M., BRAWNER, E., BATTE, K., YU, L., HUNTER, M. G., OTTERSON, G. A., NUOVO, G., MARSH, C. B. & NANA-SINKAM, S. P. (2008) MicroRNA-126 inhibits invasion in non-small cell lung carcinoma cell lines. Biochem Biophys Res Commun, 373, 607-12.

CURRAN, S. & MURRAY, G. I. (2000) Matrix metalloproteinases: molecular aspects of their roles in tumour invasion and metastasis. Eur J Cancer, 36, 1621-30.

DANESI, R., DE BRAUD, F., FOGLI, S., DE PAS, T. M., DI PAOLO, A., CURIGLIANO, G. & DEL TACCA, M. (2003) Pharmacogenetics of anticancer drug sensitivity in non-small cell lung cancer. Pharmacol Rev, 55, 57-103.

DAVID, J. R. (1975) Macrophage activation induced by lymphocyte mediators. Acta Endocrinol Suppl (Copenh), 194, 245-61.

DEUTSCH, J. M. (2003) Evolutionary algorithms for finding optimal gene sets in microarray prediction. Bioinformatics, 19, 45-52.

DHARMAWARDANA, P. G., PERUZZI, B., GIUBELLINO, A., BURKE, T. R., JR. & BOTTARO, D. P. (2006) Molecular targeting of growth factor receptor-bound 2 (Grb2) as an anti-cancer strategy. Anticancer Drugs, 17, 13-20.

DIAS, S., SHMELKOV, S. V., LAM, G. & RAFII, S. (2002) VEGF(165) promotes survival of leukemic cells by Hsp90-mediated induction of Bcl-2 expression and apoptosis inhibition. Blood, 99, 2532-40.

DILLON, J. S., TANIZAWA, Y., WHEELER, M. B., LENG, X. H., LIGON, B. B., RABIN, D. U., YOO-WARREN, H., PERMUTT, M. A. & BOYD, A. E., 3RD (1993) Cloning and functional expression of the human glucagon-like peptide-1 (GLP-1) receptor. Endocrinology, 133, 1907-10.

DOMBROSKI, B. A., MATHIAS, S. L., NANTHAKUMAR, E., SCOTT, A. F. & KAZAZIAN, H. H., JR. (1991) Isolation of an active human transposable element. Science, 254, 1805-8.

DONG, J. T., LAMB, P. W., RINKER-SCHAEFFER, C. W., VUKANOVIC, J., ICHIKAWA, T., ISAACS, J. T. & BARRETT, J. C. (1995) KAI1, a metastasis suppressor gene for prostate cancer on human chromosome 11p11.2. Science, 268, 884-6.

DORSAM, R. T. & GUTKIND, J. S. (2007) G-protein-coupled receptors and cancer. Nat Rev Cancer, 7, 79-94.

DOUMA, S., VAN LAAR, T., ZEVENHOVEN, J., MEUWISSEN, R., VAN GARDEREN, E. & PEEPER, D. S. (2004) Suppression of anoikis and induction of metastasis by the neurotrophic receptor TrkB. Nature, 430, 1034-9.

DRUCKER, D. J., PHILIPPE, J., MOJSOV, S., CHICK, W. L. & HABENER, J. F. (1987) Glucagon-like peptide I stimulates insulin gene expression and increases cyclic AMP levels in a rat islet cell line. Proc Natl Acad Sci U S A, 84, 3434-8.

DUFFY, M. J. (2002) Urokinase plasminogen activator and its inhibitor, PAI-1, as prognostic markers in breast cancer: from pilot to level 1 evidence studies. Clin Chem, 48, 1194-7.

DURING, M. J., CAO, L., ZUZGA, D. S., FRANCIS, J. S., FITZSIMONS, H. L., JIAO, X., BLAND, R. J., KLUGMANN, M., BANKS, W. A., DRUCKER, D. J. & HAILE, C. N. (2003) Glucagon-like peptide-1 receptor is involved in learning and neuroprotection. Nat Med, 9, 1173-9.

EMOTO, K., SAWADA, H., YAMADA, Y., FUJIMOTO, H., TAKAHAMA, Y., UENO, M., TAKAYAMA, T., UCHIDA, H., KAMADA, K., NAITO, A., HIRAO, S. & NAKAJIMA, Y. (2001) Annexin II overexpression is correlated with poor prognosis in human gastric carcinoma. Anticancer Res, 21, 1339-45.

ERNST, S., LANGE, C., WILBERS, A., GOEBELER, V., GERKE, V. & RESCHER, U. (2004) An annexin 1 N-terminal peptide activates leukocytes by triggering different members of the formyl peptide receptor family. J Immunol, 172, 7669-76.

ESQUELA-KERSCHER, A. & SLACK, F. J. (2006) Oncomirs - microRNAs with a role in cancer. Nat Rev Cancer, 6, 259-69.

EUER, N., SCHWIRZKE, M., EVTIMOVA, V., BURTSCHER, H., JARSCH, M., TARIN, D. & WEIDLE, U. H. (2002) Identification of genes associated with metastasis of mammary carcinoma in metastatic versus non-metastatic cell lines. Anticancer Res, 22, 733-40.

EVANS, M. J., CARLTON, M. B. & RUSS, A. P. (1997) Gene trapping and functional genomics. Trends Genet, 13, 370-4.

FELIPE, A., VICENTE, R., VILLALONGA, N., ROURA-FERRER, M., MARTINEZ-MARMOL, R., SOLE, L., FERRERES, J. C. & CONDOM, E. (2006) Potassium channels: new targets in cancer therapy. Cancer Detect Prev, 30, 375-85.

FELSENFELD, G., BOYES, J., CHUNG, J., CLARK, D. & STUDITSKY, V. (1996) Chromatin structure and gene expression. Proc Natl Acad Sci U S A, 93, 9384-8.

FEARON, E. R. & VOGELSTEIN, B. (1990) A genetic model for colorectal tumorigenesis. Cell, 61, 759-67.

FEHMANN, H. C., JIANG, J., SCHWEINFURTH, J., WHEELER, M. B., BOYD, A. E., 3RD & GOKE, B. (1994) Stable expression of the rat GLP-I receptor in CHO cells: activation and binding characteristics utilizing GLP-I(7-36)-amide, oxyntomodulin, exendin-4, and exendin(9-39). Peptides, 15, 453-6.

FENG, J., CHANG, H., LI, E. & FAN, G. (2005) Dynamic expression of de novo DNA methyltransferases Dnmt3a and Dnmt3b in the central nervous system. J Neurosci Res, 79, 734-46.

FENG, Q., MORAN, J. V., KAZAZIAN, H. H., JR. & BOEKE, J. D. (1996) Human L1 retrotransposon encodes a conserved endonuclease required for retrotransposition. Cell, 87, 905-16.

FIDLER, I. J. (2002) Critical determinants of metastasis. Semin Cancer Biol, 12, 89-96.

FIDLER, I. J. & KRIPKE, M. L. (1977) Metastasis results from preexisting variant cells within a malignant tumor. Science, 197, 893-5.

FIELDS, P. A. (2001) Review: Protein function at thermal extremes: balancing stability and flexibility. Comp Biochem Physiol A Mol Integr Physiol, 129, 417-31.

FOWLKES, J. L., SUZUKI, K., NAGASE, H. & THRAILKILL, K. M. (1994) Proteolysis of insulin-like growth factor binding protein-3 during rat pregnancy: a role for matrix metalloproteinases. Endocrinology, 135, 2810-3.

FOWLKES, J. L., THRAILKILL, K. M., SERRA, D. M., SUZUKI, K. & NAGASE, H. (1995) Matrix metalloproteinases as insulin-like growth factor binding protein-degrading proteinases. Prog Growth Factor Res, 6, 255-63.

FORTIN, S., LE MERCIER, M., CAMBY, I., SPIEGL-KREINECKER, S., BERGER, W., LEFRANC, F. & KISS, R. (2008) Galectin-1 Is Implicated in the Protein Kinase C epsilon/Vimentin-Controlled Trafficking of Integrin-beta1 in Glioblastoma Cells. Brain Pathol.

FOURNEL, M., SAPIEHA, P., BEAULIEU, N., BESTERMAN, J. M. & MACLEOD, A. R. (1999) Down-regulation of human DNA-(cytosine-5) methyltransferase induces cell cycle regulators p16(ink4A) and p21(WAF/Cip1) by distinct mechanisms. J Biol Chem, 274, 24250-6.

FRIEDL, P. & WOLF, K. (2003a) Proteolytic and non-proteolytic migration of tumour cells and leucocytes. Biochem Soc Symp, 277-85.

FRIEDL, P. & WOLF, K. (2003b) Tumour-cell invasion and migration: diversity and escape mechanisms. Nat Rev Cancer, 3, 362-74.

FRISCH, S. M. & RUOSLAHTI, E. (1997) Integrins and anoikis. Curr Opin Cell Biol, 9, 701-6.

FUJITA, A., SAKAGAMI, K., KANEGAE, Y., SAITO, I. & KOBAYASHI, I. (1995) Gene targeting with a replication-defective adenovirus vector. J Virol, 69, 6180-90.

FUKUSHIGE, S. & SAUER, B. (1992) Genomic targeting with a positive-selection lox integration vector allows highly reproducible gene expression in mammalian cells. *Proc Natl Acad Sci U S A,* 89**,** 7905-9.

GALLEGO, M. E., SIRAND-PUGNET, P. & WHITE, C. I. (1999) Positive-negative selection and T-DNA stability in Arabidopsis transformation. Plant Mol Biol, 39, 83-93.

GDULA, D. A., GERASIMOVA, T. I. & CORCES, V. G. (1996) Genetic and molecular analysis of the gypsy chromatin insulator of Drosophila. Proc Natl Acad Sci U S A, 93, 9378-83.

GHIGNA, C., GIORDANO, S., SHEN, H., BENVENUTO, F., CASTIGLIONI, F., COMOGLIO, P. M., GREEN, M. R., RIVA, S. & BIAMONTI, G. (2005) Cell motility is controlled by SF2/ASF through alternative splicing of the Ron protooncogene. Mol Cell, 20, 881-90.

GOLIC, M. M., RONG, Y. S., PETERSEN, R. B., LINDQUIST, S. L. & GOLIC, K. G. (1997) FLP-mediated DNA mobilization to specific target sites in Drosophila chromosomes. Nucleic Acids Res, 25, 3665-71.

GUIRGUIS, R., MARGULIES, I., TARABOLETTI, G., SCHIFFMANN, E. & LIOTTA, L. (1987) Cytokine-induced pseudopodial protrusion is coupled to tumour cell migration. Nature, 329, 261-3.

GLOVER, S., NATHANIEL, R., SHAKIR, L., PERRAULT, C., ANDERSON, R. K., TRAN-SON-TAY, R. & BENYA, R. V. (2005) Transient upregulation of GRP and its receptor critically regulate colon cancer cell motility during remodeling. Am J Physiol Gastrointest Liver Physiol, 288, G1274-82.

GRIMM, T., SCHAFER, A. & HOGGER, P. (2004) Antioxidant activity and inhibition of matrix metalloproteinases by metabolites of maritime pine bark extract (pycnogenol). Free Radic Biol Med, 36, 811-22.

GROBHANS, H. & FILIPOWICZ, W. (2008) Proteomics Joins the Search for MicroRNA Targets. Cell, 4, 560-562, 22.

GRZMIL, M., HEMMERLEIN, B., THELEN, P., SCHWEYER, S. & BURFEIND, P. (2004) Blockade of the type I IGF receptor expression in human prostate cancer cells inhibits proliferation and invasion, up-regulates IGF binding protein-3, and suppresses MMP-2 expression. J Pathol, 202, 50-9.

GUO, W. & GIANCOTTI, F. G. (2004) Integrin signalling during tumour progression. Nat Rev Mol Cell Biol, 5, 816-26.

HANAHAN, D. & WEINBERG, R. A. (2000) The hallmarks of cancer. Cell, 100, 57-70.

HAY, W. W., JR. (1995) Metabolic interrelationships of placenta and fetus. Placenta, 16, 19-30.

HANSEN, S. G., COPE, T. A. & HRUBY, D. E. (2002) BiZyme: a novel fusion protein-mediating selection of vaccinia virus recombinants by fluorescence and antibiotic resistance. Biotechniques, 32, 1178, 1180, 1182-7.

HE, H., JAZDZEWSKI, K., LI, W., LIYANARACHCHI, S., NAGY, R., VOLINIA, S., CALIN, G. A., LIU, C. G., FRANSSILA, K., SUSTER, S., KLOOS, R. T., CROCE, C. M. & DE LA CHAPELLE, A. (2005a) The role of microRNA genes in papillary thyroid carcinoma. Proc Natl Acad Sci U S A, 102, 19075-80.

HE, L., THOMSON, J. M., HEMANN, M. T., HERNANDO-MONGE, E., MU, D., GOODSON, S., POWERS, S., CORDON-CARDO, C., LOWE, S. W., HANNON, G. J. & HAMMOND, S. M. (2005b) A microRNA polycistron as a potential human oncogene. Nature, 435, 828-33.

HOOD, J. D. & CHERESH, D. A. (2002) Role of integrins in cell invasion and migration. Nat Rev Cancer, 2, 91-100.

HORAK, C. E. & STEEG, P. S. (2005) Metastasis gets site specific. Cancer Cell, 8, 93-5.

HORIE, H., INAGAKI, Y., SOHMA, Y., NOZAWA, R., OKAWA, K., HASEGAWA, M., MURAMATSU, N., KAWANO, H., HORIE, M., KOYAMA, H., SAKAI, I., TAKESHITA, K., KOWADA, Y., TAKANO, M. & KADOYA, T. (1999) Galectin-1 regulates initial axonal growth in peripheral nerves after axotomy. J Neurosci, 19, 9964-74.

HUNTER, K. (2006) Host genetics influence tumour metastasis. Nat Rev Cancer, 6, 141-6.

HUTVAGNER, G. & ZAMORE, P. D. (2002) A microRNA in a multiple-turnover RNAi enzyme complex. Science, 297, 2056-60.

HASTIE, C., MASTERS, J. R., MOSS, S. E. & NAABY-HANSEN, S. (2008) Interferon-gamma reduces cell surface expression of annexin 2 and suppresses the invasive capacity of prostate cancer cells. J Biol Chem, 283, 12595-603.

HAY, W. W., JR. (1995) Metabolic interrelationships of placenta and fetus. Placenta, 16, 19-30.

HEENAN, M., O'DRISCOLL, L., CLEARY, I., CONNOLLY, L. & CLYNES, M. (1997) Isolation from a human MDR lung cell line of multiple clonal subpopulations which exhibit significantly different drug resistance. Int J Cancer, 71, 907-15.

HOESS, R., ABREMSKI, K. & STERNBERG, N. (1984) The nature of the interaction of the P1 recombinase Cre with the recombining site loxP. Cold Spring Harb Symp Quant Biol, 49, 761-8.

HSU, C. W., JUAN, H. F. & HUANG, H. C. (2008) Characterization of microRNA-regulated protein-protein interaction network. Proteomics, 8, 1975-9.

HYNES, R. O. (1992) Integrins: versatility, modulation, and signaling in cell adhesion. Cell, 69, 11-25.

SHADFORTH, I.P., DUNKLEY, T.P.J., LILLEY K.S. & BESSANT, C. (2005) i-Tracker: For quantitative proteomics using iTRAQ™ , *BMC Genomics*, **6:**145.

ILIOPOULOS, D., MALIZOS, K.N., OIKONOMOU, P., TSEZOU, A. (2008) Integrative microRNA and proteomic approaches identify novel osteoarthritis genes and their collaborative metabolic and inflammatory networks. PLOS ONE, 3(11), e3740.

INAGAKI, N., INAZAWA, J. & SEINO, S. (1995) cDNA sequence, gene structure, and chromosomal localization of the human ATP-sensitive potassium channel, uKATP-1, gene (KCNJ8). Genomics, 30, 102-4.

JASIN, M., MOYNAHAN, M. E. & RICHARDSON, C. (1996) Targeted transgenesis. Proc Natl Acad Sci U S A, 93, 8804-8.

JENSEN, M. L., KIAER, H., ANDERSEN, J., JENSEN, V. & MELSEN, F. (1997) Prognostic comparison of three classifications for medullary carcinomas of the breast. Histopathology, 30, 523-32.

JELOVAC, D., MACEDO, L., HANDRATTA, V., LONG, B. J., GOLOUBEVA, O. G., INGLE, J. N. & BRODIE, A. M. (2004) Effects of exemestane and tamoxifen in a postmenopausal breast cancer model. Clin Cancer Res, 10, 7375-81.

JIANG, X., MULTHAUPT, H., CHAN, E., SCHAEFER, L., SCHAEFER, R. M. & COUCHMAN, J. R. (2004) Essential contribution of tumor-derived perlecan to epidermal tumor growth and angiogenesis. J Histochem Cytochem, 52, 1575-90.

JIN, Z. G., LUNGU, A. O., XIE, L., WANG, M., WONG, C. & BERK, B. C. (2004) Cyclophilin A is a proinflammatory cytokine that activates endothelial cells. Arterioscler Thromb Vasc Biol, 24, 1186-91.

KAGAWA, W., KURUMIZAKA, H., IKAWA, S., YOKOYAMA, S. & SHIBATA, T. (2001) Homologous pairing promoted by the human Rad52 protein. J Biol Chem, 276, 35201-8.

KAMP, T. J. & HELL, J. W. (2000) Regulation of cardiac L-type calcium channels by protein kinase A and protein kinase C. Circ Res, 87, 1095-102.

KHVOROVA, A., LESCOUTE, A., WESTHOF, E. & JAYASENA, S. D. (2003) Sequence elements outside the hammerhead ribozyme catalytic core enable intracellular activity. Nat Struct Biol, 10, 708-12.

KIM, E. J. & HELFMAN, D. M. (2003) Characterization of the metastasis-associated protein, S100A4. Roles of calcium binding and dimerization in cellular localization and interaction with myosin. J Biol Chem, 278, 30063-73.

KINZIG, K. P., D'ALESSIO, D. A. & SEELEY, R. J. (2002) The diverse roles of specific GLP-1 receptors in the control of food intake and the response to visceral illness. J Neurosci, 22, 10470-6.

KINZLER, K. W. & VOGELSTEIN, B. (1996) Lessons from hereditary colorectal cancer. Cell, 87, 159-70.

KLEMKE, R. L., CAI, S., GIANNINI, A. L., GALLAGHER, P. J., DE LANEROLLE, P. & CHERESH, D. A. (1997) Regulation of cell motility by mitogen-activated protein kinase. J Cell Biol, 137, 481-92.

KNAUPER, V., WILL, H., LOPEZ-OTIN, C., SMITH, B., ATKINSON, S. J., STANTON, H., HEMBRY, R. M. & MURPHY, G. (1996) Cellular mechanisms for human procollagenase-3 (MMP-13) activation. Evidence that MT1-MMP (MMP-14) and gelatinase a (MMP-2) are able to generate active enzyme. J Biol Chem, 271, 17124-31.

KOBLINSKI, J. E., AHRAM, M. & SLOANE, B. F. (2000) Unraveling the role of proteases in cancer. Clin Chim Acta, 291, 113-35.

KOHN, E. C., FIGG, W. D., SAROSY, G. A., BAUER, K. S., DAVIS, P. A., SOLTIS, M. J., THOMPKINS, A., LIOTTA, L. A. & REED, E. (1997) Phase I trial of micronized formulation carboxyamidotriazole in patients with refractory solid

tumors:pharmacokinetics, clinical outcome, and comparison of formulations. J Clin Oncol, 15, 1985-93.

KORNER, M., STOCKLI, M., WASER, B. & REUBI, J. C. (2007) GLP-1 receptor expression in human tumors and human normal tissues: potential for in vivo targeting. J Nucl Med, 48, 736-43.

KRICHEVSKY, A. M., KING, K. S., DONAHUE, C. P., KHRAPKO, K. & KOSIK, K. S. (2003) A microRNA array reveals extensive regulation of microRNAs during brain development. Rna, 9, 1274-81.

KURUMIZAKA, H., IKAWA, S., NAKADA, M., EDA, K., KAGAWA, W., TAKATA, M., TAKEDA, S., YOKOYAMA, S. & SHIBATA, T. (2001) Homologous-pairing activity of the human DNA-repair proteins Xrcc3.Rad51C. Proc Natl Acad Sci U S A, 98, 5538-43.

KERR, J. F., WYLLIE, A. H. & CURRIE, A. R. (1972) Apoptosis: a basic biological phenomenon with wide-ranging implications in tissue kinetics. Br J Cancer, 26, 239-57.

KINNULA, V. L., TORKKELI, T., KRISTO, P., SORMUNEN, R., SOINI, Y., PAAKKO, P., OLLIKAINEN, T., KAHLOS, K., HIRVONEN, A. & KNUUTILA, S. (2004) Ultrastructural and chromosomal studies on manganese superoxide dismutase in malignant mesothelioma. Am J Respir Cell Mol Biol, 31, 147-53.

KOHN, E. C., FIGG, W. D., SAROSY, G. A., BAUER, K. S., DAVIS, P. A., SOLTIS, M. J., THOMPKINS, A., LIOTTA, L. A. & REED, E. (1997) Phase I trial of micronized formulation carboxyamidotriazole in patients with refractory solid tumors: pharmacokinetics, clinical outcome, and comparison of formulations. J Clin Oncol, 15, 1985-93.

KONDURI, S. D., TASIOU, A., CHANDRASEKAR, N. & RAO, J. S. (2001) Overexpression of tissue factor pathway inhibitor-2 (TFPI-2), decreases the invasiveness of prostate cancer cells in vitro. Int J Oncol, 18, 127-31.

KORNER, M., STOCKLI, M., WASER, B. & REUBI, J. C. (2007) GLP-1 receptor expression in human tumors and human normal tissues: potential for in vivo targeting. J Nucl Med, 48, 736-43.

KOVALCHUK, O., FILKOWSKI, J., MESERVY, J., ILNYTSKYY, Y., TRYNDYAK, V. P., CHEKHUN, V. F. & POGRIBNY, I. P. (2008) Involvement of

microRNA-451 in resistance of the MCF-7 breast cancer cells to chemotherapeutic drug doxorubicin. Mol Cancer Ther, 7, 2152-9.

KURISETTY, V. V., JOHNSTON, P. G., JOHNSTON, N., ERWIN, P., CROWE, P., FERNIG, D. G., CAMPBELL, F. C., ANDERSON, I. P., RUDLAND, P. S. & EL-TANANI, M. K. (2008) RAN GTPase is an effector of the invasive/metastatic phenotype induced by osteopontin. Oncogene, 27, 7139-49.

LANDRISCINA, M., SOLDI, R., BAGALA, C., MICUCCI, I., BELLUM, S., TARANTINI, F., PRUDOVSKY, I. & MACIAG, T. (2001) S100A13 participates in the release of fibroblast growth factor 1 in response to heat shock in vitro. J Biol Chem, 276, 22544-52.

LANIADO, M. E., FRASER, S. P. & DJAMGOZ, M. B. (2001) Voltage-gated K(+) channel activity in human prostate cancer cell lines of markedly different metastatic potential: distinguishing characteristics of PC-3 and LNCaP cells. Prostate, 46, 262-74.

LAVROVSKY, V. A., GUVAKOVA, M. A. & LAVROVSKY, Y. V. (1992) High frequency of tumour cell reversion to non-tumorigenic phenotype. Eur J Cancer, 28, 17-21.

LEDERBERG, J. (1998) Plasmid (1952-1997). Plasmid, 39, 1-9.

LEE, J. H., MIELE, M. E., HICKS, D. J., PHILLIPS, K. K., TRENT, J. M., WEISSMAN, B. E. & WELCH, D. R. (1996) KiSS-1, a novel human malignant melanoma metastasis-suppressor gene. J Natl Cancer Inst, 88, 1731-7.

LEE, R. C., FEINBAUM, R. L. & AMBROS, V. (1993) The C. elegans heterochronic gene lin-4 encodes small RNAs with antisense complementarity to lin-14. Cell, 75, 843-54.

LEE, Y., AHN, C., HAN, J., CHOI, H., KIM, J., YIM, J., LEE, J., PROVOST, P., RADMARK, O., KIM, S. & KIM, V. N. (2003) The nuclear RNase III Drosha initiates microRNA processing. Nature, 425, 415-9.

LEE, Y., JEON, K., LEE, J. T., KIM, S. & KIM, V. N. (2002) MicroRNA maturation: stepwise processing and subcellular localization. Embo J, 21, 4663-70.

LIOTTA, L. A., KLEINERMAN, J., CATANZARO, P. & RYNBRANDT, D. (1977) Degradation of basement membrane by murine tumor cells. J Natl Cancer Inst, 58, 1427-31.

LUISI-DELUCA, C. (1995) Homologous pairing of single-stranded DNA and superhelical double-stranded DNA catalyzed by RecO protein from Escherichia coli. J Bacteriol, 177, 566-72.

LUND, E., GUTTINGER, S., CALADO, A., DAHLBERG, J. E. & KUTAY, U. (2004) Nuclear export of microRNA precursors. Science, 303, 95-8.

LAKKA, S. S., KONDURI, S. D., MOHANAM, S., NICOLSON, G. L. & RAO, J. S. (2000) In vitro modulation of human lung cancer cell line invasiveness by antisense cDNA of tissue factor pathway inhibitor-2. Clin Exp Metastasis, 18, 239-44.

LANDER, E. S., LINTON, L. M., BIRREN, B., NUSBAUM, C., ZODY, M. C., BALDWIN, J., DEVON, K., DEWAR, K., DOYLE, M., FITZHUGH, W., FUNKE, R., GAGE, D., HARRIS, K., HEAFORD, A., HOWLAND, J., KANN, L., LEHOCZKY, J., LEVINE, R., MCEWAN, P., MCKERNAN, K., MELDRIM, J., MESIROV, J. P., MIRANDA, C., MORRIS, W., NAYLOR, J., RAYMOND, C., ROSETTI, M., SANTOS, R., SHERIDAN, A., SOUGNEZ, C., STANGE-THOMANN, N., STOJANOVIC, N., SUBRAMANIAN, A., WYMAN, D., ROGERS, J., SULSTON, J., AINSCOUGH, R., BECK, S., BENTLEY, D., BURTON, J., CLEE, C., CARTER, N., COULSON, A., DEADMAN, R., DELOUKAS, P., DUNHAM, A., DUNHAM, I., DURBIN, R., FRENCH, L., GRAFHAM, D., GREGORY, S., HUBBARD, T., HUMPHRAY, S., HUNT, A., JONES, M., LLOYD, C., MCMURRAY, A., MATTHEWS, L., MERCER, S., MILNE, S., MULLIKIN, J. C., MUNGALL, A., PLUMB, R., ROSS, M., SHOWNKEEN, R., SIMS, S., WATERSTON, R. H., WILSON, R. K., HILLIER, L. W., MCPHERSON, J. D., MARRA, M. A., MARDIS, E. R., FULTON, L. A., CHINWALLA, A. T., PEPIN, K. H., GISH, W. R., CHISSOE, S. L., WENDL, M. C., DELEHAUNTY, K. D., MINER, T. L., DELEHAUNTY, A., KRAMER, J. B., COOK, L. L., FULTON, R. S., JOHNSON, D. L., MINX, P. J., CLIFTON, S. W., HAWKINS, T., BRANSCOMB, E., PREDKI, P., RICHARDSON, P., WENNING, S., SLEZAK, T., DOGGETT, N., CHENG, J. F., OLSEN, A., LUCAS, S., ELKIN, C., UBERBACHER, E., FRAZIER, M., et al. (2001) Initial sequencing and analysis of the human genome. Nature, 409, 860-921.

LAW, E., GILVARRY, U., LYNCH, V., GREGORY, B., GRANT, G. & CLYNES, M. (1992) Cytogenetic comparison of two poorly differentiated human lung squamous cell carcinoma lines. Cancer Genet Cytogenet, 59, 111-8.

LEE, J. W., KWAK, H. J., LEE, J. J., KIM, Y. N., LEE, J. W., PARK, M. J., JUNG, S. E., HONG, S. I., LEE, J. H. & LEE, J. S. (2008) HSP27 regulates cell adhesion and invasion via modulation of focal adhesion kinase and MMP-2 expression. Eur J Cell Biol, 87, 377-87.

LEWIS, B. P., BURGE, C. B. & BARTEL, D. P. (2005) Conserved seed pairing, often flanked by adenosines, indicates that thousands of human genes are microRNA targets. Cell, 120, 15-20.

LI, M., ZHAI, Q., BHARADWAJ, U., WANG, H., LI, F., FISHER, W. E., CHEN, C. & YAO, Q. (2006) Cyclophilin A is overexpressed in human pancreatic cancer cells and stimulates cell proliferation through CD147. Cancer, 106, 2284-94.

LI, Z., LIN, S. X., LIANG, Y. J. & ZONG, Y. S. (2004) [Effect of macrophage migration inhibitory factor (MIF) on expression of MMP-2,MMP-9,and IL-8 in nasopharyngeal carcinoma cell strains]. Ai Zheng, 23, 130-5.

LIM, R., ZHONG, W. X. & ZAHEER, A. (1990) Antiproliferative function of glia maturation factor beta. Cell Regul, 1, 741-6.

LIN, F. L., SPERLE, K. & STERNBERG, N. (1985) Recombination in mouse L cells between DNA introduced into cells and homologous chromosomal sequences. Proc Natl Acad Sci U S A, 82, 1391-5.

LIN, X., ZHANG, F., BRADBURY, C. M., KAUSHAL, A., LI, L., SPITZ, D. R., AFT, R. L. & GIUS, D. (2003) 2-Deoxy-D-glucose-induced cytotoxicity and radiosensitization in tumor cells is mediated via disruptions in thiol metabolism. Cancer Res, 63, 3413-7.

LIU, T., TANG, H., LANG, Y., LIU, M. & LI, X. (2008) MicroRNA-27a functions as an oncogene in gastric adenocarcinoma by targeting prohibitin. Cancer Lett.

LOWENSTEIN, E. J., DALY, R. J., BATZER, A. G., LI, W., MARGOLIS, B., LAMMERS, R., ULLRICH, A., SKOLNIK, E. Y., BAR-SAGI, D. & SCHLESSINGER, J. (1992) The SH2 and SH3 domain-containing protein GRB2 links receptor tyrosine kinases to ras signaling. Cell, 70, 431-42.

MA, L., TERUYA-FELDSTEIN, J. & WEINBERG, R. A. (2007) Tumour invasion and metastasis initiated by microRNA-10b in breast cancer. Nature, 449, 682-8.

MANDINOVA, A., SOLDI, R., GRAZIANI, I., BAGALA, C., BELLUM, S., LANDRISCINA, M., TARANTINI, F., PRUDOVSKY, I. & MACIAG, T. (2003)

S100A13 mediates the copper-dependent stress-induced release of IL-1alpha from both human U937 and murine NIH 3T3 cells. J Cell Sci, 116, 2687-96.

MENDELL, J. T. (2005) MicroRNAs: critical regulators of development, cellular physiology and malignancy. Cell Cycle, 4, 1179-84.

METZLER, M., WILDA, M., BUSCH, K., VIEHMANN, S. & BORKHARDT, A. (2004) High expression of precursor microRNA-155/BIC RNA in children with Burkitt lymphoma. Genes Chromosomes Cancer, 39, 167-9.

MICHAEL, M. Z., SM, O. C., VAN HOLST PELLEKAAN, N. G., YOUNG, G. P. & JAMES, R. J. (2003) Reduced accumulation of specific microRNAs in colorectal neoplasia. Mol Cancer Res, 1, 882-91.

MIYAGI, Y., KOSHIKAWA, N., YASUMITSU, H., MIYAGI, E., HIRAHARA, F., AOKI, I., MISUGI, K., UMEDA, M. & MIYAZAKI, K. (1994) cDNA cloning and mRNA expression of a serine proteinase inhibitor secreted by cancer cells: identification as placental protein 5 and tissue factor pathway inhibitor-2. J Biochem, 116, 939-42.

MANEVICH, Y. & FISHER, A. B. (2005) Peroxiredoxin 6, a 1-Cys peroxiredoxin, functions in antioxidant defense and lung phospholipid metabolism. Free Radic Biol Med, 38, 1422-32.

MCBRIDE, S., MELEADY, P., BAIRD, A., DINSDALE, D. & CLYNES, M. (1998) Human lung carcinoma cell line DLKP contains 3 distinct subpopulations with different growth and attachment properties. Tumour Biol, 19, 88-103.

MCBURNEY, M. W., LAU, S., JARDINE, K., YANG, X. & DAVIES, B. (2001) Reexpression of a cluster of silenced transgenes is associated with their rearrangement. Genes Chromosomes Cancer, 32, 311-23.

MERTENS-TALCOTT, S. U., CHINTHARLAPALLI, S., LI, X. & SAFE, S. (2007) The oncogenic microRNA-27a targets genes that regulate specificity protein transcription factors and the G2-M checkpoint in MDA-MB-231 breast cancer cells. Cancer Res, 67, 11001-11.

MIGLIACCIO, A. R., BENGRA, C., LING, J., PI, W., LI, C., ZENG, S., KESKINTEPE, M., WHITNEY, B., SANCHEZ, M., MIGLIACCIO, G. & TUAN, D. (2000) Stable and unstable transgene integration sites in the human genome:

extinction of the Green Fluorescent Protein transgene in K562 cells. Gene, 256, 197-214.

MIZEJEWSKI, G. J. (1999) Role of integrins in cancer: survey of expression patterns. Proc Soc Exp Biol Med, 222, 124-38.

MOTT, J. L., KOBAYASHI, S., BRONK, S. F. & GORES, G. J. (2007) mir-29 regulates Mcl-1 protein expression and apoptosis. Oncogene, 26, 6133-40.

MUKHERJI, M., BRILL, L. M., FICARRO, S. B., HAMPTON, G. M. & SCHULTZ, P. G. (2006) A phosphoproteomic analysis of the ErbB2 receptor tyrosine kinase signaling pathways. Biochemistry, 45, 15529-40.

NAGASE, H., SUZUKI, K., ITOH, Y., KAN, C. C., GEHRING, M. R., HUANG, W. & BREW, K. (1996) Involvement of tissue inhibitors of metalloproteinases (TIMPS) during matrix metalloproteinase activation. Adv Exp Med Biol, 389, 23-31.

NAKAJIMA, M., MORIKAWA, K., FABRA, A., BUCANA, C. D. & FIDLER, I. J. (1990) Influence of organ environment on extracellular matrix degradative activity and metastasis of human colon carcinoma cells. J Natl Cancer Inst, 82, 1890-8.

NEILDEZ-NGUYEN, T. M., PARISOT, A., VIGNAL, C., RAMEAU, P., STOCKHOLM, D., PICOT, J., ALLO, V., LE BEC, C., LAPLACE, C. & PALDI, A. (2008) Epigenetic gene expression noise and phenotypic diversification of clonal cell populations. Differentiation, 76, 33-40.

NEWCOMB, E. W., TAMASDAN, C., ENTZMINGER, Y., ARENA, E., SCHNEE, T., KIM, M., CRISAN, D., LUKYANOV, Y., MILLER, D. C. & ZAGZAG, D. (2004) Flavopiridol inhibits the growth of GL261 gliomas in vivo: implications for malignant glioma therapy. Cell Cycle, 3, 230-4.

NOIROT, P. & KOLODNER, R. D. (1998) DNA strand invasion promoted by Escherichia coli RecT protein. J Biol Chem, 273, 12274-80.

NASH, H. M., BRUNER, S. D., SCHARER, O. D., KAWATE, T., ADDONA, T. A., SPOONER, E., LANE, W. S. & VERDINE, G. L. (1996) Cloning of a yeast 8-oxoguanine DNA glycosylase reveals the existence of a base-excision DNA-repair protein superfamily. Curr Biol, 6, 968-80.

NEILDEZ-NGUYEN, T. M., PARISOT, A., VIGNAL, C., RAMEAU, P., STOCKHOLM, D., PICOT, J., ALLO, V., LE BEC, C., LAPLACE, C. & PALDI, A. (2008) Epigenetic gene expression noise and phenotypic diversification of clonal cell populations. Differentiation, 76, 33-40.

NIELSEN, C. B., SHOMRON, N., SANDBERG, R., HORNSTEIN, E., KITZMAN, J. & BURGE, C. B. (2007) Determinants of targeting by endogenous and exogenous microRNAs and siRNAs. Rna, 13, 1894-910.

NEWCOMB, E. W., TAMASDAN, C., ENTZMINGER, Y., ARENA, E., SCHNEE, T., KIM, M., CRISAN, D., LUKYANOV, Y., MILLER, D. C. & ZAGZAG, D. (2004) Flavopiridol inhibits the growth of GL261 gliomas in vivo: implications for malignant glioma therapy. Cell Cycle, 3, 230-4.

NUNES-DUBY, S. E., KWON, H. J., TIRUMALAI, R. S., ELLENBERGER, T. & LANDY, A. (1998) Similarities and differences among 105 members of the Int family of site-specific recombinases. Nucleic Acids Res, 26, 391-406.

ODREMAN, F., VINDIGNI, M., GONZALES, M. L., NICCOLINI, B., CANDIANO, G., ZANOTTI, B., SKRAP, M., PIZZOLITTO, S., STANTA, G. & VINDIGNI, A. (2005) Proteomic studies on low- and high-grade human brain astrocytomas. J Proteome Res, 4, 698-708.

OSSOWSKI, L. & AGUIRRE-GHISO, J. A. (2000) Urokinase receptor and integrin partnership: coordination of signaling for cell adhesion, migration and growth. Curr Opin Cell Biol, 12, 613-20.

PARDO, L. A., DEL CAMINO, D., SANCHEZ, A., ALVES, F., BRUGGEMANN, A., BECKH, S. & STUHMER, W. (1999) Oncogenic potential of EAG K(+) channels. Embo J, 18, 5540-7.

PEDERSEN, S. K., HARRY, J. L., SEBASTIAN, L., BAKER, J., TRAINI, M. D., MCCARTHY, J. T., MANOHARAN, A., WILKINS, M. R., GOOLEY, A. A., RIGHETTI, P. G., PACKER, N. H., WILLIAMS, K. L. & HERBERT, B. R. (2003) Unseen proteome: mining below the tip of the iceberg to find low abundance and membrane proteins. J Proteome Res, 2, 303-11.

PETERSEN, L. C., SPRECHER, C. A., FOSTER, D. C., BLUMBERG, H., HAMAMOTO, T. & KISIEL, W. (1996) Inhibitory properties of a novel human Kunitz-type protease inhibitor homologous to tissue factor pathway inhibitor. Biochemistry, 35, 266-72.

PETERSON, D. S. (2007) Matrix-free methods for laser desorption/ionization mass spectrometry. Mass Spectrom Rev, 26, 19-34.

PFEFFER, S., ZAVOLAN, M., GRASSER, F. A., CHIEN, M., RUSSO, J. J., JU, J., JOHN, B., ENRIGHT, A. J., MARKS, D., SANDER, C. & TUSCHL, T. (2004) Identification of virus-encoded microRNAs. Science, 304, 734-6.

POLETTE, M., NAWROCKI-RABY, B., GILLES, C., CLAVEL, C. & BIREMBAUT, P. (2004) Tumour invasion and matrix metalloproteinases. Crit Rev Oncol Hematol, 49, 179-86.

POWELL, C., SHANSKY, J., DEL TATTO, M., FORMAN, D. E., HENNESSEY, J., SULLIVAN, K., ZIELINSKI, B. A. & VANDENBURGH, H. H. (1999) Tissue-engineered human bioartificial muscles expressing a foreign recombinant protein for gene therapy. Hum Gene Ther, 10, 565-77.

PEI, L., WISER, O., SLAVIN, A., MU, D., POWERS, S., JAN, L. Y. & HOEY, T. (2003) Oncogenic potential of TASK3 (Kcnk9) depends on K+ channel function. Proc Natl Acad Sci U S A, 100, 7803-7.

PEKARSKY, Y., SANTANAM, U., CIMMINO, A., PALAMARCHUK, A., EFANOV, A., MAXIMOV, V., VOLINIA, S., ALDER, H., LIU, C. G., RASSENTI, L., CALIN, G. A., HAGAN, J. P., KIPPS, T. & CROCE, C. M. (2006) Tcl1 expression in chronic lymphocytic leukemia is regulated by miR-29 and miR-181. Cancer Res, 66, 11590-3.

PIERCE, A., BARRON, N., LINEHAN, R., RYAN, E., O'DRISCOLL, L., DALY, C. & CLYNES, M. (2008) Identification of a novel, functional role for S100A13 in invasive lung cancer cell lines. Eur J Cancer, 44, 151-9.

PIERCE, K. L., PREMONT, R. T. & LEFKOWITZ, R. J. (2002) Seven-transmembrane receptors. Nat Rev Mol Cell Biol, 3, 639-50

POOLE, A. R., TILTMAN, K. J., RECKLIES, A. D. & STOKER, T. A. (1978) Differences in secretion of the proteinase cathepsin B at the edges of human breast carcinomas and fibroadenomas. Nature, 273, 545-7.

PORTEUS, M. (2007) Using homologous recombination to manipulate the genome of human somatic cells. Biotechnol Genet Eng Rev, 24, 195-212.

RAY, M. K., FAGAN, S. P. & BRUNICARDI, F. C. (2000) The Cre-loxP system: a versatile tool for targeting genes in a cell- and stage-specific manner. Cell Transplant, 9, 805-15.

REHMSMEIER, M., STEFFEN, P., HOCHSMANN, M. & GIEGERICH, R. (2004) Fast and effective prediction of microRNA/target duplexes. Rna, 10, 1507-17.

REN, Y., TSUI, H. T., POON, R. T., NG, I. O., LI, Z., CHEN, Y., JIANG, G., LAU, C., YU, W. C., BACHER, M. & FAN, S. T. (2003) Macrophage migration inhibitory factor: roles in regulating tumor cell migration and expression of angiogenic factors in hepatocellular carcinoma. Int J Cancer, 107, 22-9.

REN, X. D., KIOSSES, W. B. & SCHWARTZ, M. A. (1999) Regulation of the small GTP-binding protein Rho by cell adhesion and the cytoskeleton. Embo J, 18, 578-85.

RHEE, H. J., KIM, G. Y., HUH, J. W., KIM, S. W. & NA, D. S. (2000) Annexin I is a stress protein induced by heat, oxidative stress and a sulfhydryl-reactive agent. Eur J Biochem, 267, 3220-5.

RISSEEUW, E., FRANKE-VAN DIJK, M. E. & HOOYKAAS, P. J. (1997) Gene targeting and instability of Agrobacterium T-DNA loci in the plant genome. Plant J, 11, 717-28.

RIVELLA, S., CALLEGARI, J. A., MAY, C., TAN, C. W. & SADELAIN, M. (2000) The cHS4 insulator increases the probability of retroviral expression at random chromosomal integration sites. J Virol, 74, 4679-87.

ROTH, N. S., CAMPBELL, P. T., CARON, M. G., LEFKOWITZ, R. J. & LOHSE, M. J. (1991) Comparative rates of desensitization of beta-adrenergic receptors by the beta-adrenergic receptor kinase and the cyclic AMP-dependent protein kinase. Proc Natl Acad Sci U S A, 88, 6201-4.

RUBIN, H. (1993) 'Spontaneous' transformation as aberrant epigenesis. Differentiation, 53, 123-37.

RUBIN, H. (2001) Selected cell and selective microenvironment in neoplastic development. Cancer Res, 61, 799-807.

RUSSELL, W. M. & KLAENHAMMER, T. R. (2001) Efficient system for directed integration into the Lactobacillus acidophilus and Lactobacillus gasseri chromosomes via homologous recombination. Appl Environ Microbiol, 67, 4361-4.

RUSSELL, D. W. & HIRATA, R. K. (1998) Human gene targeting by viral vectors. Nat Genet, 18, 325-30.

RUVKUN, G. (2001) Molecular biology. Glimpses of a tiny RNA world. Science, 294, 797-9.

RYCYZYN, M. A. & CLEVENGER, C. V. (2000) Role of cyclophilins in somatolactogenic action. Ann N Y Acad Sci, 917, 514-21.

SAHI, J., SINZ, M. W., CAMPBELL, S., MIRELES, R., ZHENG, X., ROSE, K. A., RAEISSI, S., HASHIM, M. F., YE, Y., DE MORAIS, S. M., BLACK, C., TUGNAIT, M. & KELLER, L. H. (2006) Metabolism and transporter-mediated drug-drug interactions of the endothelin-A receptor antagonist CI-1034. Chem Biol Interact, 159, 156-68.

SANTIN, A. D., ZHAN, F., CANE, S., BELLONE, S., PALMIERI, M., THOMAS, M., BURNETT, A., ROMAN, J. J., CANNON, M. J., SHAUGHNESSY, J., JR. & PECORELLI, S. (2005) Gene expression fingerprint of uterine serous papillary carcinoma: identification of novel molecular markers for uterine serous cancer diagnosis and therapy. Br J Cancer, 92, 1561-73.

SCHWARZ, D. S., HUTVAGNER, G., DU, T., XU, Z., ARONIN, N. & ZAMORE, P. D. (2003) Asymmetry in the assembly of the RNAi enzyme complex. Cell, 115, 199-208.

SCOTT, J. C., KENNEDY, M. W. & MCMANUS, D. P. (2000) Molecular and immunological characterisation of a polymorphic cytosolic fatty acid binding protein from the human blood fluke of humans, Schistosoma japonicum. Biochim Biophys Acta, 1517, 53-62.

SHENK, T. E. & BERG, P. (1976) Isolation and propagation of a segment of the simian virus 40 genome containing the origin of DNA replication. Proc Natl Acad Sci U S A, 73, 1513-7.

SHIBATA, T., OHTANI, T., CHANG, P. K. & ANDO, T. (1982) Role of superhelicity in homologous pairing of DNA molecules promoted by Escherichia coli recA protein. J Biol Chem, 257, 370-6.

SIMPSON, R. J. & DOROW, D. S. (2001) Cancer proteomics: from signaling networks to tumor markers. Trends Biotechnol, 19, S40-8.

SMALHEISER, N. R. (2003) EST analyses predict the existence of a population of chimeric microRNA precursor-mRNA transcripts expressed in normal human and mouse tissues. Genome Biol, 4, 403.

SMITHIES, O., KORALEWSKI, M. A., SONG, K. Y. & KUCHERLAPATI, R. S. (1984) Homologous recombination with DNA introduced into mammalian cells. Cold Spring Harb Symp Quant Biol, 49, 161-70.

SMIRNOV, D. A., ZWEITZIG, D. R., FOULK, B. W., MILLER, M. C., DOYLE, G. V., PIENTA, K. J., MEROPOL, N. J., WEINER, L. M., COHEN, S. J., MORENO, J. G., CONNELLY, M. C., TERSTAPPEN, L. W. & O'HARA, S. M. (2005) Global gene expression profiling of circulating tumor cells. Cancer Res, 65, 4993-7.

SONG, S. U., GERASIMOVA, T., KURKULOS, M., BOEKE, J. D. & CORCES, V. G. (1994) An env-like protein encoded by a Drosophila retroelement: evidence that gypsy is an infectious retrovirus. Genes Dev, 8, 2046-57.

SADOWSKI, P. D. (1995) The Flp recombinase of the 2-microns plasmid of Saccharomyces cerevisiae. Prog Nucleic Acid Res Mol Biol, 51, 53-91.

SARKAR, D., AZARO, M. A., AIHARA, H., PAPAGIANNIS, C. V., TIRUMALAI, R., NUNES-DUBY, S. E., JOHNSON, R. C., ELLENBERGER, T. & LANDY, A. (2002) Differential affinity and cooperativity functions of the amino-terminal 70 residues of lambda integrase. J Mol Biol, 324, 775-89.

SAWAYA, R., GO, Y., KYRITISIS, A. P., UHM, J., VENKAIAH, B., MOHANAM, S., GOKASLAN, Z. L. & RAO, J. S. (1998) Elevated levels of Mr 92,000 type IV collagenase during tumor growth in vivo. Biochem Biophys Res Commun, 251, 632-6.

SAZER, S. & DASSO, M. (2000) The ran decathlon: multiple roles of Ran. J Cell Sci, 113 (Pt 7), 1111-8.

SCOTT, G. K., MATTIE, M. D., BERGER, C. E., BENZ, S. C. & BENZ, C. C. (2006) Rapid alteration of microRNA levels by histone deacetylase inhibition. Cancer Res, 66, 1277-81.

SEIKE, M., KONDO, T., MORI, Y., GEMMA, A., KUDOH, S., SAKAMOTO, M., YAMADA, T. & HIROHASHI, S. (2003) Proteomic analysis of intestinal epithelial cells expressing stabilized beta-catenin. Cancer Res, 63, 4641-7.

SELBACH, M., SCHWANHÄUSSER, B., THIERFELDER, FANG, N.Z., KHANIN, N. and RAJEWSKY, N. (2008) Widespread changes in protein synthesis induced by microRNAs *Nature* **455**, 58-63.

SENGUPTA, S., DEN BOON, J. A., CHEN, I. H., NEWTON, M. A., STANHOPE, S. A., CHENG, Y. J., CHEN, C. J., HILDESHEIM, A., SUGDEN, B. & AHLQUIST, P. (2008) MicroRNA 29c is down-regulated in nasopharyngeal carcinomas, up-regulating mRNAs encoding extracellular matrix proteins. Proc Natl Acad Sci U S A, 105, 5874-8.

SHARMA, M. R., KOLTOWSKI, L., OWNBEY, R. T., TUSZYNSKI, G. P. & SHARMA, M. C. (2006) Angiogenesis-associated protein annexin II in breast cancer: selective expression in invasive breast cancer and contribution to tumor invasion and progression. Exp Mol Pathol, 81, 146-56.

SHERRATT, D. J., ARCISZEWSKA, L. K., BLAKELY, G., COLLOMS, S., GRANT, K., LESLIE, N. & MCCULLOCH, R. (1995) Site-specific recombination and circular chromosome segregation. Philos Trans R Soc Lond B Biol Sci, 347, 37-42.

SHICHI, H. & DEMAR, J. C. (1990) Non-selenium glutathione peroxidase without glutathione S-transferase activity from bovine ciliary body. Exp Eye Res, 50, 513-20.

SHIMIZU, T., ABE, R., OHKAWARA, A. & NISHIHIRA, J. (1999) Ultraviolet B radiation upregulates the production of macrophage migration inhibitory factor (MIF) in human epidermal keratinocytes. J Invest Dermatol, 112, 210-5.

SMIRNOV, D. A., ZWEITZIG, D. R., FOULK, B. W., MILLER, M. C., DOYLE, G. V., PIENTA, K. J., MEROPOL, N. J., WEINER, L. M., COHEN, S. J., MORENO, J. G., CONNELLY, M. C., TERSTAPPEN, L. W. & O'HARA, S. M. (2005) Global gene expression profiling of circulating tumor cells. Cancer Res, 65, 4993-7.

SMITH, G. R. (2001) Homologous recombination near and far from DNA breaks: alternative roles and contrasting views. Annu Rev Genet, 35, 243-74.

SNAPKA, R. M., GE, S., TRASK, J. & ROBERTSON, F. (1997) Unbalanced growth in mouse cells with amplified dhfr genes. Cell Prolif, 30, 385-99.

SOCINSKI, M. A. (2004) Adjuvant therapy of resected non-small-cell lung cancer. Clin Lung Cancer, 6, 162-9.

SORRENTINO, A., LIU, C. G., ADDARIO, A., PESCHLE, C., SCAMBIA, G. & FERLINI, C. (2008) Role of microRNAs in drug-resistant ovarian cancer cells. Gynecol Oncol, 111, 478-86.

STEC, D. E. & SIGMUND, C. D. (1998) Modifiable gene expression in mice: kidney-specific deletion of a target gene via the cre-loxP system. Exp Nephrol, 6, 568-75.

STOCKHOLM, D., BENCHAOUIR, R., PICOT, J., RAMEAU, P., NEILDEZ, T. M., LANDINI, G., LAPLACE-BUILHE, C. & PALDI, A. (2007) The origin of phenotypic heterogeneity in a clonal cell population in vitro. PLoS ONE, 2, e394.

SUKOH, N., ABE, S., OGURA, S., ISOBE, H., TAKEKAWA, H., INOUE, K. & KAWAKAMI, Y. (1994) Immunohistochemical study of cathepsin B. Prognostic significance in human lung cancer. Cancer, 74, 46-51.

SUN, C., ANTONIONIO, R. J. & REDPATH, J. L. (1996) Reversion of UVC-induced tumorigenic human hybrid cells to the non-tumorigenic phenotype. Eur J Cancer, 32A, 322-7.

TALMADGE, J. E. & FIDLER, I. J. (1982) Cancer metastasis is selective or random depending on the parent tumour population. Nature, 297, 593-4.

THOMAS, P. D., CAMPBELL, M. J., KEJARIWAL, A., MI, H., KARLAK, B., DAVERMAN, R., DIEMER, K., MURUGANUJAN, A. & NARECHANIA, A. (2003) PANTHER: a library of protein families and subfamilies indexed by function. Genome Res, 13, 2129-41.

THORENS, B. (1992) Expression cloning of the pancreatic beta cell receptor for the gluco-incretin hormone glucagon-like peptide 1. Proc Natl Acad Sci U S A, 89, 8641-5.

TUCK, A. B., WILSON, S. M., KHOKHA, R. & CHAMBERS, A. F. (1991) Different patterns of gene expression in ras-resistant and ras-sensitive cells. J Natl Cancer Inst, 83, 485-91.

TAKAI, D. & JONES, P. A. (2002) Comprehensive analysis of CpG islands in human chromosomes 21 and 22. Proc Natl Acad Sci U S A, 99, 3740-5.

TANAKA, T. (2003) [Therapeutic gene clusters as drug action mechanisms]. Nippon Yakurigaku Zasshi, 122 Suppl, 5P-7P.

TERADA, R., JOHZUKA-HISATOMI, Y., SAITOH, M., ASAO, H. & IIDA, S. (2007) Gene targeting by homologous recombination as a biotechnological tool for rice functional genomics. Plant Physiol, 144, 846-56.

THORENS, B. (1992) Expression cloning of the pancreatic beta cell receptor for the gluco-incretin hormone glucagon-like peptide 1. Proc Natl Acad Sci U S A, 89, 8641-5.

THYKJAER, T., FINNEMANN, J., SCHAUSER, L., CHRISTENSEN, L., POULSEN, C. & STOUGAARD, J. (1997) Gene targeting approaches using positive-negative selection and large flanking regions. Plant Mol Biol, 35, 523-30.

TURRIN, N. P. & PLATA-SALAMAN, C. R. (2000) Cytokine-cytokine interactions and the brain. Brain Res Bull, 51, 3-9.

UEBLACKER, P., WAGNER, B., VOGT, S., SALZMANN, G., WEXEL, G., KRUGER, A., PLANK, C., BRILL, T., SPECHT, K., HENNIG, T., SCHILLINGER, U., IMHOFF, A. B., MARTINEK, V. & GANSBACHER, B. (2007) In vivo analysis of retroviral gene transfer to chondrocytes within collagen scaffolds for the treatment of osteochondral defects. Biomaterials, 28, 4480-7.

UNGRIN, M. D. & HARRINGTON, L. (2006) Strict control of telomerase activation using Cre-mediated inversion. BMC Biotechnol, 6, 10.

VAN DEN BRULE, F. A., BUICU, C., BALDET, M., SOBEL, M. E., COOPER, D. N., MARSCHAL, P. & CASTRONOVO, V. (1995) Galectin-1 modulates human melanoma cell adhesion to laminin. Biochem Biophys Res Commun, 209, 760-7.

VANPOUILLE, C., DENYS, A., CARPENTIER, M., PAKULA, R., MAZURIER, J. & ALLAIN, F. (2004) Octasaccharide is the minimal length unit required for efficient

binding of cyclophilin B to heparin and cell surface heparan sulphate. Biochem J, 382, 733-40.

VETTER, I. R., NOWAK, C., NISHIMOTO, T., KUHLMANN, J. & WITTINGHOFER, A. (1999) Structure of a Ran-binding domain complexed with Ran bound to a GTP analogue: implications for nuclear transport. Nature, 398, 39-46.

VINTHER, J., HEDEGAARD, M. M., GARDNER, P. P., ANDERSEN, J. S. & ARCTANDER, P. (2006) Identification of miRNA targets with stable isotope labeling by amino acids in cell culture. Nucleic Acids Res, 34, e107.

WADE, P. A., GEGONNE, A., JONES, P. L., BALLESTAR, E., AUBRY, F. & WOLFFE, A. P. (1999) Mi-2 complex couples DNA methylation to chromatin remodelling and histone deacetylation. Nat Genet, 23, 62-6.

YAMANE-OHNUKI, N., KINOSHITA, S., INOUE-URAKUBO, M., KUSUNOKI, M., IIDA, S., NAKANO, R., WAKITANI, M., NIWA, R., SAKURADA, M., UCHIDA, K., SHITARA, K. & SATOH, M. (2004) Establishment of FUT8 knockout Chinese hamster ovary cells: an ideal host cell line for producing completely defucosylated antibodies with enhanced antibody-dependent cellular cytotoxicity. Biotechnol Bioeng, 87, 614-22.

YANAMANDRA, N., KONDRAGANTI, S., GONDI, C. S., GUJRATI, M., OLIVERO, W. C., DINH, D. H. & RAO, J. S. (2005) Recombinant adeno-associated virus (rAAV) expressing TFPI-2 inhibits invasion, angiogenesis and tumor growth in a human glioblastoma cell line. Int J Cancer, 115, 998-1005.

WANG, M., LIU, Y. E., GREENE, J., SHENG, S., FUCHS, A., ROSEN, E. M. & SHI, Y. E. (1997) Inhibition of tumor growth and metastasis of human breast cancer cells transfected with tissue inhibitor of metalloproteinase 4. Oncogene, 14, 2767-74.

WANG, Z. (2004) Roles of K+ channels in regulating tumour cell proliferation and apoptosis. Pflugers Arch, 448, 274-86.

WICKI, R., SCHAFER, B. W., ERNE, P. & HEIZMANN, C. W. (1996) Characterization of the human and mouse cDNAs coding for S100A13, a new member of the S100 protein family. Biochem Biophys Res Commun, 227, 594-9.

WOJTUKIEWICZ, M. Z., SIERKO, E., ZIMNOCH, L., KOZLOWSKI, L. & KISIEL, W. (2003) Immunohistochemical localization of tissue factor pathway inhibitor-2 in human tumor tissue. Thromb Haemost, 90, 140-6.

WOHN, K. D., KANSE, S. M., DEUTSCH, V., SCHMIDT, T., ELDOR, A. & PREISSNER, K. T. (1997) The urokinase-receptor (CD87) is expressed in cells of the megakaryoblastic lineage. Thromb Haemost, 77, 540-7.

WURM, F. M. (2004) Production of recombinant protein therapeutics in cultivated mammalian cells. Nat Biotechnol, 22, 1393-8.

WYLLIE, A. H., KERR, J. F. & CURRIE, A. R. (1980) Cell death: the significance of apoptosis. Int Rev Cytol, 68, 251-306.

YANG, M., LI, Y. & PADGETT, R. W. (2005) MicroRNAs: Small regulators with a big impact. Cytokine Growth Factor Rev, 16, 387-93.

YANO, S., MUGURUMA, H., MATSUMORI, Y., GOTO, H., NAKATAKI, E., EDAKUNI, N., TOMIMOTO, H., KAKIUCHI, S., YAMAMOTO, A., UEHARA, H., RYAN, A. & SONE, S. (2005) Antitumor vascular strategy for controlling experimental metastatic spread of human small-cell lung cancer cells with ZD6474 in natural killer cell-depleted severe combined immunodeficient mice. Clin Cancer Res, 11, 8789-98.

YI, R., QIN, Y., MACARA, I. G. & CULLEN, B. R. (2003) Exportin-5 mediates the nuclear export of pre-microRNAs and short hairpin RNAs. Genes Dev, 17, 3011-6.

YOUNG, T. W., MEI, F. C., YANG, G., THOMPSON-LANZA, J. A., LIU, J. & CHENG, X. (2004) Activation of antioxidant pathways in ras-mediated oncogenic transformation of human surface ovarian epithelial cells revealed by functional proteomics and mass spectrometry. Cancer Res, 64, 4577-84.

YU, Q. & STAMENKOVIC, I. (2000) Cell surface-localized matrix metalloproteinase-9 proteolytically activates TGF-beta and promotes tumor invasion and angiogenesis. Genes Dev, 14, 163-76.

YURCHENKO, V., ZYBARTH, G., O'CONNOR, M., DAI, W. W., FRANCHIN, G., HAO, T., GUO, H., HUNG, H. C., TOOLE, B., GALLAY, P., SHERRY, B. & BUKRINSKY, M. (2002) Active site residues of cyclophilin A are crucial for its signaling activity via CD147. J Biol Chem, 277, 22959-65.

YURCHENKO, V., ZYBARTH, G., O'CONNOR, M., DAI, W. W., FRANCHIN, G., HAO, T., GUO, H., HUNG, H. C., TOOLE, B., GALLAY, P., SHERRY, B. &
ZHONG, R., HUANG, R. B. & SONG, S. J. (2003) [Role of tissue factor pathway inhibitor-2 in ovarian tumor migration and invasion]. Ai Zheng, 22, 1038-41.

ZHONG, R., HUANG, R. B. & SONG, S. J. (2003) [Role of tissue factor pathway inhibitor-2 in ovarian tumor migration and invasion]. Ai Zheng, 22, 1038-41.

ZHU, S., SI, M. L., WU, H. & MO, Y. Y. (2007) MicroRNA-21 targets the tumor suppressor gene tropomyosin 1 (TPM1). J Biol Chem, 282, 14328-36.